



Functional Materials by Click Chemistry

Daugaard, Anders Egede; Hvilsted, Søren

Publication date:
2009

Document Version
Publisher's PDF, also known as Version of record

[Link back to DTU Orbit](#)

Citation (APA):
Daugaard, A. E., & Hvilsted, S. (2009). Functional Materials by Click Chemistry. Kgs. Lyngby, Denmark: Technical University of Denmark (DTU).

DTU Library

Technical Information Center of Denmark

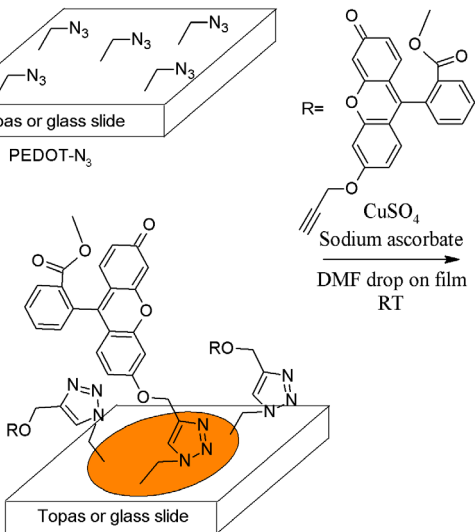
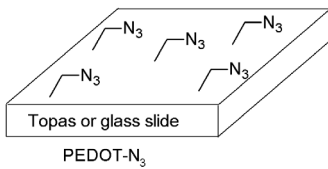
General rights

Copyright and moral rights for the publications made accessible in the public portal are retained by the authors and/or other copyright owners and it is a condition of accessing publications that users recognise and abide by the legal requirements associated with these rights.

- Users may download and print one copy of any publication from the public portal for the purpose of private study or research.
- You may not further distribute the material or use it for any profit-making activity or commercial gain
- You may freely distribute the URL identifying the publication in the public portal

If you believe that this document breaches copyright please contact us providing details, and we will remove access to the work immediately and investigate your claim.

Functional Materials by Click Chemistry



PhD thesis

Anders Egede Daugaard
2009

Functional Materials by Click Chemistry



**Danish Polymer Centre
Department of Chemical and Biochemical
Engineering
Technical University of Denmark
Kgs. Lyngby Denmark**

Anders Egede Daugaard

February 2009

Copyright © Anders Egede Dagaard, 2009
ISBN-13: 978-87-92481-00-9
Printed by J&R Frydenberg A/s, Copenhagen, Denmark

Acknowledgement

This thesis is the result of my Ph.D. project carried out at the Danish Polymer Centre (DPC) in Department of Chemical and Biochemical Engineering at the Technical University of Denmark (DTU) from 2006 to 2009. The project was financed in part by DTU and by the Danish Research Council for Technology and Production Sciences through the frame work programme “Design and Processing of Polymers for Microfluidic Applications”, grant 26-04-0074.

First and foremost I would like to thank my supervisor Professor Søren Hvilsted for giving me the opportunity of working on this interesting project. I have always appreciated your support and guidance with the project allowing me to bring my own ideas and to a large extent also to carry them out in the lab. Especially, our sometimes too long meetings with discussions of new chemistry and other approaches have been enjoyed tremendously on my behalf. I would also like to thank you for pushing me to go to California when needed and for establishing the contact to Professor Craig J. Hawker at University of California Santa Barbara (UCSB) for my external research stay.

At UCSB I would like to thank Professor Craig J. Hawker for allowing me to come to his group and experience the dynamic research environment supported by his enthusiasm for science and research. It was a great pleasure working with Ph.D. Anzar Khan both educationally and on a personal level, you really increased the value of my stay at UCSB. Also Ph.D. Jos Paulusse is thanked for the helpful discussions and for supplying the cyclic monomers when time was getting tight at the end. My lab mate Ph.D. student Denis Damiron from the University of Lyon is thanked for many great times in Santa Barbara and his impressively infectious good spirits. All the people from the Materials Research Department are appreciated for contributing to my stay by being very welcoming and always helpful with even the smallest of things. It was a very good experience sharing the spring of 2008 with all of you in Santa Barbara, and I will always remember it.

At Risø DTU I would like to thank Professor Niels B. Larsen for the discussions and collaboration in relation to the conductive polymers and for his help with XPS analyses at almost all times of the day. It has been a great inspiration working with you on this project. Also Ph.D. Thomas S. Hansen is thanked for the collaboration on the conductive polymers and always contributing with new ideas keeping things moving constantly.

From DTU nanotech I would like to thank Associate Professor Oliver Geschke, Senior Researcher Noemi Rozlosnik and Ph.D. Student Jan Kafka for all their help

with the electrochemical analyses.

I would also like to thank Kim Chi Szabo at DPC for her assistance with DSC and SEC analyses. Associate Professor Katja Jankova for clarification of all the small details and for help on polymerizations. I would like to thank my office mates Natanya M.L. Hansen, Anne Katrine K. Overgaard, Charlotte Juel Fristrup and Irakli Javakhisvili for many discussions and for creating an inspiring and relaxed atmosphere. All my other colleagues at DPC are also acknowledged for many good experiences throughout the last three years.

Finally I would also like to thank my friends and family who have always given the helpful support whenever it was needed. A special thanks to my wife Anja who has been especially tolerant of my irrational behavior during the last months of my thesis work.

Kgs. Lyngby, 26th of February 2009.

Anders Egede Daugaard

Abstract

This thesis is based on the preparation of new functional materials through the concept of click chemistry and especially by the use of the highly efficient copper catalyzed cycloaddition of alkynes and azides (CuAAC).

Initially, carboxylic acid polymer surfaces have been prepared. These functional polystyrenes have been synthesized through an approach based on poly(4-hydroxystyrene), followed by a Williamson introduction of an alkyne and subsequent cycloadditions. The approach has been applied to both commercially available homo- and copolymers illustrating the broad range of possible applications. In addition to the commercial polymers, the free radical copolymerization of 4-*tert*-butoxystyrene and styrene has been investigated for preparation of specific loadings. It was found that the copolymerization yields a perfectly random copolymer with reactivity ratios close to one. The surface properties of the prepared carboxylic acid polymers have been investigated using both X-ray photoelectron spectroscopy and contact angle measurements on thin films. The loading of functional groups and minor structural changes were found to strongly influence the accessibility of carboxylic acids on the surface.

This approach has also been applied for preparation of new monomers for photopolymer systems. The holographic systems investigated have been based on macromonomers prepared through the traditional Fréchet type benzyl ethers as well as on a new type of naphthalene end group functionalized dendrons build through thiol-ene chemistry. Application of cycloadditions for preparation of cyclic analogues were also investigated using two alkyne functional lactone acrylates. These were functionalized through cycloadditions with azides illustrating a highly efficient way of introducing substituents into the cyclic monomers before polymerization. The holographic characterizations of dendronized macromonomer photopolymer systems clearly showed that there was a beneficial effect of the dendritic structure. This results in a lowering of the volume shrinkage of the photopolymer system, while maintaining a high storage capacity.

Also novel conductive polymers based on poly(3,4-ethylenedioxythiophene) have been prepared. A new azide functional monomer was synthesized and polymerized, enabling the introduction of new functionalities to the conductive polymer. The CuAAC on the insoluble conductive polymer was optimized using a fluorescent alkyne, finding optimal conditions of 20 hours at room temperature. Additionally conductive polymers with different surface properties were prepared through the optimized method. Experiments with microwave reactions performed on the conductive polymer, were found to reduce the reaction time considerably, resulting

in reaction times on the order of minutes. In addition to this, it was found that the reaction could be localized selectively on either of a pair of interdigitated electrodes by electrochemical reduction of the catalyst. Finally, the modularity of the approach has been exploited in the preparation of new conductive polymers for applications as micro sensors. Here receptors such as a 12-crown-4 ether, biotin or ferrocene have been covalently linked to the surface. Initial investigations of the sensing properties of these conductive polymers are presented.

Resumé

Denne Ph.D. afhandling er baseret på fremstillingen af funktionelle materialer ved hjælp af konceptet click kemi. Specielt er de meget effektive kobber katalyserede cykloaditioner mellem azider og alkyner (CuAAC) anvendt i flere tilfælde.

I den første del af projektet er der arbejdet med udvikling af nye polymerfilm med carboxylsyrer på overfladen. Disse er fremstillet ud fra funktionelle polystyrener baseret på poly(4-hydroxystyren). Poly(4-hydroxystyren) er ved en Williamson ether syntese omdannet til den tilsvarende propargyl ether, der efterfølgende er funktionaliseret igennem CuAAC med carboxylsyre azider. Denne strategi er blevet anvendt på både komercielle homo- og copolymerer illustrerende de brede anvendelsesmuligheder. Udover de komercielle prøver er ligeledes fremstillingen af copolymerer af 4-*tert*-butoxystyren og styren blevet undersøgt for at kunne variere mængden af de funktionelle grupper. I den forbindelse blev reaktivitets forholdene undersøgt, og det kunne konstateres, at der ved copolymerisation at de to monomerer bliver produceret en random copolymer, da reaktivitetsforholdene var tæt på en. Kontakt vinkel målinger og X-ray photoelectron spektroskopi er blevet anvendt til undersøgelse af overfladeegenskaberne for polymerfilm fremstillet af de respektive copolymerer ved spincoating. Gennem disse undersøgelser er det vist, at selv små strukturelle ændringer samt ændringer i mængden af funktionelle grupper i copolymererne, har stor indflydelse på mængden af carboxylsyrer på overfladen.

Ligeledes er denne tilgang til funktionalisering af makromolekyler anvendt ved fremstilling af nye makromonomerer med henblik på anvendelser i photopolymer systemer til holografisk data opbevaring. De undersøgte makromonomerer har både været baseret på de velkendte Frechét type benzyl ether, samt på en ny naphthalen funktionaliseret dendron fremstillet ved thiol-en kemi. Sideløbende blev en anden strategi, rettet mod fremstilling af nye monomerer der polymeriserer ved ring åbning under fri radikal betingelser, undersøgt. Her blev forskellige cykloaditioner anvendt til reaktion af cykliske alkyn funktionelle acrylater før polymerisation, identificeret som en effektiv metode til fremstilling af nye monomerer. Karakterisering af de holografiske egenskaber for de forskellige systemer viste, at de dendritiske makromonomerer resulterede i en minimal volumen ændring ved polymerisation, hvor eksempler på volumen ændringer helt ned til 0.01% blev fundet uden en tilsvarende reduktion i lager kapaciteten.

Derudover er der udviklet en ny metode til funktionalisering af den ledende polymer poly(3,4-ethylenedioxythiophene) (PEDOT). Her er en ny azid funktionaliseret monomer fremstillet og polymeriseret til PEDOT-N₃, hvorefter funktionalisering

ved CuAAC er optimeret. Optimeringen blev udført ved reaktion med en alkyn funktionel fluorofor, hvorved en standard reaktionstid på 20 timer blev fundet. Ligeledes er metoden også anvendt til fremstilling af ledende polymerfilm med forskellige overflade egenskaber. Mikrobølgeovns reaktioner foretaget på den azid funktionelle ledende polymer viste, at denne teknik kunne anvendes til at opnå en reduktion af reaktionstiden til nogle få minutter. Ligeledes er selektiv funktionalisering af mikro elektroder baseret på PEDOT-N₃ blevet undersøgt. I dette tilfælde blev funktionalisering af to sammenflettede elektroder foretaget selektivt ved elektrokemisk reduktion af katalysatoren på hver af de to elektroder. Slutteligt er det modulære koncept i cycloadditionerne udnyttet til fremstilling af nye materialer med henblik på anvendelser i mikro sensorer. Her er det lykkedes at binde en 12-krone-4 ether, biotin eller ferrocen på overfladen af den ledende polymer. Indledende undersøgelser af disse ledende polymerers egenskaber som mikro sensorer bliver her præsenteret.

Contents

List of Abbreviations	1
1 Background and Outline	5
1.1 Functional Materials	5
1.2 Outline	6
2 Click Chemistry	7
2.1 Copper Catalyzed 1,3-Dipolar Cycloadditions of Alkynes and Azides	8
2.2 Radical Addition of Thiols to Alkenes	9
3 Carboxylic Acid Polymers and Surfaces	11
3.1 CuAAC Based Approach to Carboxylic Acid Polymers	12
3.1.1 Characterization	13
3.2 Polymer Properties by Functional Group	13
3.3 Variation of the Copolymer Composition	13
3.4 Surface Properties of Carboxylic Acid Copolymer Films	17
3.5 Conclusions	19
4 Materials for Holographic Data Storage	21
4.1 Data Storage in Three Dimensions	21
4.2 Benzyl Ether Dendronized Macromonomers in Volume Holography	23
4.3 Increased Storage Capacity	27
4.4 Cyclic Monomers	32
4.5 Conclusions	35
5 Functional Conductive Polymers	37
5.1 Monomer, Polymerization and Characterization	38
5.2 Microwave Chemistry	44
5.3 Electroclick	47
5.4 Sensors - Concept System	49
5.4.1 Biosensors	52
5.5 Conclusions	54
6 Conclusion and Outlook	55
6.1 Conclusion	55
6.2 Future Work	56

7 Experimental Work	59
7.1 General Methods and Materials	59
7.1.1 Method A	59
7.1.2 Method B	59
7.2 Experimental work	60
Bibliography	69
Appendices	
Appendix A	77
Appendix B	97
Appendix C	107
Appendix D	113
Appendix E	135

List of Abbreviations

AS	4-Acetoxystyrene
ATR	Attenuated total reflection
ATRP	Atom transfer radical polymerization
bis-MPA	Dimethylolpropionic acid
BMDO	5,6-Benzo-2-methylene-1,3-dioxepane
BuOH	Butanol
Cp*	Pentamethylcyclopentadienyl
CuAAC	Copper Catalyzed Alkyne Azide Cycloaddition
DCC	N,N'-dicyclohexylcarbodiimide
DMAP	Dimethylaminopyridine
DMF	N,N-dimethylformamide
DMPA	2,2-Dimethoxy-2-phenylacetophenone
DPC	Danish Polymer Centre
DSC	Differential Scanning Calorimetry
DTU	Technical University of Denmark
EDOT	3,4-Ethylenedioxythiophene
EI	Electron Ionization
ES	4-Ethoxystyrene
ESI-TOF	Electrospray Ionization Time-of-flight
FT-IR	Fourier Transform Infrared
HMDI	Hexamethylenediisocyanate

KHFP	Potassium hexafluorophosphate
MPEG	Methoxy poly(ethyleneglycol)
MS	4-Methoxystyrene
NMR	Nuclear Magnetic Resonance
NOESY	Nuclear Overhauser Effect Spectroscopy
PtBS	Poly(4- <i>tert</i> -butoxystyrene)
PDMS	Poly(dimethylsiloxane)
PEDOT	Poly(3,4-ethylenedioxythiophene)
PEG	Poly(ethyleneglycol)
PHS	Poly(4-hydroxystyrene)
PMMA	Poly(methyl methacrylate)
PPT	Polypropylene-triol
PS	Polystyrene
PTSA	p-Toluenesulfonic acid
RI	Refractive Index
RuAAC	Ruthenium Catalyzed Alkyne Azide Cycloaddition
SAM	Self Assembled Monolayer
St	Styrene
T_g	Glass Transition Temperature
<i>t</i> -BuOH	<i>tert</i> -Butanol
<i>t</i> -BuOK	Potassium <i>tert</i> -butoxide
<i>t</i> BS	4- <i>tert</i> -Butoxystyrene
TBAHFP	Tetrabutylammonium hexafluorophosphate
TBAP	Tetrabutylammonium perchlorate
THF	Tetrahydrofuran
TLC	Thin Layer Chromatography

UCSB	University of California Santa Barbara
WORM	Write Once Read Many
XPS	X-ray Photoelectron Spectroscopy

1 Background and Outline

1.1 Functional Materials

The general purpose of this thesis has been the preparation of new functional materials by high yielding reactions based on the “Click Chemistry” concept (see chapter 2) introduced by Kolb, Finn and Sharpless in 2001.¹ This, combined with the introduction of copper catalysis for the cycloaddition of alkynes and azides in 2002 by the groups of Meldal² and Sharpless,³ inspired the development of new materials for many different applications. It was the foundation for this project that this could be transferred to a system based on the known polymer, poly(4-hydroxystyrene). It is a commercially available polymer that would serve as a good basis for preparation of new polymeric materials. Interest in new materials for an electro osmotic micropump then formed the starting point for the project that was intended to evolve in multiple directions based on polymer functionalization. With the large number of publications already available within the area when the project started in mind, it was speculated that it should somehow be possible to exploit the approach for the preparation of new micro sensor materials. This was based only on the high selectivity and versatility of the technique and not with a specific system in mind. If time would permit, it was intended to start testing such systems and potentially start the preparation of new microfluidic systems.

For the preparation of new functional materials three different approaches were taken in this project:

- A postpolymerization functionalization performed in solution based on poly(4-hydroxystyrene) for development of the modular polymer concept with application as a new material for an electro osmotic micropump in mind.
- Prepolymerization functionalization of monomers for application in holographic data storage systems.
- Postpolymerization functionalization of an insoluble conductive polymer with sensor applications in mind.

The research projects covered in this thesis span several topics, though all of them to some extent touches upon click chemistry or reactions that in principle fulfill the requirements for this.

1.2 Outline

The thesis initially briefly introduces click chemistry in Chapter 2, where the most relevant literature is treated. This is intended as a short introduction and not as a review.

The first topic has been the preparation of linear polymers functionalized with carboxylic acids, presented in Chapter 3. These were envisioned for applications in electro osmotic micropumps and therefore both the synthesis and film properties have been of major importance.

The second topic has been new materials for holographic data storage, presented in Chapter 4. This part is the result of a research stay at University of California Santa Barbara in the research group of Professor Craig J. Hawker. The research stay was focused on preparation of low shrinkage monomers that would polymerize under free radical conditions. Both the application of dendronized macromonomers as well as new cyclic monomers were investigated.

The third part is focused on the preparation of a conductive functional material based on poly(3,4-ethylenedioxythiophene) (PEDOT) through click chemistry, presented in Chapter 5. This was intended for the preparation of sensor materials by exploitation of the conductive properties in combination with the modularity attained through click chemistry.

This is followed by a general conclusion and outlook in Chapter 6.

The unpublished synthesis work mentioned in the thesis can be found in the experimental work in Chapter 7 after the conclusion, whereas experimental details of the published work is available in the appendices with the respective papers. All references can be found in the bibliography after the experimental work.

The papers published as part of the Ph.D. study can be found in the following appendices:

Appendix A. A.D. Thomsen, E. Malmström, S. Hvilsted. “Novel Polymers with a High Carboxylic Acid Loading”. *Journal of Polymer Science: Part A: Polymer Chemistry* **2006**, *44*, 6360–6377.

Appendix B A.E. Daugaard and S. Hvilsted. “The Influence of Pendant Carboxylic Acid Loading on Surfaces of Statistical Poly[(4-hydroxystyrene)-co-styrene]s”. *Macromolecular Rapid Communications* **2008**, *29*, 1119–1125.

Appendix C and D A. Khan, A.E. Daugaard, A. Bayles, S. Koga, Y. Miki, K. Sato, J. Enda, S. Hvilsted, G.D. Stucky and C.J. Hawker. “Dendronized Macromonomers for Three-Dimensional Data Storage”. *Chemical Communications* **2009**, 425–427 and supporting info.

Appendix E A.E. Daugaard, S. Hvilsted, T.S. Hansen and N.B. Larsen. “Conductive Polymer Functionalization by Click Chemistry”. *Macromolecules* **2008**, *41*, 4321–4327.

2 Click Chemistry

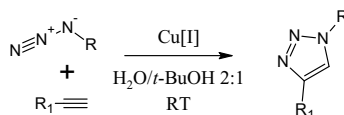
In 2001 Kolb, Finn and Sharpless¹ defined a set of selection criteria in order to identify especially good reactions that would be well suited for the construction of large molecules by modular formation of heteroatom links. They termed this approach “click chemistry” which has also been used as a common denominator for reactions fulfilling these requirements. Their interest in these reactions were for pharmaceutical applications, inspired by Nature's modular approach to the synthesis of large molecules. Subsequently the approach has found widespread use within especially materials research. By their definition a click reaction should be:

- Modular - facilitates construction of larger structures
- Wide in scope
- Very high yielding
- Generating only inoffensive byproducts
- Stereospecific
- Simple to perform
- Insensitive to water and oxygen
- Based on readily available starting materials and reagents
- Run in a mild or easily removable solvent
- Easy to purify by non-chromatographic methods

There is nothing new in the interest for reactions that fulfill these requirements. Chemists have always been interested in such reactions and have used them throughout time. The advantage of click chemistry is that it has put a strong emphasis on the formation of a desired product with certain properties in a simple and easy way. Many known reactions fulfill these criteria to some extent e.g. dipolar cycloadditions, Diels Alder reactions, nucleophilic substitutions and reactions involving carbonyl chemistry. Of these reactions mainly the copper catalyzed 1,3-dipolar cycloaddition of alkynes and azides (CuAAC) that was developed by the groups of Meldal² and Sharpless³ has found increased application within macromolecular chemistry with the introduction of click chemistry.

2.1 Copper Catalyzed 1,3-Dipolar Cycloadditions of Alkynes and Azides

The development of Cu(I) catalysis of the 1,3-dipolar cycloaddition of alkynes and azides resulted in a large reduction in reaction time and regioselective formation of only the 1,4-triazoles, in contrary to the thermal cycloaddition investigated by Huisgen in 1963.⁴ Thermal cycloadditions are known to produce a mixture of the 1,4- and 1,5-triazole products after reaction times on the order of days at temperatures around 120°C. The copper catalyzed reaction, see Scheme 2.1, is highly selective, tolerates a number of other functional groups, and in general proceeds in high yields. Under certain circumstances byproducts may be formed, though this is rare a few examples have been mentioned in the review by Meldal and Tornøe.⁵ Generally, it gives a high yield at ambient conditions or at moderate temperature. Depending on the copper source it can be highly tolerant to oxygen and be performed in a number of solvents.



Scheme 2.1. Cu(I) catalyzed 1,3-dipolar cycloaddition of an azide and an alkyne regioselectively yielding a 1,4-triazole.

The catalyst is most often Cu(I) added as a salt or generated *in situ* by a reduction of CuSO₄ with sodium ascorbate, where the latter is preferred due to lower cost, high purity of the active catalyst and stability towards oxygen. For use in purely organic solvents several different ligated copper species have been prepared, making the system widely applicable. Recently the use of microwave irradiation has been shown to result in even shorter reaction times of 10-15 minutes.⁶ There are numerous examples of the use of CuAAC in macromolecular chemistry and several reviews have been written, where especially reviews by Binder and Sachsenhofer^{7,8} provide a broad overview of the many applications. Here a few selected papers will be touched upon, giving a short introduction to the possibilities of click chemistry.

CuAAC has been used for end group functionalization both by post and pre-polymerization strategies making this a very efficient approach for building new block copolymers or other advanced structures that would otherwise be difficult to attain. This has both been achieved by initiation using azide functional initiators⁹ and silyl protected alkyne initiators.¹⁰ Post polymerization strategies using low conversion and subsequent nucleophilic substitution of the halogen endgroup after an atom transfer radical polymerization (ATRP)¹⁰ is another approach; though this is best suited for low molecular weight polymers in order to retain full con-

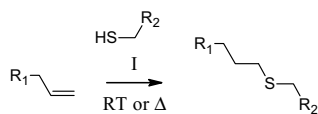
version of the end group. The high reactivity has been exploited for the synthesis of the branching structure of dendrimers,¹¹ surface functionalization as well as for reactions of the core moiety.¹² A large number of polymers have been grafted using CuAAC, providing poly(ethyleneglycol) (PEG) or short peptide sequences grafted poly(ϵ -caprolactone) from alkyne functional poly(ϵ -caprolactone).¹³ Alternatively, azide functional acrylates¹⁴ have been polymerized. Also 4-vinyl-1,2,3-triazole monomers have been prepared, leading to new polymers with a highly versatile structure.¹⁵ The selectivity of the CuAAC has been investigated and one-pot reactions have been shown to be possible. This includes examples of *in situ* azide formation⁹ as well as a CuAAC conducted simultaneously with an ester synthesis.¹⁶ For a review on multi-step reactions see Lundberg et al.¹⁷ Click reactions have also been used for heterogeneous reactions on nanotubes^{18,19} or self assembled monolayers (SAM) on gold.²⁰ The high yield and selectivity of the reaction facilitates surface modifications using this approach and it has broadened the field of possible surface functionalities. A step by step approach was published by Nandivada et al.²¹ who functionalized an alkyne surface by coating it with an azide reagent, which reacted through exposure to a structured poly(dimethylsiloxane) (PDMS) stamp containing the copper catalyst. This resulted in a patterned surface clearly showing that the click chemistry approach has great potential for surface reactions.²¹ Similarly Rozkiewicz et al.²² performed a microcontact printing method on a SAM of an aliphatic alkyne on gold reacted with ethynylferrocene without copper catalysis. However, the same authors also found that the copper catalysis was essential for the coupling of carbohydrates to the SAM by the same method.²³

Finally, the preparation of a copper free variant of the CuAAC through strained alkynes (“springloaded”) that react without the copper catalysis should also be mentioned. These systems are especially suitable for biological systems, where Baskin et al. showed that *in vivo* click reactions could be performed within minutes.²⁴ The coupling reactions under these conditions are very interesting from a biological perspective and that the reaction can be performed *in vivo* substantially broadens the applicability. However, a more general approach to the ring strained alkynes would be needed in order for this approach to gain more widespread use. In this case the cyclic alkyne was prepared through a twelve step synthesis, which makes it of less use from a general perspective.

2.2 Radical Addition of Thiols to Alkenes

Recently another reaction has been advocated as a possible click reaction. The radical reaction of thiols with alkenes (thiol-ene reaction) by either photo or thermal initiation as shown in Scheme 2.2 has been shown to give good results.²⁵

Thiols are known transfer agents and their reaction with alkenes proceed both under thermal and photoinitiation in good yields. Normally a large excess of one



Scheme 2.2. The thiol-ene reaction, where I is either a thermal or a photoinitiator.

of the reagents is necessary in order for the reaction to go to completion without byproduct formation.²⁶ Thiol-ene chemistry has found several applications during the last decades. PEG^{27,28} and dendrimers^{29,30} have been functionalized, polybutadiene^{26,31-33} as well as poly(2-(3-butenyl)-2-oxazoline)³⁴ have been grafted with small molecules. Recently Campos et al.²⁵ showed that the thiol-ene reaction is orthogonal to the CuAAC by end group functionalization of an asymmetric telechelic polystyrene. This indicates the potential from a combination of thiol-ene and CuAAC. The reaction has also found application for preparation of different networks,^{30,35,36} where the absence of the transition metal catalyst from CuAAC potentially can be exploited for preparation of biocompatible materials.

During the last few years click chemistry has been established as a very efficient frame for preparation of novel materials. The applications of this approach is steadily increasing and it is expected that this development will continue in the years to come.

3 Carboxylic Acid Polymers and Surfaces

This Ph.D. was initiated with a study of the preparation of functional materials based on a polystyrene backbone. These materials were believed to have applications for electroosmotic micropumps. Electro osmotic micropumps are based on the formation of a mobile charge layer on the surface of a microchannel. The ions in the mobile layer will move in the presence of an electrical field and by viscous drag an electrically neutral liquid will flow as shown in Figure 3.1.

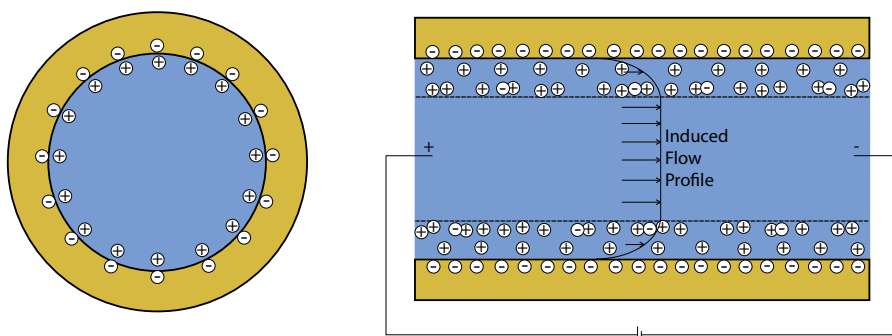
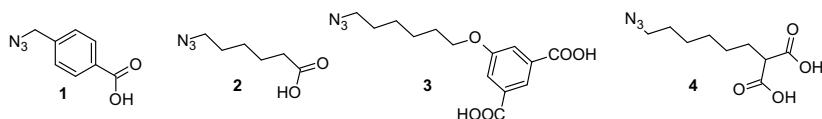


Figure 3.1. Principle of an electroosmotic micropump in a capillary, where the mobile charge layer on the surface will move and induce a flow by application of a voltage at the ends of the channel.

Traditionally, the mobile layer is created on the surface of glass particles, where proton donation creates a charged surface.³⁷ An all polymer electroosmotic micropump that could replace the traditional glass spheres would be very interesting for preparation of novel microfluidic devices. A polystyrene surface with carboxylic acid groups were targeted for this application, whereby the proton donating layer could be based solely on a polymer. Polymers containing carboxylic acids can be prepared from protected monomers. However, in the light of the recent developments within click chemistry a modular post polymerization strategy based on the CuAAC was chosen. This research project resulted in two publications^{38,39} that can be found in appendices A and B.

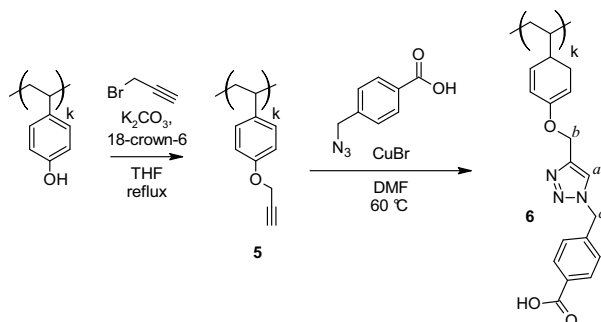
3.1 CuAAC Based Approach to Carboxylic Acid Polymers

The CuAAC enables two synthesis paths, either an azide or an alkyne would have to be bound to the polymer backbone. Subsequently, the inverse functional group could then be applied for postfunctionalization. Given the interest in introduction of carboxylic acids to the polymer backbone the approach with an alkyne on the backbone was chosen. This enabled the preparation of the carboxylic acid azides shown in Scheme 3.1 through nucleophilic substitutions with NaN_3 of the respective bromides.



Scheme 3.1. Carboxylic acid azides prepared directly from the respective bromides by nucleophilic substitution with NaN_3 .

The alkyne functional polymer based on polystyrene was prepared from commercially available poly(4-hydroxystyrene) (PHS) that was reacted with propargyl bromide under Williamson conditions as shown in Scheme 3.2. The advantage of this approach is that the starting materials are cheap and readily available.



Scheme 3.2. Preparation of the alkyne functionalized PHS followed by a CuAAC with **1** in dimethylformamide (DMF) with CuBr as catalyst, introducing benzoic acid.

The alkyne functionalized polymer was then reacted with the prepared azides providing a polystyrene backbone loaded with carboxylic acids, as shown in Scheme 3.2 with **1**. The method provides the desired polymers in high yields with no unreacted alkynes and without any detected byproducts clearly underlining the efficiency and selectivity of CuAAC.

3.1.1 Characterization

The standard analysis tools have been applied for the structure determination of the triazole products. As both alkynes and the azides are strongly absorbing in FT-IR spectroscopy this is a very well suited technique for determination of the extent of reaction as well as presence of even trace amounts of excess reagents. The most characteristic peak in the $^1\text{H-NMR}$ spectrum is the triazole proton (*a* in Scheme 3.2) that appears at approximately 8 ppm. Likewise the methylenes close to the triazole (*b* and *c* in Scheme 3.2) are also very distinct with down field shifts from 4.6 to 5.1 ppm and 4.3 to 5.7 ppm, respectively. In addition to this, nuclear overhauser effect spectroscopy (NOESY) has been applied to confirm the formation of only the 1,4 triazole regioisomer.³⁸

3.2 Polymer Properties by Functional Group

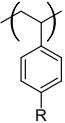
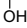
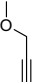
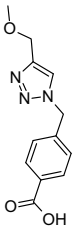
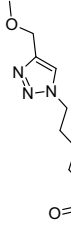

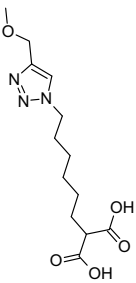
The advantages of the postpolymerization functionalization approach by CuAAC is the modularity attained by the high selectivity of the reaction and the high yields that results in complete functionalization of the backbone. Thereby a number of different functionalities could in principle be introduced on the backbone as has been done here with carboxylic acids. Since the same backbone is applied for the preparation of all the polymers the method is extremely well suited for the preparation of model systems for investigations of the influence of changes with different functional groups. This could be used to investigate the effects on e.g. the glass transition temperature (T_g) as shown in Table 3.1.

From the table it is obvious that large effects can be obtained by changing from aromatic to aliphatic substituents or the number of functional groups from the mono to the divalent carboxylic acids. Compared to an evaluation of polymer properties with different functional groups on polymers prepared from different monomers, this approach is much simpler. Here the influence of the backbone and changes in polydispersity can be neglected, since the products origin from the same backbone. Thus it is possible to visualize the effect of even very small changes like the length of a spacer without having to attribute parts of the change to the effects of the polymerization and monomer reactivity.

3.3 Variation of the Copolymer Composition

The carboxylic acid polymers indicated in Table 3.1 were used for an initial study of film properties, and it was found in these preliminary studies that random copolymers would be best suited for preparation of functional surfaces. Therefore the preparation of a selection of random copolymers of 4-hydroxystyrene and styrene was investigated. Poly(4-hydroxystyrene) can be prepared from either

Table 3.1. T_g 's of different backbones with various carboxylic acids [$^{\circ}\text{C}$].

						
PHS, 8K	123	46	98	54	118	60
PHS-co-PMMA, 3K (75% PHS)	131	60	–	–	90	65
PHS-block-PS, 55K (10% PHS)	101	99	–	–	100	104

4-*tert*-butoxystyrene (*t*BS) or 4-acetoxystyrene (AS) by either controlled conditions or free radical polymerization. Experience from working with AS in ATRP showed that it could be polymerized,⁴⁰ though the deprotection was complicated by crosslinking.⁴¹ Since 4-methoxystyrene⁴² (MS) and 4-ethoxystyrene⁴³ (ES) has been shown to copolymerize with styrene (St) with reactivity ratios close to one ($r_{\text{MS,St}}=1.16$ and $r_{\text{St,MS}}=0.82$; $r_{\text{ES,St}}=0.71$ and $r_{\text{St,ES}}=0.98$) it was decided to investigate the copolymerization of *t*BS with styrene. In order to determine the reactivity ratios, polymerizations were conducted with different feed compositions and stopped at approximately 5-10% conversion. By assuming a constant ratio of monomers in the feed at low conversion the copolymer compositions obtained from NMR on these polymers could be used to determine the reactivity ratios by the method of Kelen and Tüdös,^{44,45} as shown in Figure 3.2.

The plot clearly shows linearity and was therefore used directly to calculate the reactivity ratios to $r_{\text{tBS,St}}=0.97$ and $r_{\text{St,tBS}}=1.12$. As these are very close to unity it could be concluded that a true random copolymer would be formed throughout the copolymerization without modification of the feed. Standard free radical polymerizations targeting copolymers containing 25, 50, 75% *t*BS were then conducted and the copolymers shown in Table 3.2 were obtained.

¹H-NMR was applied to confirm the composition of the copolymers and verified that the monomer ratios in the copolymers corresponded to the feed composition. The prepared copolymers were then deprotected under standard acidic conditions and subsequently the alkyne functional backbone could be prepared by the Williamson reaction as mentioned above. Having prepared the backbone, the

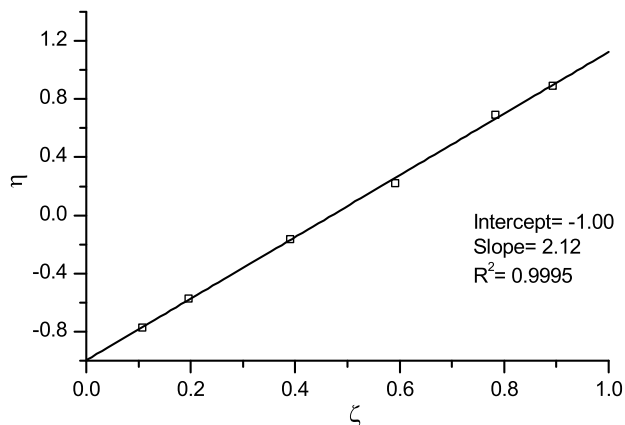


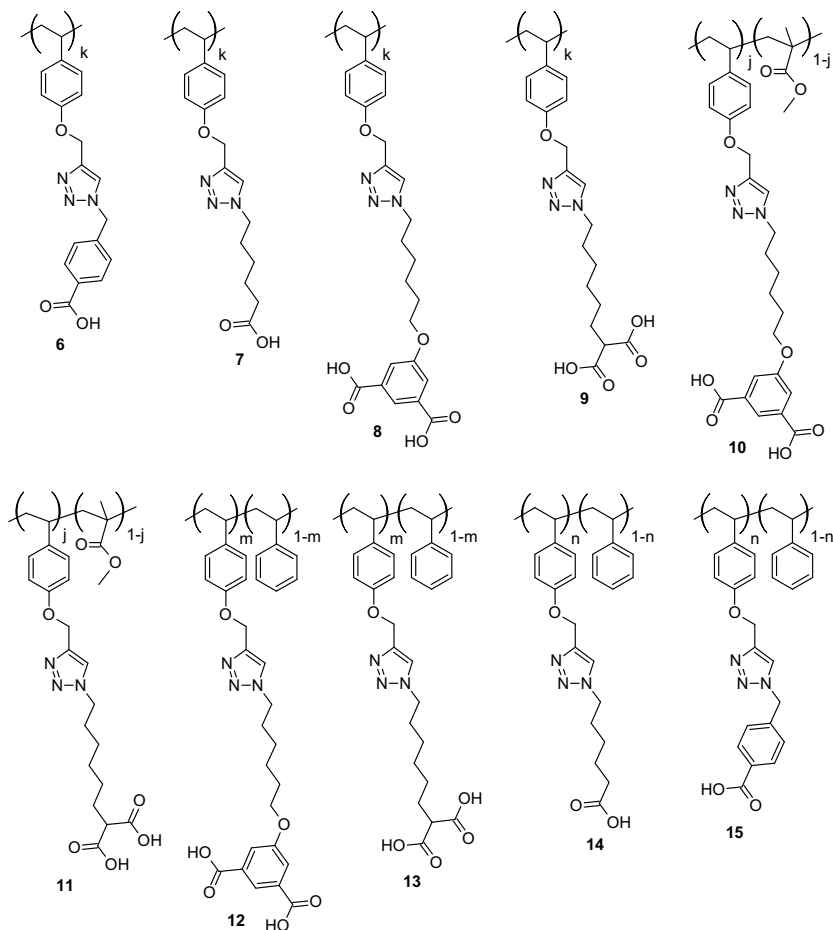
Figure 3.2. Kelen and Tüdös plot that shows linearity between the two parameters, validating that the two parameter model can be applied here. Based on the slope and intercept reactivity ratios of $r_{tBS,St}=0.97$ and $r_{St,tBS}=1.12$ were calculated.

Table 3.2. (Co)polymer composition and molecular weight.

(Co)polymer	Feed Composition [mol-%]		Mn [kg/mol]	PDI	T _g [°C]	Copolymer Composition [†] [mol-%]	
	<i>t</i> BS	St				<i>t</i> BS	St
PS	0	100	11.3	1.9	86[90] ⁴⁶		
<i>Pt</i> BS- <i>ran</i> -PS	25.0	75.0	13.3	1.8	88	24.5	75.5
<i>Pt</i> BS- <i>ran</i> -PS	50.2	49.8	16.0	1.7	94	47.2	52.8
<i>Pt</i> BS- <i>ran</i> -PS	75.0	25.0	17.2	1.7	96	72.8	27.2
<i>Pt</i> BS	100	0	19.3	1.7	94[103] ⁴⁷		

[†] Determined by ¹H-NMR

alkyne functional copolymers were postfunctionalized through the CuAAC with the two carboxylic acids **1** and **2** yielding the desired carboxylic acid functional random copolymers. An overview of all the prepared materials is shown in Scheme 3.3.



Scheme 3.3. Carboxylic acid (co)polymers; $k=1$; $j=0.75$ (copolymers); $m=0.9$ (block copolymers) and $n=0.25, 0.5, 0.75$ (random copolymers).

3.4 Surface Properties of Carboxylic Acid Copolymer Films

For the application in the electroosmotic micropump it is essential to identify the copolymers with the highest concentration of carboxylic acids on the surface of thin films. In order to determine the surface properties of the random copolymers, thin polymer films were prepared by spincoating onto a glass slide. These were characterized with both X-ray Photoelectron Spectroscopy (XPS) and contact angle measurements. XPS showed atom concentrations corresponding to approximately the bulk concentration. High resolution data from the carbon peak showed that the carboxylic acids were present in the upper 10 nm of the samples, where especially the aromatic carboxylic acid showed a high concentration on the surface.³⁹ Contact angle measurements were performed on the same samples, resulting in a nice correlation to the loading as shown in Figure 3.3.

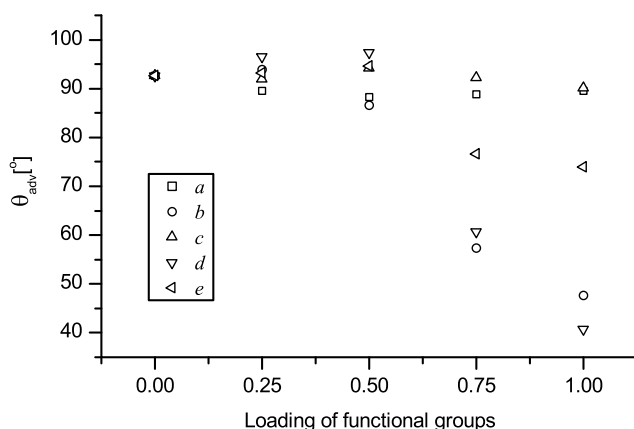


Figure 3.3. Advancing contact angles of H₂O on the copolymer thin films as a function of the different functional groups, *a*: *tert*-butoxy, *b*: hydroxy, *c*: prop-2-ynyl, *d*: aromatic acid and *e*: aliphatic acid.

Interestingly, the influence of some of the functional groups upon the contact angle of H₂O on the surface reach a point where the contact angle cannot be changed by an increased loading. This is true for all the unpolar substituents (*a* and *c* in Figure 3.3), but also for the aliphatic carboxylic acid (*e* in Figure 3.3), whereas the aromatic carboxylic acid and the unreacted phenol exhibits an increased influence throughout the range investigated (*b* and *d* in Figure 3.3). This indicates that there may be an optimum loading dependent on the type of functional group and the mobility of that group. Normally, carboxylic acids would

be buried in the surface in order to minimize the surface free energy. However, with the inflexible structures created with especially the aromatic carboxylic acid, sufficient strain is achieved and the functional groups are therefore to some extent available on the surface. This observed effect was much more pronounced in the receding contact angle measurements as shown in Figure 3.4.

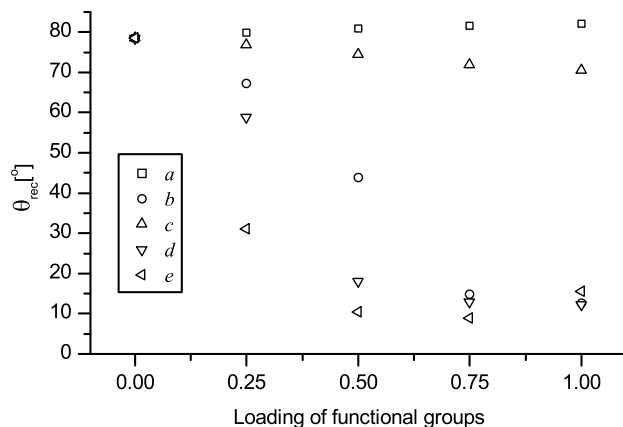


Figure 3.4. Receding contact angles of H₂O on the copolymer thin films as a function of the different functional groups, *a*: *tert*-butoxy, *b*: hydroxy, *c*: prop-2-ynyl, *d*: aromatic acid and *e*: aliphatic acid.

As with the advancing contact angle measurements the effect upon the receding contact angle with increased loading is limited on the less polar copolymers (*a* and *c* in Figure 3.4). The interesting tendency in the receding contact angle measurements is that the effects of the polar groups (*b*, *d* and *e* in Figure 3.4) have an earlier onset. Compared to the effects on the advancing contact angle, observed for copolymers with above 50 % loading, the effects are already seen in the receding contact angles of copolymers with 25 % loading. It appears that effects on the advancing contact angle are largely dependent on the majority component, whereas a minority component may influence the receding contact angle. As an effect of the earlier onset the copolymers reach constant values of the receding contact angle at lower copolymer compositions. This is interesting from an application point of view, where a lower loading might be sufficient in some cases and therefore the receding contact angle would be best suited for determination of the right material properties. In this case, it would be a selection between a copolymer with a composition of approximately 50 or 100 % functionality, having a considerable influence on the cost of the material. Unfortunately the polymer films were never tested for the application as an electroosmotic micropump since collaborators lost interest in the project.

3.5 Conclusions

A click approach based on PHS was developed and applied for preparation of a number of carboxylic acid functional (co)polymers. It was found that poly(4-hydroxy-*ran*-styrene) copolymers could be prepared by free radical copolymerization between styrene and 4-butoxystyrene. These could easily be deprotected and converted into the alkyne functional analogues for the postfunctionalization with CuAAC. The materials prepared here were used for determination of the influence of the pendant groups on the glass transition temperature but could easily have been used to examine other properties of interest like e.g. degradation temperatures by thermo gravimetric analysis. The film forming properties of the prepared (co)polymers were also tested and it was found that especially the random copolymers with styrene form well defined films on support. Here contact angle measurements and XPS were applied to test the accessibility of the carboxylic acids on the surface. It was found that steric hindrance and rigidity counteract effects from the high surface free energy of the carboxylic acid groups. In principle the approach could be applied for preparation of other polymer grafts. This has recently been corroborated in our group, where sulfonic acids and amines were coupled to the backbone.⁴⁸

4 Materials for Holographic Data Storage

4.1 Data Storage in Three Dimensions

With the increasing demand for higher data storage capacity and flexibility there is a need for development of new storage techniques as well as new materials. Presently used two dimensional techniques like harddrives and other disc media have limits as to how far storage capacity can be extended. In order to achieve sufficient storage capacities in the future one solution is to store data in three dimensions by volume holography. There is currently one commercial application of holographic data storage produced by the company InPhase Technologies. They produce a write once read many (WORM) storage system with a storage capacity of 300-1600 GB pr. storage medium.⁴⁹

In volume holography data is stored as optical interference patterns throughout a photosensitive material. This interference pattern is created by intersection of two laser beams, where one contains the information to be written and the other is a reference beam used to read out the written holograms afterwards. When the beams intersect they cause chemical or physical changes in the material resulting in a modulation in e.g. the refractive index or the density of the material. Additional holograms can then be recorded by angling of the sample and thereby the storage capacity can be increased. Presently, volume holography still faces some material challenges and thus continued development is still needed. The ideal material should have a high photosensitivity, high storage capacity, fast recording, nondestructive readout, dimensional stability, be prepared in millimeter thick samples and be of low cost.^{50,51} A photopolymer system,⁵²⁻⁵⁴ as outlined in Figure 4.1 fulfills many of these criteria.

In these systems a (macro)monomer is dissolved in an inert matrix together with a photoinitiator. Polymerization of the (macro)monomer can then take place through localized initiation by exposure to light. During the polymerization a concentration gradient is formed in the material as monomer diffuses to the bright areas, which causes a modulation of the refractive index and thereby a hologram is created. Traditionally monomers of low molecular weight have been used and that results in a substantial shrinkage upon polymerization as the polymer takes up less volume than the monomers. This writing induced shrinkage causes distortion of the holograms and in practice makes readout impossible. This problem becomes

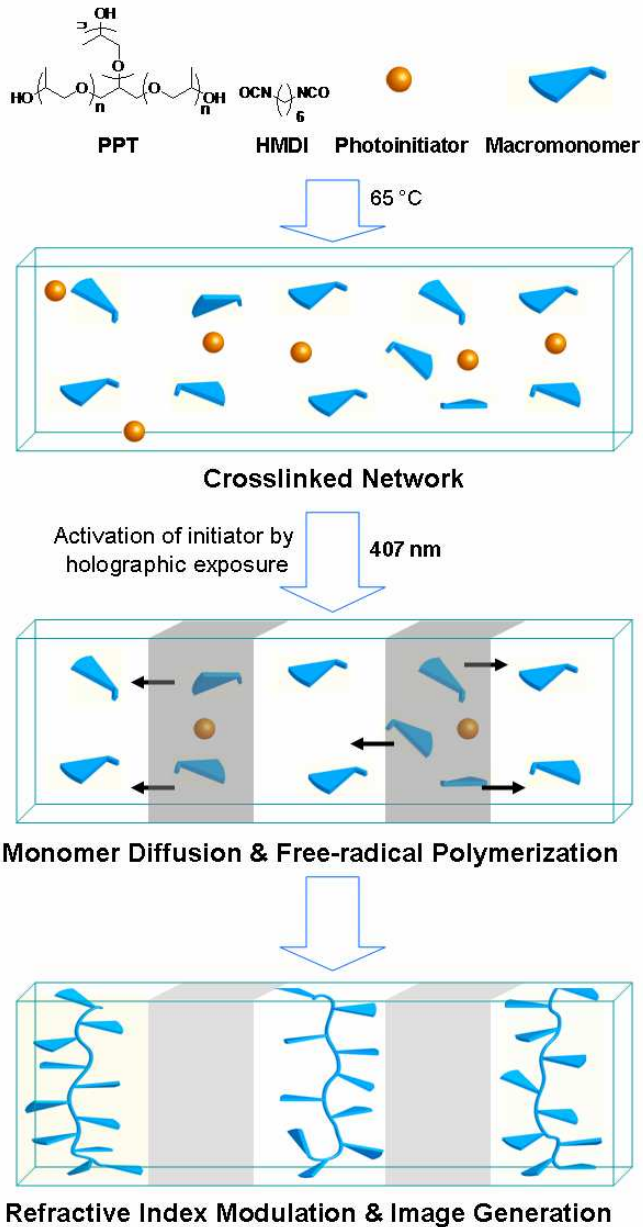


Figure 4.1. Schematic of the refractive index modulation in a matrix by photopolymerization of dendronized macromonomers.⁵⁵

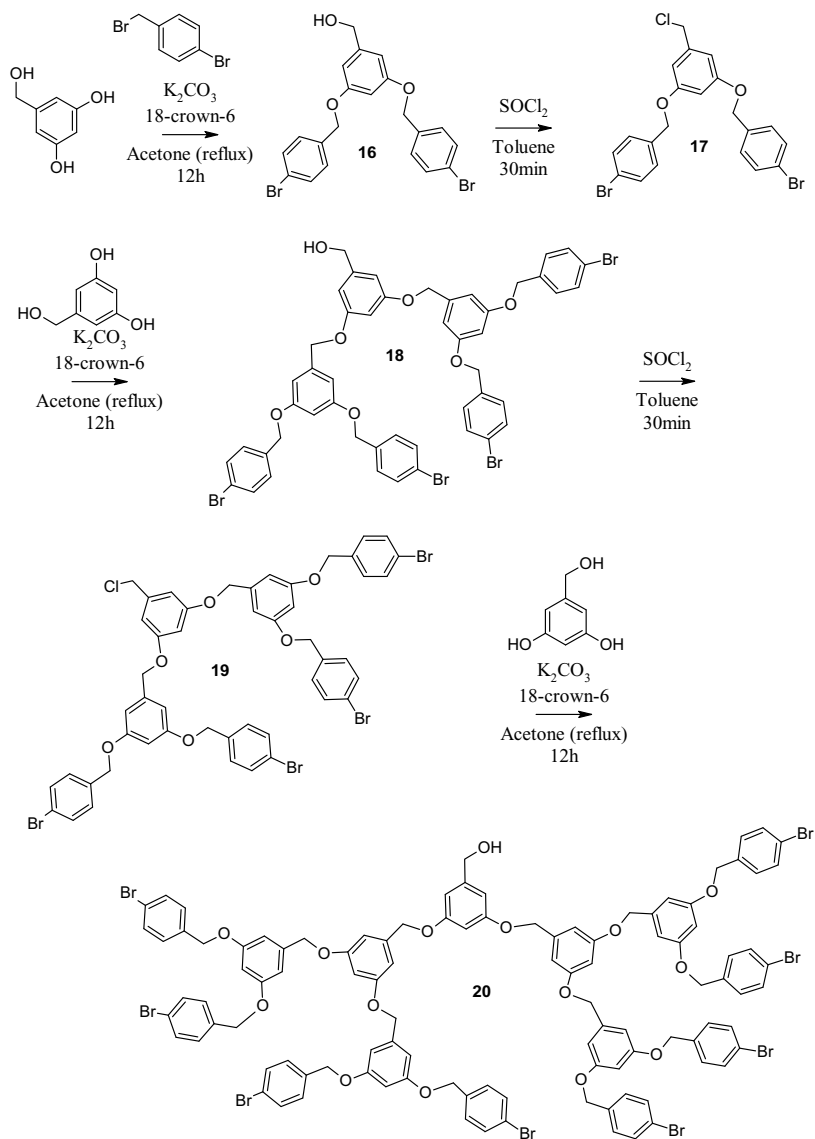
even more important with increasing film thickness and therefore a significant reduction in volume shrinkage is of great importance for the exploitation of the full potential of holographic data storage by the use of photopolymer systems. New monomers that have low viscosity (good diffusivity), high refractive index (high storage capacity) and low shrinkage upon polymerization therefore needs to be developed. This research project resulted in one publication⁵⁵ that can be found in appendices C and D.

4.2 Benzyl Ether Dendronized Macromonomers in Volume Holography

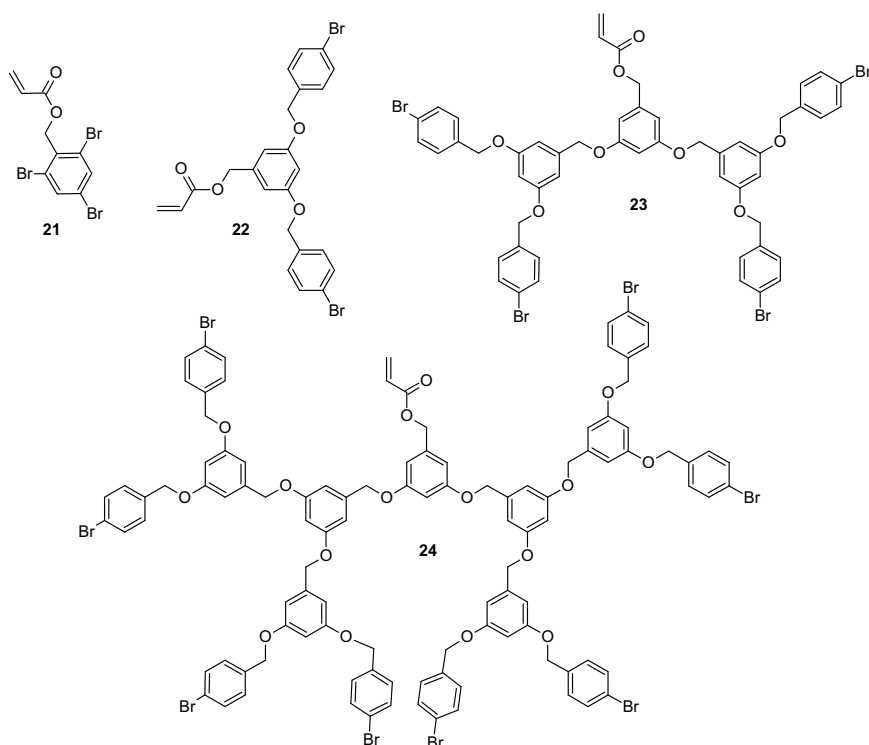
In order to prepare monomers with lower volume shrinkage several solutions could be imagined. Monomers that polymerize by ring opening have been shown to have lower volume shrinkage.⁵⁶ For applications in photopolymer systems it is necessary for the polymerization to occur through a free radical mechanism to enable photoinitiation. As an alternative to highly complex synthetic schemes towards cyclic monomers it was decided to investigate the application of dendritic macromonomers in a photopolymer system. The advantage of a dendritic macromonomer is that it contains a number of branches to a functional core that can easily be converted into a polymerizable acrylate. Thereby the concentration of polymerizable group is low in the material, resulting in an inherent low volume shrinkage by mass. The branches can be of high refractive index, whereby the sensitivity and storage capacity is kept high. Finally the known low viscosities of dendrimers⁵⁷ makes diffusion occur easily, maintaining high mobility. Dendritic macromonomers based on benzyl ethers (Fréchet type) were prepared by a convergent approach,⁵⁸ by minor changes of the method published by Wooley et al.,⁵⁹ as shown in Scheme 4.1.

Repeated Williamson ether syntheses and chlorination of the hydroxyl group in the core using thionyl chloride, instead of bromination with triphenylphosphine and CBr_4 , were performed to obtain the first to the third generation dendron. Subsequent ester syntheses of the hydroxyl functional dendrons with acryloyl chloride provided the respective acrylates **21**, **22**, **23**, and **24** shown in Scheme 4.2.

The matrix for the photopolymer system was prepared through the orthogonal reaction of polypropylene-triol (PPT, $M_n=1000 \text{ g/mol}$) and hexamethylenediisocyanate (HMDI) at moderate temperature (henceforth referred to as the polypropylene matrix). These reaction conditions are compatible with the acrylate monomer and the photoinitiator (Lucirine) that can be suspended in the mixture prior to the network formation, as indicated in Figure 4.1. Thereby thick films of the crosslinked network can be prepared. The network is optically transparent and thus well suited for holographic applications, where the transparency is of utmost importance in order to obtain a high sensitivity system. The crosslinked matrix



Scheme 4.1. Convergent synthesis of the 1st to the 3rd generation Fréchet dendrons.



Scheme 4.2. Prepared dendritic acrylates of increasing generations from **21** to **24**.

is then exposed to the laser light and the interference pattern is written into the film. In the exposed areas the laser light initiates polymerization and additional monomer diffuses to the activated areas due to the concentration gradient, as indicated in step 2 in Figure 4.1. When the polymerization has been completed the diffusion of monomer throughout the polymerization has created a higher concentration of the polymerized monomer in the bright areas. If the monomer has a higher refractive index compared to the matrix a modulation of the refractive index is attained and the interference pattern can be read out at a later stage by exposure of the sample to only the reference beam.

The high sensitivity of this system allows at least 60 holograms to be individually recorded in each volume of the holographic disc with a high angular selectivity as shown in Figure 4.2.

Here the signal is read out after angular rotation of the disc, containing the 60 holograms, and thus the diffraction efficiency of each hologram can be determined. It can then be used to calculate the dynamic range, illustrating the response of the system throughout the matrix.⁶⁰ This can also be regarded as an expression of

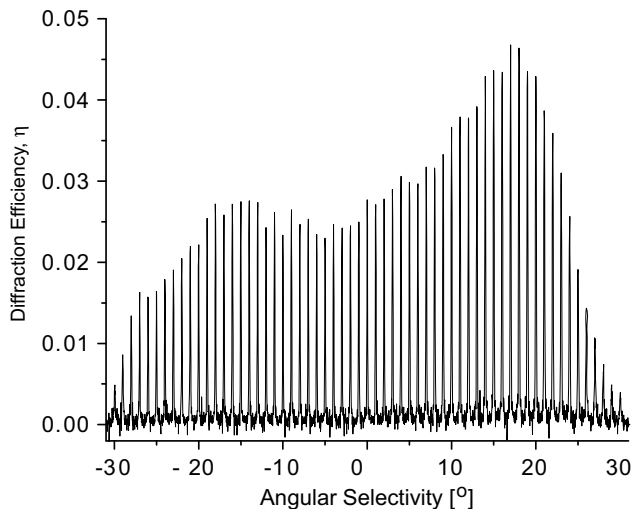


Figure 4.2. Angular selectivity curves of the 60 holograms recorded in 0.5 mm thick holographic disc containing the second generation dendritic macromonomer **23**.

the storage capacity of the system. The dynamic range (M# number) is defined as shown in equation 4.1, where η_i is the diffraction efficiency of the i^{th} hologram.

$$M\# = \sum_{i=1}^n \sqrt{\eta_i} \quad (4.1)$$

The results for each of the dendronized macromonomers are shown in Table 4.1.

Table 4.1. Holographic data from the different systems.

Monomer	M#	Sensitivity [cm/mJ]	Volume Shrinkage [%]	RI
21 [†]	8	0.20	0.23	1.614
22 [†]	8	0.37	0.10	1.616
23 [†]	10	0.46	0.04	1.647
24 [‡]	6	0.05	0.03	1.663

[†] Polypropylene matrix

[‡] Polycarbonate matrix

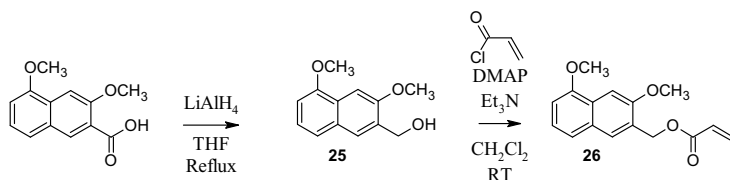
The change in volume shrinkage as an effect of the different monomers was evaluated in accordance with the method of Dhar and co-workers.⁶¹ As can be

seen from Table 4.1 there is a clear tendency for a reduction in the volume shrinkage from the unbranched acrylate to the third generation dendronized macromonomer. The 0.23% volume shrinkage obtained from the unbranched reference compound corresponds to shrinkages evaluated for other acrylates.⁵⁶ A reduction of the shrinkage to 0.04 or 0.03% is a substantial decrease compared to known systems. In addition to this, the branched structure of the dendron also has a beneficial effect upon the storage capacity, through an increase in the refractive index with increasing generations of the dendron. The best performance was found with the second generation dendron that is well soluble in the matrix and has the highest sensitivity. The third generation gave very poor results in the applied matrix as the monomer is poorly soluble. It was decided to prepare a different matrix that could dissolve the third generation monomer. The new matrix was prepared from a blend of polycarbonatediol ($M_n = 800$) and trimethylolpropane (9:1) as well as the HMDI and the photoinitiator Lucirine (henceforth referred to as the polycarbonate matrix). In the polycarbonate matrix the third generation dendronized monomer gave a lower shrinkage with only 0.03% as shown in Table 4.1. However, both a low sensitivity and a low storage capacity was found compared to the other dendronized monomers. A test of the other macromonomers in the polycarbonate matrix showed that this was an effect of this matrix, which apparently did not have as good mobility as the polypropylene matrix. Through these experiments it has been demonstrated that dendronized macromonomers have a beneficial effect on the volume shrinkage in a photopolymer system. In addition to this, introduction of high refractive index end groups of the dendron has been shown to be one approach to an increased storage capacity. The optimal ratio between branching and core functionality was found to be the second generation dendronized macromonomer, **23**. It had a higher storage capacity, lower shrinkage and higher sensitivity compared to all the other monomers investigated in this series. An increased storage capacity is very important for the commercial application of photopolymer systems. The volume shrinkage in the dendronized benzyl ether system was found to be negligible, which allows for good readout properties and the high sensitivity allows for fast data recording.

4.3 Increased Storage Capacity

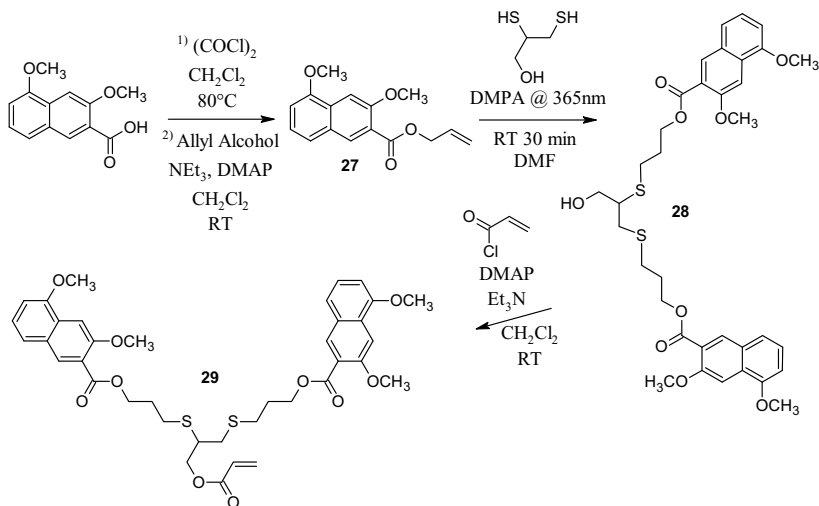
In an effort to improve the photopolymer system based on the dendronized macromonomers, focus was put upon development of new monomers with a higher storage capacity compared to the benzyl ether system. The storage capacity is directly dependent on the modulation of the refractive index upon writing, thus a monomer with a higher refractive index could give a higher contrast to the background resulting in a better diffraction efficiency. Several compounds are known to have a high refractive index, e.g. brominated compounds like the benzyl ethers from above, carbazoles and naphthalenes^{62,63} and all of these could fulfill the re-

quirements. In view of the recent developments within thiol-ene chemistry (see Chapter 2), it was decided to use a thiol-ene reaction for the construction of a new dendronized macromonomer with a naphthalene end group. Another advantage of the thiol-ene approach is that it introduces sulfurs in the branching structure, which also increases the overall refractive index. The simplest naphthalene monomer was prepared as shown in Scheme 4.3.



Scheme 4.3. Preparation of the 0th generation naphthalene acrylate, **26**.

Commercially available 3,5-dimethoxy-2-naphthoic acid was reduced using lithium aluminum hydride providing the alcohol, **25**. It was then converted to the acrylate, **26**, by reaction with acryloyl chloride under standard conditions employing DMAP as catalyst and triethylamine as base. Thereby the 0th generation monomer was prepared. The branched naphthalenes were prepared through a convergent approach by consecutive thiol-ene and ester syntheses as shown in Scheme 4.4.



Scheme 4.4. Preparation of the 1st generation dendronized macromonomer, **29**.

Initially the alkene starting material was prepared from 3,5-dimethoxy-2-naphthoic acid via the acid chloride by an oxalyl chloride activation followed by reaction

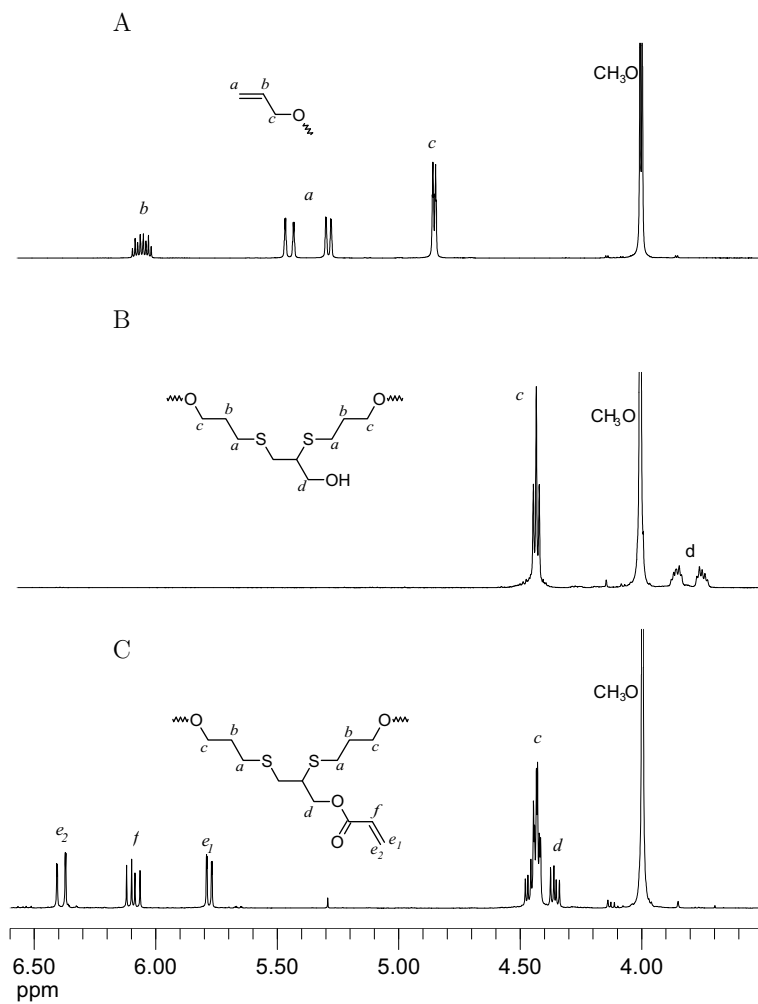
with allyl alcohol directly after preparation providing the allylic ester, **27**. The first generation dendron was prepared from **27** by UV initiation with 2,2-dimethoxy-2-phenylacetophenone (DMPA @ 365 nm) in the presence of 2,3-dimercapto-1-propanol. A minor excess of **27** gave the fully functionalized dendron, **28**, in 76% yield. An unidentified byproduct originating from **27** by degradation of the naphthalene structure was observed in addition to the mercapto alcohol resulting from mono reacted 2,3-dimercapto-1-propanol. Interestingly, NMR showed that the alkenes in the byproducts were intact after irradiation. Thus, no cyclization products were identified as was otherwise observed in the grafting of polybutadiene by thiol-ene chemistry.^{26,34} Both byproducts result in a reduction of the yield. Since the reaction in essence is a radical reaction and it is performed with thiol as the minority component the formation of byproducts was not unexpected, but the amount was considered acceptable. **28** was then converted to the equivalent acrylate, **29**, using a similar approach. The preparation of the first generation dendron, **29**, is easily illustrated by very distinct changes in the ¹H-NMR spectra in the region from 3.5 to 6.5 ppm, as shown in Figure 4.3.

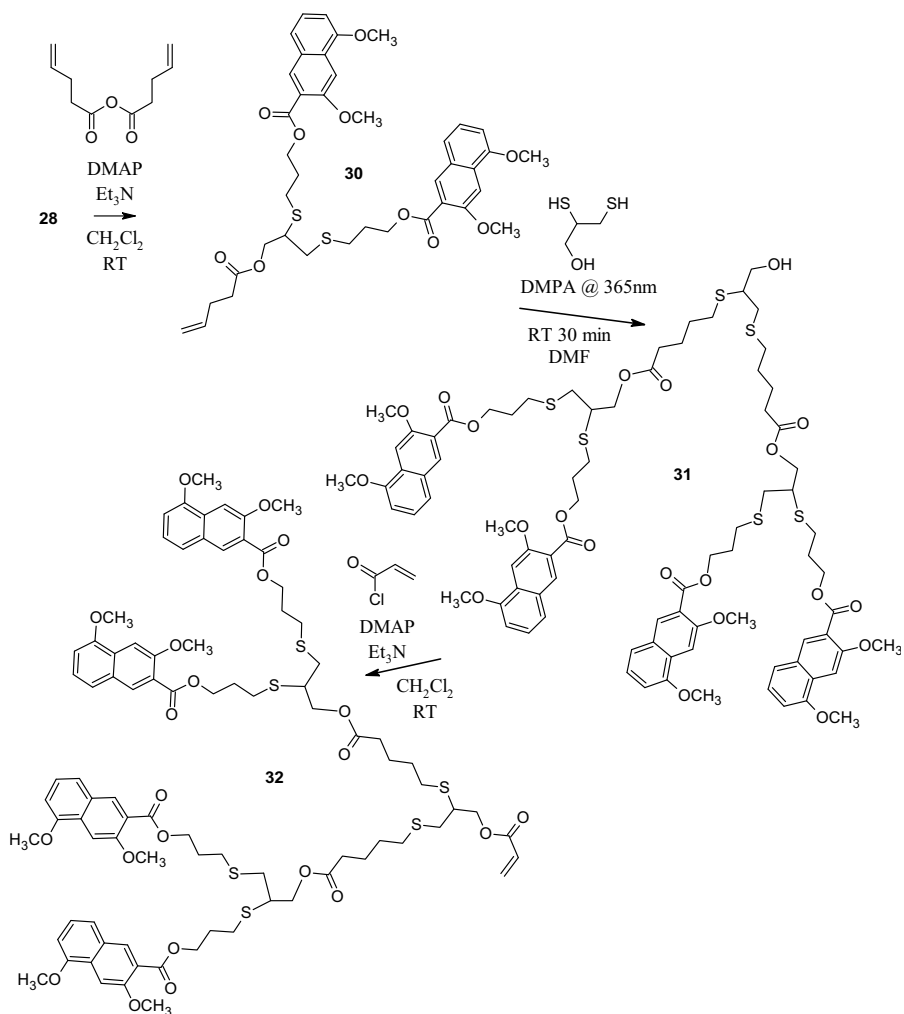
Initially **27** is identified by the alkene (*a*, *b* and *c* in Figure 4.3, A), and the upfield shift of these protons (*a*, *b* off scale) after the thiol-ene reaction is very indicative of the product, **28** (Figure 4.3, B). By conversion of the alcohol to the acrylate the diastereotopic protons (*d* in Figure 4.3, B and C) shift downfield from 3.8 ppm in **28** to overlap with the triplet at 4.5 ppm in **29** and the acrylic protons appear (*e*, *f* in Figure 4.3, C). Similar spectroscopic changes were observed in the synthesis of the second generation naphthalene, **31**, and the equivalent acrylate, **32**.

The second generation dendronized macromonomer was prepared from **28** in three steps. First an esterification of **28** with 4-pentenoic anhydride, DMAP catalysis and triethyl amine provided the dendritic alkene **30**, as shown in Scheme 4.5.

The subsequent thiol-ene reaction of **30** with 2,3-dimercapto-1-propanol yielded the second generation dendritic alcohol, **31**, in only 47%. Optimization of the reaction was attempted; however, it was not possible to obtain higher yields. This was attributed to the earlier mentioned byproduct formation. Since the dendron is prepared by a convergent approach a minor byproduct formation gives a significant reduction in the yield of the product. Finally **31** was converted to its acrylate, **32**.

The holographic performance of the prepared 0th, 1st and 2nd generation dendronized macromonomers was then intended to be investigated in the photopolymer system with the polypropylene matrix that was used for the benzyl ether system. Unfortunately the laser in the holographic setup broke down directly before these measurements could be conducted. The 1st generation dendronized monomer (**29**) was tested before the incident and it was found to have a M# number of 11 and a volume shrinkage of only 0.01%. These preliminary results clearly show that the approach with the naphthalenes on the periphery was ben-



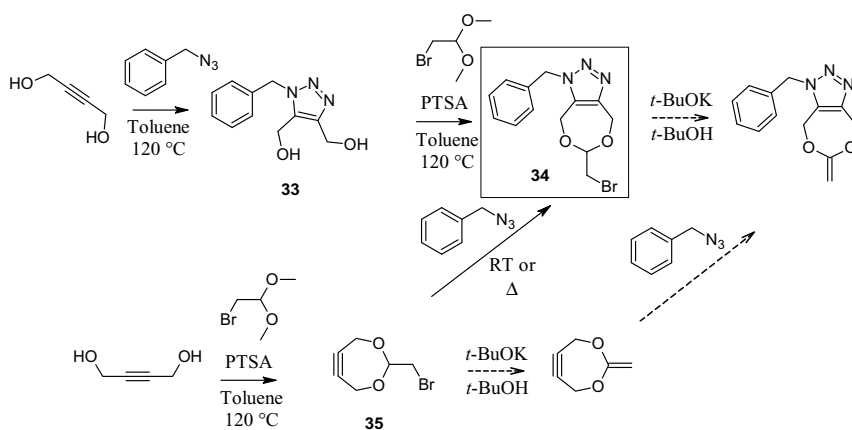


Scheme 4.5. Preparation of the 2nd generation dendronized macromonomer, **32**.

eficial for the properties as a photopolymer system. Data from the remaining 0th (**26**) and 2nd generation monomer (**32**) is anticipated in the near future. It will be very interesting to see whether the increased loading of the 2nd generation macromonomer will show the corresponding increase in performance as observed for the benzyl ether system.

4.4 Cyclic Monomers

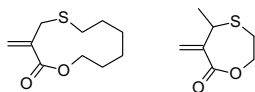
Another approach towards low shrinkage monomers for photopolymer systems is cyclic monomers that perform ring opening polymerization under free radical conditions. Some monomers of this type are known.⁵⁶ However, preparation of new cyclic monomers that perform likewise can be difficult and may also give only partial ring opening after even minor changes to a monomer that is known to perform ring opening.⁶⁴ 5,6-Benzo-2-methylene-1,3-dioxepane (BMDO) is one of the cyclic monomers that has been proven to undergo exclusively ring opening polymerization under free radical conditions.^{65,66} Inspired by this a preparation of an alkyne functional analogue as shown in Scheme 4.6 was undertaken.



Scheme 4.6. Synthesis strategy for a novel seven membered cyclic monomer based on BMDO, where the stippled arrows signify steps that were not carried out.

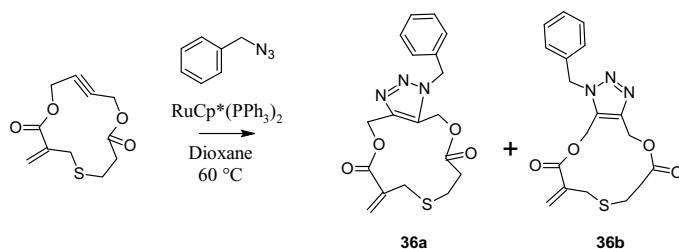
Based on the results on the copper free cycloaddition promoted by ring strain in an eight membered cyclic alkyne that was presented by Bertozzi and coworkers²⁴ it was expected that ring strain would have a similar effect in this seven membered system. In addition to this, the alkyne intermediate would facilitate preparation of a selection of materials with different refractive index. However, it was found that the seven membered ring did not have sufficient ring strain to promote a cycloaddition and that even prolonged reaction time at elevated temperature was insufficient to provide the product in reasonable yields. Due to these unsatisfactory results the project was stopped at this point.

In parallel, a project on cyclic acrylates containing more than 10 ring atoms based on the cyclic monomers developed by Evans et al.⁶⁷ has been performed in the research group of Professor Hawker. Evans et al. found that these β -stabilized lactone acrylates, shown in Scheme 4.7, exclusively gave ring opening under free radical conditions.



Scheme 4.7. β -Stabilized lactone acrylates prepared by Evans et al. that exclusively performs ring opening polymerization under free radical conditions.

Application of their strategy on larger sized rings provided ring opening polymerization under free radical conditions, as expected. However, monomers of this type were found to have a relatively low storage capacity in the holographic photopolymer system. One way of improving this could be to increase the refractive index of the monomers. In light of the results from the strained seven membered rings it was speculated that the less strained rings would be easier to functionalize through a cycloaddition before polymerization and that the refractive index of the monomers thus could be increased. A 13 membered lactone acrylate monomer containing an internal alkyne was reacted with benzyl azide under ruthenium catalysis, as shown in Scheme 4.8, resulting in the formation of a mixture of the two regioisomers (**36a** and **36b**).

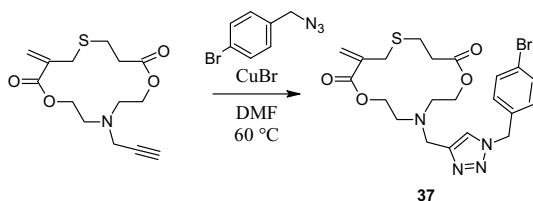


Scheme 4.8. The RuAAC of an internal alkyne with benzyl azide.

Ruthenium catalysis of the cycloaddition of alkynes and azides (RuAAC) has recently been introduced as an alternative to the CuAAC. In the RuAAC on terminal alkynes the 1,5 regioisomer can be formed selectively^{68–70} as opposed to the 1,4-regioisomer with the CuAAC. Another advantage of the RuAAC is that it can be performed with internal alkynes as well and thus allows for lower reaction temperatures and shorter reaction times compared to the purely thermal cycloaddition. Depending on the reactants and ligands, RuAACs on internal alkynes usually result in mixtures of regioisomers.⁷¹ Even though the regioselectivity is low for the internal alkynes, a reduced temperature and reaction time is still gained. The regioisomers can normally be separated by column chromatography, though that was not possible in this case. The two regioisomers were expected to perform similarly under polymerization, and therefore no additional efforts were invested in the separation.

Likewise a 14 membered lactone acrylate containing an external alkyne was

reacted with 4-bromobenzyl azide under copper catalysis providing the triazole, **37**, as shown in Scheme 4.9.



Scheme 4.9. CuAAC of an external alkyne with 4-bromobenzyl azide.

The CuAAC on the external alkyne provides a much cleaner reaction and the yield was considerably higher (98% for the terminal alkyne versus 60% for the internal alkyne). This is of course not a direct comparison between the ruthenium and copper catalyzed cycloadditions, but rather that of a disubstituted alkyne and a terminal alkyne. However, it illustrates how the internal alkynes in some cases are less reactive compared to the terminal alkynes. Which alkyne would be best suited for the preparation of other monomers with even higher refractive index, depends largely on the holographic data that could be obtained with these monomers. The holographic tests were performed in the polypropylene matrix as described for the benzyl ethers. Initially the diffraction efficiency of **37** was compared to that of the 7 and 11 membered cyclic monomers prepared by Evans et al.,⁶⁷ as shown in Scheme 4.4.

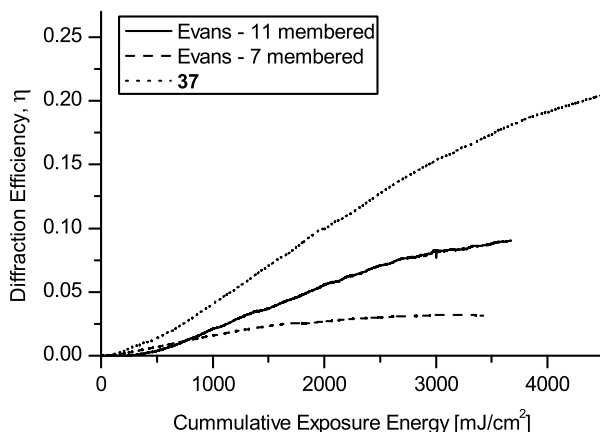


Figure 4.4. The diffraction efficiency with extended exposure to light in the polypropylene matrix.

In these experiments the diffraction efficiency of the monomers were measured with respect to exposure time. Here it was found that **37** had a substantially higher diffraction efficiency compared to the other cyclic monomers. This clearly illustrates that the introduction of the triazole and the brominated phenyl resulted in an improvement of the holographic properties of the system. Unfortunately, the weakness of cyclic monomers that perform ringopening polymerization under free radical conditions, is that this type of monomers usually results in a low conversion. This is also the case for these systems, where a conversion of less than 10% was found. This is a problem, since the sensitivity of the system is considerably reduced and thereby it is not possible to write the required high number of holograms in each volume of the holographic disc. Due to the low conversion it has not been possible to calculate a $M\#$ number for this system.

4.5 Conclusions

It has been shown that dendronized macromonomers have a beneficial effect upon the volume shrinkage of photopolymer systems in volume holography. The properties of dendritic molecules have been exploited, especially the low viscosity relative to the molecular weight of the dendronized macromonomers has facilitated the diffusion of the large molecules, resulting in high sensitivity materials. Exploitation of the substitutions on the periphery of the dendron has been illustrated with the benzyl ethers showing an increased $M\#$ number from the first to the second generation. Preparation of the naphthalene substituted dendrons with higher refractive index clearly showed that the dendritic structure can be exploited to further improve the performance of the holographic system. Preparation of a modular monomer based on BMDO that would undergo free radical ring opening polymerization was less successful. However, it supplied the inspiration to try the similar approach on the sulfur stabilized acrylic lactones. The holographic data from these larger ring sized monomers were unfortunately not as good as anticipated. The prepared monomers were found to have improved properties due to the extension of the ring system. However, they did not polymerize to a sufficiently high conversion and therefore were not suited for application in new photopolymer systems.

5 Functional Conductive Polymers

During the past few decades conductive polymers have been studied extensively and many new applications have been found.⁷² Based on the experience from functionalization of polystyrenes with CuAAC (Chapter 2) it was expected that a click approach for functionalization of a conductive polymer could result in novel functional materials. Especially the preparation of new sensor materials was the long term objective for this project and conjugated polymers have found many applications within this area.⁷³ Many challenges have been met for development of new conductive polymer materials, though there are still some incompatibilities with large biomolecules and specific molecules may be incompatible with the polymerization conditions normally applied. This motivates the use of a postpolymerization strategy that would enable coupling of delicate compounds. The idea was that coupling of specific receptors to a conductive polymer backbone would allow conversion of an ionic response into an electrochemical signal that could be exploited for construction of a sensing device as sketched in Figure 5.1.

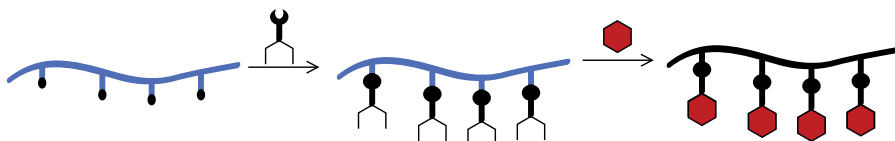


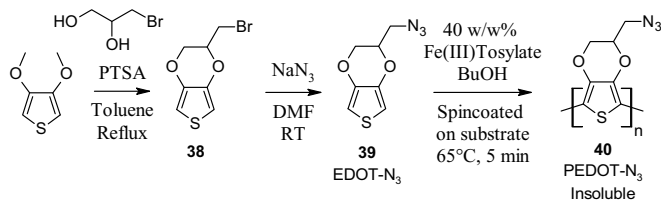
Figure 5.1. Conductive polymer with functional site that can be reacted selectively with a receptor, which would result in a specific response from the polymer backbone upon binding of an analyte.

For this approach to work it is central that the conductive polymer would be influenced by small changes in the environment of the backbone. That the receptor is distanced from the backbone reduces the influence on the conductivity as structural changes cannot directly change the length of conjugation. However, there are examples of receptors covalently bound to conductive polymers that are showing good responses without influencing the length of conjugation e.g. carboxylic acids,⁷⁴ crown ethers,^{75–77} oligooxyethylenes⁷⁸ as well as blending of receptors into conductive polymers.⁷⁹ Poly(3,4-ethylenedioxythiophene) (PEDOT) was chosen for the project due to its good properties of high electrical conductivity and high stability in ambient and aqueous environments.⁸⁰ During polymerization the polymer becomes insoluble, and further functionalization becomes difficult. Combination of the conductive properties of PEDOT and the advantages of modularity,

high selectivity, and high yields of click chemistry would permit preparation of new PEDOTs for many different applications. Both pre- and postfunctionalization have been studied by others. With regards to biological active molecules the most successful methods so far is physical absorption after polymerization or entrapment during polymerization.⁸¹ Covalent postfunctionalization has been achieved through peptide bonding.^{82,83} The click approach is a good alternative that gives a controlled functionalization without protective groups through high selectivity. This research project resulted in one publication⁸⁴ that can be found in appendix E.

5.1 Monomer, Polymerization and Characterization

To functionalize PEDOT through a CuAAC approach a new monomer had to be synthesized containing either the alkyne or azide group. However, given the oxidative polymerization of 3,4-ethylenedioxythiophene, it was anticipated that a deprotection step could be avoided by preparation of the azide. Therefore it was prepared instead of the alkyne, as shown in Scheme 5.1. In principle the functionalities could be reversed if a certain demand for the alkyne functional polymer would arise.



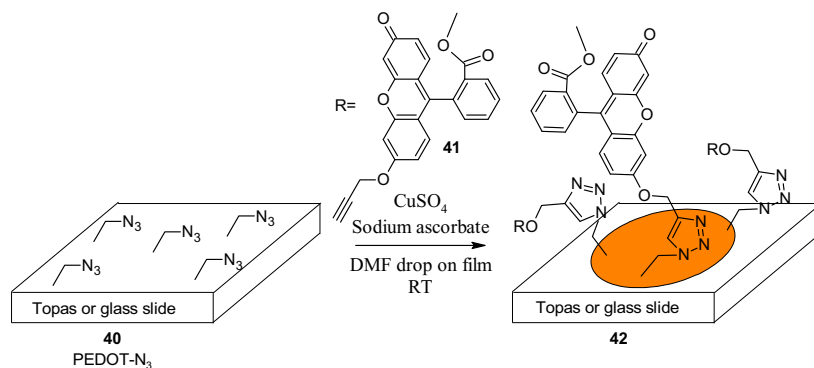
Scheme 5.1. EDOT-N₃ synthesis and polymerization.

A transesterification using 3-bromo-1,2-propanediol provided the bromine functional monomer, **38**. This was converted to the azide, EDOT-N₃ (**39**) by a substitution with NaN₃. The reactivity of the monomer was checked in a model reaction using standard CuAAC conditions where the triazole product was formed.

PEDOT can be prepared by a chemically oxidative polymerization performed through spin coating of a thin film from a butanol solution of EDOT, Fe(III)tosylate and pyridine.⁸⁵ The thin film is then heated to 65 °C for 5 minutes during this period the polymerization takes place. In principle this polymerization can take place on any surface that is stable at 65 °C for 5 minutes, which is a considerable advantage over standard electrochemical oxidative polymerizations that need to take place on a conductive surface. This enables the preparation of all polymer microfluidic systems giving access to a number of possible future applications. The polymerization of **39** was attempted applying the equivalent condi-

tions; however, no polymer was formed. Omission of the pyridine inhibitor from the polymerization mixture provided the polymer directly, as indicated in Scheme 5.1. Pyridine is a necessary inhibitor for the preparation of ordinary PEDOT, which otherwise forms irregular films, though apparently the functional monomer polymerizes slower and therefore the inhibition is not required. As the polymer is insoluble, characterization can only be performed using spectroscopy techniques such as FT-IR, UV-vis or XPS. Attenuated total reflection (ATR) FT-IR gave no signals from the conductive polymer, which is attributed to the very thin films. By transmission FT-IR of a thin film on a polymer substrate it was possible to obtain a vague signal at 2100 cm^{-1} corresponding to the azide, however this absorption was not strong enough to be used for conclusive identification. XPS showed the presence of azides on the surface and the right ratio of carbon, oxygen and nitrogen confirmed the structure of the polymer. The pristine PEDOT- N_3 was found to be moderately conductive, with a conductivity of 60 S/cm . A similar approach was developed simultaneously by Bu et al.,⁸⁶ who prepared the EDOT- N_3 from the chlorinated analogue and applied it in electro oxidative polymerization on platinum substrates.

To investigate the reactivity of the azides on the surface an alkyne fluorophore based on fluorescein (**41**) was synthesized⁸⁴ and reacted with **40** as shown in Scheme 5.2.



Scheme 5.2. CuAAC of the fluorophore **41** with the thin PEDOT- N_3 film on the substrate. The reaction taking place in a drop of DMF with a catalyst system of CuSO_4 /sodium ascorbate.

Fluorescence microscopy clearly showed a fluorescent positive sample, confirming the reaction. Likewise **42** was also investigated by UV-vis spectroscopy, where a distinct signal from the fluorophore was identified. Optimization of the reaction time and catalyst concentration could then be performed using UV-vis spectroscopy as shown in Figure 5.2 for the reaction time.

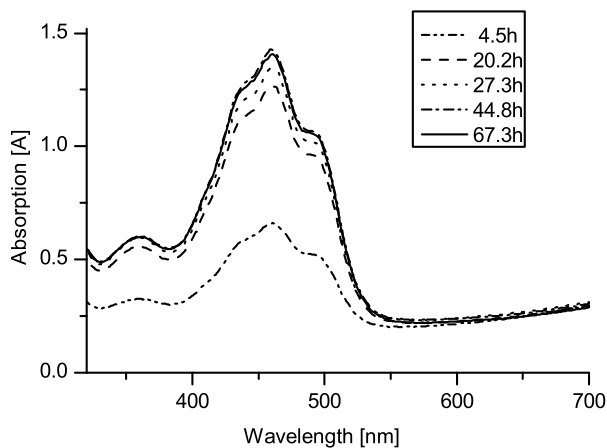


Figure 5.2. Absorption as a function of reaction time investigated by UV-vis spectroscopy for samples of **42**.

Most of the reaction proceeds during the first 20 hours, whereafter the rate of the reaction is reduced. The reaction is expected to be limited by diffusion, since mechanical stirring is not possible on the substrate. In addition to this, steric effects would also be expected to have an increasing influence at a higher degree of reaction. Similarly, profilometry measurements on **42** the same reaction times showed a substantial increase in the thickness of the samples with increasing reaction time as shown in Figure 5.3.

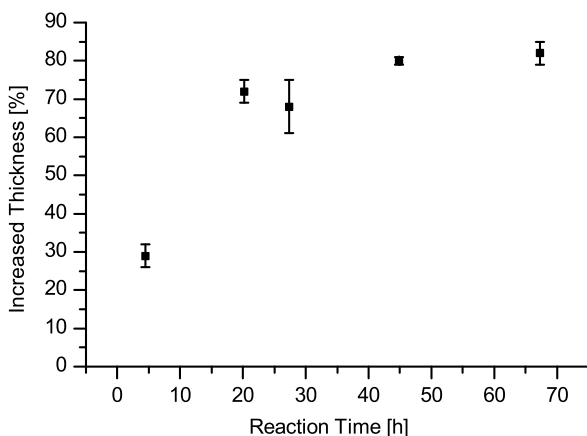


Figure 5.3. Increased thickness as a function of reaction time monitored by profilometry for samples of **42**.

The thicknesses were measured several days after the reactions took place and a blank reference sample, exposed to the reaction mixture without copper, showed no increase in thickness. These profilometry measurements clearly corroborate that the reaction continues even after long reaction times. However, the majority of the reaction has clearly been conducted within the first 20 hours. The increase in thickness naturally influences the conductivity that was found to be 0.2-0.3 S/cm after the reaction. This is partly a result of the exposure to sodium ascorbate in the reaction mixture, which reduces the film to a low conductive state, and partly a result of the large increase in volume, which directly lowers the conductivity. However, reoxidation with an aqueous solution of Fe(III)tosylate restored the conductivity to approximately 15 S/cm. Considering the increase in thickness of approximately 75 %, and the reduced conductivity as a result of the volume expansion, the total decrease in conductivity was found acceptable.

Copolymerization of EDOT-N₃ and EDOT is possible by simple mixing of the two feed mixtures. As earlier mentioned it was observed that EDOT-N₃ polymerizes only without pyridine. That is not the case for EDOT, where pyridine inhibition is required in order to control the polymerization, thus an amount of pyridine relative to EDOT is necessary in the copolymerization mixture in order to obtain proper films. The obtained copolymers show different thicknesses, though whether this is an effect of the different polymerization rates or some other effect has not been established. The copolymers show similar reactivity compared to the homopolymers and can be functionalized under equivalent conditions. The conductivity of PEDOT-N₃ reacted with the fluorescein alkyne was investigated as a function of the copolymer ratio as shown in Figure 5.4.

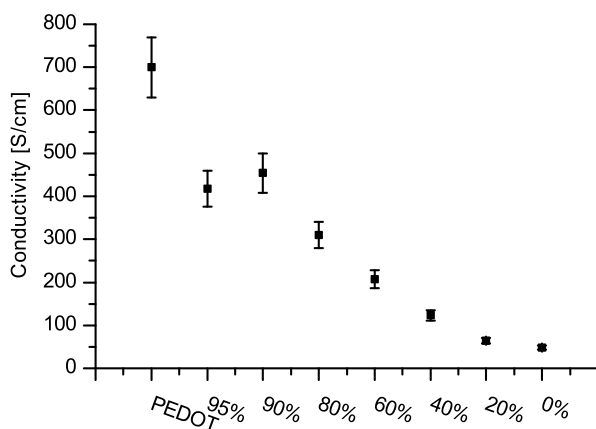


Figure 5.4. Conductivity of the functionalized copolymers relative to the content of EDOT, where 0 % corresponds to **42**.

The conductivity of the copolymers is clearly decreasing with an increasing loading of the functionalized group. This can be exploited for the preparation of films with a certain loading while still retaining a high conductivity. Depending on the eventual application a certain loading can be selected by variation of the feed ratios. An alternative approach to an increased conductivity is to prepare an ordinary PEDOT and subsequently add a layer of PEDOT-N₃. Thereby a high conductivity is obtained while the surface can still be functionalized.

It is known from the literature that the CuAAC is very chemoselective and a number of different compounds could be reacted with the PEDOT-N₃ film. An overview of the different prepared reactants is given in Table 5.1 illustrating the potential of the system.

In this way a number of properties could be obtained e.g. a change in the surface free energy by introduction of either the fluorous hydrocarbon, **43**, or the MPEG, **45**. Contact angle measurements on these surfaces were performed and the results are shown in Figure 5.5.

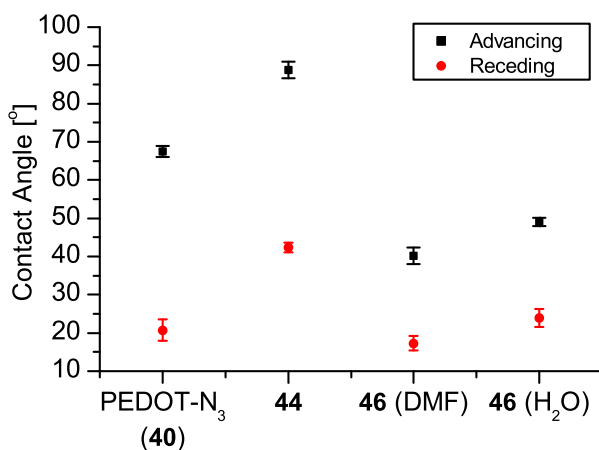
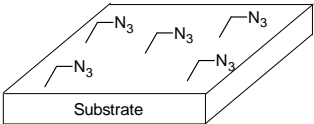
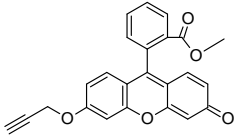
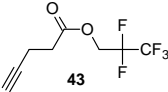
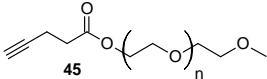
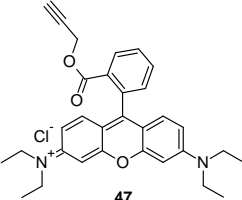
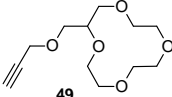
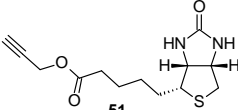
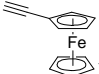


Figure 5.5. Contact angles of H₂O on the surface of PEDOT-N₃, the fluoro functionalized surface with **44** and the MPEGylated surface with **46** prepared in both H₂O and DMF.

Here it is obvious that there is an increase in the contact angle of H₂O on the surface with the fluorous hydrocarbon, **44**. This indicates the increase in hydrophobicity of the surface resulting from a decrease in the surface free energy as is a known effect from introduction of fluor on a surface.⁸⁷ Normally a larger effect would have been expected; however, the tosylate counter ions present in the film would affect the surface oppositely. Similarly introduction of the MPEG, **45**, on the surface results in an increase of the surface free energy, which is shown

Table 5.1. Prepared products on PEDOT-N₃.

Polymer	Reactant	Product & Notes
 <p data-bbox="284 984 361 1026">Substrate 40 PEDOT-N₃</p>	 <p data-bbox="718 615 739 633">41</p>	42
	 <p data-bbox="680 711 700 729">43</p>	44
	 <p data-bbox="628 802 649 820">45</p>	46 $M_n = 5000$ g/mol
	 <p data-bbox="692 1021 713 1039">47</p>	48
	 <p data-bbox="667 1135 687 1153">49</p>	50
	 <p data-bbox="687 1263 708 1281">51</p>	52
 <p data-bbox="713 1354 734 1372">53</p>	53	

† Commercially available

by a decrease in the contact angle of H₂O on the surface of **46**. Since MPEG is water soluble, the CuAAC was performed both in H₂O and DMF. Interestingly, there appears to be a higher advancing contact angle of H₂O on the surface when the reaction has been conducted in H₂O rather than DMF. Somehow the reaction proceeds less efficiently in H₂O, resulting in a less pronounced effect on the advancing contact angle. This could be an effect of several things, like better swelling of the surface by DMF than H₂O resulting in better access to the surface or alternatively an effect of a conformational change of **45** when it is dissolved in H₂O, which could result in a screening of the alkyne.

5.2 Microwave Chemistry

There seems to be a general trend that bulk film functionalization by CuAAC takes at least 20 hours or longer,^{21,86} sometimes days. For many applications a substantial reduction of this reaction time would make the method much more attractive. One approach to reach this possible requirement is to use microwave irradiation to heat sealed reaction vessels at high temperature and pressure resulting in reaction times on the order of minutes. There are many examples of applications of this methodology in solution;⁶ however, there appears to be no reports of the use of microwave irradiation for a CuAAC on a polymer film.

In an effort to reduce the reaction time the possibility of performing the CuAAC on polymer films under microwave irradiation in an ordinary microwave oven was investigated. A standard kitchen microwave oven was used for the experiments as this could facilitate the reaction of polymer films of different sizes and shapes in addition to being cost effective. The chemical oxidative polymerization of EDOT-N₃ assists the use of different substrates and in the experiments conducted here a commercially available copolymer of ethylene and norbornene (Topas®) was used as substrate. Any solid substrate tolerant to a heating to 60 °C for 5 minutes could in principle be applied. As mentioned this facilitates preparation of all polymer devices for a number of applications. Initial experiments with microwave heating showed that the conductive polymer became very hot in the microwave where irradiation for a few seconds resulted in cracking and destruction of the thin polymer films. This is in accordance with Lakshimi et al.,⁸⁸ who showed that conductive polymers absorb an amount of energy from microwave irradiation resulting in heating of the polymer related to the conductivity, dielectric constant, dielectric loss and absorption coefficients of the polymers. Polymers with lower conductivity generally were shown to absorb less energy than more conductive polymers. Similarly, poly(aniline) has been used for welding of PMMA plates together with microwave irradiation.⁸⁹ The prepared PEDOT-N₃ film is in its conductive state after polymerization and would therefore absorb a high amount of energy in the microwave oven. By chemical reduction with sodium ascorbate the polymer conductivity was reduced from 60 S/cm to 0.2 S/cm. This was sufficient

for the film to remain intact under microwave irradiation for several minutes. A step by step method was developed, as outlined in Scheme 5.6.

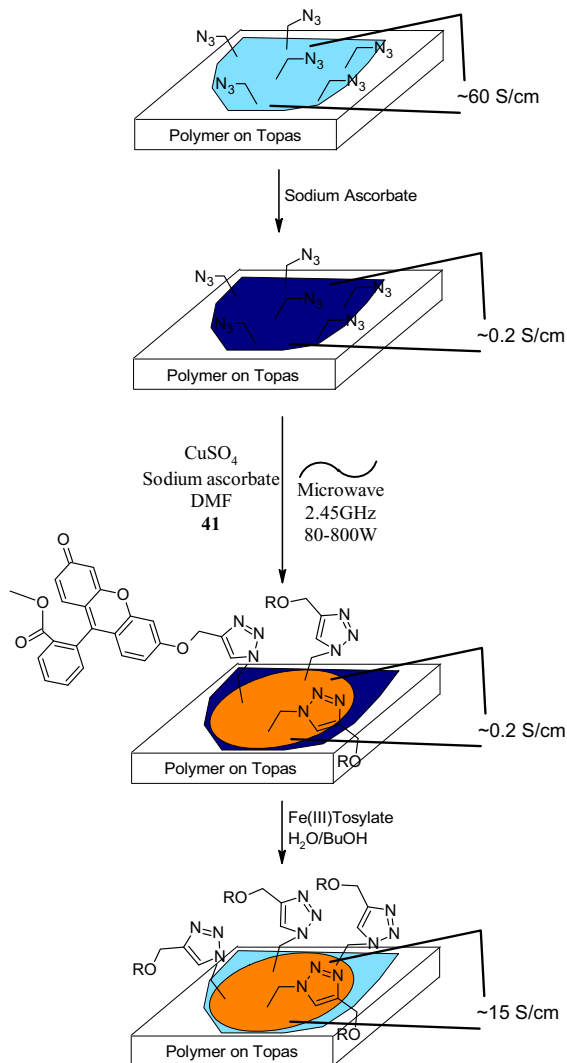


Figure 5.6. Overview of the step by step method for microwave activation of the CuAAC on PEDOT-N₃.

Before the reaction the samples were reduced with a solution of sodium ascorbate. Thereafter the reaction was conducted, as at room temperature, with the

additional microwave irradiation. The samples were rinsed and reoxidated with an aqueous solution of Fe(III)tosylate providing the conductive functionalized product. Investigation of the effects of power input and reaction time was performed with **41** and the catalytic system of CuSO₄/sodium ascorbate. The extent of the reaction was monitored using UV/Vis spectroscopy as shown in Figure 5.7.

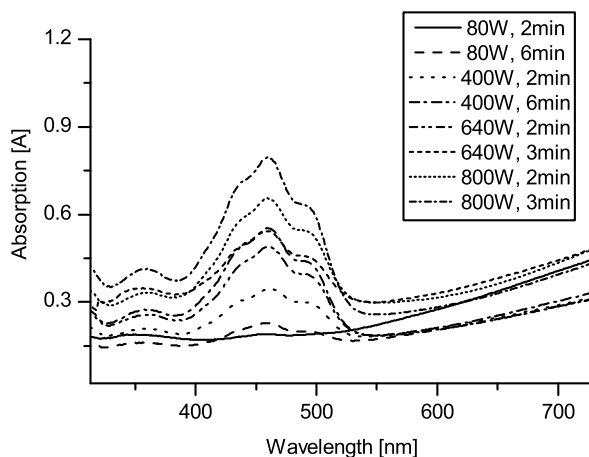


Figure 5.7. UV-vis spectra of 0.8 cm² samples of **42** prepared at different input power and reaction time.

At 80 W and 400 W reaction times of 2 and 6 minutes were used. However, at 640 W and 800 W similar reaction times resulted in evaporation of the reaction mixture, therefore only 2 and 3 minutes were used for these samples. In general an increase of the input power or reaction time resulted in an increase in degree of reaction, as seen from the enhanced absorption. As it was found that 800 W of power for 2-3 minutes resulted in the highest loading, it was decided to test a larger sample under the equivalent conditions. Interestingly, a sample with an area of 2.5 cm² was found to react much faster than the 0.8 cm² sample used for the input power investigation, as shown in Figure 5.8.

This is believed to be a result of the approximately three times larger surface being covered with only two times the reaction mixture. A larger surface corresponds to a larger heating source, and combined with a lower volume of the reaction mixture on the surface, this gives a higher reaction temperature. Reactions performed at 800 W for 1, 2x1.5, 2 and 3 minutes showed that the optimal reaction time for this area/volume ratio is 2 minutes. A sample run at room temperature for 20 hours gave an absorbance of 1.3 A at 448 nm, which corresponds to the loading obtained after 2 minutes at 800 W. A blank sample

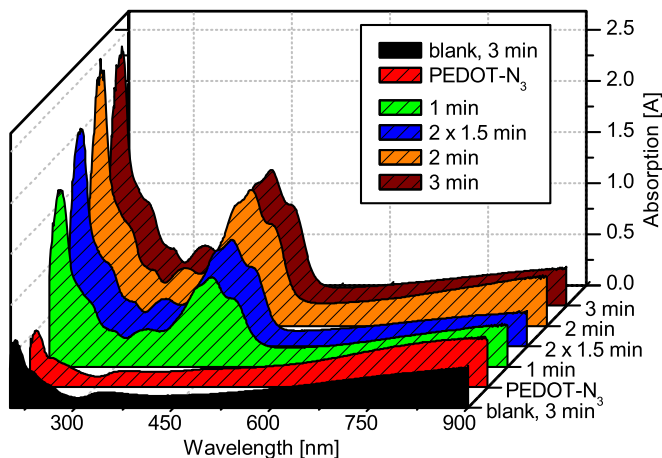


Figure 5.8. UV-vis spectra of 2.5 cm² samples of **42** prepared at 800 W with varied reaction time.

exposed to the same conditions omitting the CuSO₄ showed no reaction even after 3 minutes at 800 W. This confirms that the reaction occurring is still the CuAAC and not just a thermal cycloaddition. However, it is not possible to get proof of the regioselectivity as the conductive polymer is insoluble. An interesting detail was found by irradiation of one reaction mixture for two times 1.5 minute, where the consecutive irradiations resulted in an absorption corresponding to a reaction time of between 1 and 2 minutes. An explanation could be that the solution needs to be kept at the activated temperature sufficiently long for the bulk reaction to occur. An eventual increase in the absorption would have to come from additional reactions in the bulk of the film, since the surface groups are expected to have reacted during the first irradiation. When the microwave is stopped, the solution rapidly returns to room temperature and the repeated irradiation therefore only has a moderate influence on the loading.

5.3 Electroclick

In an effort to control the functionalization on a macroscopic scale experiments have also been conducted on a patterned surface. The idea was that by electrochemical reduction of the catalyst the reaction could be conducted on one electrode selectively. In order to investigate this a pair of interdigitated electrodes were prepared from PEDOT-N₃ through a masking strategy applying UV sensitive photoresist and reactive ion etching by an earlier published method.⁹⁰ Thereby

the pair of electrodes (1 and 2 shown in Figure 5.9, A) was prepared.

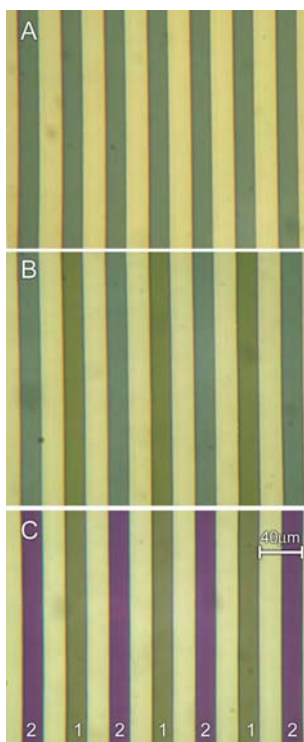


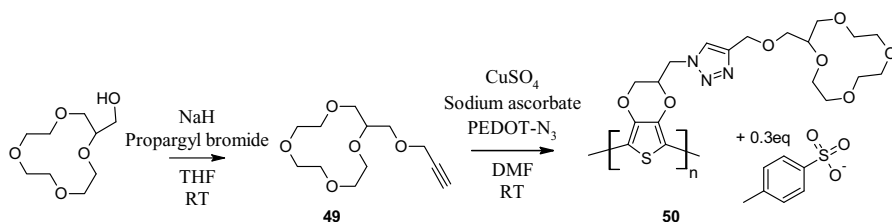
Figure 5.9. Interdigitated electrodes of PEDOT-N₃ (1 and 2); A: Pristine electrodes; B: Electrode 1 reacted with **41**/CuSO₄; C: Electrode 2 reacted with **47**/CuSO₄.

An electrochemical cell was constructed from the two electrodes, and a reaction solution containing only the fluorescein alkyne, **41**, and CuSO₄ in DMF was placed on the surface. By fixing a negative potential on one electrode it was possible to reduce copper selectively at this electrode. The localized reduction of copper catalyzed the reaction solely on that electrode, resulting in the pattern shown in Figure 5.9, B. Thereafter the current could be reversed providing localized activation of the catalyst at the other electrode. As an illustration of the concept a new click solution containing the rhodamine alkyne, **47**, and CuSO₄ in DMF was placed on the surface and the reaction was repeated on the same electrodes, providing the color change shown in Figure 5.9, C. A similar activation of the copper catalyst has been demonstrated on a SAM of thiols on a gold electrode by Devaraj et al⁹¹ in 2006. The efficiency of the electrode activation versus the

general method is currently under investigation.

5.4 Sensors - Concept System

The CuAAC has been shown to have an extremely good selectivity and to be applicable under a multitude of conditions. Therefore it would be well suited for introduction of chemically diverse molecules onto a target substrate. As outlined in the introduction this would be a very interesting property for new sensors, since different materials could be prepared through a standardized approach only dependent on introduction of an alkyne to the respective receptors. PEDOT can easily be prepared on non conductive polymer substrates and device fabrication would therefore be possible through standard fabrication procedures. In order to test this approach different receptors were considered, where especially a selective response to one specific analyte was prioritized. There are numerous examples of sensors in the literature, where the covalent linking of crown ethers was found to have resulted in highly selective systems. Especially two systems where a 12-crown-4 ether was bonded to polythiophene^{75,76} and equivalently where 1-aza-15-crown-5 ether was bonded to polypyrrole⁷⁷ was found interesting. Analyses by cyclic voltametry performed in both cases showed distinct changes upon exposure of the conductive polymers to increasing ion concentrations. Here the oxidation potential was found to increase and the exchanged current was diminished with increasing ion concentrations. Therefore it was chosen to use this concept for investigation of the ionic response of the functionalized conductive polymers. An alkyne functionalized 12-crown-4 ether, **49**, was prepared and subsequently coupled to PEDOT-N₃ following the general method as shown in Scheme 5.3.



Scheme 5.3. Synthesis of **49** and the subsequent CuAAC with PEDOT-N₃ to give the crown ether functionalized surface, **50**.

XPS data of the prepared material (Table 5.2) clearly confirm that the surface has been functionalized as shown in Scheme 5.3 in accordance with earlier results.

Initial experiments performed in an aqueous phosphate electrolyte in an electrochemical chamber for aqueous electrolytes on **50** showed no effects upon addition of small aliquots of LiOCl₄. This is in accordance with results presented from

Table 5.2. XPS results on **50**.

Atom	Content Found [atom-%]	Calculated [†] [atom-%]
C	62.7	63.4
O	23.9	23.7
N	8.6	9.0
S	4.8	3.9

[†] Including 0.3 eq tosylate.

other groups on the topic. One theory is that an aqueous environment ligates alkali ions well in solution, and therefore a response from a surface bound receptor would be expected to be low. Consequently an organic electrolyte of tetrabutylammonium perchlorate (TBAP) in acetonitrile was prepared and applied in the experiments henceforth. In order to perform the experiments on a smaller scale a PDMS chamber for the electrochemical cell was produced and the experimental setup showed in Figure 5.10 was constructed.

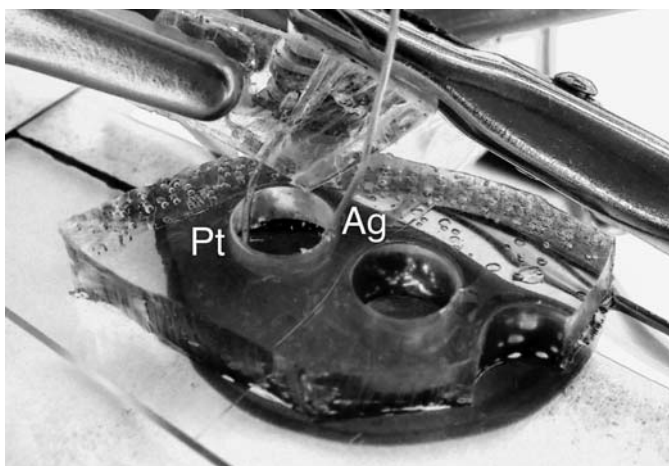


Figure 5.10. Electrochemical cell setup on a 12-crown-4 functionalized PEDOT-N₃, **50**, showing two chambers on separate cells. In the active cell a reference electrode of Ag and a counter electrode of Pt was used. The working electrode was connected to the film on the backside of the chamber.

On the picture it is clear to see the advantage of changing the size of the electrochemical cell to this smaller version. Here it is possible to conduct several measurements on the same surface in different cells, while still maintaining short

distance between the working electrode and the actual cell. In addition to this, the cell cannot be moved on the surface, maintaining a constant area and access to the exact same functional area on the film throughout all the measurements. In Figure 5.11 cyclic voltamograms obtained for **50** in the TBAP electrolyte with an increasing concentration of LiOCl_4 are shown.

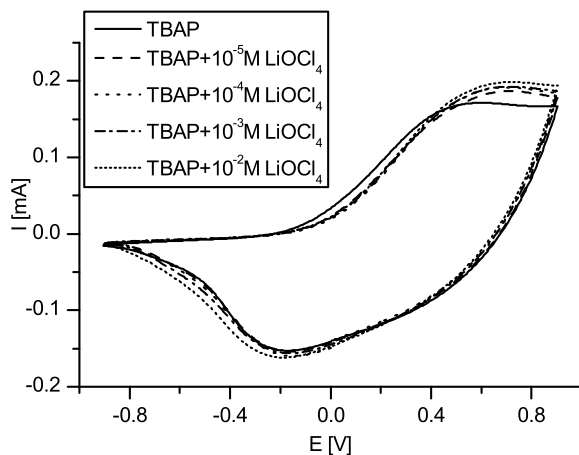


Figure 5.11. Cyclic voltamograms obtained on **50** with different TBAP electrolytes containing increasing concentrations of LiOCl_4 in acetonitrile.

The effects found here are much less pronounced compared to the literature results mentioned earlier. No gradual disappearance of the oxidation peak was observed for any of the measurements and the oxidation peak clearly does not decrease in intensity with increasing ion concentrations. As these experiments have been performed on a polymer substrate and the original data were obtained on a platinum surface this might change the properties of the system and therefore other substrates were also investigated. Samples prepared on glass and gold showed a shift of the oxidation peak potential in the cyclic voltamogram compared to the samples prepared on the polymer substrates. However, the general trend of an irreversible change after exposure to the lowest ion concentration were observed in all cases.

In search of an explanation for the low sensitivity a different approach was based on the assumption that a high surface coverage could have changed the responsiveness of the surface significantly compared to the earlier mentioned literature, where electropolymerization had made it necessary to have a lower coverage as polymerization of the pure monomer was not possible. Therefore, tests with sodium and potassium salts were performed. Especially potassium is known to show a tendency for ligation in sandwich complexes with smaller crown ethers,⁹²

since the cavity in e.g. a 12-crown-4 ether is too small to fit the whole potassium ion inside. Unfortunately the perchlorate salt of potassium is almost insoluble in acetonitrile, and therefore these measurements had to be performed with potassium hexafluorophosphate (KHFP) and the corresponding electrolyte, tetrabutylammonium hexafluorophosphate (TBAHFP). In order to be able to compare the effects from the different salts, the relative change of the oxidation peak potential was measured as presented in Table 5.3.

Table 5.3. Change in the oxidation peak of **50** with exposure to different electrolytes.

Scan rate [mV/s]	Δ Oxidation Peak Potential [mV]		
	LiOCl ₄ [†]	NaOCl ₄ [†]	KHFP ^{††}
100	+96	+190	+124
10	-22	+45	- [‡]

[†] Relative to TBAP.

^{††} Relative to TBAHFP.

[‡] The oxidation peak potential with the TBAHFP electrolyte could not be determined accurately. A very distinct oxidation peak was observed in the KHFP electrolyte.

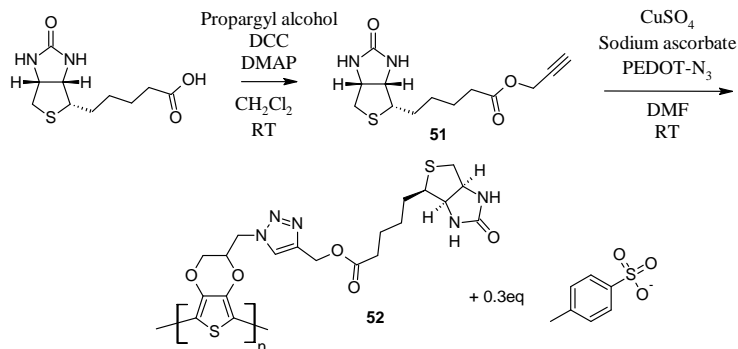
As can be seen from the table the oxidation peak potential is influenced by changes in the electrolyte. Here especially the sodium salt shows the largest change compared to the ammonium electrolyte with a shift in the oxidation peak potential of 190 mV. The increase is considerable compared to the other salts, though the selectivity is not as high as indicated in the literature references. This sensor setup was based on the influence of ions complexed at the surface of the film, where the positively charged alkali ions were expected to influence the oxidation potential of the polymer. This has been found to be possible to achieve with the system, though it appears that some optimization is still required in order to gain the necessary sensitivity and selectivity of a sensing system. Recently in a pH sensitive PEDOT, employing a carboxylic acid covalently bound to PEDOT,⁷⁴ Ali et al. showed that a minor change in a linker from an ether to an ester strongly influenced the sensitivity. Something similar could be the case here where the effects of the triazole unit and the length of the linker has not been investigated.

5.4.1 Biosensors

Finally, the first steps towards biosensors by this approach have been taken. Two different systems are currently under investigation, the first based on detection of antigens through a layer by layer strategy employing biotin and streptavidin and the second based on the analysis of glucose. The projects are based on collabora-

tions with Thomas S. Hansen and Professor Niels B. Larsen from Risø DTU and Jan Kafka from DTU Nanotech, respectively.

For the first system an alkyne functional biotin was prepared as shown in Scheme 5.4.



Scheme 5.4. Synthesis of **51** by dicyclohexylcarbodiimide (DCC) coupling, followed by the reaction with PEDOT-N₃.

The subsequent functionalization of PEDOT-N₃ was performed in accordance with the optimized method. The strategy was that the biotin functionalized surface then could be exposed to streptavidin followed by a biotin-antibody, which should result in a surface that would respond selectively on exposure to a sample containing the corresponding antigen. The initial experiments have until now been challenged by the need to prevent unspecific bonding of proteins to the surface. This could be envisioned attained through modification of the surface with PEG or MPEG, and this approach is currently under investigation at Risø DTU.

Similarly initial work was done towards a variant of the well known glucose sensor based on glucose oxidase.^{93,94} Recent results on a graphite electrode covered with an ionic film has shown that hydrogen peroxide can be sensed through the redox process of the iron in ferrocene.⁹⁵ This could be exploited for the preparation of a glucose sensor, which is normally based on a combination of the enzyme glucose oxidase that produces hydrogen peroxide from H₂O by oxidation of glucose and a mediator that converts this to an electrical signal. The formed hydrogen peroxide can then be reoxidized by the mediator, which could be e.g. ferrocene or Prussian blue loaded into the polymer during the polymerization. Electrochemical reoxidation of the mediator then generates the electrical signal that directly corresponds to the glucose concentration. Alternatively an oxygen free variant can also be prepared, where the mediator is directly reduced in the oxidation of glucose.⁹⁶ Based on the results of Zhao et al.⁹⁵ the investigation of the direct bonding of ferrocene onto the conductive polymer electrode was undertaken. Ethynylferrocene is commercially available and could easily be reacted onto

the surface. Currently the investigation of the sensing abilities of this system is under investigation.

5.5 Conclusions

The monomer EDOT-N₃ was prepared in a two step synthesis and was applied in a chemically oxidative polymerization with good results. The prepared polymer was shown to be conductive and the azide groups were intact after polymerization. CuAAC were utilized to functionalize the conductive polymer, and optimization of the reaction conditions led to reaction times of approximately 20 hours at ambient conditions. The diversity of the different alkynes applied here clearly illustrated the versatility of the process and shows that the method is generally applicable. Microwave irradiation was tested as an accelerator for the reaction and was found very efficient, resulting in reaction times on the order of minutes. The reaction was also performed on a pair of interdigitated electrodes, where localized reduction of the catalyst resulted in controlled reaction on one electrode selectively. Finally the method was applied for preparation of sensor systems. Preparation of both a 12-crown-4 ether, a biotin, and a ferrocene functionalized surface shows that the system is well suited for the introduction of receptors on the surface of the conductive polymer. However, until now the prepared systems still lack in sensitivity and selectivity and further development will be necessary in order for the full potential of the system to be realized.

6 Conclusion and Outlook

6.1 Conclusion

The overall objective of this Ph.D. research project was the preparation of novel functional materials by high yielding reactions inspired by the frame of click chemistry.

During the project three different applications have been targeted. In the first application example the strategy was based on postpolymerization functionalization in solution followed by preparation of the functional film surfaces intended for the application in an electro osmotic micropump. In this case, the preparation of the alkyne functional polymers both from commercial samples and from copolymers prepared from 4-*tert*-butoxystyrene and styrene was standardized and found to be directly applicable to several different systems. The postfunctionalization through CuAAC was shown to be extremely effective and applicable to all the systems investigated. In addition to this, it was proven that random copolymers with a variable loading could be prepared by a free radical copolymerizations of 4-*tert*-butoxystyrene and styrene potentially enabling total control of the loading. Preparation of thin polymer films of these materials followed by investigations of the surface properties by both contact angle measurements and XPS efficiently identified polymer films with a high surface loading of carboxylic acids.

In the second case, work was done on both dendritic macromonomers but also on new cyclic monomers for holographic data storage based on photopolymer systems. The dendritic macromonomers were found to have beneficial effects upon the inherent problem of high volume shrinkage in photopolymer systems. It was proven that the branched macromonomers could reduce the volume shrinkage to insignificant levels. Additionally, the dendritic structure was exploited for end-group functionalization in a new dendritic macromonomer with high refractive index naphthalenes on the periphery. The final testing of these materials still remains, though the initial results are looking very promising. In parallel to the dendritic approach towards new monomers with low volume shrinkage, two projects working on cyclic monomers through a prepolymerization functionalization strategy were conducted. Unfortunately the strategy based on BMDO stranded on low yields and nonreactive intermediates. However, the approach based on the larger ring sized lactone acrylates provided an easy and efficient approach to new monomers with higher refractive index. By introduction of the alkynes in the parent monomer access to a number of substituents on the monomer was en-

abled. The prepared monomers were tested in the photopolymer system, where they unfortunately were found to polymerize with too low conversion in order to attain the necessary sensitivity and storage capacity. However, the strategy of prepolymerization functionalization was found to be highly effective.

The third strategy was also based on postpolymerization functionalization as in the first case. The PEDOT functionalization was performed on the surface of the insoluble polymer and not in solution as in the PHS approach. The method was optimized and a standard protocol for preparation of new materials was developed. Several different functionalities were introduced to the conductive polymer film, enabling access to a conductive polymer with both a more hydrophobic and a highly hydrophilic surface through introduction of fluor or MPEG onto the polymer, respectively. In an effort to increase the number of possible applications a microwave activated protocol was also developed enabling reaction times on the order of minutes. Through this protocol a quick and efficient access to new materials was ensured. Additional experiments on interdigitated electrodes enabled area selective reactions on the surface of the substrates, which would be a very useful property for the future development of sensor devices on this functional material. Since the conductive polymer can easily be prepared on different polymer substrates it is highly suited for the preparation of microfluidic devices of this kind. As an effort towards a functional microsystem initial steps with covalent anchoring of receptors onto the conductive polymer were taken. The initial investigations of the prepared materials with especially the 12-crown-4 receptor on the surface were performed, though it remains to be proven that the approach can yield selective and highly sensitive materials.

6.2 Future Work

From the presented data, it would be easy to extend the preparation of carboxylic acid functional copolymers to other functional groups such as amines, alcohols or polymer grafts. The approach presented here has only been applied to this one functional group, but the potential for preparation of other types can easily be seen from the number of publications on CuAAC. A postpolymerization strategy for polymer grafting (a “graft to” approach) compared to the traditional sequential polymerization methods (a “graft from” approach) would enable the complete characterization of both the backbone and the grafts before combination in the copolymer. This would result in a more highly defined system. Through the high selectivity of the CuAAC it would be possible to introduce polymers containing a high number of different functional groups, which would provide a good alternative to existing “graft to” protocols. In addition to this, grafts could easily be prepared through different polymerization techniques like anionic polymerization or ATRP combined with free radical polymerizations.

The holography research project is continued at UCSB with development of

other dendrimers with different high refractive index groups. It could also be interesting to investigate known dendrimers, like dimethylolpropionic acid (bis-MPA) dendrons that could be end group functionalized with groups of a high refractive index, in the photopolymer system. Furthermore, the benzyl ether strategy could also be extended through orthogonal functionalization of the periphery of the benzyl ether dendrons exploiting the relatively high refractive index of the branching structure. Future development of the system will have to focus on a continued increase in storage capacity and sensitivity. Additionally, actual implementation into a device could be extremely interesting and would certainly have a commercial interest.

With the conductive polymer system the foundation for many new applications have been created. The modularity of the system makes it possible to prepare the conductive polymer with whatever surface properties would be needed for new applications. Given that the reaction can also be conducted at very short reaction times, on different types of substrates and by selective activation on different electrodes there is a large potential for preparation of new microsensors. For further development of this part of the project it would be very beneficial to get collaborators from either industry or other research groups interested in the project. This would facilitate testing of possible devices for e.g. biosensors under more relevant conditions, which is essential in order to fully develop the potential of the system.

7 Experimental Work

7.1 General Methods and Materials

7.1.1 Method A

At UCSB all chemicals were acquired from Sigma-Aldrich and used without further purification. Analytical Thin layer chromatography (TLC) was performed on commercial Merck plates coated with silica gel GF254 (0.24 mm thick). Column chromatography was performed on a Biotage SP1 Flash Purification System using FLASH 40+M and FLASH 25+M cartridges. FT-IR was performed on a Perkin Elmer Spectrum 100 with a Universal ATR sampling accessory. NMR measurements were performed on a Bruker AC 500 (^1H -NMR (500 MHz) and ^{13}C -NMR (125 MHz)) or a Bruker AC 200 (^1H (200 MHz) and ^{13}C -NMR (50 MHz)) at $23\pm 2^\circ\text{C}$ using residual protonated solvent signal as internal standard (^1H : $\delta(\text{CHCl}_3) = 7.26$ ppm and ^{13}C : $\delta(\text{CHCl}_3) = 77.16$ ppm). Differential Scanning Calorimetry (DSC) measurements were performed with a TA Instruments DSC 2920 with a heating ramp of $5^\circ\text{C}/\text{min}$. Data was collected during third cycle in the selected temperature ranges. Melting transition temperatures (T_m) were determined by peak maxima of the transition. Mass spectroscopy was run on a Micromass QTOF2 Quadrupole/Time-of-Flight Tandem mass spectrometer using electron ionization (EI) or electrospray ionization (ESI-TOF).

7.1.2 Method B

At DTU all chemicals were acquired from Sigma-Aldrich too and used without further purification. Analytical TLC was performed on Merck plates coated with silica gel GF254 (0.24 mm thick). Kieselgel for column chromatography was Merck Kieselgel 60 (230-400 mesh). NMR was run on a 300 MHz Cryomagnet from Spectrospin & Bruker at room temperature using residual protonated solvent signal as internal standard (^1H : $\delta(\text{CHCl}_3) = 7.26$ ppm and ^{13}C : $\delta(\text{CHCl}_3) = 77.16$ ppm). FT-IR was performed on a PerkinElmer Spectrum One model 2000 Fourier transform infrared system with a universal ATR sampling accessory on a ZnSe/diamond composite. The conductivity was measured with a four-point probe (Jandel Engineering Ltd, Linslade, UK) connected to a four-point source meter (Keithley 2400, Cleveland, US).

7.2 Experimental work

2-Methanol-3,5-dimethoxynaphthalene (25)

3,5-Dimethoxy-2-naphthoic acid (3.00 g, 13 mmol) was placed in a Soxhlet timple and loaded into a Soxhlet extractor. LiAlH_4 (0.61 g, 16 mmol) was suspended in dry THF (75 mL) and the mixture was heated at reflux for 6.5 h under nitrogen. The excess LiAlH_4 was quenched with H_2O , causing the product to precipitate. The crude was obtained by filtration and recrystallized from hexanes giving a white solid (2.30 g, 82%, $T_m = 99\text{--}100^\circ\text{C}$). Characterization was performed by method A.

IR (cm^{-1}): 3365 (OH); 3000, 2950, 2835 (C-H); 1635, 1605 (C=C); 1230, 1035 (C-O).

$^1\text{H-NMR}$ (500 MHz) CDCl_3 , δ_{H} (ppm): 4.01, 4.02 (2s, 6H, CH_3O); 4.84 (s, 2H, CH_2OH); 6.83 (d, 1H, ArH, $^3J = 7.6\text{ Hz}$); 7.27 (m, 1H, ArH); 7.38 (d, 1H, ArH, $^3J = 8.2\text{ Hz}$); 7.55 (s, 1H, ArH); 7.70 (s, 1H, ArH).

$^{13}\text{C-NMR}$ (125 MHz) CDCl_3 , δ_{C} (ppm): 55.5 (2C, CH_3O); 62.5 (1C, CH_2OH); 99.9 (1C, arom. CH); 104.5 (1C, arom. CH); 120.2 (1C, arom. CH); 123.9 (1C, arom. CH); 126.0 (1C, arom. CCH_2OH); 127.3 (1C, arom. CH); 129.7 (1C, arom. C); 130.9 (1C, arom. C); 154.5 (1C, arom. COCH_3); 155.8 (1C, arom. COCH_3).

Mass spectroscopy (m/z) EI: 218 M^+ ; ESI-TOF: 241 $\{\text{M}+\text{Na}\}^+$.

General procedure for synthesis of naphthalene acrylates, (3,5-dimethoxynaphthalen-2-yl)methyl acrylate (26)

25 (0.149 g, 0.7 mmol) was dissolved in CH_2Cl_2 (1.5 mL) whereafter dimethylaminopyridine (DMAP, 0.018 g, 0.1 mmol) and Et_3N (0.556 g, 0.76 mL, 5.5 mmol) were added. Acryloyl chloride (0.249 g, 0.11 mL, 1.4 mmol) was added dropwise to the solution, and the resulting slurry was stirred for 16 h at RT under nitrogen. The reaction mixture was filtered and the organic layer was extracted with NaHSO_4 (1 M, x3), NaHCO_3 (x3) and brine (x1). The organic layer was dried with MgSO_4 , filtered and concentrated *in vacuo*. The product was obtained as an oil (0.119 g, 64%). Characterization was performed by method A.

IR (cm^{-1}): 3050, 2965, 2930 (C-H); 1720 (C=O); 1635, 1605 (C=C); 1250, 1195 (C-O).

$^1\text{H-NMR}$ (500 MHz) CDCl_3 , δ_{H} (ppm): 3.97, 4.01 (2s, 6H, CH_3O); 5.40 (s, 2H, CH_2OCO); 5.87 (dd, 1H, $\text{CH}_2=\text{CH}$ -, $^2J = 1.3\text{ Hz}$, $^3J = 10.4\text{ Hz}$); 6.23 (dd, 1H, $\text{CH}_2=\text{CH}$ -, $^3J = 10.4\text{ Hz}$, $^3J = 17.3\text{ Hz}$); 6.49 (dd, 1H, $\text{CH}_2=\text{CH}$ -, $^2J = 1.4\text{ Hz}$, $^3J = 17.3\text{ Hz}$); 6.83 (d, 1H, ArH, $^3J = 7.6\text{ Hz}$); 7.26 (m, 1H, ArH); 7.37 (d, 1H, ArH, $^3J = 8.2\text{ Hz}$); 7.54 (s, 1H, ArH); 7.76 (s, 1H, ArH).

$^{13}\text{C-NMR}$ (125 MHz) CDCl_3 , δ_{C} (ppm): 55.58, 55.63 (2C, CH_3O); 62.2 (1C, CH_2OCO); 100.0 (1C, arom. CH); 104.6 (1C, arom. CH); 120.2 (1C, arom. CH); 123.8 (1C, arom. CH); 126.2 (1C, arom. $\text{C-CH}_2\text{OCO}$); 126.3 (1C, arom.

C); 128.3 (1C, arom. CH); 128.6 (1C, -CH=CH₂); 129.4 (1C, arom. C); 131.0 (1C, -CH=CH₂); 154.5 (1C, arom. COCH₃); 155.5 (1C, arom. COCH₃); 166.2 (1C, -COO-).

Mass spectroscopy (m/z) ESI-TOF: 295 {M+Na}⁺, 567 {2M+Na}⁺.

Prop-2-enyl 3,5-dimethoxynaphthalene-2-carboxylate (27)

3,5-Dimethoxy-2-naphthoic acid (5.09 g, 21.5 mmol) was suspended in oxalyl chloride (13 mL, 154 mmol) at 0 °C. The suspension was heated to reflux for 3 h and the excess oxalyl chloride was removed *in vacuo*. The acid chloride was dissolved in CH₂Cl₂ (35 mL), whereafter Et₃N (8.8 mL, 64 mmol) and DMAP (0.53 g, 4.3 mmol) were added to the solution. The mixture was stirred at 0 °C and allyl chloride (3.0 mL, 37 mmol) was added dropwise. After addition, the mixture was stirred under nitrogen overnight. The suspension was dissolved in CH₂Cl₂/H₂O and extracted with brine (x3), dried with MgSO₄, filtered and concentrated *in vacuo*. The product was isolated as an oil that may crystallize upon standing (5.14 g, 94 %, T_m = 62-63 °C). Characterization was performed by method A.

IR (cm⁻¹): 3000, 2950, 2835 (C-H); 1730 (C=O); 1630, 1600 (C=C); 1230, 1100, 1055 (C-O).

¹H-NMR (500 MHz) CDCl₃, δ_H (ppm): 4.01, 4.02 (2s, 6H, CH₃O); 4.87 (dt, 2H, CH₂O-, ³J = 5.6 Hz, ⁴J = 1.3 Hz); 5.31 (dq, 1H, C=CH₂, ³J = 10.4 Hz, ⁴J = 1.3 Hz); 5.47 (ddt, 1H, C=CH₂, ²J = 1.5 Hz, ³J = 17.2 Hz, ⁴J = 1.3 Hz); 6.08 (ddt, 1H, -CH=CH₂, ³J = 10.5 Hz, ³J = 17.1 Hz, ³J = 5.6 Hz); 6.86 (d, 1H, ArH, ³J = 7.6 Hz); 7.29 (t, 1H, ArH, ³J = 8.0 Hz); 7.41 (d, 1H, ArH, ³J = 8.2 Hz); 7.62 (s, 1H, ArH); 8.29 (s, 1H, ArH).

¹³C-NMR (125 MHz) CDCl₃, δ_C (ppm): 55.7, 56.1 (2C, CH₃O); 65.8 (1C, CH₂O-); 101.7 (1C, arom. CH); 106.1 (1C, arom. CH); 118.3 (1C, CH=CH₂); 120.9 (1C, arom. CH); 122.0 (1C, arom. CCOO-); 124.4 (1C, arom. CH); 128.3 (1C, arom. C); 128.5 (1C, arom. C); 132.43 (1C, arom. CH); 132.47 (1C, CH₂=CH); 154.3 (1C, arom. COCH₃); 155.7 (1C, arom. COCH₃); 166.0 (1C, -COOC).

Mass spectroscopy (m/z) ESI-TOF: 295 {M+Na}⁺, 567 {2M+Na}⁺.

Naphthalene-G1-OH (28)

27 (0.3 g, 1.2 mmol) was dissolved in DMF (0.5 mL). To the solution 2,3-dimercapto-1-propanol (0.07 g, 5.4 mmol) and 2,2-dimethoxy-2-phenylacetophenone (0.06 g, 2.8 mmol) were added. The mixture was stirred under a 365 nm UV lamp for 30 min. The mixture was dissolved in EtOAc and H₂O was added. The aqueous phase was extracted with EtOAc (x3). The combined organics were extracted with H₂O (x5), dried with MgSO₄, filtered and concentrated *in vacuo*. The crude was purified by column chromatography and the product was isolated as a colorless oil (0.27 g, 76 %). Characterization was performed by method A.

IR (cm^{-1}): 3495 (OH); 3000, 2935, 2835 (C-H); 1730, 1710 (C=O); 1630, 1600 (C=C); 1270, 1200, 1105, 1060 (C-O).

$^1\text{H-NMR}$ (500 MHz) CDCl_3 , δ_{H} (ppm): 2.07 (m, 4H, $\text{CH}_2\text{-CH}_2\text{-CH}_2$); 2.33 (t, 1H, CH_2OH , 5.8 Hz); 2.76 (m, 4H, $\text{CH}_2\text{-S}$); 2.81 (dd, 1H, $\text{S-CH}_2\text{-CH}$, $^2J = 13.3$ Hz, $^3J = 8.6$ Hz); 2.88 (dd, 1H, $\text{S-CH}_2\text{-CH}$, $^2J = 13.3$ Hz, $^3J = 5.6$ Hz); 2.98 (m, 1H, $\text{CH}_2\text{-CHS-CH}_2$); 3.74 (m, dd if OH exchanged, 1H, $\text{-CH}_2\text{-OH}$, $^2J = 11.5$ Hz, $^3J = 5.7$ Hz); 3.85 (m, dd if OH exchanged, 1H, $\text{-CH}_2\text{-OH}$, $^2J = 11.5$ Hz, $^3J = 5.0$ Hz); 4.00 (s, 12H, CH_3O); 4.43 (t, 4H, $\text{CH}_2\text{O-}$, $^3J = 6.1$ Hz); 6.85 (d, 2H, ArH , $^3J = 7.7$ Hz); 7.28 (t, 2H, ArH , $^3J = 7.7$ Hz); 7.40 (br d, 2H, ArH , $^3J = 8.2$ Hz); 7.59 (s, 2H, ArH); 8.22 (s, 2H, ArH).

$^{13}\text{C-NMR}$ (125 MHz) CDCl_3 , δ_{C} (ppm): 27.9, 29.0, 29.3, 29.7 (4C, $\text{CH}_2\text{-CH}_2$); 34.8 (1C, $\text{SCH}_2\text{-CHS}$); 49.0 (1C, $\text{CH}_2\text{-CHS}$); 55.7, 56.2 (4C, CH_3O); 63.3, 63.5, 63.6 (3C, CH_2O); 101.7 (2C, arom. CH); 106.1 (2C, arom. CH); 120.9 (2C, arom. CH); 122.1 (2C, arom. C-COO-); 124.4 (2C, arom. CH); 128.3 (2C, arom. C); 128.5 (2C, arom. C); 132.3 (2C, arom. CH); 154.3 (2C, arom. COCH_3); 155.6 (2C, arom. COCH_3); 166.0 (2C, Ar- COOC).

Mass spectroscopy (m/z) ESI-TOF: 691 $\{\text{M}+\text{Na}\}^+$, 1359 $\{2\text{M}+\text{Na}\}^+$.

Naphthalene-G1-acrylate (29)

The product was prepared from **28** by the general procedure, giving an oil (0.133 g, 98%). Characterization was performed by method A.

IR (cm^{-1}): 3000, 2930, 2835 (C-H); 1720 (C=O); 1630, 1600 (C=C); 1270, 1180, 1105, 1065 (C-O).

$^1\text{H-NMR}$ (500 MHz) CDCl_3 , δ_{H} (ppm): 2.07 (m, 4H, $\text{CH}_2\text{-CH}_2\text{-CH}_2$); 2.82 (m, 6H, $\text{CH}_2\text{-S}$); 3.12 (m, 1H, $\text{CH}_2\text{-CHS-CH}_2$); 4.00 (s, 12H, CH_3O); 4.36 (dd, 1H, $\text{-OCH}_2\text{-CHS}$, $^3J = 6.7$ Hz, $^2J = 11.5$ Hz); 4.43 (m, 5H, $\text{CH}_2\text{O-}$, $\text{-OCH}_2\text{-CHS}$); 5.78 (dd, 1H, $\text{CH}_2=\text{C}$, $^2J = 1.3$ Hz, $^3J = 10.4$ Hz); 6.09 (dd, 1H, $\text{CH}_2=\text{CH-}$, $^3J = 10.4$ Hz, $^3J = 17.3$ Hz); 6.39 (dd, 1H, $\text{CH}_2=\text{CH-}$, $^2J = 1.3$ Hz, $^3J = 17.3$ Hz); 6.85 (d, 2H, ArH , $^3J = 7.6$ Hz); 7.28 (t, 2H, ArH , $^3J = 8.0$ Hz); 7.40 (2 br d, 2H, ArH , $^3J = 8.2$ Hz); 7.59 (s, 2H, ArH); 8.22, 8.23 (2s, 2H, ArH).

$^{13}\text{C-NMR}$ (125 MHz) CDCl_3 , δ_{C} (ppm): 28.5, 29.0, 29.2, 30.0 (4C, $\text{CH}_2\text{-CH}_2$); 35.1 (1C, $\text{SCH}_2\text{-CHS}$); 45.0 (1C, $\text{CH}_2\text{-CHS}$); 55.7, 56.1 (4C, CH_3O); 63.58, 63.60 (2C, $\text{CH}_2\text{O-}$); 65.7 (1C, $\text{CH}_2\text{O-CO}$); 101.7 (2C, arom. CH); 106.1 (2C, arom. CH); 120.9, 121.0 (2C, arom. CH); 122.1, 122.2 (2C, arom. C-COO-); 124.39, 124.41 (2C, arom. CH); 128.1 (1C, -CH=CH_2); 128.2 (2C, arom. C); 128.5 (2C, arom. C); 131.5 (1C, -CH=CH_2); 132.31, 132.35 (2C, arom. CH); 154.3 (2C, arom. COCH_3); 155.6 (2C, arom. COCH_3); 165.9 (1C, -COOC); 166.4 (2C, -COOC).

Mass spectroscopy (m/z) ESI-TOF: 745 $\{\text{M}+\text{Na}\}^+$.

Naphthalene-G1-ene (30)

28 (0.23 g, 0.4 mmol) was dissolved in CH_2Cl_2 (1.5 mL). 4-Pentenoic anhydride (0.1 mL, 0.5 mmol), DMAP (0.009 g, 0.07 mmol) and Et_3N (0.2 mL, 1.4 mmol) were added, and the reaction was stirred at room temperature overnight. The excess anhydride was quenched with H_2O and the mixture was diluted with CH_2Cl_2 and separated. The organic phase was extracted with NaHSO_4 (x3), NaHCO_3 (x3) and brine (x1), dried with MgSO_4 , filtered and concentrated *in vacuo*. The crude was purified by column chromatography and was isolated as a colorless oil (0.19 g, 80 %). Characterization was performed by method A.

IR (cm^{-1}): 3000, 2935, 2835 (C-H); 1725 (C=O); 1675 (C=C); 1630, 1600 (Ar C=C); 1270, 1180, 1105, 1065 (C-O).

$^1\text{H-NMR}$ (500 MHz) CDCl_3 , δ_{H} (ppm): 2.07 (m, 4H, $\text{CH}_2\text{-CH}_2\text{-CH}_2$); 2.32, 2.40 (2 x m, 4H, $\text{CO-CH}_2\text{-CH}_2\text{-C=CH}_2$); 2.76 (m, 6H, $\text{CH}_2\text{-S}$); 3.06 (m, 1H, $\text{CH}_2\text{-CHS-CH}_2$); 3.98 (2 x s, 12H, CH_3O); 4.26 (dd, 1H, $\text{CH-CH}_2\text{O-}$, $^3J = 6.6$ Hz, $^2J = 11.4$ Hz); 4.37 (dd, 1H, $\text{CH-CH}_2\text{O-}$, $^3J = 5.1$ Hz, $^2J = 11.4$ Hz); 4.42 (t, 4H, 6.2 Hz); 4.96 (dq, 1H, -HC=CH_2 , $^3J = 10.2$ Hz, $^4J = 1.3$ Hz); 5.01 (ddt, 1H, -HC=CH_2 , $^2J = 1.6$ Hz, $^3J = 17.1$ Hz, $^4J = 1.4$ Hz); 5.76 (ddt, 1H, -CH=CH_2 , $^3J = 10.4$ Hz, $^3J = 17.0$ Hz, $^3J = 6$ Hz); 6.84 (d, 2H, ArH, $^3J = 7.6$ Hz); 7.28 (t, 2H, ArH, $^3J = 7.9$ Hz); 7.40 (2 x d, 2H, ArH, $^3J = 8.2$ Hz); 7.59 (s, 2H, ArH); 8.22 (2 x s, 2H, ArH).

$^{13}\text{C-NMR}$ (125 MHz) CDCl_3 , δ_{C} (ppm): 28.3, 28.8, 29.0, 29.2, 29.9, 33.5 (6C, $\text{CH}_2\text{-CH}_2$); 34.8 (1C, $\text{SCH}_2\text{-CHS}$); 44.9 (1C, $\text{CH}_2\text{-CHS}$); 55.6, 56.1 (4C, CH_3O); 63.6 (2C, $\text{CH}_2\text{O-}$); 65.4 (1C, $\text{CH}_2\text{O-}$) 101.7 (2C, arom. CH); 106.1 (2C, arom. CH); 115.7 (1C, -CH=CH_2); 120.9 (2C, arom. CH); 122.1 (2C, arom. CCOO-); 124.4 (2C, arom. CH); 128.2 (2C, arom. C); 128.5 (2C, arom. C); 132.3 (2C, arom. CH); 136.6 (1C, -CH=CH_2); 154.2 (2C, arom. C-OCH_3); 155.6 (2C, arom. COCH_3); 166.3 (2C, Ar- COOC); 172.8 (1C, $\text{CH}_2\text{-COO-C}$).

Mass spectroscopy (m/z) ESI-TOF: 773 $\{\text{M+Na}\}^+$, 1523 $\{2\text{M+Na}\}^+$.

Naphthalene-G2-OH (31)

31 was prepared by the same procedure as **28**, giving a colorless oil (0.220 g, 47 %). Characterization was performed by method A.

IR (cm^{-1}): 3495 (O-H); 3015, 2930, 2835 (C-H); 1725 (C=O); 1630, 1600 (Ar C=C); 1270, 1180, 1105, 1065 (C-O).

$^1\text{H-NMR}$ (500 MHz) CDCl_3 , δ_{H} (ppm): 1.57 (m, 4H, $\text{-CH}_2\text{-CH}_2\text{-CH}_2$); 1.67 (m, 4H, $\text{-CH}_2\text{-CH}_2\text{-CH}_2$); 2.06 (m, 8H, $\text{OCH}_2\text{-CH}_2\text{-CH}_2\text{S}$); 2.30 (t, 4H, $\text{O=C-CH}_2\text{-CH}_2$, $^3J = 7.2$ Hz); 2.50 (m, 4H, $\text{CH}_2\text{-CH}_2\text{-S}$); 2.69-2.85 (m, 15H, S-CH_2 , $\text{SCH}_2\text{-CHS}$); 3.06 (m, 2H, $\text{SCH}_2\text{-CHS}$); 3.65 (ddd, 1H, $\text{SCH-CH}_2\text{-OH}$, $^3J = 5.7$ Hz, $^3J = 5.7$ Hz, $^2J = 11.5$ Hz); 3.75 (ddd, 1H, $\text{SCH-CH}_2\text{-OH}$, $^3J = 5.7$ Hz, $^3J = 5.7$ Hz, $^2J = 11.2$ Hz); 3.99 (s, 24H, CH_3O); 4.28 (2dd, 2H, $\text{O-CH}_2\text{-CHS}$, $^3J = 6.4$ Hz, $^2J = 11.4$ Hz); 4.36 (dd, 2H, $\text{O-CH}_2\text{-CHS}$, $^3J = 5.3$ Hz, $^2J = 11.4$ Hz); 4.43 (t, 8H,

$\text{OCH}_2\text{-CH}_2\text{-}$, $^3J = 6.2\text{ Hz}$); 6.85 (d, 4H, ArH, $^3J = 7.6\text{ Hz}$); 7.27 (t, 4H, ArH, $^3J = 7.9\text{ Hz}$); 7.40, 7.41 (2 br d, 4H, ArH, $^3J = 8.2\text{ Hz}$); 7.59 (s, 4H, C=CH); 8.22, 8.23 (2s, 4H, ArH).

$^{13}\text{C-NMR}$ (125MHz) CDCl_3 , δ_{C} (ppm): 23.93, 23.98 (4C, $\text{CH}_2\text{-CH}_2\text{-CH}_2\text{-CH}_2$); 28.2, 28.9, 29.0, 29.2 (6C, $-\text{CH}_2\text{-CH}_2$); 29.8, 30.6, 32.6, 33.5, 33.6, 34.6, 34.9 (9C, $-\text{S-CH}_2$); 44.8 (2C, $\text{SCH}_2\text{-CHS}$); 48.6 (1C, $\text{SCH}_2\text{-CHS}$); 55.5, 56.0 (8C, CH_3O); 63.2, 63.4, 65.2 (7C, CH_2O); 101.6 (4C, arom. CH); 106.0 (4C, arom. CH); 120.8 (4C, arom. CH); 122.0 (4C, arom. CCOO-); 124.3 (4C, arom. CH); 128.1 (4C, arom. C); 128.4 (4C, arom. C); 132.15, 132.19 (4C, arom. CH); 154.1 (4C, arom. COCH_3); 155.5 (4C, arom. COCH_3); 166.2 (4C, $-\text{COO-C}$), 172.9, 173.0 (2C, $-\text{COO-C}$).

Mass spectroscopy (m/z) ESI-TOF: 1623 M^+ , 1647 $\{\text{M+Na}\}^+$, 1663 $\{\text{M+K}\}^+$.

Naphthalene-G2-acrylate (32)

The product was prepared from **31** by the general procedure, giving an oil (0.040 g, 45%). Characterization was performed by method A.

IR (cm^{-1}): 3000, 2930, 2855 (C-H); 1725 (C=O); 1630, 1600 (C=C); 1270, 1180, 1105, 1065 (C-O).

$^1\text{H-NMR}$ (500 MHz) CDCl_3 , δ_{H} (ppm): 1.57 (m, 4H, $-\text{CH}_2\text{-CH}_2\text{-CH}_2$); 1.67 (m, 4H, $-\text{CH}_2\text{-CH}_2\text{-CH}_2$); 2.06 (m, 8H, $\text{OCH}_2\text{-CH}_2\text{-CH}_2\text{S}$); 2.30 (t, 4H, $\text{O=C-CH}_2\text{-CH}_2$, $^3J = 7.2\text{ Hz}$); 2.50, 2.55 (2m, 4H, $\text{CH}_2\text{-CH}_2\text{-S}$); 2.69-2.85 (m, 12H, S-CH_2); 2.99 (m, 1H, $\text{SCH}_2\text{-CHS}$); 3.06 (m, 2H, $\text{SCH}_2\text{-CHS}$); 3.99 (s, 24H, CH_3O); 4.27 (dd, 2H, $\text{OCH}_2\text{-CHS}$, $^3J = 6.6\text{ Hz}$, $^2J = 11.3\text{ Hz}$); 4.36 (dd, 2H, $\text{OCH}_2\text{-CHS}$, $^3J = 5.2\text{ Hz}$, $^2J = 11.4\text{ Hz}$); 4.43 (t (8H) and m (2H), 10H, $\text{OCH}_2\text{-CH}_2$, $\text{OCH}_2\text{-CHS}$, $^3J = 6.2\text{ Hz}$); 5.83 (br d, 1H, CH=CH_2 , $^3J = 10.4\text{ Hz}$); 6.11 (dd, 1H, $-\text{CH=CH}_2$, $^3J = 10.4\text{ Hz}$, $^3J = 17.3\text{ Hz}$); 6.40 (br d, 1H, $-\text{CH=CH}_2$, $^3J = 17.3\text{ Hz}$); 6.85 (d, 4H, ArH, $^3J = 7.6\text{ Hz}$); 7.27 (t, 4H, ArH, $^3J = 7.9\text{ Hz}$); 7.40, 7.41 (2 br d, 4H, ArH, $^3J = 8.1\text{ Hz}$); 7.59 (s, 4H, ArH); 8.21, 8.22 (2s, 4H, ArH).

$^{13}\text{C-NMR}$ (125MHz) CDCl_3 , δ_{C} (ppm): 24.08, 24.11 (4C, $\text{CH}_2\text{-CH}_2\text{-CH}_2\text{-CH}_2$); 28.4, 29.0, 29.1, 29.2, 29.3 (6C, $-\text{CH}_2\text{-CH}_2$); 29.85, 30.0, 31.4, 32.1, 33.0, 35.0, 35.1 (9C, $-\text{S-CH}_2$); 44.8, 45.0 (3C, $\text{SCH}_2\text{-CHS}$); 55.7, 56.2 (8C, CH_3O); 63.6, 63.6, 65.3, 65.6 (7C, CH_2O); 101.7 (4C, arom. CH); 106.1 (4C, arom. CH); 120.9, 121.0 (4C, arom. CH); 122.1, 122.2 (4C, arom. CCOO-); 124.4 (4C, arom. C-H); 128.22 (1C, $-\text{CH=CH}_2$), 128.24 (4C, arom. C); 128.5 (4C, arom. C); 131.4 (1C, $-\text{CH=CH}_2$), 132.31, 132.35 (4C, arom. CH); 154.3 (4C, arom. COCH_3); 155.6 (4C, arom. COCH_3); 166.4 (5C, COOC), 173.0, 173.1 (2C, COOC).

Mass spectroscopy (m/z) ESI-TOF: 1702 $\{\text{M+Na}\}^+$.

36a/b, RuAAC

Pentamethylcyclopentadienyl ruthenium chloride (6.7 mg, 0.008 mmol) was dissolved in dioxane (2 mL) and the acrylate (93 mg, 0.4 mmol) was added in a so-

lution of dioxane (1 mL). Finally a solution of benzyl azide (58 mg, 0.4 mmol) in dioxane (1 mL) was added to the mixture and it was stirred at 60 °C for 21 h under nitrogen. The solvent was removed *in vacuo* and the concentrate was purified by gradient column chromatography eluting with 1:4 EtOAc:Hex, 1:1 EtOAc:Hex and finally EtOAc. An inseparable mixture of the 1,4- and 1,5-regioisomers (40 (A) : 60 (B)) was obtained as a colorless oil (87 mg, 60 %). Characterization was performed by method A.

IR (cm⁻¹): 3060, 2930 (C-H); 1725 (C=O); 1630, 1495 (C=C); 1231, 1175, 1130 (C-O); 725 (mono subst. ph).

¹H-NMR (500 MHz) CDCl₃, δ_H (ppm): 2.47 (t, 2H (A), CH₂CO, ³J = 6.3 Hz); 2.61 (t, 2H (B), CH₂CO, ³J = 6.1 Hz); 2.68 (t, 2H (A), CH₂-S, ³J = 6.3 Hz); 2.75 (t, 2H (B), CH₂-S, ³J = 6.1 Hz); 3.32 (s, 2H (B), S-CH₂-C=); 3.39 (s, 2H (A), S-CH₂-C=); 5.03 (s, 2H (A), =C-CH₂-OCO); 5.18 (s, 2H (B), =C-CH₂-OCO); 5.29 (s, 2H (B), =C-CH₂-OCO); 5.44 (s, 2H (A), =C-CH₂-OCO); 5.64 (m, 3H (B), Ph-CH₂- (2H), CH₂=C (1H)); 5.70 (m, 3H (A), Ph-CH₂- (2H), CH₂=C (1H)); 6.12 (s, 1H (B), CH₂=C); 6.23 (s, 1H (A), CH₂=C); 7.17-7.20 (m, 2H (A+B), ArH); 7.27-7.35 (m, 3H, ArH).

¹³C-NMR (50 MHz) CDCl₃, δ_C (ppm): 27.1, 27.3 (2C (A+B), -CH₂-CH₂-COO); 32.9, 33.4 (2C (A+B), CH₂-CH₂-S); 34.2, 34.5 (2C (A+B), CH₂=C-CH₂-S); 52.7 (2C (A+B), Ph-CH₂-N); 52.9, 53.2 (2C (A+B), OCO-CH₂-C=C); 57.3, 57.5 (2C (A+B), OCO-CH₂-C=C); 127.3, 127.4 (4C (A+B), C=CH); 128.3, 128.8 (2C (A+B), C=CH₂); 128.7 (2C (A+B), C=CH); 129.1, 129.2 (4C (A+B), C=CH); 130.7, 131.1 (2C (A+B), OCH₂-C=C-CH₂O); 134.6, 134.8 (2C (A+B), N-CH₂-C=CH); 136.3, 136.6 (2C (A+B), OCH₂-C=C-CH₂O); 143.4, 143.9 (2C (A+B), -OOC); 171.1, 171.3 (2C (A+B), -OOC).

Mass Spectroscopy (e/z) ESI/TOF: 374 M+H⁺, 396 M+Na⁺, 796 2M+Na⁺.

37, CuAAC

4-Bromobenzyl azide (0.25 g, 1.2 mmol), CuBr (0.032 g, 0.22 mmol) and the acrylate (0.27 g, 0.9 mmol) were suspended in DMF (5 mL) and stirred for 14 h at 60 °C under nitrogen. The reaction mixture was diluted with H₂O and extracted with EtOAc (x3). The combined organics were extracted with H₂O (x5), dried with MgSO₄, filtered and concentrated *in vacuo* giving an yellow oil. The crude was purified by gradient column chromatography eluting with 2:1 EtOAc followed by EtOAc. The product was obtained as a colorless oil (0.44 g, 98 %).

IR (cm⁻¹): 3140, 2955, 2820 (C-H); 1715 (br, C=O); 1630 (C=C); 1215, 1190 (C-O).

¹H-NMR (500 MHz) CDCl₃, δ_H (ppm): 2.44 (t, 2H, SCH₂-CH₂COO, ³J = 5.8 Hz); 2.70 (t, 2H, OCH₂-CH₂-N-CH₂, ³J = 4.4 Hz); 2.75 (m, 4H, CH₂-CH₂-N-CH₂, SCH₂-CH₂COO, ³J = 5.8 Hz); 3.38 (s, 2H, H₂C=CCH₂S); 3.79 (s, 2H, N-CH₂-C=C); 4.14 (m, 2H, OCH₂-CH₂-N); 4.32 (t, 2H, OCH₂-CH₂-N, ³J = 4.4 Hz); 5.44 (s, 2H, N-CH₂-Ph); 5.54 (s, 1H, CH₂=C); 6.02 (s, 1H, CH₂=C);

7.13 and 7.48 (ABq, 4H, ArH, $^3J = 8.3$ Hz); 7.86 (s, 1H, C=CH-N).

^{13}C -NMR (125 MHz) CDCl_3 , δ_{C} (ppm): 27.4 (1C, OC-CH₂CH₂-S); 33.5, 34.0 (2C, SCH₂-CH₂-CO, =C-CH₂-S); 49.3 (1C, N-CH₂-C=CH); 53.2, 53.5, 53.8 (CH₂-N); 61.08, 61.14 (2C, CH₂-O); 122.5 (1C, arom. C-Br); 124.0 (1C, C=CH-N); 125.9 (1 C, CH₂=C); 129.6 (2C, arom. CH); 132.1 (2C, arom. CH); 134.3 (1 C, arom. C); 137.6 (1C, CH₂=C); 146.5 (1 C, CH₂-C(N)=CH); 165.8 (1 C, H₂C=C-COO-); 171.8 (1 C, CH₂-COO-).

Rhodamine B prop-2-ynyl ester (47)

Rhodamine B (2.00 g, 4.18 mmol), propargyl alcohol (0.35 g, 6.3 mmol) and DMAP (0.15 g, 1.4 mmol) were dissolved in CH_2Cl_2 (13 mL) and cooled to 0 °C. A solution of DCC (0.90 g, 4.4 mmol) in CH_2Cl_2 (3 mL) was added dropwise and the mixture was left stirring under nitrogen at room temperature for 48 h. The mixture was filtered and the filtrate was mixed with silica gel where after the solvent was removed *in vacuo*. The solid was applied directly for column chromatography eluting the product with EtOAc/MeOH (1:1). The product was isolated as a sticky dark purple substance (1.11 g, 51 %). Characterization was performed by method B.

IR(cm^{-1}): 3300 (C≡C-H stretch); 3100-2800 (C-H stretch); 2155 (C≡C stretch); 1725 (C=O stretch).

^1H -NMR (300 MHz) CDCl_3 , δ_{H} (ppm): 1.33 (t, 12H, CH₃-CH₂, $^3J = 7.1$ Hz); 2.43 (t, 1H, C≡C-H, $^4J = 2.5$ Hz); 3.66 (q, 8H, N-CH₂-CH₃, $^3J = 7.1$ Hz); 4.62 (d, 2H, OCH₂-C≡CH, $^4J = 2.5$ Hz); 6.86 (d, 2H, Ar-H, $^4J = 2.4$ Hz); 6.93 (dd, 2H, Ar-H, $^3J = 9.5$ Hz, $^4J = 2.5$ Hz); 7.07 (d, 2H, Ar-H, $^3J = 9.5$ Hz); 7.35 (dd, 1H, Ar-H, $^3J = 7.6$ Hz, $^4J = 1.2$ Hz); 7.75 (ddd, 1H, Ar-H, $^3J = 7.8$ Hz, $^3J = 7.8$ Hz, $^4J = 1.3$ Hz); 7.85 (ddd, 1H, Ar-H, $^3J = 7.6$ Hz, $^3J = 7.6$ Hz, $^4J = 1.3$ Hz); 8.32 (dd, 1H, Ar-H, $^3J = 7.8$ Hz, $^4J = 1.2$ Hz).

^{13}C -NMR (75 MHz) CDCl_3 , δ_{C} (ppm): 12.5 (4C, CH₃-CH₂); 46.0 (4C, N-CH₂-CH₃); 52.7 (1C, OCH₂-C≡C); 75.4 (1C, C≡C-H); 76.3 (1C, CH₂-C≡C); 96.1, 113.3, 114.2, 129.0, 130.1, 130.3, 131.0, 131.3, 133.3, 133.5, 155.4, 157.6, 158.0 (19C, arom. C); 164.0 (1C, Ar-COOC).

2-(prop-2-ynyloxymethyl)-12-crown-4 ether(49)

NaH (0.039 g, 60 % suspension in oil, 0.97 mmol) was suspended in THF (2 mL) under nitrogen and a solution of 2-hydroxymethyl-12-crown-4 ether (0.20 g, 0.97 mmol) in THF (1 mL) was added dropwise at 0 °C. This was followed by dropwise addition of a solution of propargyl bromide (0.23 g, 1.90 mmol) in THF (2 mL) and the suspension was refluxed overnight. The mixture was filtered, concentrated *in vacuo*, dissolved in CH_2Cl_2 and extracted with H₂O and brine. The organics were dried with MgSO_4 , filtered and concentrated *in vacuo* to provide the compound as a clear oil (0.152 g, 87 %). Characterization was performed by method B.

IR(cm^{-1}): 3240 (C \equiv C-H stretch); 3000-2800 (C-H stretch); 2115 (C \equiv C stretch); 1090 (C-O stretch).

$^1\text{H-NMR}$ (300 MHz) CDCl_3 , δ_{H} (ppm): 2.42 (t, 1H, C \equiv CH, $^4J = 2.4$ Hz); 3.5-3.8 (m, 17H, O-CH-CH $_2$ -O); 4.18 (d, 2H, O-CH $_2$ -C \equiv C, $^4J = 2.4$ Hz).

$^{13}\text{C-NMR}$ (75 MHz) CDCl_3 , δ_{C} (ppm): 58.5 (1C, O-CH $_2$ -C \equiv C); 69.8, 70.1, 70.3, 70.5, 70.56, 70.59, 70.8, 71.5 (8C, CH $_2$ -O); 74.6 (1C, C \equiv C-H); 78.4 (1C, CH-O); 79.5 (1C, CH $_2$ -C \equiv CH).

Biotin prop-2-ynyl ester (51)

Biotin (0.75 g, 3.01 mmol), DMAP (0.11 g, 0.92 mmol) and propargyl alcohol (0.26 g, 4.60 mmol) were dissolved in CH_2Cl_2 (5 mL) at 0 °C, and a solution of DCC (0.64 g, 3.1 mmol) in CH_2Cl_2 (2 mL) was added dropwise under nitrogen. The reaction mixture was stirred overnight at room temperature, filtered, and concentrated *in vacuo*. The crude was dissolved in EtOAc, filtered, extracted with an aqueous solution of HCl (10%), NaHCO_3 and brine. The organic phase was dried with MgSO_4 , filtered and concentrated *in vacuo*. The crude product was purified by column chromatography EtOAc/MeOH (95:5). The product was obtained as a white solid (0.16 g, 19%, $T_{\text{m}} = 108$ °C). Characterization was performed by method B.

IR(cm^{-1}): 3440 (C \equiv C-H stretch); 3240 (NH stretch); 3100-2800 (C-H stretch); 2122 (C \equiv C stretch); 1730 (OC=O stretch); 1690 (NC=O stretch).

$^1\text{H-NMR}$ (300 MHz) CDCl_3 , δ_{H} (ppm): 1.43 (m, 2H, CH $_2$ -CH $_2$ -CH $_2$); 1.69 (m, 4H, SCH-CH $_2$, CH $_2$ -CH $_2$ COO); 2.39 (t, 2H, CH $_2$ CO, $^3J = 7.5$ Hz); 2.48 (t, 1H, C \equiv CH, $^4J = 2.5$ Hz); 2.74 (d, 1H, CH-CH $_2$ S diastereotopic, $^1J = 12.8$ Hz); 2.91 (dd, 1H, CH-CH $_2$ S diastereotopic, $^1J = 12.8$ Hz, $^3J = 5.0$ Hz); 3.15 (m, 1H, CH-CH(CH $_2$)-S); 4.31 (ddd, 1H, NH-CH(CH)-CH, $^3J = 1.0$ Hz, $^3J = 4.6$ Hz, $^3J = 7.7$ Hz); 4.50 (dd, 1H, NH-CH(CH)CH $_2$ S, $^3J = 5.0$ Hz, $^3J = 7.7$ Hz); 4.67 (d, 2H, OCH $_2$ -C \equiv CH, $^4J = 2.5$ Hz); 5.48 (s, 1H, NH); 5.98 (s, 1H, NH).

$^{13}\text{C-NMR}$ (75 MHz) CDCl_3 , δ_{C} (ppm): 24.7, 28.2, 28.4 (3C, CH $_2$ -CH $_2$); 33.7 (1C, CH $_2$ -COO); 40.6 (1C, CH $_2$ -S); 51.9 (1C, O-CH $_2$ -C \equiv C); 55.6 (1C, CH-S); 60.2, 62.0 (2C, NH-CH-CH-NH); 75.0 (1C, C \equiv CH); 77.9 (1C, CH $_2$ C \equiv CH); 164.1 (1C, CH $_2$ COOCH $_2$); 172.9 (1C, NH-CO-NH).

Bibliography

- (1) Kolb, H.; Finn, M.; Sharpless, K. *Angew. Chem., Int. Ed.* **2001**, *40*, 2004–2021.
- (2) Tornøe, C.; Christensen, C.; Meldal, M. *J. Org. Chem.* **2002**, *67*, 3057–3064.
- (3) Rostovtsev, V.; Green, L.; Fokin, V.; Sharpless, K. *Angew. Chem., Int. Ed.* **2002**, *41*, 2596–2599.
- (4) Huisgen, R. *Angew. Chem., Int. Ed.* **1963**, *2*, 565–598.
- (5) Meldal, M.; Tornøe, C. *Chem. Rev.* **2008**, *108*, 2952–3015.
- (6) Appukkuttan, P.; Dehaen, W.; Fokin, V.; Van der Eycken, E. *Org. Lett.* **2004**, *6*, 4223–4226.
- (7) Binder, W.; Sachsenhofer, R. *Macromol. Rapid Commun.* **2007**, *28*, 15–54.
- (8) Binder, W.; Sachsenhofer, R. *Macromol. Rapid Commun.* **2008**, *29*, 952–981.
- (9) Mantovani, G.; Ladmiral, V.; Tao, L.; Haddleton, D. *Chem. Commun.* **2005**, 2089–2091.
- (10) Opsteen, J.; van Hest, J. *Chem. Commun.* **2005**, 57–59.
- (11) Wu, P.; Feldman, A.; Nugent, A.; Hawker, C.; Scheel, A.; Voit, B.; Pyun, J.; Fréchet, J.; Sharpless, K.; Fokin, V. *Angew. Chem., Int. Ed.* **2004**, *43*, 3928–3932.
- (12) Wu, P.; Malkoch, M.; Hunt, J.; Vestberg, R.; Kaltgrad, E.; Finn, M.; Fokin, V.; Sharpless, K.; Hawker, C. *Chem. Commun.* **2005**, 5775–5777.
- (13) Parrish, B.; Breitenkamp, R.; Emrick, T. *J. Am. Chem. Soc.* **2005**, *127*, 7404–7410.
- (14) Sumerlin, B.; Tsarevsky, N.; Louche, G.; Lee, R.; Matyjaszewski, K. *Macromolecules* **2005**, *38*, 7540–7545.
- (15) Takizawa, K.; Nulwala, H.; Thibault, R.; Lowenhielm, P.; Yoshinaga, K.; Wooley, K.; Hawker, C. *J. Polym. Sci., Part A: Polym. Chem.* **2008**, *46*, 2897–2912.

- (16) Malkoch, M.; Thibault, R.; Drockenmuller, E.; Messerschmidt, M.; Voit, B.; Russell, T.; Hawker, C. *J. Am. Chem. Soc.* **2005**, *127*, 14942–14949.
- (17) Lundberg, P.; Hawker, C.; Hult, A.; Malkoch, M. *Macromol. Rapid Commun.* **2008**, *29*, 998–1015.
- (18) Li, H.; Cheng, F.; Duft, A.; Adronov, A. *J. Am. Chem. Soc.* **2005**, *127*, 14518–14524.
- (19) Voggu, R.; Suguna, P.; Chandrasekaran, S.; Rao, C. *Chem. Phys. Lett.* **2007**, *443*, 118–121.
- (20) Collman, J.; Devaraj, N.; Chidsey, C. *Langmuir* **2004**, *20*, 1051–1053.
- (21) Nandivada, H.; Chen, H.; Bondarenko, L.; Lahann, J. *Angew. Chem., Int. Ed.* **2006**, *45*, 3360–3363.
- (22) Rozkiewicz, D.; Janczewski, D.; Verboom, W.; Ravoo, B.; Reinhoudt, D. *Angew. Chem., Int. Ed.* **2006**, *45*, 5292–5296.
- (23) Michel, O.; Ravoo, B. *Langmuir* **2008**, *24*, 12116–12118.
- (24) Baskin, J.; Prescher, J.; Laughlin, S.; Agard, N.; Chang, P.; Miller, I.; Lo, A.; Codelli, J.; Bertozzi, C. *Proc. Natl. Acad. Sci. U. S. A.* **2007**, *104*, 16793–16797.
- (25) Campos, L.; Killops, K.; Sakai, R.; Paulusse, J.; Dameron, D.; Drockenmuller, E.; Messmore, B.; Hawker, C. *Macromolecules* **2008**, *41*, 7063–7070.
- (26) David, R.; Kornfield, J. *Macromolecules* **2008**, *41*, 1151–1161.
- (27) Cammas, S.; Nagasaki, Y.; Kataoka, K. *Bioconjugate Chem.* **1995**, *6*, 226–230.
- (28) Hiki, S.; Kataoka, K. *Bioconjugate Chem.* **2007**, *18*, 2191–2196.
- (29) Killops, K.; Campos, L.; Hawker, C. *J. Am. Chem. Soc.* **2008**, *130*, 5062–5064.
- (30) Nilsson, C.; Simpson, N.; Malkoch, M.; Johansson, M.; Malmström, E. *J. Polym. Sci., Part A: Polym. Chem.* **2008**, *46*, 1339–1348.
- (31) Boutevin, B.; Hervaud, Y.; Moulédous, G. *Polym. Bull.* **1998**, *41*, 145–151.
- (32) ten Brummelhuis, N.; Diehl, C.; Schlaad, H. *Macromolecules* **2008**, *41*, 9946–9947.
- (33) Hordyjewicz-Baran, Z.; You, L.; Smarsly, B.; Sigel, R.; Schlaad, H. *Macromolecules* **2007**, *40*, 3901–3903.

- (34) Gress, A.; Volkel, A.; Schlaad, H. *Macromolecules* **2007**, *40*, 7928–7933.
- (35) Burget, D.; Mallein, C.; Fouassier, J. *Polymer* **2004**, *45*, 6561–6567.
- (36) Campos, L.; Meinel, I.; Guino, R.; Schierhorn, M.; Gupta, N.; Stucky, G.; Hawker, C. *Adv. Mater.* **2008**, *20*, 3728–3733.
- (37) Zeng, S.; Chen, C.; Mikkelsen, J.; Santiago, J. *Sens. Actuators, B* **2001**, *79*, 107–114.
- (38) Thomsen, A.; Malmström, E.; Hvilsted, S. *J. Polym. Sci., Part A: Polym. Chem.* **2006**, *44*, 6360–6377.
- (39) Daugaard, A.; Hvilsted, S. *Macromol. Rapid Commun.* **2008**, *29*, 1119–1125.
- (40) Gao, B.; Chen, X.; Ivan, B.; Kops, J.; Batsberg, W. *Macromol. Rapid Commun.* **1997**, *18*, 1095–1100.
- (41) Chen, X.; Jankova, K.; Kops, J.; Batsberg, W. *J. Polym. Sci., Part A: Polym. Chem.* **1999**, *37*, 627–633.
- (42) Braun, D.; Cerwinski, W.; Disselhoff, F.; Tüdös, F.; Kelen, T.; Turcsanyi, B. *Angew. Makromol. Chem.* **1984**, *125*, 161–205.
- (43) Walling, C.; Briggs, E.; Wolfstirn, K.; Mayo, F. *J. Am. Chem. Soc.* **1948**, *70*, 1537–1542.
- (44) Kennedy, J.; Kelen, T.; Tüdös, F. *J. Polym. Sci., Part A: Polym. Chem.* **1975**, *13*, 2277–2289.
- (45) Kelen, T.; Tüdös, F. *J. Macromol. Sci., Chem.* **1975**, *A 9*, 1–27.
- (46) Murthy, S. *J. Polym. Sci., Part B: Polym. Phys.* **1993**, *31*, 475–480.
- (47) Conlon, D.; Crivello, J.; Lee, J.; O'Brien, M. *Macromolecules* **1989**, *22*, 509–516.
- (48) Dimitrov, I.; Jankova, K.; Hvilsted, S. In preparation.
- (49) InPhase Technologies; visited 28.01.2009; <<http://www.inphase-technologies.com>>.
- (50) Haw, M. *Nature* **2003**, *422*, 556–558.
- (51) Zilker, S. *ChemPhysChem* **2002**, *3*, 333–334.
- (52) Trentler, T.; Boyd, J.; Colvin, V. *Chem. Mater.* **2000**, *12*, 1431–1438.

- (53) Schilling, M.; Colvin, V.; Dhar, L.; Harris, A.; Schilling, F.; Katz, H.; Wysocki, T.; Hale, A.; Blyler, L.; Boyd, C. *Chem. Mater.* **1999**, *11*, 247–254.
- (54) Schnoes, M.; Dhar, L.; Schilling, M.; Patel, S.; Wiltzius, P. *Opt. Lett.* **1999**, *24*, 658–660.
- (55) Khan, A.; Daugaard, A.; Bayles, A.; Koga, S.; Miki, Y.; Sato, K.; Enda, J.; Hvilsted, S.; Stucky, G.; Hawker, C. *Chem. Commun.* **2009**, 425–427.
- (56) Sanda, F.; Endo, T. *J. Polym. Sci., Part A: Polym. Chem.* **2001**, *39*, 265–276.
- (57) Mourey, T.; Turner, S.; Rubinstein, M.; Fréchet, J.; Hawker, C.; Wooley, K. *Macromolecules* **1992**, *25*, 2401–2406.
- (58) Wooley, K.; Hawker, C.; Fréchet, J. *J. Am. Chem. Soc.* **1991**, *113*, 4252–4261.
- (59) Wooley, K.; Hawker, C.; Fréchet, J. *J. Chem. Soc. Perk. Trans. 1* **1991**, 1059–1076.
- (60) *Holographic data storage*; Coufal, H., Psaltis, D., Sincerbox, G., Eds.; Springer: New York, 2000; Vol. 76.
- (61) Dhar, L.; Schnoes, M.; Wysocki, T.; Bair, H.; Schilling, M.; Boyd, C. *Appl. Phys. Lett.* **1998**, *73*, 1337–1339.
- (62) Katritzky, A.; Sild, S.; Karelson, M. *J. Chem. Inf. Comput. Sci.* **1998**, *38*, 840–844.
- (63) *CRC Handbook of Chemistry and Physics*, 89th ed.; Lide, D., Ed.; CRC Press/Taylor and Francis: Boca Raton, FL, 2008–2009.
- (64) Ochiai, B.; Endo, T. *J. Polym. Sci., Part A: Polym. Chem.* **2007**, *45*, 2827–2834.
- (65) Bailey, W.; Ni, Z.; Wu, S. *Macromolecules* **1982**, *15*, 711–714.
- (66) Wickel, H.; Agarwal, S. *Macromolecules* **2003**, *36*, 6152–6159.
- (67) Evans, R.; Moad, G.; Rizzardo, E.; Thang, S. *Macromolecules* **1994**, *27*, 7935–7937.
- (68) Zhang, L.; Chen, X.; Xue, P.; Sun, H.; Williams, I.; Sharpless, K.; Fokin, V.; Jia, G. *J. Am. Chem. Soc.* **2005**, *127*, 15998–15999.
- (69) Rasmussen, L.; Boren, B.; Fokin, V. *Org. Lett* **2007**, *9*, 5337–5339.

- (70) Boren, B.; Narayan, S.; Rasmussen, L.; Zhang, L.; Zhao, H.; Lin, Z.; Jia, G.; Fokin, V. *J. Am. Chem. Soc.* **2008**, *130*, 8923–8930.
- (71) Majireck, M.; Weinreb, S. *J. Org. Chem.* **2006**, *71*, 8680–8683.
- (72) Inzelt, G.; Pineri, M.; Schultze, J.; Vorotyntsev, M. *Electrochim. Acta* **2000**, *45*, 2403–2421.
- (73) McQuade, D.; Pullen, A.; Swager, T. *Chem. Rev.* **2000**, *100*, 2537–2574.
- (74) Ali, E.; Kantchev, E.; Yu, H.; Ying, J. *Macromolecules* **2007**, *40*, 6025–6027.
- (75) Bäuerle, P.; Scheib, S. *Adv. Mater.* **1993**, *5*, 848–853.
- (76) Scheib, S.; Bäuerle, P. *J. Mater. Chem.* **1999**, *9*, 2139–2150.
- (77) Youssoufi, H.; Hmyene, M.; Garnier, F.; Delabouglise, D. *J. Chem. Soc., Chem. Commun.* **1993**, 1550–1552.
- (78) McCullough, R.; Williams, S. *J. Am. Chem. Soc.* **1993**, *115*, 11608–11609.
- (79) Migdalski, J.; Blaz, T.; Lewenstam, A. *Anal. Chim. Acta* **1996**, *322*, 141–149.
- (80) Groenendaal, B.; Jonas, F.; Freitag, D.; Pielartzik, H.; Reynolds, J. *Adv. Mater.* **2000**, *12*, 481–494.
- (81) Ahuja, T.; Mir, I.; Kumar, D.; Rajesh, *Biomaterials* **2007**, *28*, 791–805.
- (82) Higgins, S.; Mouffouk, F. International Patent WO2006018643–A2, 2006.
- (83) Rahman, M.; Park, D.; Chang, S.; McNeil, C.; Shim, Y. *Biosens. Bioelectron.* **2006**, *21*, 1116–1124.
- (84) Daugaard, A.; Hvilsted, S.; Hansen, T.; Larsen, N. *Macromolecules* **2008**, *41*, 4321–4327.
- (85) Winther-Jensen, B.; Breiby, D.; West, K. *Synth. Met.* **2005**, *152*, 1–4.
- (86) Bu, H.; Götz, G.; Reinold, E.; Vogt, A.; Schmid, S.; Blanco, R.; Segura, J.; Bäuerle, P. *Chem. Commun.* **2008**, 1320–1322.
- (87) Borkar, S.; Jankova, K.; Siesler, H.; Hvilsted, S. *Macromolecules* **2004**, *37*, 788–794.
- (88) Lakshmi, K.; John, H.; Joseph, R.; George, K.; Mathew, K. *Microw. Opt. Tech. Lett.* **2008**, *50*, 504–508.

-
- (89) Yussuf, A.; Sbarski, I.; Hayes, J.; Solomon, M.; Tran, N. *J. Micromech. Microeng.* **2005**, *15*, 1692–1699.
- (90) Hansen, T.; West, K.; Hassager, O.; Larsen, N. *J. Micromech. Microeng.* **2007**, *17*, 860–866.
- (91) Devaraj, N.; Dinolfo, P.; Chidsey, C.; Collman, J. *J. Am. Chem. Soc.* **2006**, *128*, 1794–1795.
- (92) Kim, J.; McQuade, D.; McHugh, S.; Swager, T. *Angew. Chem., Int. Ed.* **2000**, *39*, 3868–3872.
- (93) Raba, J.; Mottola, H. *Crit. Rev. Anal. Chem.* **1995**, *25*, 1–42.
- (94) Cass, A.; Davis, G.; Francis, G.; Hill, H.; Aston, W.; Higgins, I.; Plotkin, E.; Scott, L.; Turner, A. *Anal. Chem.* **1984**, *56*, 667–671.
- (95) Zhao, G.; Xu, M.; Zhang, Q. *Electrochem. Commun.* **2008**, *10*, 1924–1926.
- (96) Urban, G. *Meas. Sci. Technol.* **2009**, *20*, 012001.

Appendices

Appendix A

A.D. Thomsen, E. Malmström, S. Hvilsted. “Novel Polymers with a High Carboxylic Acid Loading”. *Journal of Polymer Science: Part A: Polymer Chemistry* **2006**, *44*, 6360–6377.

Novel Polymers with a High Carboxylic Acid Loading

ANDERS D. THOMSEN,¹ EVA MALMSTRÖM,² SØREN HVILSTED¹

¹Danish Polymer Centre, Department of Chemical Engineering, Technical University of Denmark, Building 423, DK-2800 Kgs. Lyngby, Denmark

²KTH Fibre and Polymer, School of Chemical Science and Engineering, Royal Institute of Technology, Stockholm, Sweden

Received 26 June 2006; accepted 8 August 2006

DOI: 10.1002/pola.21730

Published online in Wiley InterScience (www.interscience.wiley.com).

ABSTRACT: Click chemistry has been used to prepare a range of novel polymers with pendant carboxylic acid side groups. Four azido carboxylic acids, either mono- or difunctional and aliphatic or aromatic, have been prepared and thoroughly characterized. Extensive model reactions with 1-ethyl-4-hydroxybenzene, the simplest model for poly(4-hydroxystyrene), and the four azido carboxylic acids have been conducted to establish the proper reaction conditions and provide an analytical frame for the corresponding polymers. Poly(4-hydroxystyrene) moieties in three different polymers—poly(4-hydroxystyrene), poly(4-hydroxystyrene-co-methyl methacrylate), and poly(4-hydroxystyrene-*b*-styrene)—have been quantitatively transformed into oxypropynes by the use of either Williamson or Mitsunobu strategies and subsequently reacted with the azido carboxylic acids. Detailed differential scanning calorimetry investigations of all the polymers in general exhibit [when poly(4-hydroxystyrene) is a substantial part] significant changes in the glass-transition temperature from the polar poly(4-hydroxystyrene) (120–130 °C) to the much less polar alkyne polymers (46–60 °C). A direct correlation between the nature of the pendant groups in the derivatized polymers and the glass-transition temperature has emerged: the aromatic carboxylic acids give high glass-transition temperatures (90–120 °C), and the aliphatic carboxylic acids give lower glass-transition temperatures (50–65 °C). © 2006 Wiley Periodicals, Inc. *J Polym Sci Part A: Polym Chem* 44: 6360–6377, 2006

Keywords: block copolymers; carboxylic acids; click chemistry; functionalization of polymers; glass transition; polystyrene

INTRODUCTION

Functional block copolymers with a predetermined composition and functionality can be made by several routes. Living anionic or controlled radical polymerization techniques often allow the design of precise architectures with specific functionality provided that the proper monomers can be polymerized. Another possibility is the modular approach via the coupling of different pre-

formed polymers. A third possibility is the use of precursor scaffold polymers, into which the desired functionality is introduced through postfunctionalization reactions. This last method, however, requires chemical reaction strategies that perform irreversibly in a 100% yield. Recently developed click chemistry,¹ especially Huisgen's² 1,3-dipolar cycloaddition between azides and alkynes, revived through Cu(I) catalysis,^{3,4} has proved very versatile for the synthesis of polymers.⁵ Among the first to apply click chemistry in macromolecular chemistry were Finn et al.,⁶ who used cycloaddition to form a polymer as an adhesive between two copper plates. Subsequently, polymers have been

Correspondence to: S. Hvilsted (E-mail: sh@kt.dtu.dk)

Journal of Polymer Science: Part A: Polymer Chemistry, Vol. 44, 6360–6377 (2006)
© 2006 Wiley Periodicals, Inc.

end-functionalized,⁷ functional polymers have been coupled,^{8,9} dendritic polymers have been prepared,¹⁰ and protected alkyne monomers,¹¹ azide monomers, and azide initiators¹² have been polymerized and applied through click chemistry. Linear polymers have been functionalized with dendrons¹³ and poly(ethylene glycol)s,¹⁴ and even simultaneous orthogonal ester and click reactions on polymer backbones have been performed,¹⁵ clearly highlighting the potential of click chemistry. For applications in electro-osmotic (EO) micropumps, proton-donating polymers are especially interesting. EO micropumps are based on the formation of a mobile charge layer (Debye layer) on a surface. The Debye layer will move in the presence of an electrical field and by viscous drag move an electrically neutral liquid. Traditionally, the Debye layer is created on the surface of glass particles, where proton donation creates a charged surface. As an alternative, we are testing the application of proton-donating polymers on a surface. Carboxylic acid containing polymers cannot be made by atom transfer radical polymerizations of the acid monomers because the carboxylic acid interacts with the catalyst, and thus they have to be made through protected acryl- or styrene-based monomers, followed by a deprotection step, or from the respective carboxylate salts, which yield carboxylic acids directly on the polymer backbone.¹⁶ In light of the recent advances within click chemistry, an alternative and highly efficient postfunctionalization method has appeared with fewer limitations for the polymer backbone; therefore, we decided to use click chemistry to functionalize polymer scaffolds. This strategy has proved very flexible in terms of the degree of functionality of the backbone, the number of carboxylic acids per polymer repeat unit, and a possible change in the length of the flexible spacer, as indicated by the double-headed arrows shown in Scheme 1.

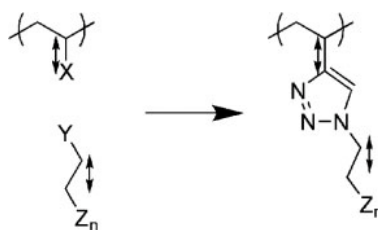
We here present the versatility of the concept that we believe in principle can be extended to almost all chemical functionalities.

EXPERIMENTAL

General Laboratory Practice

All compounds were characterized with IR spectroscopy, ¹H NMR, and ¹³C NMR. The polymers were additionally characterized with size exclusion chromatography (SEC) and differential scanning calorimetry (DSC). The reactions were monitored with thin-layer chromatography (TLC), IR,

Journal of Polymer Science: Part A: Polymer Chemistry
DOI 10.1002/pola



Scheme 1. Precursor scaffold strategy based on click-chemistry postfunctionalization. X and Y represent the azides and alkynes, respectively, and Z represents the functional group(s).

or NMR. TLC was run on a Merck Kieselgel 60 (F₂₅₄) on aluminum sheets.

IR Spectroscopy

The IR analysis was performed on a PerkinElmer Spectrum One model 2000 Fourier transform infrared system with a universal attenuated total reflection sampling accessory on a ZnSe/diamond composite. Sixteen scans were used for all samples, with a resolution of 4 cm⁻¹ in the range from 525 to 4000 cm⁻¹.

NMR Spectroscopy

NMR experiments were performed on a Bruker Avance 400-MHz NMR instrument. ¹H NMR spectra were acquired with a spectral window of 20 ppm, an acquisition time of 4 s, and a relaxation delay of 1 s. ¹³C NMR spectra were acquired with a spectral window of 240 ppm, an acquisition time of 0.7 s, and a relaxation delay of 2 s. Nuclear Overhauser and exchange spectroscopy (NOESY) was performed with a relaxation time of 2 s on nonpolymeric compounds and with a relaxation time of 0.3 s on polymers. Spectra have been referenced in accordance with Gottlieb et al.¹⁷ In the assignment of the shifts, the protons and carbons are numbered starting from the polymer backbone or its equivalent, as shown later in Scheme 3. The numbering in the azides starts from the azide functionality.

SEC

Two different systems were used, both with tetrahydrofuran (THF) as the mobile phase. With system one, SEC was performed in THF at 35 °C with a Viscotek TDA model 301 equipped with two GMHHR-M columns with TSKgel (mixed bed, molecular weight resolving range = 300–

100,000) from Tosoh Biosep, a VE 5200 GPC auto-sampler, a VE 1121 GPC solvent pump, and a VE 5710 GPC degasser (all from Viscotek Corp.). Corrections for the flow rate fluctuations were made with toluene as an internal standard. Viscotek OmniSEC (version 4.0) software was used to process data. With system two, SEC analysis was performed in THF with or without an Irganox standard on a system with a Shimadzu SIL-10AD auto injector and a Shimadzu LC10AD pump operating on two columns. Both columns were Polymer Laboratories PLgel 5- μ m Mixed-D (300×7.5 mm). The detector was a Viscotek model 200 differential refractometer. For each sample, approximately 1–5 mg of the compound was dissolved in 1 mL of THF, the injection volume was 100 μ L, and a flow rate of 1 mL/min was used for the analyses. The number-average molecular weight (M_n) and polydispersity index (PDI) values were determined with either polystyrene (PS) standards or universal calibration.

DSC

DSC thermograms were collected with a Mettler–Toledo DSC820 or a DSCQ1000 differential scanning calorimeter from TA Instruments. The thermal analysis was performed at a heating and cooling rate of 10 $^{\circ}$ C min $^{-1}$. The melting temperatures (T_m 's) are reported as the peak temperatures of the endothermal melting peaks. The glass-transition temperatures (T_g 's) were measured at the inflection point.

Chemicals

Chemicals were acquired from Aldrich and were used as received unless otherwise specified. Polymers poly(4-hydroxystyrene) (PHS) and poly(4-hydroxystyrene-*co*-methyl methacrylate) (PHS-*co*-PMMA), were from Aldrich, whereas poly(4-butoxystyrene-*b*-styrene) was synthesized by living anionic polymerization.¹⁸ Diethyl ether, acetone, THF, and dimethylformamide (DMF) were dried with 4-Å molecular sieves. Silica gel 60 (35–70 μ m) was used for flash chromatography and medium-pressure liquid chromatography. CuP(OEt)₃I was provided by Andreas Nyström, KTH.

General Procedure for Azide Syntheses in DMF

4-(Azidomethane)benzoic Acid (1)

4-(Bromomethyl)benzoic acid (2.95 g, 12.9 mmol) and NaN₃ (2.59 g, 39.8 mmol) were dissolved in DMF (100 mL). The solution was stirred at

110 $^{\circ}$ C under N₂ overnight. The heating was turned off, and the reaction was stopped by the dropwise addition of aqueous HCl (10 mL, pH = 1; caution: HN₃ is formed and can be removed by a stream of N₂ bubbled through a concentrated aqueous solution of KOH).¹⁹ The solution was stirred until the temperature had decreased to room temperature. The solution was extracted with ethyl acetate (EtOAc; 4 \times 50 mL), and the combined EtOAc phases were extracted with aqueous HCl (5 \times 50 mL, pH = 1) and with brine (1 \times 50 mL). The organic phase was dried with MgSO₄, filtered, and concentrated *in vacuo*. **1** was isolated as a white, crystalline compound (2.11 g, 86%, T_m = 134 $^{\circ}$ C).

IR (cm $^{-1}$): 3400–2300 (COO–H stretching); 3000–2850 (C–H stretching); 2107 (N $^{-}$ =N $^{+}$ =N stretching); 1677 (HOC=O stretching); 1290 (OC–OH stretching); 932 (O–H out-of-plane bending); 841 (para-substituted Ar–H out-of-plane bending). ¹H NMR [dimethyl sulfoxide-*d*₆ (DMSO-*d*₆), 400 MHz, δ_H , ppm]: 3.71 (s, 2H, H₁); 6.63 (d, 2H, H₃, ³*J* = 8.3 Hz); 7.12 (d, 2H, H₄, ³*J* = 8.3 Hz); 12.15 (s, 1H, H₆). ¹³C NMR (DMSO-*d*₆, 100 MHz, δ_C , ppm): 53.1 (C₁); 128.3 (C₃), 129.7 (C₄); 130.5 (C₅); 140.6 (C₂); 167.0 (C₆).

6-Azidohexanoic Acid (2)

6-Bromohexanoic acid (6.00 g, 30.8 mmol) and NaN₃ (5.38 g, 82.8 mmol) were reacted according to the general procedure for azide synthesis. **2** was isolated as a transparent oil (4.49 g, 93%).

IR (cm $^{-1}$): 3400–2300 (COO–H stretching); 3000–2850 (C–H stretching); 2091 (N $^{-}$ =N $^{+}$ =N stretching); 1705 (HOC=O stretching); 1254 (OC–OH stretching); 931 (O–H out-of-plane bending). ¹H NMR (DMSO-*d*₆, 400 MHz, δ_H , ppm): 1.41 (m, 2H, H₃); 1.64 (m, 4H, H_{2,4}); 2.35 (t, 2H, H₅, ³*J* = 7.4 Hz); 3.25 (t, 2H, H₁, ³*J* = 6.8 Hz); 10.54 (s, 1H, H₆); the assignment has been corroborated with a correlation spectroscopy (COSY) spectrum. ¹³C NMR (DMSO-*d*₆, 100 MHz, δ_C , ppm): 24.3 (C₄), 26.2 (C₃); 28.6 (C₂); 33.9 (C₅); 51.3 (C₁); 179.5 (C₆).

5-(6-Azidohexoxy)isophthalic Acid (3)

Dimethyl 5-hydroxyisophthalate (3.98 g, 18.9 mmol), K₂CO₃ (2.27 g, 22.7 mmol), and tetrabutylammonium bromide (TBAB; 0.61 g, 1.89 mmol) were dissolved in dry DMF (15 mL) and heated to 60 $^{\circ}$ C. 1,6-Dibromohexane (8.07 mL, 53.0 mmol) was added to the refluxing solution, and the reaction was monitored with TLC. The reaction was

stopped after 5 days of reaction. The crude product was purified with column chromatography, eluting with a gradient from 1:9 EtOAc/heptane to 1:4 EtOAc/heptane. Dimethyl 5-(6-bromohexoxy)isophthalate was isolated as a colorless oil (3.58 g, 51%).

IR (cm^{-1}): 3000–2850 (C–H stretching); 1716 (MeOC=O stretching); 1591 (C=C stretching); 1240, 1229 (Ph–O, OC–OMe stretching); 1041 (C–O stretching); 873, 670 (1,3,5-substituted Ar–H out-of-plane bending); 648 (C–Br stretching). ^1H NMR (CDCl_3 , 400 MHz, δ_{H} , ppm): 1.5 (m, 4H, $\text{H}_{3,4}$); 1.81 (m, 2H, H_5); 1.89 (m, 2H, H_2); 3.41 (t, 2H, H_1 , $^3J = 6.8$ Hz); 3.92 (s, 6H, H_{12}); 4.03 (t, 2H, H_6 , $^3J = 6.3$ Hz); 7.71 (s, 2H, H_8); 8.24 (s, 1H, H_{10}); the assignment has been corroborated with a COSY spectrum. ^{13}C NMR (CDCl_3 , 100 MHz, δ_{C} , ppm): 25.3 (C_4); 29.0 (C_5); 32.8 (C_2); 33.8 (C_1); 52.5 (C_{12}); 68.4 (C_6); 120.0 (C_8); 122.9 (C_{10}); 131.8 (C_9); 159.2 (C_7); 166.3 (C_{11}).

Dimethyl 5-(6-bromohexoxy)isophthalate (4.97 g, 0.013 mol) was reacted with NaN_3 (2.18 g, 0.335 mmol) at 0 °C according to the general procedure for azide synthesis, and dimethyl 5-(6-azidohexoxy)isophthalate was isolated as a pale yellow oil without further purification (4.32 g, 97%).

IR (cm^{-1}): 3000–2850 (C–H stretching); 2093 ($\text{N}^-=\text{N}^+=\text{N}$ stretching); 1721 (MeOC=O stretching); 1682, 1595 (C=C stretching); 1235 (Ph–O, OC–OMe stretching); 1044 (C–O stretching); 875, 673 (1,3,5-substituted Ar–H out-of-plane bending). ^1H NMR (CDCl_3 , 400 MHz, δ_{H} , ppm): 1.5 (m, 4H, $\text{H}_{3,4}$); 1.63 (m, 2H, H_2); 1.82 (m, 2H, H_5); 3.28 (t, 2H, H_1 , $^3J = 6.9$ Hz); 3.92 (s, 6H, H_{12}); 4.03 (t, 2H, H_6 , $^3J = 6.3$ Hz); 7.72 (d, 2H, H_8 , $^4J = 1.4$ Hz); 8.24 (d, 1H, H_{10} , $^4J = 1.4$ Hz); the assignment has been corroborated with a COSY spectrum. ^{13}C NMR (CDCl_3 , 100 MHz, δ_{C} , ppm): 25.7 (C_4); 26.6 (C_3); 28.9 (C_2); 29.1 (C_5); 51.5 (C_1); 52.5 (C_{12}); 68.4 (C_6); 119.9 (C_8); 122.9 (C_{10}); 131.8 (C_9); 159.2 (C_7); 166.3 (C_{11}).

Dimethyl 5-(6-azidohexoxy)isophthalate (2.43 g, 72.5 mmol) was dissolved in EtOH (20 mL) and 2 N NaOH (20 mL) and was refluxed for 8.5 h. EtOH was removed *in vacuo*, and the residue was diluted with H_2O (10 mL). The aqueous phase was made acidic to pH = 1–2 with concentrated HCl, and **3** was isolated as a white, crystalline compound by filtration and dried *in vacuo* (1.89 g, 85%, $T_m = 216$ °C).

IR (cm^{-1}): 3400–2300 (COO–H stretching); 3000–2850 (C–H); 2089 ($\text{N}^-=\text{N}^+=\text{N}$); 1705, 1685 (HOC=O); 1593 (C=C stretching); 1271

(Ph–O, OC–OH); 1045 (O–CH stretching); 931 (O–H out-of-plane bending); 885, 686 (1,3,5-substituted Ar–H out-of-plane bending). ^1H NMR (CDCl_3 , 400 MHz, δ_{H} , ppm): 1.41 (m, 4H, $\text{H}_{3,4}$); 1.55 (m, 2H, H_2); 1.73 (m, 2H, H_5); 3.32 (t, 2H, H_1 , $^3J = 6.8$ Hz); 4.06 (t, 2H, H_6 , $^3J = 6.4$ Hz); 7.62 (d, 2H, H_8 , $^4J = 1.4$ Hz); 8.05 (d, 1H, H_{10} , $^4J = 1.4$ Hz); 13.27 (s, 2H, H_{11}); the assignment has been corroborated with a COSY spectrum. ^{13}C NMR (CDCl_3 , 100 MHz, δ_{C} , ppm): 25.0 (C_4); 25.9 (C_3); 28.3 (C_2); 28.5 (C_5); 50.7 (C_1); 68.0 (C_6); 119.0 (C_8); 122.2 (C_{10}); 132.7 (C_9); 158.8 (C_7); 166.5 (C_{11}).

2-(6-Azidohexyl)malonic Acid (4)

Diethyl 2-(6-bromohexyl)malonate, prepared according to Salmon-Legagneur et al.,²⁰ (20.01 g, 61.9 mmol) was reacted with NaN_3 (10.06 g, 154.7 mmol) according to the general procedure for azide synthesis but at 0 °C. Diethyl 2-(6-azidohexyl)malonate was isolated as a transparent oil (17.39 g, 99%).

IR (cm^{-1}): 3000–2850 (C–H stretching); 2093 ($\text{N}^-=\text{N}^+=\text{N}$ stretching); 1749, 1730 (EtOC=O stretching); 1240 (OC–OEt stretching); 1031 (O–Et stretching); 728 (long-chain band). ^1H NMR (CDCl_3 , 400 MHz, δ_{H} , ppm): 1.25 (t, 6H, H_{10} , $^3J = 7.1$ Hz); 1.34 (m, 6H, $\text{H}_{3,4,5}$); 1.57 (p, 2H, H_2 , $^3J = 7.0$ Hz); 1.88 (dt, 2H, H_6 , $^3J = 7.3$, 7.4 Hz); 3.24 (t, 2H, H_1 , $^3J = 6.9$ Hz); 3.29 (t, 1H, H_7 , $^3J = 7.5$ Hz); 4.17 (q, 4H, H_9 , $^3J = 7.1$ Hz); the assignment has been corroborated with a COSY spectrum. ^{13}C NMR (CDCl_3 , 100 MHz, δ_{C} , ppm): 14.2 (C_{10}); 26.5 (C_4); 27.2 (C_5); 28.7 (C_3); 28.8 (C_6); 28.8 (C_2); 51.4 (C_1); 52.1 (C_7); 61.4 (C_9); 169.6 (C_8).

Diethyl 2-(6-azidohexyl)malonate (8.51 g, 29.8 mmol) was dissolved in a mixture of EtOH (75 mL) and 2 N NaOH (75 mL). The reaction mixture was stirred at the refluxing temperature for 5 h and monitored by TLC [95:5 EtOAc/methanol (MeOH) plus two to three drops of concentrated HCl]. EtOH was removed *in vacuo*, and the residual aqueous solution was extracted with CH_2Cl_2 (30 mL). The aqueous phase was acidified to pH = 1–2 with concentrated HCl. The aqueous phase was extracted with CH_2Cl_2 (3 × 30 mL). The combined organics were dried with MgSO_4 , filtered, and concentrated *in vacuo*. **4** was isolated as a white, crystalline compound (5.86 g, 86%, $T_m = 58$ °C).

IR (cm^{-1}): 3500–2400 (COO–H stretching); 3000–2850 (C–H stretching); 2088 ($\text{N}^-=\text{N}^+=\text{N}$)

stretching); 1699 (HOC=O stretching); 1292 (OC—OH stretching); 929 (O—H out-of-plane bending); 727 (long-chain band). ^1H NMR (CDCl_3 , 400 MHz, δ_{H} , ppm): 1.38 (m, 6H, $\text{H}_{3,4,5}$); 1.60 (m, 2H, H_2); 1.94 (m, 2H, H_6); 3.26 (t, 2H, H_1 , $^3J = 6.9$ Hz); 3.44 (t, 1H, H_7 , $^3J = 7.4$ Hz); 10.42 (s, 2H, H_8); the assignment has been corroborated with a COSY spectrum. ^{13}C NMR (CDCl_3 , 100 MHz, δ_{C} , ppm): 26.2 (C_4); 26.9 (C_5); 28.4 (C_3); 28.5 ($\text{C}_{2,6}$); 51.2 (C_1); 51.5 (C_7); 175.0 (C_8).

General Alkyne Synthesis Procedure: 1-Ethyl-4-(prop-2-ynoxy)benzene (5)

4-Ethylphenol (8.01 g, 65.6 mmol) was dissolved in THF (100 mL), 18-crown-6-ether (0.70 g, 2.65 mmol) and K_2CO_3 (9.87 g, 98.7 mmol) were added, and the solution was heated to reflux. After 1 h, propargyl bromide (80% in toluene, 9.5 mL, 91.8 mmol) was added, and the reaction was left stirring at the refluxing temperature for 17 h and monitored with TLC (3:7 EtOAc/heptane plus two to three drops of concentrated HCl). The crude reaction mixture was filtered and evaporated to dryness *in vacuo*. The residue was dissolved in CH_2Cl_2 (100 mL), washed with H_2O (2×50 mL) and brine (1×50 mL), and dried with MgSO_4 . The heterogeneous mixture was filtered, and the solution was concentrated *in vacuo* for 1 h to remove traces of propargyl bromide (bp = 90 °C). **5** was isolated as a yellow oil (9.82 g, 94%).

IR (cm^{-1}): 3293 (C≡C—H stretching); 3000–2850 (C—H stretching); 2122 (C≡C stretching); 1609, 1509 (C=C stretching); 1214 (Ph—O stretching); 1028 (CH_2 —O stretching); 827 (para-substituted Ar—H out-of-plane bending). ^1H NMR (CDCl_3 , 400 MHz, δ_{H} , ppm): 1.26 (t, 3H, H_1 , $^3J = 7.6$ Hz); 2.54 (t, 1H, H_9 , $^3J = 2.4$ Hz); 2.645 (q, 2H, H_2 , $^3J = 7.6$ Hz); 4.70 (d, 2H, H_7 , $^3J = 2.4$ Hz); 6.95 (d, 2H, H_5 , $^3J = 8.7$ Hz); 7.17 (d, 2H, H_4 , $^3J = 8.7$ Hz). ^{13}C NMR (CDCl_3 , 100 MHz, δ_{C} , ppm): 15.9 (C_1); 28.1 (C_2); 56.0 (C_7); 75.4 (C_9); 78.9 (C_8); 114.9 (C_5); 128.8 (C_4); 137.4 (C_3); 155.7 (C_6); the assignment has been corroborated with a heteronuclear multiple quantum coherence (HMQC) NMR spectrum.

General Procedure for Model Click Reactions in DMF: 1-(4-Carboxybenzyl)-1H-1,2,3-triazol-4-[methyloxy(4-ethylbenzene)] (6)

5 (55.0 mg, 0.34 mmol) and CuBr (29.1 mg, 0.20 mmol) were dissolved in evacuated DMF (1.5 mL). The reaction flask was degassed and

backfilled with Ar three times, and this produced a yellow solution. In parallel, **1** (61.0 mg, 0.34 mmol) was dissolved in degassed DMF (1.5 mL) to give a colorless solution, which was transferred to the reaction flask with an Ar-purged syringe. The reaction was left under Ar and followed by TLC (6:4 EtOAc/heptane plus two to three drops of concentrated HCl). After 2 h, the azide had been consumed, and the color of the solution had changed to green. The reaction mixture was diluted with H_2O (10 mL) and EtOAc (20 mL), and concentrated HCl was added until the pH was 1. The phases were separated, and the H_2O /DMF phase was extracted with EtOAc (5×10 mL). The combined organic phases were extracted with brine (1×25 mL), dried with MgSO_4 , filtered, and concentrated *in vacuo* to give **6** as a white, crystalline compound (92.0 mg, 79%, $T_{\text{m}} = 197$ °C).

IR (cm^{-1}): 3400–2300 (COO—H stretching); 3000–2850 (C—H stretching); 1685 (HOC=O stretching); 1612, 1515 (C=C stretching); 1255 (Ph—O stretching); 1050 (C—O stretching); 941 (O—H out-of-plane bending); 829 (para-substituted Ar—H out-of-plane bending). ^1H NMR ($\text{DMSO}-d_6$, 400 MHz, δ_{H} , ppm): 1.19 (t, 3H, H_1 , $^3J = 7.6$ Hz); 2.58 (t, 2H, H_2 , $^3J = 7.6$ Hz); 5.16 (s, 2H, H_7); 5.76 (s, 2H, H_{10}); 6.98 (d, 2H, H_4 , $^3J = 8.6$ Hz); 7.17 (d, 2H, H_5 , $^3J = 8.6$ Hz); 7.44 (d, 2H, H_{12} , $^3J = 8.2$ Hz); 7.99 (d, 2H, H_{13} , $^3J = 8.2$ Hz); 8.35 (s, 1H, H_9); 13.09 (s, 1H, H_{15}); the assignment has been corroborated with a COSY and two NOESY spectra. ^{13}C NMR ($\text{DMSO}-d_6$, 100 MHz, δ_{C} , ppm): 15.9 (C_1); 27.3 (C_2); 52.4 (C_{10}); 61.1 (C_7); 114.6 (C_5); 124.8 (C_9); 127.9 (C_{13}); 128.6 (C_4); 129.8 (C_{12}); 130.6 (C_{14}); 136.1 (C_3); 140.8 (C_{11}); 143.3 (C_8); 156.1 (C_6); 166.9 (C_{15}); the assignment has been corroborated with a ^{13}C distortionless enhancement by polarization transfer (DEPT) 135 spectrum.

General Procedure for Model Click Reactions in H_2O /THF: (6)

5 (55.5 mg, 0.35 mmol) and **1** (61.3 mg, 0.35 mmol) were dissolved in THF (1.5 mL) and H_2O (1.5 mL), giving a clear solution. Freshly prepared sodium ascorbate (35.0 μL , 1.0 M, 0.04 mmol) and CuSO_4 (17.5 μL , 1.0 M, 0.02 mmol) were added, and the reaction was stirred vigorously for 2 h while it was monitored by TLC (6:4 EtOAc/heptane plus two to three drops of concentrated HCl). **6** precipitated as the reaction proceeded and was isolated by filtration and dried *in vacuo*; it was obtained as a white, crystalline compound (83.0 mg, 71%, $T_{\text{m}} = 212$ °C).

1-(6-Carboxyhexyl)-1H-1,2,3-triazol-4-[methyloxy(4-ethylbenzene)] (7)

5 (46.3 mg, 0.29 mmol), CuBr (23.3 mg, 0.16 mmol), and **2** (50.2 mg, 0.30 mmol) were reacted according to the general click procedure in DMF. **7** was isolated as an oil that crystallized as white crystals upon storage *in vacuo* for 3 days (86 mg, 94%, $T_m = 97^\circ\text{C}$).

IR (cm^{-1}): 3400–2300 (COO—H stretching); 3000–2850 (C—H stretching); 1733 (HOC=O stretching); 1612, 1511 (C=C stretching); 1236 (Ph—O stretching); 1050 (C—O stretching); 829 (para-substituted Ar—H out-of-plane bending). ^1H NMR (DMSO- d_6 , 400 MHz, δ_{H} , ppm): 1.19 (t, 3H, H_1 , $^3J = 7.6$ Hz); 1.28 (m, 2H, H_{12}); 1.56 (p, 2H, H_{13} , $^3J = 7.2, 7.4$ Hz); 1.86 (p, 2H, H_{11} , $^3J = 7.2, 7.4$ Hz); 2.24 (m, 2H, H_{14}); 2.58 (q, 2H, H_2 , $^3J = 7.6$ Hz); 4.39 (t, 2H, H_{10} , $^3J = 7.1$ Hz); 5.13 (s, 2H, H_7); 6.98 (d, 2H, H_5 , $^3J = 8.5$ Hz); 7.16 (d, 2H, H_{12} , $^3J = 8.5$ Hz); 8.25 (s, 1H, H_9); 12.05 (s, 1H, H_{15}); the assignment has been corroborated with a COSY spectrum. ^{13}C NMR (CDCl_3 , 100 MHz, δ_{C} , ppm): 15.9 (C_1); 24.0 (C_{13}); 25.9 (C_{12}); 28.0 (C_2); 29.9 (C_{11}); 33.7 (C_{14}); 50.4 (C_{10}); 62.0 (C_7); 114.7 (C_5); 128.8 (C_4); 137.1 (C_3); 156.3 (C_6); 178.5 (C_{15}); the assignment has been corroborated with ^{13}C DEPT 135 and HMQC spectra. ^{13}C NMR (DMSO- d_6 , 100 MHz, δ_{C} , ppm): 15.9 (C_1); 24.0 (C_{13}); 25.4 (C_{12}); 27.3 (C_2); 29.5 (C_{11}); 33.8 (C_{14}); 49.2 (C_{10}); 61.2 (C_7); 114.6 (C_5); 124.3 (C_9); 128.6 (C_4); 136.0 (C_3); 142.8 (C_8); 156.1 (C_6); 174.1 (C_{15}).

1-(6-Oxy-3,5-dicarboxyphenylhexyl)-1H-1,2,3-triazol-4-[methyloxy(4-ethylbenzene)] (8)

5 (124.6 mg, 0.77 mmol), CuBr (27.9 mg, 0.19 mmol), and **3** (239.7 mg, 0.78 mmol) were reacted according to the general click procedure in DMF. **8** was isolated as an oil that crystallized into white crystals (239 mg, 65%, $T_m = 173^\circ\text{C}$).

IR (cm^{-1}): 3400–2300 (COO—H stretching); 3000–2850 (C—H stretching); 1691 (HOC=O stretching); 1595, 1510 (C=C stretching); 1237 (Ph—O stretching); 1042 (C—O stretching); 826 (para-substituted Ar—H out-of-plane bending); 910, 667 (1,3,5-substituted Ar—H out-of-plane bending). ^1H NMR (DMSO- d_6 , 400 MHz, δ_{H} , ppm): 1.15 (t, 3H, H_1 , $^3J = 7.6$ Hz); 1.31 (m, 2H, H_{12}); 1.46 (m, 2H, H_{13}); 1.73 (m, 2H, H_{14}); 1.86 (m, 2H, H_{11}); 2.52 (q, 2H, H_2 , $^3J = 7.6$ Hz); 4.06 (t, 2H, H_{15} , $^3J = 6.4$ Hz); 4.38 (t, 2H, H_{10} , $^3J = 7.0$ Hz); 5.10 (s, 2H, H_7); 6.94 (d, 2H, H_5 , $^3J = 8.6$ Hz); 7.12 (s, 2H, H_4 , $^3J = 8.5$ Hz); 7.65 (d, 2H,

H_{17} , $^4J = 1.2$ Hz); 8.10 (t, 1H, H_{19} , $^4J = 1.2$ Hz); 8.21 (s, 1H, H_9); 13.24 (s, 2H, H_{20}); the assignment has been corroborated with a COSY spectrum. ^{13}C NMR (DMSO- d_6 , 100 MHz, δ_{C} , ppm): 15.9 (C_1); 24.8 (C_{13}); 25.6 (C_{12}); 27.3 (C_2); 28.3 (C_{14}); 29.6 (C_{11}); 49.3 (C_{10}); 61.2 (C_7); 67.9 (C_{15}); 114.6 (C_5); 119.0 (C_{17}); 122.3 (C_{19}); 124.3 (C_9); 128.6 (C_4); 132.6 (C_{18}); 136.0 (C_3); 142.8 (C_8); 156.1 (C_6); 158.8 (C_7); 166.4 (C_{20}).

1-(7,7-Dicarboxyheptyl)-1H-1,2,3-triazol-4-[methyloxy(4-ethylbenzene)] (9)

5 (52.2 mg, 0.33 mmol), CuBr (26.3 mg, 0.18 mmol), and **4** (75.2 mg, 0.33 mmol) were reacted according to the general click procedure in DMF. **9** was isolated as a transparent oil (53.0 mg, 80%).

IR (cm^{-1}): 3400–2300 (COO—H stretching); 3000–2850 (C—H stretching); 1713 (HOC=O stretching); 1611, 1510 (C=C stretching); 1215 (Ph—O stretching); 1017 (C—O stretching); 828 (para-substituted Ar—H out-of-plane bending). ^1H NMR (CDCl_3 , 400 MHz, δ_{H} , ppm): 1.17 (t, 3H, H_1 , $^3J = 7.6$ Hz); 1.32 (m, 6H, $\text{H}_{12,13,14}$); 1.86 (m, 4H, $\text{H}_{11,15}$); 2.55 (q, 2H, H_2 , $^3J = 7.6$ Hz); 3.38 (t, 1H, H_{16} , $^3J = 7.1$ Hz); 4.29 (t, 2H, H_{10} , $^3J = 6.9$ Hz); 5.16 (s, 2H, H_7); 6.87 (d, 2H, H_5 , $^3J = 8.4$ Hz); 7.08 (s, 2H, H_4 , $^3J = 8.5$ Hz); 7.62 (s, 1H, H_9); 9.14 (s, 2H, H_{17}); the assignment has been corroborated with a COSY spectrum. ^{13}C NMR (CDCl_3 , 100 MHz, δ_{C} , ppm): 15.9 (C_1); 26.0 (C_{13}); 26.9 (C_{12}); 28.0 (C_{14}); 28.5 (C_{15}); 28.9 (C_2); 30.0 (C_{11}); 50.8 (C_{10}); 51.4 (C_{16}); 61.7 (C_7); 114.8 (C_5); 123.2 (C_9); 128.9 (C_4); 137.3 (C_3); 144.3 (C_8); 156.2 (C_6); 173.7 (C_{17}).

Poly[4-(prop-2-ynoxy)styrene] (10)

PHS (6.51 g, $M_n = 8000$, PDI = 1.8, 54.2 mmol of the functional group) was reacted according to the general alkyne procedure with 18-crown-6-ether (0.58 g, 2.2 mmol), K_2CO_3 (8.11 g, 81.1 mmol), and propargyl bromide (80% in toluene, 7.7 mL, 74.4 mmol). In addition to the general procedure, the polymer was dissolved in THF (20 mL) and precipitated into MeOH (300 mL), the precipitate was filtered off and dissolved in THF (100 mL), and the solvent was removed *in vacuo* to give **10** as a yellow-white, solid foam (6.33 g, 74%, $T_g = 46^\circ\text{C}$, $M_n = 11,100$, PS standard on system two, PDI = 1.7).

IR (cm^{-1}): 3287 (C≡C—H stretching); 3000–2850 (C—H stretching); 2120 (C≡C stretching); 1608, 1507 (C=C stretching); 1214 (Ph—O stretching); 1025 (C—O stretching); 827 (para-substituted Ar—H out-of-plane bending). ^1H NMR

(CDCl₃, 400 MHz, δ_{H} , ppm): 1.2–1.9 (m, 3H, H₁₊₂); 2.52 (s, 1H, H₉); 4.62 (s, 2H, H₇); 6.5, 6.7 (m, 4H, H_{4,5}); a COSY spectrum shows coupling between H₇ and H₉. ¹³C NMR (CDCl₃, 100 MHz, δ_{C} , ppm): 39.7 (C₂); 44.2 (C₁); 56.0 (C₇); 75.6 (C₉); 79.0 (C₈); 114.4 (C₅); 128.6 (C₄); 138.3 (C₃); 155.6 (C₆); the assignment has been corroborated through ¹³C DEPT 135 and HMQC NMR spectra).

General Procedure for Polymer Click Reactions in DMF

Poly[1-(4-carboxybenzyl)-1H-1,2,3-triazol-4-(4-methyloxystyrene)] (11)

10 (200 mg, 1.26 mmol of the functional group) and CuBr (45.7 mg, 0.32 mmol) were dissolved in degassed DMF (5 mL). The reaction flask was degassed and backfilled with Ar three times, and this produced a yellow solution. In parallel, **1** (225 mg, 1.27 mmol) was dissolved in degassed DMF (5 mL) to give a colorless solution, which was transferred to the reaction flask with an Ar-purged syringe. The reaction was stirred at room temperature under Ar overnight, and crude NMR showed that the reaction had been completed. The crude reaction mixture was precipitated dropwise into acidic MeOH (100 mL), and the precipitate was filtered, redissolved in DMF, and precipitated into aqueous HCl (10 v/v%). The precipitate was isolated by filtration to give **11** as a white, solid compound (362 mg, 85.5%, $T_{\text{g}} = 98\text{ }^{\circ}\text{C}$).

IR (cm⁻¹): 3400–2300 (COO–H stretching); 3000–2850 (C–H stretching); 1711 (HOC=O stretching); 1611, 1508 (C=C stretching); 1230 (Ph–O stretching); 1019 (C–O stretching); 828 (para-substituted Ar–H out-of-plane bending). ¹H NMR (DMSO-*d*₆, 400 MHz, δ_{H} , ppm): 1.0–2 (m, 3H, H_{1,2}); 4.99 (s, 2H, H₁₀); 5.58 (s, 2H, H₇); 6.40, 6.69 (m, 4H, H_{4,5}); 7.29 (s, 2H, H₁₂); 7.87 (s, 2H, H₁₃); 8.21 (s, 1H, H₉); 13.0 (s, 1H, H₁₅). ¹³C NMR (DMSO-*d*₆, 100 MHz, δ_{C} , ppm): 52.4 (C₁₀); 61.1 (C₇); 114.1 (C₅); 124.8 (C₉); 127.9 (C₁₃); 129.8 (C₁₂); 130.6 (C₁₄); 137.7 (C₃); 140.6 (C₁₁); 143.3 (C₈); 156.0 (C₆); 166.9 (C₁₅); the assignment has been corroborated with a ¹³C DEPT 135 spectrum, although carbons C₁ and C₂ could not be verified.

Poly[1-(6-carboxyhexyl)-1H-1,2,3-triazol-4-(4-methyloxystyrene)] (12)

10 (497 mg, 3.16 mmol of the functional group), CuBr (141.4 mg, 0.99 mmol), and **2** (528.1 mg, 3.54 mmol) were reacted according to the general click procedure in DMF for polymers at 60 °C.

The compound was purified by precipitation into aqueous HCl (300 mL, <10 v/v %) twice, filtered, and washed with H₂O to give **12** as a white, solid compound (529.0 mg, 53%, $T_{\text{g}} = 54\text{ }^{\circ}\text{C}$).

IR (cm⁻¹): 3400–2300 (COO–H stretching); 3000–2850 (C–H stretching); 1709 (HOC=O stretching); 1608, 1508 (C=C stretching); 1236 (Ph–O stretching); 1012 (C–O stretching); 827 (para-substituted Ar–H out-of-plane bending). ¹H NMR (DMSO-*d*₆, 400 MHz, δ_{H} , ppm): 1.0–2.2 (m, 11H, H_{1,2,12,13,11,14}); 4.29 (s, 2H, H₁₀); 5.03 (s, 2H, H₇); 6.45–6.75 (m, 4H, H_{4,5}); 8.14 (s, 1H, H₉); 12.01 (s, 1H, H₁₅). ¹³C NMR (DMSO-*d*₆, 100 MHz, δ_{C} , ppm): 23.9 (C₁₃); 25.5 (C₁₂); 29.5 (C₁₁); 33.5 (C₁₄); 39.7 (C₂); 41.2 (C₁); 49.3 (C₁₀); 61.2 (C₇); 114.1 (C₅); 124.2 (C₉); 128.3 (C₄); 137.7 (C₃); 142.8 (C₈); 156.1 (C₆); 174.4 (C₁₅); the assignment has been corroborated with a ¹³C DEPT 135 spectrum.

Poly[1-(6-oxy-3,5-dicarboxyphenylhexyl)-1H-1,2,3-triazol-4-(4-methyloxystyrene)] (13)

10 (99.6 mg, 0.63 mmol of the functional group), CuBr (45.3 mg, 0.32 mmol), and **3** (196.0 mg, 0.64 mmol) were reacted according to the general click procedure in DMF for polymers at 60 °C. The crude product was precipitated into aqueous HCl (300 mL, <10 v/v %), filtered, dissolved in THF (10 mL), precipitated into EtOAc (200 mL), filtered, dissolved in THF (10 mL), precipitated into H₂O (200 mL), filtered, washed with H₂O, and dried *in vacuo* to give **13** as a white, solid compound (207.6 mg, 71%, $T_{\text{g}} = 118\text{ }^{\circ}\text{C}$).

IR (cm⁻¹): 3400–2300 (COO–H stretching); 3000–2850 (C–H stretching); 1698 (HOC=O stretching); 1594, 1509 (C=C stretching); 1222 (Ph–O stretching); 1042 (C–O stretching); 827 (para-substituted Ar–H out-of-plane bending); 886, 668 (1,3,5-substituted Ar–H out-of-plane bending). ¹H NMR (DMSO-*d*₆, 400 MHz, δ_{H} , ppm): 1.0–2.2 (m, 11H, H_{1,2,12,13,14,11}); 3.95 (s, 2H, H₁₅); 4.28 (s, 2H, H₁₀); 5.01 (s, 2H, H₇); 6.45–6.75 (m, 4H, H_{4,5}); 7.57 (s, 2H, H₁₇); 8.04 (s, 1H, H₁₉); 8.14 (s, 1H, H₉); 13.23 (s, 2H, H₂₀). ¹³C NMR (DMSO-*d*₆, 100 MHz, δ_{C} , ppm): 24.9 (C₁₃); 25.6 (C₁₂); 28.3 (C₁₄); 29.6 (C₁₁); 49.3 (C₁₀); 61.2 (C₇); 67.9 (C₁₅); 114.0 (C₅); 119.2 (C₁₇); 122.6 (C₁₉); 124.2 (C₉); 128.4 (C₄); 132.9 (C₁₈); 137.0 (C₃); 143.0 (C₈); 156.2 (C₆); 159.0 (C₁₆); 166.4 (C₂₀).

Poly[1-(7,7-dicarboxyheptyl)-1H-1,2,3-triazol-4-(4-methyloxystyrene)] (14)

10 (117.0 mg, 0.74 mmol of the functional group), CuBr (36.0 mg, 0.25 mmol), and **4** (208.6 mg,

0.91 mmol) were reacted according to the general click procedure in DMF for polymers at 60 °C. The compound was isolated by precipitation into aqueous HCl (100 mL, <10 v/v %), filtered, dissolved in THF (4 mL), precipitated into diethyl ether (100 mL), filtered, and dried *in vacuo* at 50 °C overnight to give **14** as a white, solid compound (209.1 mg, 73%, $T_g = 48$ °C).

IR (cm⁻¹): 3400–2300 (COO–H stretching); 3000–2850 (C–H stretching); 1723 (HOC=O stretching); 1609, 1508 (C=C stretching); 1215 (Ph–O stretching); 1014 (C–O stretching); 827 (para-substituted Ar–H out-of-plane bending). ¹H NMR (DMSO-*d*₆, 400 MHz, δ_H , ppm): 1.0–2.2 (m, 13H, H_{1,2,13,12,14,15,11}); 3.17 (s, 1H, H₁₆); 4.29 (s, 2H, H₁₀); 5.03 (s, 2H, H₇); 6.40–6.74 (m, 4H, H_{4,5}); 8.14 (s, 1H, H₉); 12.60 (s, 2H, H₁₇). ¹³C NMR (DMSO-*d*₆, 100 MHz, δ_C , ppm): 25.7 (C₁₃); 26.7 (C₁₂); 28.1 (C₁₄); 28.3 (C₁₅); 29.6 (C₁₁); 39.8 (C₂); 49.3 (C₁₀); 51.7 (C₁₆); 61.1 (C₇); 114.1 (C₅); 124.2 (C₉); 128.2 (C₄); 138.1 (C₃); 142.8 (C₈); 156.1 (C₆); 170.9 (C₁₇); the assignment has been corroborated with a ¹³C DEPT 135 spectrum.

Poly[4-(prop-2-ynoxy)styrene]-co-methyl methacrylate (**15**)

Poly(hydroxystyrene-co-methyl methacrylate) (10.0 g, $M_n = 2810$, PDI = 3.2, estimated 65.3 mmol of the functional group) was reacted according to the general alkyne synthesis with propargyl bromide (80% in toluene, 9.4 mL, 125 mmol) in the presence of 18-crown-6-ether (0.89 g, 3.4 mmol) and K₂CO₃ (17.3 g, 125 mmol). In addition to the general procedure, the polymer was dissolved in THF (35 mL) and precipitated dropwise into MeOH (600 mL), the precipitate was filtered off and redissolved in THF (10 mL), and the solvent was removed *in vacuo* to give **15** as a pale yellow, solid foam (8.51 g, 68%, $T_g = 60$ °C, $M_n = 5416$, universal calibration on system one, PDI = 2.1).

IR (cm⁻¹): 3288 (C≡C–H stretching); 3000–2850 (C–H stretching); 2124 (C≡C stretching); 1722 (MeOC=O stretching); 1609, 1507 (C=C stretching); 1214 (Ph–O stretching); 1109 (H₃C–O stretching); 1025 (C–O stretching); 828 (para-substituted Ar–H out-of-plane bending). ¹H NMR (acetone-*d*₆, 400 MHz, δ_H , ppm): 0.6–2 (m, 8H, H_{12,1,10}); 2.46 (s, 1H, H₂); 3.04 (s, 1.8H, H₉); 3.46 (s, 1H, H₁₄); 4.73 (s, 2H, H₇); 6.9 (m, 4H, H_{4,5}). ¹³C NMR (acetone-*d*₆, 100 MHz, δ_C , ppm): 20.6 (C₁₂); 38.4 (C₂); 46.1 (C₁₁); 51.2 (C_{10,1,14}); 56.2 (C₇); 76.8 (C₉); 80.0 (C₈); 115.2 (C₅); 130.1 (C₄); 139.3 (C₃); 156.8 (C₆); 177.1 (C₁₃); the assignment has been

corroborated with ¹³C DEPT 135 and HMQC spectra.

Poly[[1-(6-oxy-3,5-dicarboxyphenyl)hexyl]-1H-1,2,3-triazol-4-(4-methyloxystyrene)]-co-methyl methacrylate (**16**)

15 (113.1 mg, 0.59 mmol of the functional group), CuBr (34.7 mg, 0.24 mmol), and **3** (308.0 mg, 1.00 mmol) were reacted according to the general click procedure in DMF for polymers at 60 °C. The compound was precipitated into aqueous HCl (150 mL, <10 v/v %), filtered, dissolved in THF (4 mL), precipitated into EtOAc (150 mL), filtered, and dried *in vacuo* at 50 °C overnight to give **16** as an off-white, solid compound (166.8 mg, 56%, $T_g = 90$ °C).

IR (cm⁻¹): 3400–2300 (COO–H stretching); 3000–2850 (C–H stretching); 1719 (HOC=O, MeOC=O stretching); 1596, 1509 (C=C stretching); 1207 (Ph–O stretching); 1040 (C–O stretching); 829 (para-substituted Ar–H out-of-plane bending); 886, 665 (1,3,5-substituted Ar–H out-of-plane bending). ¹H NMR (DMSO-*d*₆, 400 MHz, δ_H , ppm): 0.90 (s, 1H, H₂₃); 1.0–1.9 (m, 13H, H_{1,2,21,12,13,14,11}); 2.89 (s, 1H, H₂₅); 4.02 (s, 2H, H₁₅); 4.33 (s, 2H, H₁₀); 5.03 (s, 2H, H₇); 6.79 (m, 4H, H_{4,5}); 7.61 (s, 2H, H₁₇); 8.06 (s, 1H, H₁₉); 8.16 (s, 1H, H₉); 13.15 (s, 2H, H₂₀). ¹³C NMR (DMSO-*d*₆, 100 MHz, δ_C , ppm): 18.8 (C₂₃); 24.8 (C₁₃); 25.6 (C₁₂); 28.3 (C₁₄); 29.6 (C₁₁); 39.8 (C₂); 44.8 (C₂₂); 49.3 (C₁₀); 50.4 (C_{25,1,21}); 60.9 (C₇); 67.9 (C₁₅); 113.9 (C₅); 118.9 (C₁₉); 122.1 (C₁₇); 124.2 (C₉); 128.7 (C₄); 132.5 (C₁₈); 136.8 (C₃); 142.8 (C₈); 156.0 (C₆); 158.7 (C₁₆); 166.4 (C₂₀); 176.0 (C₂₄); the assignment has been corroborated with a ¹³C DEPT 135 spectrum.

Poly[[1-(7,7-dicarboxyheptyl)-1H-1,2,3-triazol-4-(4-methyloxystyrene)]-co-methyl methacrylate (**17**)

15 (135.5 mg, 0.71 mmol of the functional group), CuBr (34.2 mg, 0.24 mmol), and **4** (196.1 mg, 0.86 mmol) were reacted according to the general click procedure in DMF for polymers at 60 °C. The compound was precipitated into aqueous HCl (150 mL, <10 v/v %), filtered, dissolved in THF (4 mL), precipitated into diethyl ether (100 mL), filtered, and dried *in vacuo* at 50 °C overnight to give **17** as an off-white, solid compound (147.7 mg, 46%, $T_g = 65$ °C).

IR (cm⁻¹): 3400–2300 (COO–H stretching); 3000–2850 (C–H stretching); 1722 (HOC=O stretching); 1609, 1509 (C=C stretching); 1211 (Ph–O stretching); 1014 (C–O stretching); 830

(para-substituted Ar—H out-of-plane bending). ^1H NMR (DMSO- d_6 , 400 MHz, δ_{H} , ppm): 0.92 (s, 1H, H₂₀); 1.0–2.0 (m, 13H, H_{1,2,18,14,13,12,15,11}); 2.89 (s, 1H, H₂₂); 3.18 (m, 1H, H₁₆); 4.32 (s, 2H, H₁₀); 5.04 (s, 2H, H₇); 6.81 (m, 4H, H_{4,5}); 8.17 (s, 1H, H₉); 12.48 (s, 2H, H₁₇). ^{13}C NMR (DMSO- d_6 , 100 MHz, δ_{C} , ppm): 19.8 (C₂₀); 27.7 (C₁₃); 26.6 (C₁₂); 28.1 (C₁₄); 28.4 (C₁₅); 29.7 (C₁₁); 44.9 (C₁₉); 49.3 (C₁₀); 51.5 (C_{22,18}); 61.0 (C₇); 114.2 (C₅); 124.3 (C₉); 129.0 (C₄); 137.1 (C₃); 142.8 (C₈); 156.3 (C₆); 171.0 (C₁₇); 174.5 (C₂₁); the assignment has been corroborated with a ^{13}C DEPT 135 spectrum.

Poly[4-(prop-2-ynoxy)styrene]-*b*-styrene] (18)

Poly(4-butoxystyrene-*b*-styrene), synthesized as part of earlier work in our group¹⁸ (5.1 g, $M_n = 52,000$, PDI = 1.3, 1:9, estimated 4.6 mmol of the functional group), was dissolved in THF (200 mL), and the solution was cooled to 0 °C. CF₃SO₃H (30 drops) was added dropwise, and the reaction was stirred overnight, while the reaction temperature was allowed to reach room temperature. The crude mixture was concentrated *in vacuo* and precipitated into MeOH (800 mL). The precipitate was filtered off and dried *in vacuo* at 50 °C to give poly(4-hydroxystyrene-*b*-styrene) (PHS-*b*-PS) as a white solid (3.33 g, 68%, $T_g = 101$ °C, $M_n = 42,500$, PS standard on system two, PDI = 1.3).

IR (cm⁻¹): 3400 (O—H stretching); 3060–2850 (C—H stretching); 1605–1450 (C=C stretching); 1232 (Ph—O stretching); 828 (para-substituted Ar—H out-of-plane bending); 754, 696 (monosubstituted Ar—H out-of-plane bending). ^1H NMR (acetone- d_6 , 400 MHz, δ_{H} , ppm): 1–2.5 (m, 3.2H, H_{1,2}); 6.5–7.2 (m, 4.9H, H_{10,8,4,5,9}); 7.95 (s, 0.1H, H₆). ^{13}C NMR (acetone- d_6 , 100 MHz, δ_{C} , ppm): 42.2 (C₂); 45.3 (C₁); 116.6 (C₅); 127.6 (C_{9,10}); 129.9 (C_{4,8}); 147.6 (C_{3,7}); 157.0 (C₆).

PHS-*b*-PS (2.26 g, estimated 2.1 mmol of the functional group) and triphenylphosphine (TPP; 1.68 g, 6.4 mmol) were dissolved in THF (145 mL). Diethyl azodicarboxylate (DEAD, 1.11 g, 6.4 mmol) was added, and the solution changed color from clear to light yellow. Propargyl alcohol (0.36 g, 6.4 mmol) was added with a syringe, and the solution became colorless again. The reaction flask was evacuated and backfilled with Ar three times and was stirred overnight. The crude mixture was precipitated into MeOH (900 mL), filtered, and dried *in vacuo* at 50 °C to give **18** as a white, solid compound (1.76 g, 75%, $T_g = 99$ °C, $M_n = 52,500$, PS standard on system two, PDI = 1.3).

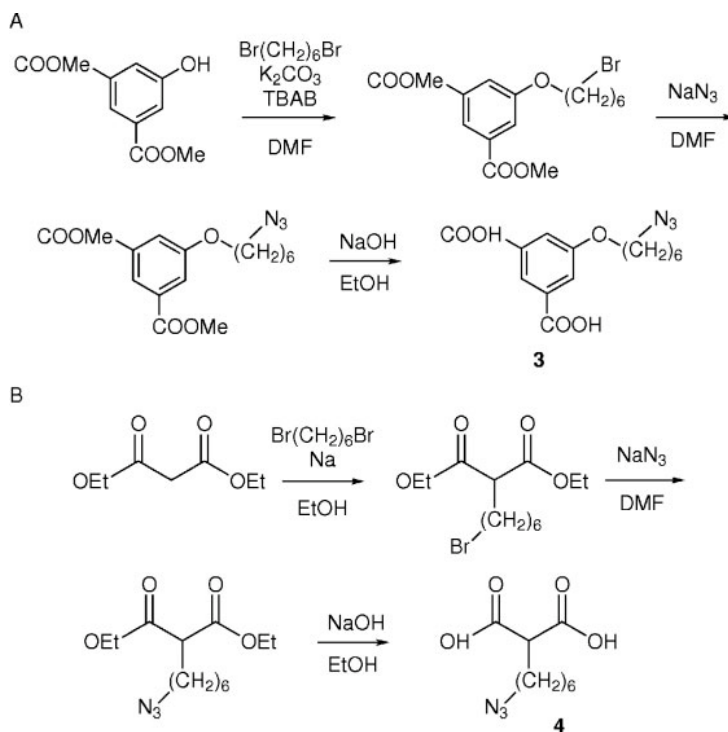
IR (cm⁻¹): 3291 (C≡C—H stretching); 3060–2850 (C—H stretching); 1605–1450 (C=C stretching); 1218 (Ph—O stretching); 1029 (C—O stretching); 829 (para-substituted Ar—H out-of-plane bending); 756, 697 (monosubstituted Ar—H out-of-plane bending). ^1H NMR (DMSO- d_6 , 400 MHz, δ_{H} , ppm): 1–2.3 (m, 3.2H, H_{1,2}); 2.56 (s, 0.05 H, H₉); 4.67 (s, 0.1 H, H₇); 6.3–7.2 (m, 4.9H, H_{4,11,13,5,12}). ^{13}C NMR (acetone- d_6 , 100 MHz, δ_{C} , ppm): 40.7 (C₂); 44.0 (C₁); 56.2 (C₇); 75.8 (C₉); 79.1 (C₈); 114.7 (C₅); 125.9 (C_{12,13}); 127.9, 128.3 (C_{4,11}); 145.9 (C_{3,10}); 155.8 (C₆); the assignment has been corroborated with a ^{13}C DEPT 135 spectrum.

General Click Procedure in THF with CuP(OEt)₃I

Poly[[1-(6-oxy-3,5-dicarboxyphenyl)hexyl]-1H-1,2,3-triazol-4-(4-methyloxystyrene)]-*b*-styrene] (19)

18 (94.0 mg, 0.09 mmol of the functional group), **3** (44.0 mg, 0.14 mmol), and CuP(OEt)₃I (32.5 mg, 0.09 mmol) were dissolved in dry THF (5 mL). *N,N*-Diisopropylethylamine (DIPEA; 80 μL , 0.46 mmol) was added with a syringe, and the reaction flask was sealed with a stopper and stirred overnight at room temperature. NMR showed that the reaction was complete, and the crude mixture was precipitated into acidic MeOH (pH = 1, HCl; 100 mL). The precipitate was filtered and washed with MeOH and was dried *in vacuo* at 50 °C to give **19** as a white, solid compound (111.0 mg, 92%, $T_g = 100$ °C).

IR (cm⁻¹): 3400–2300 (COO—H stretching); 3000–2850 (C—H stretching); 1704 (HOC=O stretching); 1600, 1509 (C=C stretching); 1237 (Ph—O stretching); 1028 (C—O stretching); 828 (para-substituted Ar—H out-of-plane bending); 759, 697 (monosubstituted Ar—H out-of-plane bending). ^1H NMR (1:1 DMSO- d_6 /CDCl₃, 400 MHz, δ_{H} , ppm): 1.0–2.2 (m, 3.8H, H_{1,12,13,14,11,2}); 3.93 (m, 0.1H, H₁₅); 4.27 (s, 0.1H, H₁₀); 4.95 (s, 0.1H, H₇); 6.51, 6.98 (m, 4.9H, H_{4,5}); 7.57 (s, 0.1H, H₁₇); 7.94 (s, 0.1H, H₁₉); 8.07 (s, 0.1H, H₉); 12.8 (s, 0.1H, H₂₀); the solvent peak for DMSO has been used as a reference value. ^{13}C NMR (1:1 DMSO- d_6 /CDCl₃, 100 MHz, δ_{C} , ppm): 25.5 (C₁₃); 26.0 (C₁₂); 28.2 (C₁₄); 29.5 (C₁₁); 43.4 (C₁); 49.3 (C₁₀); 61.0 (C₇); 67.6 (C₁₅); 113.8 (C₅); 118.8 (C₁₇); 122.3 (C₁₉); 123.6 (C₉); 125.3 (C_{22,24}); 127.1, 127.6 (C_{4,23}); 132.2 (C₁₈); 144.7 (C_{8,3,21}); 155.9 (C₆); 158.4 (C₁₆); 166.4 (C₂₀); the assignment has been corroborated with a ^{13}C DEPT 135 spectrum, and the solvent peak for DMSO has been used as a reference value.



Scheme 2. Preparation of (A) **3** and (B) **4**.

Poly{[1-(7,7-dicarboxyheptyl)-1H-1,2,3-triazol-4-(4-methoxystyrene)]-*b*-styrene} (20**)**

18 (700.1 mg, 0.6 mmol of the functional group), **4** (474.0 mg, 2.07 mmol), CuP(OEt)₃I (398 mg, 1.11 mmol), and DIPEA (1.26 mL, 7.2 mmol) were reacted according to the general click procedure in THF at room temperature for 12 h and at 50 °C for an additional 12 h. Crude NMR showed that the reaction was complete, and the mixture was precipitated into aqueous HCl (500 mL, <10 v/v %). The precipitate was filtered and washed with H₂O, dried *in vacuo*, dissolved in THF, and precipitated into heptane (300 mL). The precipitate was filtered and dried *in vacuo* at 50 °C, and **20** was isolated as a white, solid compound (618.0 mg, 73%, *T_g* = 104 °C).

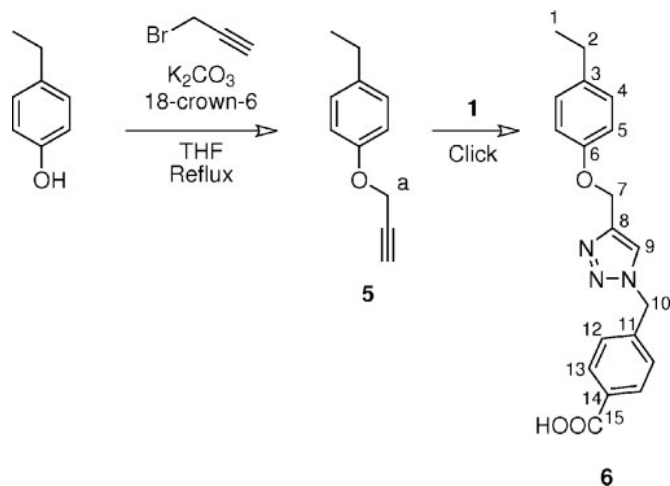
IR (cm⁻¹): 3400–2300 (COO–H stretching); 3000–2850 (C–H stretching); 1730 (HOC=O stretching); 1601, 1509 (C=C stretching); 1216 (Ph–O stretching); 1028 (C–O stretching); 829 (para-substituted Ar–H out-of-plane bending); 755, 697 (monosubstituted Ar–H out-of-plane bending). ¹H NMR (7:2 DMSO-*d*₆/CDCl₃, 400 MHz, δ_H,

ppm): 1.0–2.2 (m, 4H, H_{1,13,12,14,2,15,11}); 3.16 (s, 0.1H, H₁₆); 4.31 (s, 0.1 H, H₁₀); 5.02 (s, 0.05H, H₇); 6.53, 6.81 (m, 4.9H, H_{4,20,5,19,21}); 12.43 (s, 0.1H, H₁₇); the solvent peak for DMSO has been used as a reference value.

For ¹³C NMR (DMSO-*d*₆, 100 MHz, δ_C, ppm), the registered peaks were 39.6 (C₂), 44.1 (C₁), 125.0 (C_{19,21}), 126.7 and 127.2 (C_{4,20}), and 144.2 (C_{3,18}); the assigned peaks were confirmed with a ¹³C DEPT 135 spectrum.

RESULTS AND DISCUSSION

In applying click chemistry to the synthesis of a (co)polymer with pendant carboxylic acid groups, either an azide- or alkyne-functional polymer could in principle be used. The alkyne polymer was chosen because it is easily available through a Williamson ether synthesis from PHS or copolymers of PHS. In addition, the carboxylic acid derivatives needed for the click reactions could be synthesized directly from their equivalent bromides.



Scheme 3. Preparation of the model alkyne (**5**) and its model click reaction with **1** (click conditions: CuBr in DMF at room temperature/60 °C or CuSO₄/sodium ascorbate in H₂O/THF at room temperature).

Azide Synthesis

Four different carboxylic acid derivatives were synthesized from the corresponding bromides by a reaction with sodium azide. The two monofunctional carboxylic acids (**1** and **2**) were prepared from 4-(bromomethyl)benzoic acid and 6-bromohexanoic acid, respectively. The two difunctional carboxylic acids (**3** and **4**), on the other hand, were prepared by different methods, as shown in Scheme 2.

Model Reactions

A number of model reactions were performed to obtain conclusive characterization data for each of the triazoles and to test different reaction conditions with different catalysts. An analysis of the monomeric model compounds eased the identification of the subsequently synthesized polymers considerably. The model reactions were performed on a model alkyne and the four carboxylic acid azides. 1-Ethyl-4-(1-oxyprop-2-yne)benzene was chosen as a model alkyne to mimic the alkyne-functionalized PHS backbone, whereas **1** especially was used to find the proper reaction conditions, as shown in Scheme 3.

In the characterization of the triazoles, the peaks from protons 7, 9, and 10 in Scheme 3 have been found especially useful for monitoring the reactions and for identifying the products. The

methylenes (7 and 10) shift downfield from $\delta_{\text{H}} = 4.7$ ppm to $\delta_{\text{H}} = 5.1$ ppm and from $\delta_{\text{H}} = 3.7$ ppm to $\delta_{\text{H}} = 5.8$ ppm in the reactants and the product, respectively. In addition, the appearance of the triazole proton (9) at $\delta_{\text{H}} = 8.35$ ppm also clearly indicates the formation of the product. In the less electron-deficient triazoles, the triazole proton appears slightly upfield from this. Apart from NMR, IR is also very efficient for the detection of residual reactants because the azide especially gives a very sharp and distinct peak at approximately 2100 cm⁻¹.

The efficiency of the 1,3-dipolar cycloaddition was investigated with two different solvent systems: first DMF with CuBr as a catalyst and second a mixture of H₂O and THF with CuSO₄/sodium ascorbate as a catalyst system. The DMF/CuBr system appeared to be easier to apply to different reactants and gave purer products, with only minor adjustments of the reaction conditions. The H₂O/THF system, on the other hand, was also very efficient, but the ratio of the solvents apparently influenced the reactivity considerably, and it was expected that this ratio would have to be changed with every set of reactants. Because of these minor differences and because the H₂O/THF system was expected to give additional difficulties with the polymer, we decided to use the DMF/CuBr system.

Bunz et al.²¹ found that an increased reaction temperature gave both the 1,5- and 1,4-regioisomers

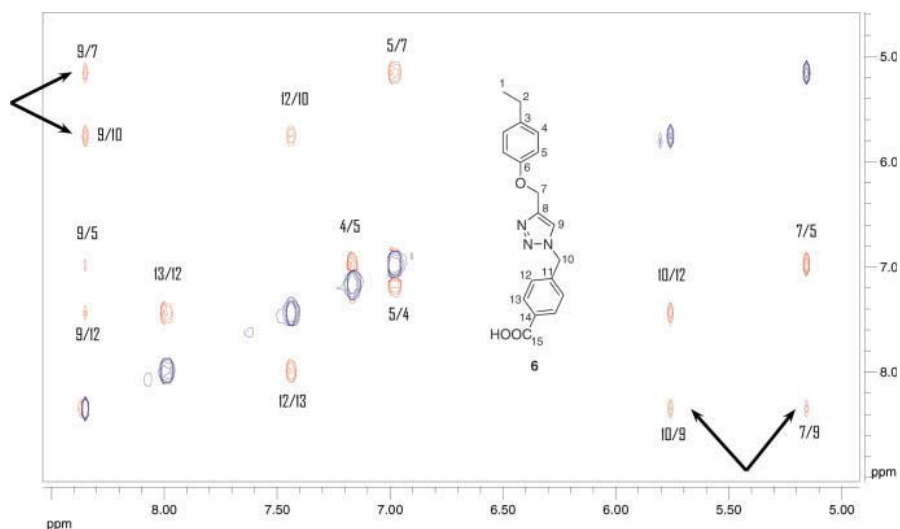


Figure 1. NOESY spectrum of triazole product **6** (prepared as shown in Scheme 3). The arrows indicate the NOEs between the triazole proton (9) and the two methylenes (7 and 10).

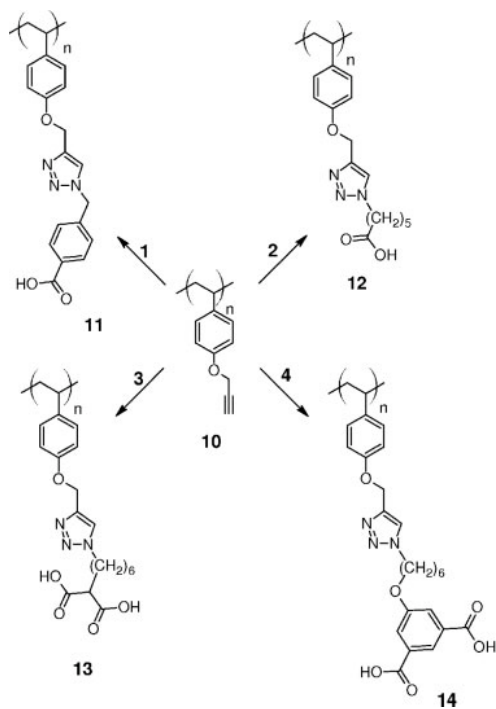
of the triazole product with a solvent mixture of H_2O and THF, so it was additionally tested if the DMF/CuBr system would give a similar result with reactions run at room temperature and at 60°C . Both products were analyzed with NMR, and NOESY clearly showed that the 1,4-regioisomer had been formed regioselectively in both cases, as shown in Figure 1.

The NOESY spectrum clearly shows a strong nuclear Overhauser and exchange (NOE) effect between the triazole proton (9) and the methylenes (7 and 10), which strongly implies that these are in close proximity, as would be expected in a 1,4-substituted triazole.

Polymer Synthesis

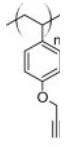
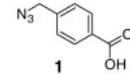
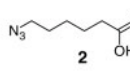
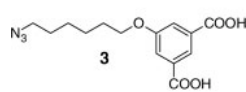
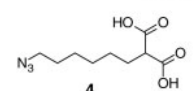
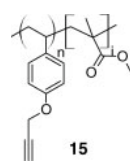
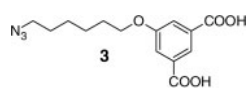
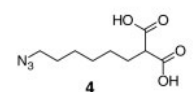
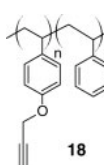
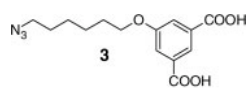
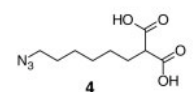
The results from the model reactions showed that the formation of the triazoles from azides and alkynes could be conducted in high yields through a fairly straightforward method. In addition to this, the model experiments also provided valuable spectroscopic data that were used to interpret the analysis data from the polymer reactions. PHS was alkyne-functionalized through a highly efficient Williamson ether synthesis that gave the completely alkyne-substituted PHS (**10**), without any trace of unreacted phenol from the starting material, in a yield of 74%. Subsequently, **10** was

Journal of Polymer Science: Part A: Polymer Chemistry
DOI 10.1002/pola



Scheme 4. Click reactions of **10** and the four azido carboxylic acids (**1–4**) catalyzed with CuBr in DMF at 60°C .

Table 1. Polymer Click Products

Alkyne	Azide	Triazole Product	Yield (%)	T_g (°C)
 10	 1	11	86	98
	 2	12	53	54
	 3	13	71	118
	 4	14	73	60
 15	 3	16	56	90
	 4	17	46	65
 18	 3	19	92	100
	 4	20	73	104

clicked with azides 1–4, as shown in Scheme 4, to obtain targeted carboxylic acid polymers 11–14.

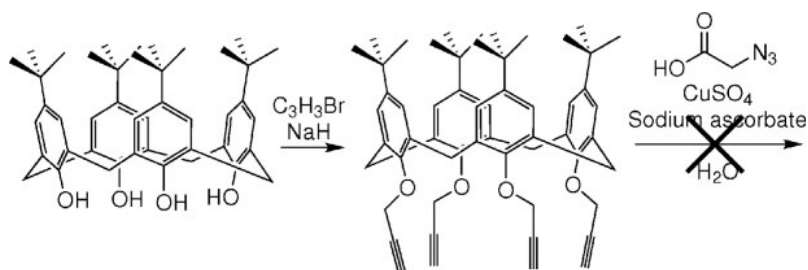
Furthermore, an increase in the reaction temperature to 60 °C and the use of a slight excess of the azides gave fully functionalized polymers in good yields, as shown in Table 1, for all the click products.

With all the clicked polymers, the disappearance of the alkyne and azide absorptions in IR clearly confirms the efficiency of the reaction and thus complete functionalization of the polymers, as well as the complete removal of the excess azides. All four carboxylic acid polymers were isolated in moderate to high yields (53–86%), which were largely dependent on the purifica-

tion. The purification of the polymers was performed by precipitation into MeOH, for example, and subsequently into EtOAc, for example, to remove the remaining catalyst and excess of the azides. SEC of the products in THF was attempted, though without any success; this was attributed to the very high polarity of the clicked polymers.

The complete functionalization is in contrast to the work published by Ryu and Zhao,²² who found that the equivalent synthesis on a calix[4]-arene very similar to the polymer backbone was not feasible, as shown in Scheme 5.

Ryu and Zhao²² attributed their results to a difference in the solubility of the azide and their calix [4]arene as well as an observed homocoupling of



Scheme 5. Preparation of water-soluble calix[4]arenes by click chemistry.

the alkynes. In our case, the homocoupling of the alkynes was not observed, not even with increasing reaction temperature, and the fully substituted polymers were isolated in all cases. It is not known whether this difference in reactivity is related to the ring strain in the calix[4]arene or perhaps to the solvent and catalyst system, although this has not been investigated further.

The synthetic strategy was transferred to a random copolymer of PHS and poly(methyl methacrylate), which was obtained commercially. The ratio of the two repeating units in the polymer was unknown, so it was investigated with NMR. The determination of the ratio of PHS-*co*-PMMA was very difficult to assess by NMR because it was troublesome to obtain a decent spectrum, most likely because of the amphiphilic character of the polymer. Hence, the corresponding alkyne

was synthesized through the Williamson reaction and subsequently investigated with NMR (Fig. 2). As can be seen from the HMQC spectrum in Figure 2, even this approach was rather difficult, although an estimate of the ratio was made through a comparison of protons 14 and 7, resulting in approximately 75% PHS. In addition to this, Figure 2 shows no traces of the phenol groups from the starting material, which are expected at $\delta_{\text{H}} = 8.9$ – 9.1 ppm.

Applying similar reaction conditions from the click reactions on **10** gave the two carboxylic acid polymers, **16** and **17**, as shown in Scheme 6.

The final polymer was a block copolymer of PHS and PS. The starting material was a PBS-*b*-PS in a ratio of 1:9 with a molecular weight of 52,000 g/mol. The removal of the butoxy protective groups by acid hydrolysis, followed by a Mitsunobu ether synthesis provided the corre-

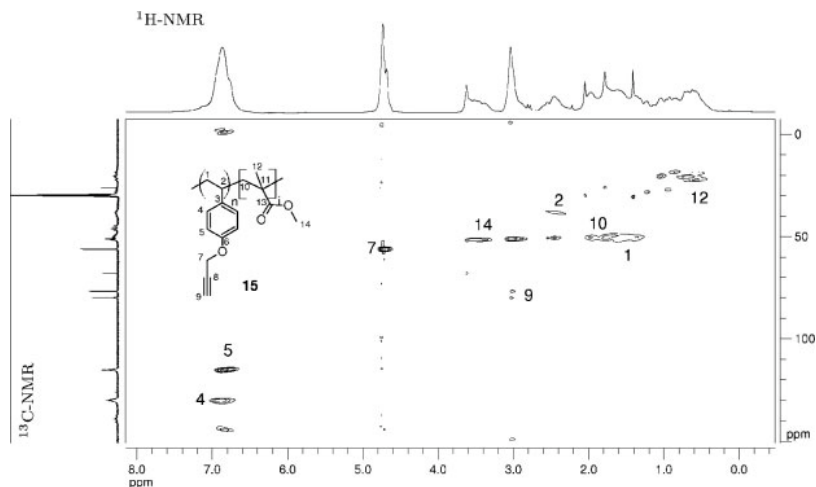
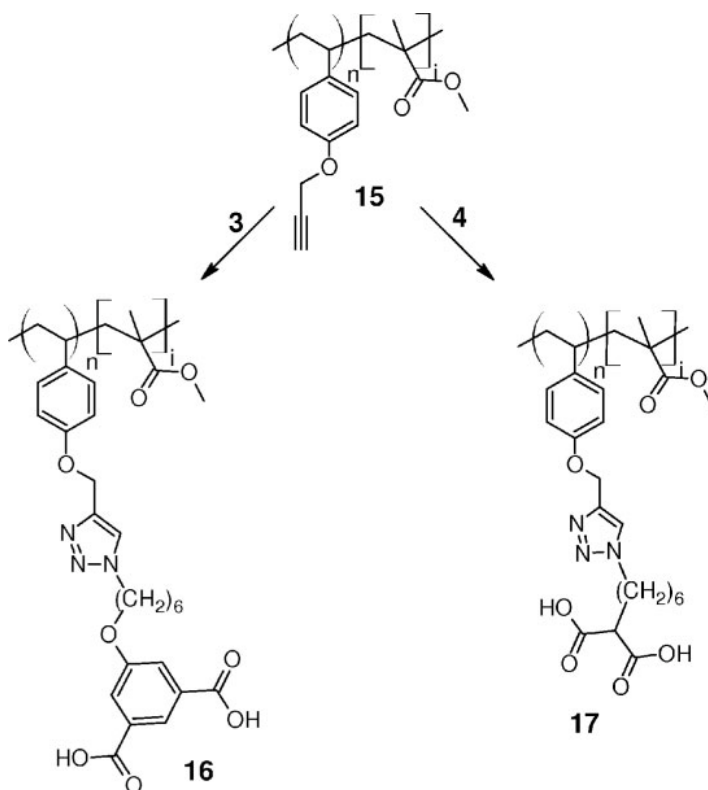


Figure 2. HMQC spectrum of **15** (H–C correlation in DMSO- d_6).

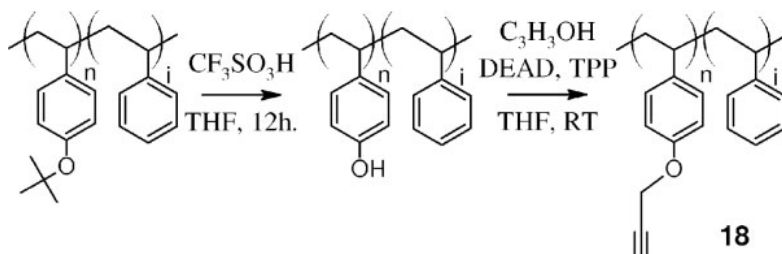


Scheme 6. Click reactions of **15** in DMF with CuBr and **3** or **4**.

sponding alkyne block copolymer (**18**), as shown in Scheme 7.

Two different methods for the deprotection of the copolymer were attempted. First, deprotection with concentrated HCl in acetone was explored. Unfortunately, the polymer precipitated upon the addition of the acid to the solution, and the isolated compound still contained the protective group, as

detected by ^1H and ^{13}C NMR. It is believed that the water content in the concentrated acid solution precipitated the polymer. As an alternative, it was found that deprotection with trifluoromethanesulfonic acid in THF was a very efficient route for removing the butoxy protective groups quantitatively. The deprotected polymer was isolated in a yield of 68% by precipitation into H_2O .



Scheme 7. Preparation of the alkyne block copolymer (**18**).

We also attempted to perform the functionalization with the same method used for the two other polymers through a Williamson ether synthesis. Unfortunately, this was found to be difficult because the polymer precipitated during the reaction. It is believed that this precipitation was due to the formation of water during the reaction, which acted as a nonsolvent. Two different solutions to this problem were investigated. One was to run the reaction in the presence of molecular sieves (4 Å) and dried solvents to minimize the exposure to water as much as possible during the reaction. The other was to perform the reaction as a Mitsunobu reaction with propargyl alcohol, DEAD, and TPP in dry THF under anhydrous conditions.

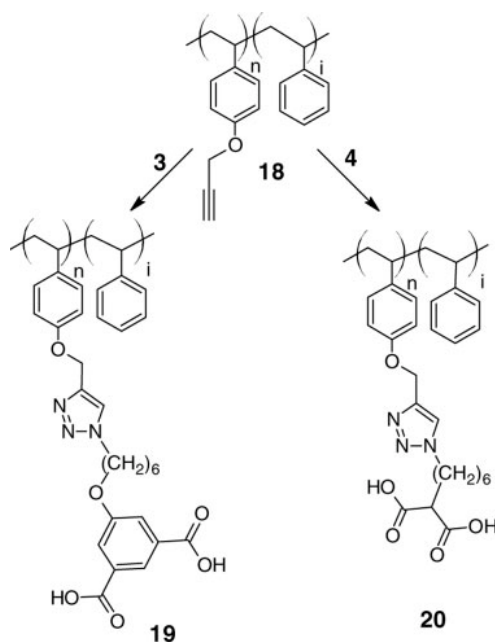
The first approach, using molecular sieves, worked in the sense that the product was formed, although it was very difficult to remove the molecular sieves completely after the reaction. The problem arose when the heterogeneous mixture was filtered because the polymer precipitated and stuck to the filter. Even the addition of solvents (CH_2Cl_2 and THF) could not redissolve the polymer and force it through the filter without also carrying the granulated molecular sieves through the filter with the polymer.

The Mitsunobu reaction was very easy to perform and gave very good results. The reaction seemed to proceed almost instantaneously, and the pure copolymer was isolated in a 79% yield after precipitation into MeOH.

Click products **19** and **20** of block copolymer **18** could not be synthesized through the same procedure used for the other polymers because the polymer was not soluble in DMF. It was decided to run the syntheses in THF with an organic source for Cu(I), as shown in Scheme 8.

The click reactions on **18** were performed with organosoluble $\text{CuP}(\text{OEt})_3\text{I}$ and base DIPEA in THF. Hawker et al.¹¹ published syntheses with this catalyst and found that an amine base was necessary to make the reaction proceed. As can be seen in Table 1, both block copolymers were isolated in good yields (73–92%) after the click reactions, although in these cases no apparent effect could be seen in the change of T_g . This reduced influence from the pendant groups is believed to be due to the ratio between the PHS and PS of the polymer backbone because, with only 10 v/v % PHS, the effects seen in the earlier discussed polymers are less distinct here.

The identifications of the last two functionalized block copolymers by NMR were complicated by the fact that neither could be dissolved in pure



Scheme 8. Click reactions in THF with $\text{CuP}(\text{OEt})_3\text{I}$ and DIPEA between **18** and **3** or **4**, respectively.

$\text{DMSO-}d_6$, CDCl_3 , or acetone- d_6 . As an alternative method, mixtures of $\text{DMSO-}d_6$ and CDCl_3 were used to obtain sufficiently dissolved samples. With this solvent mixture, it was possible to obtain spectra of the products in which no traces of the starting materials could be seen. IR spectroscopy showed no traces of the reactants, and this indicated that the purification was efficient. These analysis difficulties are attributed to the amphiphilic nature of the products and also indicate that the products were formed, especially when the chemoselectivity from the earlier reactions is considered.

Thermal Properties

An overview of the T_g 's found in the DSC investigations of the different polymer products and their starting materials is shown in Figure 3.

It is evident that when the polymer contains more than the 10% functional groups, as in **15**, an effect can be seen in the change in the T_g 's with every modification of the backbone. There is a clear drop in T_g from the starting material with the hydroxy groups on the backbone (120–130 °C) to alkyne-substituted polymers **10** and

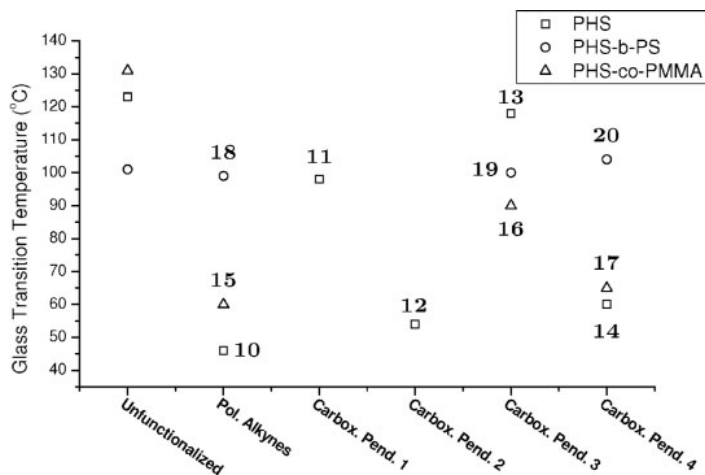


Figure 3. Overview of T_g values for the polymers (the numbers refer to the polymers shown in Table 1).

15 (46–60 °C). This change is believed to be directly related to hydrogen-bonding and dipole-dipole interactions in the unsubstituted polymers, which reduce the rotational freedom in the polymers and thereby lead to increased T_g 's. The carboxylic acid substituted polymers from **10** and **15** also show a clear pattern in which the aromatic carboxylic acid substituents (**1** and **3**) give higher T_g 's around 90–120 °C (**11**, **13**, and **16**), and the aliphatic carboxylic acids (**2** and **4**) give T_g 's around 50–65 °C (**12**, **14**, and **17**). An explanation for this difference could be that the pendant six-carbon chain has a plasticizing effect and thereby reduces T_g in general for all the products. In the case of the aromatic groups, this is counterbalanced by the rigidity and steric hindrance of the terminal phenyl groups interacting along the backbone, whereas the aliphatic equivalents lack these interactions and hence without this counter effect give lower T_g 's.

CONCLUSIONS

Both CuBr in DMF and CuSO₄/sodium ascorbate in H₂O/THF at room temperature catalyzed the click reaction satisfactorily. Through NOESY NMR, it was evidenced that an increased reaction temperature (up to 60 °C) did not effect the regioselectivity of the reaction.

An alkyne-functionalized PHS showed excellent reactivity through click reactions, for which

four different azides were used in postfunctionalizations, and provided fully substituted polymers. The applicability of the approach has been illustrated through postfunctionalizations of both a random copolymer, PHS-co-PMMA, and a block copolymer, PHS-b-PS, with only minor changes to the reaction conditions.

Thermal analysis by DSC has shown a clear correlation between functional group modifications and grafting of the polymer backbone. Especially when aromatic and aliphatic side chains have been compared, a clear tendency toward high and low T_g 's, respectively, has been found.

The presented method has developed novel unprecedented polymers with a high carboxylic acid loading otherwise very difficult to prepare. Moreover, the modular concept in principle allows for great design freedom in the functional moiety to be linked to a polymer main chain because of the versatility and robustness of the click chemistry.

In addition to this, the strategy can be extended to other intriguing functionalities, and we envision localized fixation of receptor and detector couples on macromolecules by this method. Currently, the surface characteristics of thin films prepared from the polymers are being investigated.

A. D. Thomsen thanks the Reinholdt W. Jorck og Hustrus fund, the Sokrates/Erasmus study program, and the Danish Research Council for Technology and Production Sciences (through the framework program

“Design and Processing of Polymers for Microfluidic Applications”, grant 26-04-0074) for their financial support.

REFERENCES AND NOTES

- Kolb, H. C.; Finn, M. G.; Sharpless, K. B. *Angew Chem Int Ed* 2001, 40, 2004–2021.
- Huisgen, R. *Angew Chem Int Ed* 1963, 2, 565–598.
- Rostovtsev, V. V.; Green, L. G.; Fokin, V. V.; Sharpless, K. B. *Angew Chem Int Ed* 2002, 41, 2596–2599.
- Tornøe, C. W.; Christensen, C.; Meldal, M. *J Org Chem* 2002, 67, 3057–3064.
- Hawker, C. J.; Wooley, K. L. *Science* 2005, 309, 1200–1204.
- Diaz, D. D.; Punna, S.; Holzer, P.; McPherson, A. K.; Sharpless, K. B.; Fokin, V. V.; Finn, M. G. *J Polym Sci Part A: Polym Chem* 2004, 42, 4392–4403.
- Lutz, J.; Börner, H. G.; Weichenhan, K. *Macromol Rapid Commun* 2005, 26, 514–518.
- Opsteen, J. A.; van Hest, J. C. M. *Chem Commun* 2005, 57–59.
- Sumerlin, B. S.; Tsarevsky, N. V.; Louche, G.; Lee, R. Y.; Matyjaszewski, K. *Macromolecules* 2005, 38, 7540–7545.
- Wu, P.; Feldman, A. K.; Nugent, A. K.; Hawker, C. J.; Scheel, A.; Voit, B.; Pyun, J.; Fréchet, J. M. J.; Sharpless, K. B.; Fokin, V. V. *Angew Chem Int Ed* 2004, 43, 3928–3932.
- Malkoch, M.; Schleicher, K.; Drockenmuller, E.; Hawker, C. J.; Russell, T. P.; Wu, P.; Fokin, V. V. *Macromolecules* 2005, 38, 3663–3678.
- Mantovani, G.; Ladmiral, V.; Tao, L.; Haddleton, D. M. *Chem Commun* 2005, 2089–2091.
- Helms, B.; Mynar, J. L.; Hawker, C. J.; Fréchet, J. M. J. *J Am Chem Soc* 2004, 126, 15020–15021.
- Parrish, B.; Breitenkamp, R. B.; Emrick, T. *J Am Chem Soc* 2005, 127, 7404.
- Malkoch, M.; Thibault, R. J.; Drockenmuller, E.; Messerschmidt, M.; Voit, B.; Russell, T. P.; Hawker, C. J. *J Am Chem Soc* 2005, 127, 14942–14949.
- Coessens, V.; Pintauer, T.; Matyjaszewski, K. *Prog Polym Sci* 2001, 26, 337–377.
- Gottlieb, H. E.; Kotlyar, V.; Nudelman, A. *J Org Chem* 1997, 62, 7512–7515.
- Borkar, S. *Synthesis and Characterization of Functional Diblock Copolymers*. Thesis, Universität Duisburg-Essen, 2003.
- Rozycki, M.; Bartha, R. *Appl Environ Microbiol* 1981, 41, 833–836.
- Salmon-Legagneur, F.; Neveu, C.; Belot, A. *Bull Soc Chim Fr* 1957, 1463–1469.
- Englert, B. C.; Bakbak, S.; Bunz, U. H. F. *Macromolecules* 2005, 38, 5868–5877.
- Ryu, E.; Zhao, Y. *Org Lett* 2005, 7, 1035–1037.

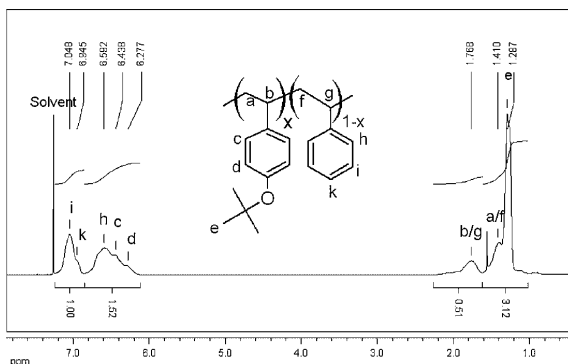
Appendix B

A.E. Daugaard and S. Hvilsted. “The Influence of Pendant Carboxylic Acid Loading on Surfaces of Statistical Poly[(4-hydroxystyrene)-*co*-styrene]s”. *Macromolecular Rapid Communications* **2008**, *29*, 1119–1125.

The Influence of Pendant Carboxylic Acid Loading on Surfaces of Statistical Poly[(4-hydroxystyrene)-*co*-styrene]

Anders Egede Daugaard, Søren Hvilsted*

Copolymers of 4-*tert*-butoxystyrene (tBS) and styrene (S) have been prepared by free radical copolymerization and the copolymer ratios of $r_{\text{tBS}} = 0.97$ and $r_{\text{S}} = 1.12$ have been determined by the Kelen-Tüdös method. After deprotection to 4-hydroxystyrene, alkynes were introduced by a Williamson ether synthesis with propargyl bromide and the copolymers were functionalized with pendant aliphatic or aromatic carboxylic acids by click chemistry. Differential scanning calorimetry of the copolymers demonstrates the large influence on T_{g} of the different functional groups and the backbone composition. In particular, aliphatic and aromatic pendant groups differ by 92 °C in T_{g} . Contact angle measurements on spin coated films have shown a maximum effect of the functional groups in the advancing contact angle at a 75/100 copolymer loading. In addition to this, X-ray photoelectron spectroscopy shows the presence of acid groups on the surface.



Introduction

The polymer materials community is constantly developing novel functional polymers, not least functional polymer surfaces. One approach is the use of precursor linear (co)polymers that can be functionalized by various synthetic strategies. Click chemistry, especially the 1,3-dipolar cycloaddition of azides and alkynes has most recently proved to be a very powerful synthetic tool due to high selectivity and almost complete conversion under

mild reaction conditions. For an extensive overview see reviews by Binder and Sachsenhofer,^[1] Lutz,^[2] and Schubert et al.^[3] Many different functionalities have thus been coupled to linear polymers for the preparation of novel materials, e.g., end-functional polymers,^[4] dendronized polymers,^[5] peptide and poly(ethylene glycol) (PEG)-functionalized polyesters,^[6] functional polysaccharides,^[7,8] functional PMMAs from alkyne^[9] or azide^[10] functional polymers, and crown ether functional conductive polymers.^[11] The selectivity of the cycloaddition has further been demonstrated through simultaneous orthogonal synthesis of esters and triazoles on the same polymer backbone.^[12]

Recently we published a method to obtain new functional polymers based on three different polymer backbones poly(4-hydroxystyrene), poly[(hydroxystyrene-*co*-methyl

A. E. Daugaard, S. Hvilsted

Danish Polymer Centre, Department of Chemical and Biochemical Engineering, Technical University of Denmark, Building 423, 2800 Kgs. Lyngby, Denmark
E-mail: sh@kt.dtu.dk

methacrylate)], and polystyrene-*block*-poly (hydroxystyrene) through a click chemistry approach.^[13] The surface properties of the produced polymers are of interest in order to find suitable candidates for application in an electro-osmotic micropump.

The preliminary results indicated that copolymers or homopolymers were well suited for the preparation of functional surfaces by this approach. The polystyrene backbone appeared promising as the products are normally amorphous polymers and easy to handle. However, it was discovered that the effect of a different loading and the effects of different functional groups would have to be investigated in greater detail. To elucidate this it was decided to prepare new copolymers with different compositions of the backbone. Based on previous experience,^[13] poly(4-hydroxystyrene) can easily be derivatized by the click approach. For the preparation of new copolymers of styrene and 4-hydroxystyrene the choice of polymerization was free radical polymerization. This was based on earlier results from atom transfer radical polymerization (ATRP) on 4-acetoxystyrene (AS),^[14] 4-*tert*-butoxystyrene (tBS), and anionic polymerization of tBS in our group. Of the two monomers it was found that only AS could be polymerized by ATRP. However, the deprotection of the poly(4-acetoxystyrene) was complicated by crosslinking,^[15] and thus other alternatives were considered. Anionic polymerization of tBS is possible and gives well defined polymers, though it would not be well suited for the targeted copolymers since the preparation time would be considerable. In addition the gain of a narrower polydispersity was expected to be of minor importance. Recently the application of nitroxide-mediated free radical polymerization of AS has been used to prepare poly(hydroxystyrene/styrene) copolymers that were post functionalized by a similar approach.^[16]

Here we present the preparation of statistic copolymers of styrene and tBS for the preparation of polymers with variable loadings of functional groups through click chemistry.

Experimental Part

General Methods

Thin layer chromatography (TLC) was performed on Merck plates coated with silica gel F254. Kiesegel for column chromatography was Merck Kiesegel 60 (230–400 mesh). ¹H NMR spectra were obtained using a 250 MHz Cryomagnet from Spectrospin & Bruker at room temperature. Infrared spectroscopy (IR) was performed on a PerkinElmer Spectrum One model 2000 Fourier transform infrared system with a universal attenuated total reflection sampling accessory on a ZnSe/diamond composite. Differential scanning calorimetry (DSC) was performed on a DSCQ1000 from TA Instruments. The thermal analyses were performed at a heating and cooling rate of 10 °C · min⁻¹. The glass transition

temperatures (T_g s) are reported as the temperature at the inflection point. Size exclusion chromatography (SEC) analyses were performed in tetrahydrofuran (THF) at a flow rate of 1 mL · min⁻¹ with an Irganox standard using a Shimadzu SIL-10AD auto injector and a Shimadzu LC10AD pump operating on two Polymer Laboratories PLgel 5 μm Mixed-D (300 × 7.5 mm²) columns. The detector was a Viscotek model 200 differential refractometer. Molecular weights were determined using a polystyrene (PS) standard. Contact angle measurements were conducted on a Dataphysics OCA 20. Initially a drop of 6 μL was placed on the surface with the needle inside, and the drop was expanded and retracted at a rate of 0.125 μL · s⁻¹. All contact angles reported are an average of three measurements on three different drops on the surface. XPS analysis was performed on a Thermo Fisher Scientific K Alpha (East Grinstead, UK) using monochromatized aluminium K_α radiation in a 400 μm spot on the sample. Survey and high resolution spectra were acquired and analyzed using the manufacturer's Avantage software package.

Chemicals

Chemicals were acquired from Aldrich and were used as received unless otherwise specified. Styrene (S) and 4-*tert*-butoxystyrene (tBS) were purified on neutral Al₂O₃.

General Procedure for Free Radical Copolymerization, Poly(4-*tert*-butoxystyrene)-*ran*-styrene] (11)

2,2'-Azobisisobutyronitrile (AIBN, 0.184 g, 1.1 mmol), tBS (6.8 mL, 36 mmol) and S (4.1 mL, 36 mmol) were mixed with xylene (22 mL) in a Schlenk tube. The tube was connected to a vacuum line, frozen in liquid N₂, evacuated for 10 min and backfilled with N₂ three times. The reaction mixture was heated to 65 °C and stirred for 16 h. The reaction mixture was precipitated drop wise into methanol (300 mL), filtered, and the solid dried under vacuum to provide the copolymer as a white solid (7.21 g, 72% conversion, $\bar{M}_n = 16\,000$ g · mol⁻¹, PDI = 1.68, $T_g = 94$ °C).

IR (ATR): 1364/1388 (*tert*-butyl bends), 1236 (ph-O stretch), 1162, cm⁻¹ (tBu-O stretch).

¹H NMR (CDCl₃, 250 MHz): δ = 1.1–1.6 (m, 6.5H, H_{a,e,f}), 1.6–2.2 (m, 1H, H_{b,g}), 6.2–6.85 (m, 3H, H_{c,d,h}), 6.85–7.2 (m, 1.5, H_{k,i}) (for proton assignments refer to Figure 1).

Determination of the Copolymer Reactivity Ratios

Copolymerizations were started in accordance with the general procedure. The reactions were stopped after 30 min at 65 °C (<4% conversion) and the reaction mixture was precipitated dropwise into methanol. The copolymer was dissolved in THF and precipitated dropwise into MeOH to remove any excess monomer, filtered off, and dried under vacuum to yield the copolymers as white solids. The copolymer composition was determined by ¹H NMR spectroscopy.

General Deprotection Procedure,^[17] Poly(4-hydroxystyrene)-*ran*-styrene) (12)

Polymer **11** (6.29 g) was dissolved in THF (100 mL) and conc. HCl (10 mL) was added. The solution was heated to reflux and stirred

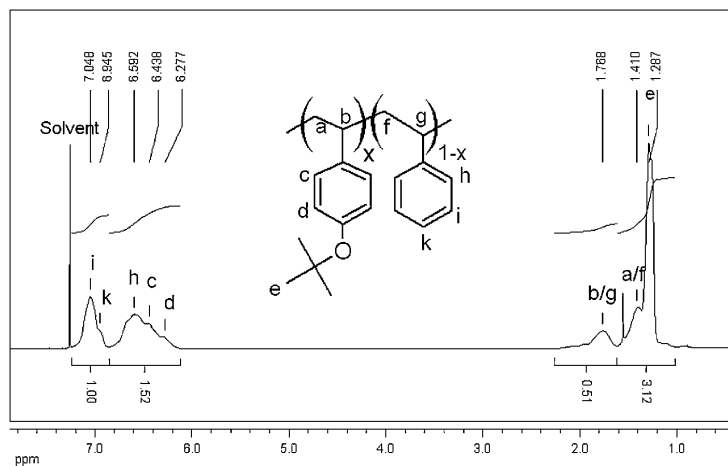


Figure 1. ^1H NMR spectrum of poly[(4-*tert*-butoxystyrene)-*co*-styrene] with 40 mol-% tBS in the feed.

for 20 h. The solution was concentrated to approximately 30 mL and precipitated dropwise into an aqueous solution of HCl (10%, 800 mL). The precipitate was filtered off, rinsed with H_2O several times, and dried under vacuum to provide the deprotected copolymer as a white solid (4.99 g, 99.3%).

IR (ATR): 3 349 (O–H stretch), 1 225 cm^{-1} (ph–O stretch).

^1H NMR (CDCl_3 , 250 MHz): δ = 1.1–1.6 (m, 2H, $\text{H}_{a,t}$), 1.6–2.2 (m, 1H, $\text{H}_{b,g}$), 6.2–6.85 (m, 3H, $\text{H}_{c,d,h}$), 6.85–7.2 (m, 1.5H, $\text{H}_{k,i}$), 9.00 (s, 0.5H, ph–OH) (for proton assignments refer to Figure 1).

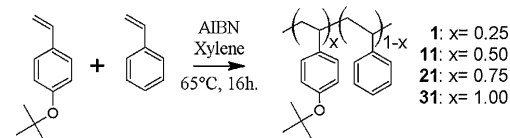
Preparation of Polymer Films

Glass slides were thoroughly rinsed with methanol and THF. A solution of the copolymers in THF (20 $\text{mg} \cdot \text{mL}^{-1}$) was spin coated on the clean glass slides at 1 000 rpm. The films were subsequently annealed in an oven at 30 $^\circ\text{C}$ above the T_g for 16 h.

Results and Discussion

Synthesis of Copolymers

Copolymers of S and tBS were produced by a free radical polymerization using AIBN as shown in Scheme 1.



Scheme 1. Copolymerization of styrene and tBS in different ratios.

The copolymer reactivity ratios were calculated using the method of Kelen and Tüdös^[18,19] in order to investigate the copolymer sequence composition. Accordingly copolymerizations with 10, 20, 40, 60, 80, and 90% of tBS and S were performed. The copolymerizations were terminated below 4% conversion in order to keep the monomer feed approximately constant. As shown in Figure 1 the aromatic *meta* and *para* protons of S are separated from the other aromatic protons. The ratios of the two areas of all the aromatic protons were used for the determination of the copolymer composition.

Based on the NMR data and the monomer feed composition the Kelen–Tüdös plot shown in

Figure 2 was constructed.

With a well-correlated linear relationship, the simple two-parameter model can be applied. From the slope and the intercept in the plot the copolymer reactivity ratios were calculated to be $r_S = 1.12$ and $r_{tBS} = 0.97$. The results correlate well with earlier reported results on copolymers of 4-methoxystyrene (MS)^[20] or 4-ethoxystyrene (ES)^[21] with S where copolymer ratios of $r_{MS} = 1.16$, $r_S = 0.82$, and $r_{ES} = 0.71$, $r_S = 0.98$ were found. Since the copolymer reactivity ratios and the product of these are close to unity the formation of random copolymers most likely will be accomplished over the entire conversion range. Therefore, copolymers can be prepared with higher conversions without effecting the copolymer composition. Random copolymers with compositions of approximately 25/75,

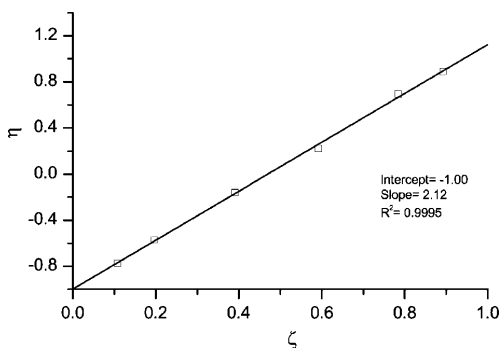


Figure 2. Kelen–Tüdös plot, giving copolymer reactivity ratios of $r_S = 1.12$ and $r_{tBS} = 0.97$.

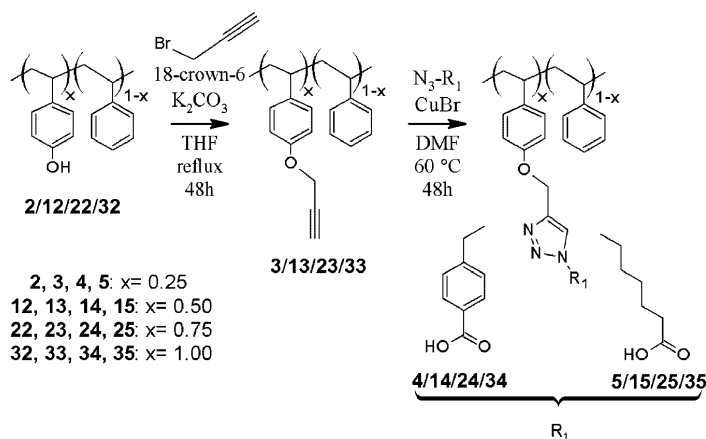
Table 1. Polymer composition and molecular weight.

Polymer	Feed composition		\bar{M}_n	PDI	$T_g^a)$	Polymer composition	
	mol-%					kg · mol ⁻¹	°C
	tBS	S	tBS	S			
PS	0	100	11.3	1.9	86 (90) ^[22]	0	100
1	25.0	75.0	13.3	1.8	88	24.5	75.5
11	50.2	49.8	16.0	1.7	94	47.2	52.8
21	75.0	25.0	17.2	1.7	96	72.8	27.2
31	100	0	19.3	1.7	94 (103) ^[17]	100	0

^{a)}The numbers in parenthesis are values from the same polymers with higher molecular weight provided in the cited references.

50/50, and 75/25 tBS/S were prepared from the equivalent monomer feeds. The obtained copolymer compositions, as determined by ¹H NMR spectra and listed in Table 1, proved almost equivalent to the monomer feed composition.

The *tert*-butoxy protective groups were removed using HCl in THF, to give the poly[(4-hydroxy)-*ran*-styrenes] **2**, **12**, **22**, and **32**. These were then etherified in accordance with the earlier reported procedure^[13] through a Williamson synthesis with propargyl bromide to provide the corresponding alkyne functional copolymers **3**, **13**, **23**, and **33**. The linear backbones were then modified through a click reaction to give different carboxylic acid copolymers as shown in Scheme 2. All products were characterized by IR and NMR spectroscopy and were in accordance with the earlier published results.^[13] The conversions were complete in all cases.



■ Scheme 2. Copolymer functionalization by click chemistry.

Thermal Properties

The thermal properties of these polymers were investigated by DSC. All the copolymers were amorphous and exhibited single T_g s. As shown in Table 1 the neat samples of PS and PtBS show slightly lower T_g s compared to the reference values because of the relatively low molecular weights of the homopolymers. The effect of changes in both the pendant groups as well as changes in the copolymer composition on the T_g is shown in Figure 3.

With an increasing content of the pendant group in the copolymer backbone a larger effect on the T_g is observed, as seen in the case of the poly(4-hydroxystyrene-*ran*-styrene) copolymers **2**, **12**, **22**, and **32** (b in Figure 3). In this case an increase in the content of hydroxy groups from 25 to 100% raises the T_g from 111 to 169 °C. This effect is also seen for the other copolymers, although it is less pronounced.

Interestingly the hydrogen bonding of the carboxylic acids appears to be less important compared to the effects of rigidity and flexibility. The drop in T_g through the aliphatic carboxylic acid substituted polymers **5**, **15**, **25**, and **35** (e in Figure 3) is clearly a result of the plasticizing effect of the aliphatic chain, which should be counterbalanced by increased hydrogen bonding from the carboxylic acids. However, this effect appears to be of minor importance here.

On the other hand, in the case of the aromatic carboxylic acid substituted copolymers **4**, **14**, **24**, and **34** (d in Figure 3) an increased loading apparently has only a minor effect (T_g from 121 to

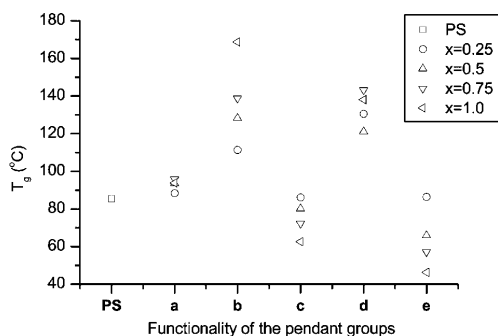


Figure 3. The changes in the glass transition temperatures of the (co)polymers as a function of the pendant groups and the compositions of the (co)polymers. a) *tert*-butoxy, b) hydroxy, c) prop-2-ynyl, d) aromatic acid, and e) aliphatic acid as shown in Schemes 1 and 2.

143 °C). Thus the copolymer with a 25% loading (**4**) has already reached a T_g of 131 °C, which is in proximity of the completely loaded **34** ($T_g = 138$ °C). It is believed that the bulkiness of the triazole and the aromatic carboxylic acid rings in each pendant group is the reason for this. Introduction of such bulky groups, even in a low concentration, imparts considerable steric hindrance on the backbone, and thus possibly prevents rotation and stabilization by interchain hydrogen bonding. The increased content of aromatic groups in the copolymer has only a minor effect as the backbone already has a rigid structure.

Functional Surfaces

The intended application of these copolymers was the preparation of functional polymer surfaces for uses within electro-osmotic micropumps. In order for the different chemistries to have an effect, the functional groups should be accessible to a solution placed on the surface. To investigate the accessibility it was decided to apply contact angle (CA) measurements as a screening method.

Polymer films of all the copolymers were prepared by spin coating on glass slides. Initial CA measurements on the pristine films demonstrated that it was necessary to anneal the films in order to get constant contact angles. After annealing for 16 h at 30 °C above the T_g the films appeared to have reached equilibrium conditions, and no changes were observed with longer annealing times.

Water CA measurements were conducted under dynamic conditions to obtain both the advancing and the receding contact angle. The changes in the contact angle from chemically different pendant groups are shown in Figure 4 with the series based on the functional homopolymer.

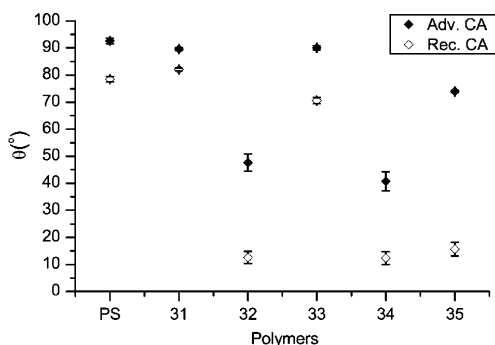


Figure 4. The advancing and receding contact angle as a function of the different pendant groups on the different homopolymers **31**, **32**, **33**, **34** and **35**. The polymer structures can be seen in Schemes 1 and 2.

The data in Figure 4 show that the polar compounds on the backbone afford a lowering of the CAs of water on the surface, which implies an increase in the surface free energy as expected. This effect is observed for both the hydroxy (**32**) and acid functional (**34**, **35**) polymers, though surprisingly the aliphatic carboxylic acid (**35**) gives a rather high advancing CA. For these substituents a substantial contact angle hysteresis is observed (25–60 °C), which is in accordance with a chemically heterogeneous surface. There appears to be a large difference in the advancing contact angle with attachment of an aromatic or an aliphatic acid to the backbone. This effect is believed to be a result of higher flexibility of the aliphatic chain compared to the aromatic ring that has a strong influence on the mobility of the groups in the immediate surface layer. Since carboxylic acids will increase the surface free energy, counteracting rearrangements would be expected. The ability to rearrange would also be an explanation for the large difference in CA hysteresis observed when comparing the hydroxy, aromatic, and aliphatic carboxylic acids. It is known from observations by others that rearrangement of polar groups in the upper surface may decrease the interfacial surface tension.^[23–25]

The effect of the copolymer composition on the advancing CA is shown in Figure 5.

The effects from polar substituents (b, d, and e in Figure 5) are clearly seen, while changes in the unpolar substituents have less influence on the contact angle because of the similarity to the S backbone. An increased loading of the backbone gives a more pronounced effect for the polar substituents. Interestingly the copolymer with pendant aliphatic carboxylic acids (e in Figure 5) seems to approach a constant value where the influence upon the advancing contact angle with increased loading levels off. The hydroxy and aromatic carboxylic acid substituted

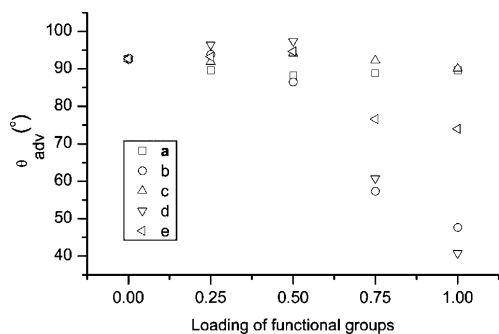


Figure 5. Advancing contact angle (θ_{adv}) as a function of the composition of the polymer backbone, error bars have been omitted for clarity, the measurements deviate by less than $\pm 4^\circ$. a) *tert*-butoxy, b) hydroxy, c) prop-2-ynyl, d) aromatic acid, and e) aliphatic acid as shown in Schemes 1 and 2.

copolymers (b and d in Figure 5) affect the advancing contact angle throughout the range of compositions. This trend is very interesting from an application point of view, since it indicates that it is possible to test a substrate for the influence of a specific functionality and find an optimal loading.

It is not possible to directly identify the chemical functionality on the surface from these measurements. CA measurements on polymer surfaces are influenced by many effects such as surface roughness, chemical heterogeneity, mobility in the surface, and swelling.^[24] On the other hand, since the films are prepared by the same procedure the influence of these effects are believed to be averaged from film to film and thus a relative comparison should be possible. Thereby the CA measurements could be used as a measurement of the polarity or, in this case, the change in concentration of the polar groups on the surface. To corroborate the CA measurements a direct correlation to chemical composition through X-ray photoelectron spectroscopy (XPS) analysis has been conducted, giving the results shown in Table 2.

The XPS results in the table are compared to the reference values calculated based on the composition of

Table 2. XPS results on selected copolymers.

Polymer	C ^{a)}	C calc.	O ^{a)}	O calc.	N ^{a)}	N calc.
	%	%	%	%	%	%
32	85.6	88.9	14.4	11.1	0	0
33	87.6	91.7	12.4	8.3	0	0
24	83.3	81.8	11.8	9.1	4.9	9.1
25	80.7	80.6	12.9	9.7	6.4	9.7
34	76.6	76.0	15.9	12.0	7.4	12.0
35	76.1	73.9	14.7	13.0	9.2	13.0

^{a)}A correction of the data to remove the effects from a minor silicone impurity (<4%) originating from our labs has been performed. It was not possible to prepare samples without the silicone impurity.

the bulk film. As can be seen there is a relatively good correlation between the contents of carbon and oxygen from the samples compared to the reference values. Interestingly, the nitrogen content is slightly lower compared to the calculated values. The bulk polymer is well characterized by NMR and IR spectroscopy, and contains only minor impurities. The deviation from the calculated composition could be an effect of surface rearrangement, though this would have to be confirmed with XPS analyses run at an angle. Such an analysis has been performed, however, the results were inconclusive. To elucidate the surface composition the high resolution XPS peak from carbon was curve fitted in order to quantify the different types of carbon in the surface. The results are shown in Table 3.

Table 3 compares the high resolution data to the calculated composition of different carbons in the bulk (co)polymers. In general the results mirror the bulk composition, except that there appears to be a slightly lower concentration of carboxylic acids on the surface. The only exception to this is **34** (aromatic acid, homopolymer), which is the only sample that shows approximately the same composition as the bulk. The higher contents of

Table 3. The high-resolution data in at.-% from the carbon peak in XPS.

Carbons	Binding energies	14 ^{a)}	14 bulk ^{b)}	15 ^{a)}	15 bulk ^{b)}	34 ^{a)}	34 bulk ^{b)}	35 ^{a)}	35 bulk ^{b)}
eV									
C–C	284	79.8	77.8	73.6	76.0	69.6	68.4	63.8	64.7
C–O, C–N	285	17.6	18.5	23.6	20.0	24.9	26.3	32.0	29.4
COOH	290	2.6	3.7	2.8	4.0	5.5	5.3	4.2	5.9

^{a)}A correction of the data to remove the effects from a minor silicone impurity (<4%) originating from our labs has been performed. It was not possible to prepare samples without the silicone impurity; ^{b)}Calculated values based on the composition of the (co)polymer.

COOH in **34** correlates well with the observed effects from the contact angle measurements, where **34** clearly afforded a much larger effect on the advancing CA compared to the other samples.

Conclusion

It has been shown that free radical copolymerization of 4-*tert*-butoxystyrene and styrene is an efficient way to produce well-defined random copolymers. The copolymer reactivity ratios have been determined as $r_{\text{tBS}} = 0.97$ and $r_{\text{S}} = 1.12$ using the Kelen-Tüdös method. After deprotection to 4-hydroxystyrene and subsequent alkyne derivatization the copolymers can be applied in a click postfunctionalization to obtain carboxylic acid functional copolymers with variable composition.

All the copolymers have been characterized thermally and it was possible to directly identify the effects upon the glass transition from different functional groups, which ranged from 46–143 °C for the aliphatic or aromatic carboxylic acids. Copolymer films have been prepared from these copolymers, giving functional surfaces with the desired chemical groups. Contact angle measurements on the homopolymers revealed that the aromatic groups result in an advancing contact angle of 41°, approximately 30° lower than the more flexible aliphatic carboxylic acid. In addition, it was also possible to identify constant contact angles independent of a further increase in copolymer composition. The results were corroborated using XPS and showed that the surfaces contain carboxylic acids. A high concentration of acids was found on the surface, especially in the case of **34**.

Acknowledgements: Niels B. Larsen at Risø, DTU Nanotech is thanked for assistance with the XPS analyses. The Danish Research Council for Technology and Production Sciences (through the framework program "Design and Processing of Polymers for Microfluidic Applications", grant 26-04-0074) is thanked for financial support.

Received: February 25, 2008; Revised: March 12, 2008; Accepted: March 13, 2008; DOI: 10.1002/marc.200800113

Keywords: copolymerisation; films; functionalization of polymers; polystyrene (PS); surfaces

- [1] W. H. Binder, R. Sachsenhofer, *Macromol. Rapid Commun.* **2007**, *28*, 15.
- [2] J. F. Lutz, *Angew. Chem. Int. Ed.* **2007**, *46*, 1018.
- [3] D. Fournier, R. Hoogenboom, U. S. Schubert, *Chem. Soc. Rev.* **2007**, *36*, 1369.
- [4] J. F. Lutz, H. G. Börner, K. Weichenhan, *Macromol. Rapid Commun.* **2005**, *26*, 514.
- [5] B. Helms, J. L. Mynar, C. J. Hawker, J. M. J. Frechet, *J. Am. Chem. Soc.* **2004**, *126*, 15020.
- [6] B. Parrish, R. B. Breitenkamp, T. Emrick, *J. Am. Chem. Soc.* **2005**, *127*, 7404.
- [7] T. Liebert, C. Hänsch, T. Heinze, *Macromol. Rapid Commun.* **2006**, *27*, 208.
- [8] J. Hafren, W. Zou, A. Cordova, *Macromol. Rapid Commun.* **2006**, *27*, 1362.
- [9] V. Ladmiral, G. Mantovani, G. J. Clarkson, S. Cauet, J. L. Irwin, D. M. Haddleton, *J. Am. Chem. Soc.* **2006**, *128*, 4823.
- [10] B. S. Sumerlin, N. V. Tsarevsky, G. Louche, R. Y. Lee, K. Matyjaszewski, *Macromolecules* **2005**, *38*, 7540.
- [11] B. C. Englert, S. Bakbak, U. H. F. Bunz, *Macromolecules* **2005**, *38*, 5868.
- [12] M. Malkoch, R. J. Thibault, E. Drockenmüller, M. Messerschmidt, B. Voit, T. P. Russell, C. J. Hawker, *J. Am. Chem. Soc.* **2005**, *127*, 14942.
- [13] A. D. Thomsen, E. Malmström, S. Hvilsted, *J. Polym. Sci., Part A: Polym. Chem.* **2006**, *44*, 6360.
- [14] B. Gao, X. Y. Chen, B. Ivan, J. Kops, W. Batsberg, *Macromol. Rapid Commun.* **1997**, *18*, 1095.
- [15] X. Y. Chen, K. Jankova, J. Kops, W. Batsberg, *J. Polym. Sci., Part A: Polym. Chem.* **1999**, *37*, 627.
- [16] B. Sieczkowska, M. Millaruelo, M. Messerschmidt, B. Voit, *Macromolecules* **2007**, *40*, 2361.
- [17] D. A. Conlon, J. V. Crivello, J. L. Lee, M. J. O'Brien, *Macromolecules* **1989**, *22*, 509.
- [18] T. Kelen, F. Tüdös, *J. Macromol. Sci. Chem.* **1975**, *A9*, 1.
- [19] J. P. Kennedy, T. Kelen, F. Tüdös, *J. Polym. Sci., Part A: Polym. Chem.* **1975**, *13*, 2277.
- [20] D. Braun, W. Cerwinski, F. Disselhoff, F. Tüdös, T. Kelen, B. Turcsanyi, *Angew. Makromol. Chem.* **1984**, *125*, 161.
- [21] C. Walling, E. R. Briggs, K. B. Wolfstirn, F. R. Mayo, *J. Am. Chem. Soc.* **1948**, *70*, 1537.
- [22] S. S. N. Murthy, *J. Polym. Sci., Part B: Polym. Phys.* **1993**, *31*, 475.
- [23] M. X. Xu, W. G. Liu, J. Wang, W. Gao, K. De Yao, *Polym. Int.* **1997**, *44*, 421.
- [24] T. Kasemura, S. Takahashi, T. Okada, T. Maegawa, T. Oshibe, T. Nakamura, *J. Adhes.* **1996**, *59*, 61.
- [25] T. Teraya, A. Takahara, T. Kajiyama, *Polymer* **1990**, *31*, 1149.

Appendix C

A. Khan, A.E. Daugaard, A. Bayles, S. Koga, Y. Miki, K. Sato, J. Enda, S. Hvilsted, G.D. Stucky and C.J. Hawker. “Dendronized Macromonomers for Three-Dimensional Data Storage”. *Chemical Communications* **2009**, 425–427

Dendronized macromonomers for three-dimensional data storage†

Anzar Khan,^a Anders E. Daugaard,^b Andrea Bayles,^a Shogo Koga,^c Yasuaki Miki,^c Ken Sato,^c Jun Enda,^c Soren Hvilsted,^b Galen D. Stucky^a and Craig J. Hawker^{*a}

Received (in Cambridge, UK) 17th September 2008, Accepted 25th November 2008

First published as an Advance Article on the web 11th December 2008

DOI: 10.1039/b816298k

A series of dendritic macromonomers have been synthesized and utilized as the photoactive component in holographic storage systems leading to high performance, low shrinkage materials.

A continuing trend in information storage is the desire for greater storage capacity, a feature that demands the development of both new storage techniques as well as new materials. One of the most promising approaches for achieving high density data storage is based on volume holography which allows data to be stored in 3 dimensions. This significant increase in capacity is in direct contrast to the fundamental size limitations found in traditional 2-D systems such as magnetic hard disk drives.¹ In volume holography, information is stored in the form of optical interference patterns throughout the volume of a photosensitive material. This is accomplished by intersecting two coherent laser beams with the first, called the object beam, containing the information to be stored. The second, called the reference beam, is used to retrieve the stored information. When the object beam and the reference beam intersect in the storage medium, they cause a change in the chemical or physical properties of the material which results in refractive index modulation. By shifting the angular position of the storage media, multiple interference patterns (holograms) can be recorded within the same volume, enabling high density information storage.‡

While promising, this 3-D volumetric storage strategy has limited commercial implementation due to a variety of material challenges. An ideal storage media must meet numerous stringent requirements including high photosensitivity, high storage capacity, non-volatile read-out, dimensional stability, millimetre thickness, and low-cost.² Photopolymer systems³ fulfill many of these requirements and are promising candidates for three-dimensional data storage applications. Typically they consist of a mixture of monomer and photoinitiator dissolved in a thick, crosslinked network (Fig. 1). Upon holographic exposure, a polymerization reaction initiates in the bright regions of the holographic media leading to consumption of the monomer in the bright regions and generation of a concentration gradient with associated diffusion of the

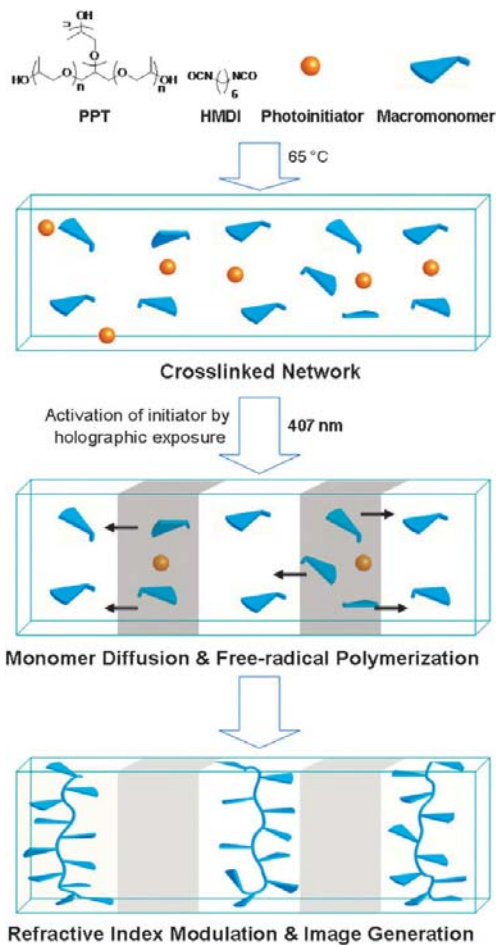


Fig. 1 Schematic representation of refractive index modulation and hologram formation due to the photopolymerization of dendronized monomers dispersed within a thick, crosslinked film.

monomers from the dark regions. This monomer diffusion results in a permanent compositional and density change in the recording material and creates a refractive index modulation. However an intrinsic problem with the photopolymer system is the writing induced shrinkage of the recording material due to the monomer diffusion and the formation of new covalent

^a Department of Chemistry and Biochemistry, Materials Department, Materials Research Laboratory, and Mitsubishi Chemical Center for Advanced Materials, University of California, Santa Barbara, CA 93106-9510, USA. E-mail: hawker@mrl.ucsb.edu

^b Department of Chemical and Biochemical Engineering, Technical University of Denmark, Building 423 Produktionstorvet, DK-2800 Kgs Lyngby, Denmark

^c Mitsubishi Chemical Group Science and Technology Research Center Inc., 1000 Kamoshida-cho, Aoba-ku, Yokohama 227-8502, Japan

† Electronic supplementary information (ESI) available: 19 pages of experimental data. See DOI: 10.1039/b816298k

bonds during polymerization. This dimensional instability has a detrimental effect on the retrieval of the data from stored holograms (hologram position shifts from the original position) and hence severely limits the commercial viability of the photopolymer system for volume holographic applications.^{2,4} This issue becomes even more critical for high capacity storage systems as holograms recorded in thicker films are more sensitive to dimensional changes than those recorded in thin films.⁴ To overcome these limitations, new monomers need to be developed that have low viscosities for efficient diffusion, do not lead to appreciable shrinkage on polymerization and possess a high refractive index.

Here, we demonstrate that the use of highly branched dendritic macromonomers can address many of these issues and allow writing induced shrinkage to be successfully reduced to negligible values. A critical feature of dendritic macromonomers is their inherent large volume to functional group ratio where the influence of the single focal point unit decreases with increasing generation number. In addition, the highly branched molecular architecture maintains a low viscosity⁵ and consequently high mobility in the initial crosslinked matrix. Finally, the incorporation of numerous high refractive index moieties at the chain ends increases the average refractive index of the macromonomer and leads to enhanced data storage capacity. The use of novel dendritic macromonomers therefore permits development of a low shrinkage photopolymer based holographic material without sacrificing the sensitivity or the storage capacity of the recording media. The modular nature of dendrimer chemistry and the precise control over the generation number, nature of chain ends, focal point, and repeat units also allows a direct structure–property relationship to be developed for these materials.^{6,7}

Benzyl ether based dendrimers were selected for initial investigations due to their ease of synthesis, relatively high refractive index, increased solubility and unique hydroxyl group at the focal point. The dendritic acrylate monomers **2**, **3**, and **4** were synthesized convergently from 4-bromobenzylbromide and 3,5-dihydroxybenzyl alcohol in 2, 4, and 6 steps with overall yields of 70–80%, respectively, followed by facile functionalization by reaction with acryloyl chloride (Fig. 2).⁸

In order to fabricate millimetre thick transparent optical films suitable for holographic recording; monomers **1**, **2**, **3**, or **4** (3 wt%) were individually mixed with polyurethane based

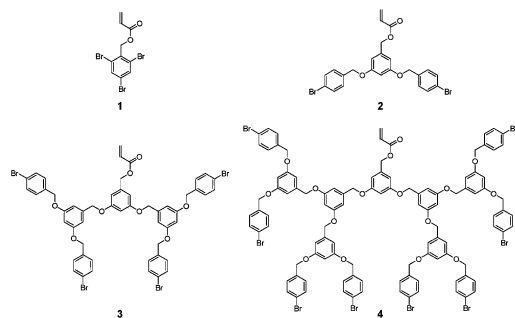


Fig. 2 Chemical structures of the dendritic monomers examined for holographic storage.

matrix precursors hexamethylenediisocyanate (19.48 wt%), polypropylene-triol ($M_n = 1000$) (77.2 wt%), and dioctyltin dilaurate (0.02 wt%) with 2,4,6-trimethylbenzoyldiphenylphosphine oxide (Lucirine) (0.3 wt%) added as a photoinitiator. Initial orthogonal reaction between the triol and diisocyanate derivatives afforded crosslinked thick films of high optical quality with no observed phase separation of the unreacted dendritic macromonomer or photoinitiator. Illumination of these crosslinked thick films with an interference pattern from two collimated 407 nm laser beams (total optical power density of $\sim 6 \text{ mW cm}^{-2}$ and beam diameter of $\sim 5 \text{ mm}$) initiates the photopolymerization and associated diffusion of unreacted dendritic macromonomers **1**, **2**, **3**, or **4** to generate a refractive index modulation. The high sensitivity of this system allows at least 60 holograms to be individually recorded in each holographic disc and from these data, the storage capacity ($M/\#$)⁹ of holographic systems containing **1**, **2**, **3**, or **4** was calculated to be 8, 8, 10, and 6, respectively (Table 1). Fig. 3 shows angular selectivity response of the 60 holograms recorded by utilizing monomer **3** as the photoactive component in the holographic disks (see also Fig. S1 in the ESI†).

Volume shrinkage due to holographic recording was then calculated according to the method reported by Dhar and co-workers.^{†10} For the control system containing the tribromo acrylate monomer **1** a volume shrinkage of 0.23% was observed after recording of 60 holograms in a standard 0.5 mm disk format (see ESI†). Use of the first generation dendritic monomer **2** led to materials with the same storage capacity as **1** (Table 1—similar refractive index (RI) of the monomers **1** (RI = 1.614) and **2** (RI = 1.616)),^{†11} while

Table 1 Holographic properties of the data storage systems containing monomer **1**, **2**, **3**, or **4**

Monomer	Storage capacity ($M/\#$)	Sensitivity/ cm mJ^{-1}	Volume shrinkage (%)	Refractive index
1	8	0.20	0.23	1.614
2	8	0.37	0.10	1.616
3	10	0.46	0.04	1.647
4	6	0.05	0.03	1.663

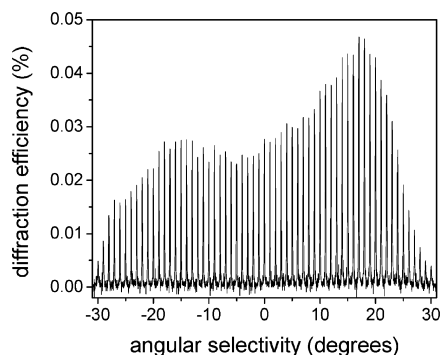


Fig. 3 Angular selectivity curves of the 60 holograms recorded in 0.5 mm thick holographic disc containing second generation based monomer **3**.

volume shrinkage was reduced to 0.1%. To further understand the relationship between generation number and volume shrinkage, the second generation dendritic macromonomer **3** having 4 chain end bromophenyl groups was synthesized and utilized as the photoactive component in a series of holographic discs. The experimental results reveal that the increased refractive index (1.647) of **3** leads to an increased storage capacity ($M/\# = 10$) and the higher generation number per molecular weight resulted in a further reduction in volume shrinkage to 0.04%. Significantly, the high solubility of **3** allowed thick, photosensitive (0.46 cm MJ^{-1}) systems to be prepared and demonstrated the effect of increasing generation number and branched structure on the performance of dendritic macromonomers as holographic storage components. Further increasing the generation number gives the third generation derivative, **4**, which was found to exhibit poor solubility in the original matrix components. As a result, the oligomeric matrix precursor polypropylene-triol ($M_n = 1000$) was replaced with a mixture of polycarbonatediol ($M_n = 800$) and trimethylolpropane (9 : 1) (referred to as polycarbonate matrix henceforth), which allowed for fabrication of thick films suitable for holographic recording. Utilization of monomer **4** resulted in an additional decrease in the volume shrinkage to 0.03% and displayed a similar storage capacity to **1** and **2**. However the sensitivity was reduced (Table 1), presumably due to the unfavorable nature of the polycarbonate matrix.¹² This is confirmed by utilizing monomers **1**, **2**, and **3** in the polycarbonate matrix which led to a decrease in the sensitivity and storage capacity of all the storage systems.†

In conclusion, we have demonstrated the synergistic effect that dendritic branching has on the performance of photopolymerizable materials for holographic storage. Careful design of the molecular structure of the dendritic macromonomers allowed the second generation, poly(benzyl ether) **3** to be identified as the optimal structure for this material set. Negligible volume shrinkage, high $M/\#$, as well as excellent photosensitivity was observed. Significantly, the minimal volume shrinkage assures high fidelity for data recovery, while the high $M/\#$ imparts elevated storage capacity to the recording material with good photosensitivity allowing for rapid recording speed. The general approach of exploiting the unique structural features of functionalized dendritic macromonomers for shrinkage reduction presented here will also be useful for materials used in optical devices that require high dimensional stability such as holographic optical elements (HOEs), gradient refractive index (GRIN) materials, optical circuits, and optical waveguides. These results also demonstrate a further advantage of the dendritic architecture in the design of materials with improved properties,¹³ in this case significant reduction in volume shrinkage for a photopolymer system without sacrificing the photosensitivity of the storage medium.

Financial support from MC-CAM and the central facilities of the UCSB Materials Research Laboratory (NSF Grant DMR05-20415) is gratefully acknowledged. A. D. would like

to thank the Berg, Niensens legat, Aage Corrits legat, Otto Mønstedts fund and the Danish Research Council for Technology and Production Sciences (through the framework program "Design and Processing of Polymers for Microfluidic Applications", grant 26-04-0074) for financial support.

Notes and references

† *Hologram recording*: Experimental setup for recording of holograms was assembled on an optical table suspended on vibration damping supports. The output of a blue diode laser (SONY SBL-N001A, 404 nm, 45 mW, single longitudinal mode) was split into two beams with equal power using a continuously adjustable beam splitter consisting of two half-wavelength plates and a polarizer cube. The resulting beams passed through spatial filters and collimating lenses, which produced beams with a diameter of ~ 5 mm. The angle between the recording beams was 37.4° . Optical power density in a single recording beam was ~ 6 mW cm.

- (a) D. Gabor, *Nature*, 1948, **161**, 777; (b) D. Gabor, *Science*, 1972, **177**, 299; (c) *Holographic Data Storage*, ed. H. Coufal, D. Psaltis and G. Sincerbox, Springer-Verlag, New York, 2000; (d) M. Hackle, L. Kador, D. Kropp and H. W. Schmidt, *Adv. Mater. (Weinheim, Ger.)*, 2006, **19**, 227; (e) S. J. Zilker, *ChemPhysChem*, 2000, **1**, 72.
- (a) S. J. Zilker, *ChemPhysChem*, 2002, **3**, 333; (b) M. Haw, *Nature*, 2003, **422**, 556.
- (a) D. H. Close, A. D. Jacobson, J. D. Margerum, R. G. Brault and F. J. Meclung, *Appl. Phys. Lett.*, 1969, **14**, 159; (b) L. Dhar, A. Hale, H. E. Katz, M. Schilling, M. G. Schnoes and F. C. Schilling, *Opt. Lett.*, 1999, **24**, 487; (c) T. J. Trentler, J. E. Boyd and V. L. Colvin, *Chem. Mater.*, 2002, **12**, 1431; (d) L. Dhar, A. Hale, H. E. Katz, M. L. Schilling and M. L. Schnoes, *U.S. Patent*, 6 103 454, 2000; (e) M. L. Schilling, V. L. Colvin, L. Dhar, A. L. Harris, C. F. Schilling, H. E. Katz, T. Wysocki, A. Hale, L. L. Blyler and C. Boyd, *Chem. Mater.*, 1999, **11**, 247.
- J. E. Boyd, T. J. Trentler, R. K. Wahi, Y. I. Vega-Cantu and V. L. Colvin, *Appl. Opt.*, 2000, **39**, 2353.
- The absence of physical entanglement in dendrimeric structures due to branching is described in: C. J. Hawker, P. J. Farrington, M. E. Mackey, K. L. Wooley and J. M. J. Fréchet, *J. Am. Chem. Soc.*, 1995, **117**, 4409.
- (a) J. M. J. Fréchet, *Science*, 1994, **263**, 1710; (b) D. A. Tomalia and J. M. J. Fréchet, *J. Polym. Sci., Part A: Polym. Chem.*, 2002, **40**, 2719; (c) S. M. Grayson and J. M. J. Fréchet, *Chem. Rev.*, 2001, **101**, 3819.
- (a) R. Freudenberger, W. Claussen, A. D. Schlüter and H. Wallmeier, *Polymer*, 1994, **35**, 4496; (b) A. D. Schlüter, *Top. Curr. Chem.*, 2005, **245**, 151.
- (a) K. L. Wooley, C. J. Hawker and J. M. J. Fréchet, *J. Chem. Soc., Perkin Trans. 1*, 1991, 1059; (b) K. L. Wooley, C. J. Hawker and J. M. J. Fréchet, *J. Am. Chem. Soc.*, 1991, **113**, 4252.
- $M/\#$ is a measure of how many holograms of a given diffraction efficiency can be stored in a common volume. Higher $M/\#$ represent higher storage capacity.
- L. Dhar, M. G. Schones, T. L. Wysocki, H. Bair, M. Schilling and C. Boyd, *Appl. Phys. Lett.*, 1998, **73**, 1337.
- Refractive index contrast (between the matrix and the resulting photopolymer) is one of the major factors that determine the storage capacity of a recording material. In general, the higher the refractive index contrast, the higher will be the storage capacity.
- Most likely the high crosslinking density/low porosity is responsible for the decreased sensitivity of the monomers in the polycarbonate matrix system. For an example of the influence of the matrix on holographic properties of a recording system, see ref. 3c.
- C. Pitois, D. Wiesmann, M. Lindgren and A. Hult, *Adv. Mater. (Weinheim, Ger.)*, 2001, **13**, 1483.

Appendix D

A. Khan, A.E. Daugaard, A. Bayles, S. Koga, Y. Miki, K. Sato, J. Enda, S. Hvilsted, G.D. Stucky and C.J. Hawker. “Dendronized Macromonomers for Three-Dimensional Data Storage”. *Chemical Communications* **2009**, 425–427, supporting information.

SUPPORTING INFORMATION**Dendronized Macromonomers for Three-Dimensional Data Storage**

Anzar Khan,[†] Anders E. Daugaard,[‡] Andrea Bayless,[†] Shogo Koga,[§] Yasuaki Miki,[§] Ken Sato,[§]

Jun Enda,[§] Søren Hvilsted,[‡] Galen D. Stucky, and Craig J. Hawker^{*†,§}

Departments of Chemistry and Biochemistry, Materials Department, Materials Research Laboratory, and Mitsubishi Chemical Center for Advanced Materials, University of California, Santa Barbara, California 93106-9510. Department of Chemical and Biochemical Engineering, Technical University of Denmark, Building 423 Produktionstorvet, DK-2800 Kgs, Lyngby, Denmark. Mitsubishi Chemical Group Science and Technology Research Center, Inc.1000 Kamoshida-cho, Aoba-ku, Yokohama 227-8502, Japan

E-mail: hawker@mrl.ucsb.edu

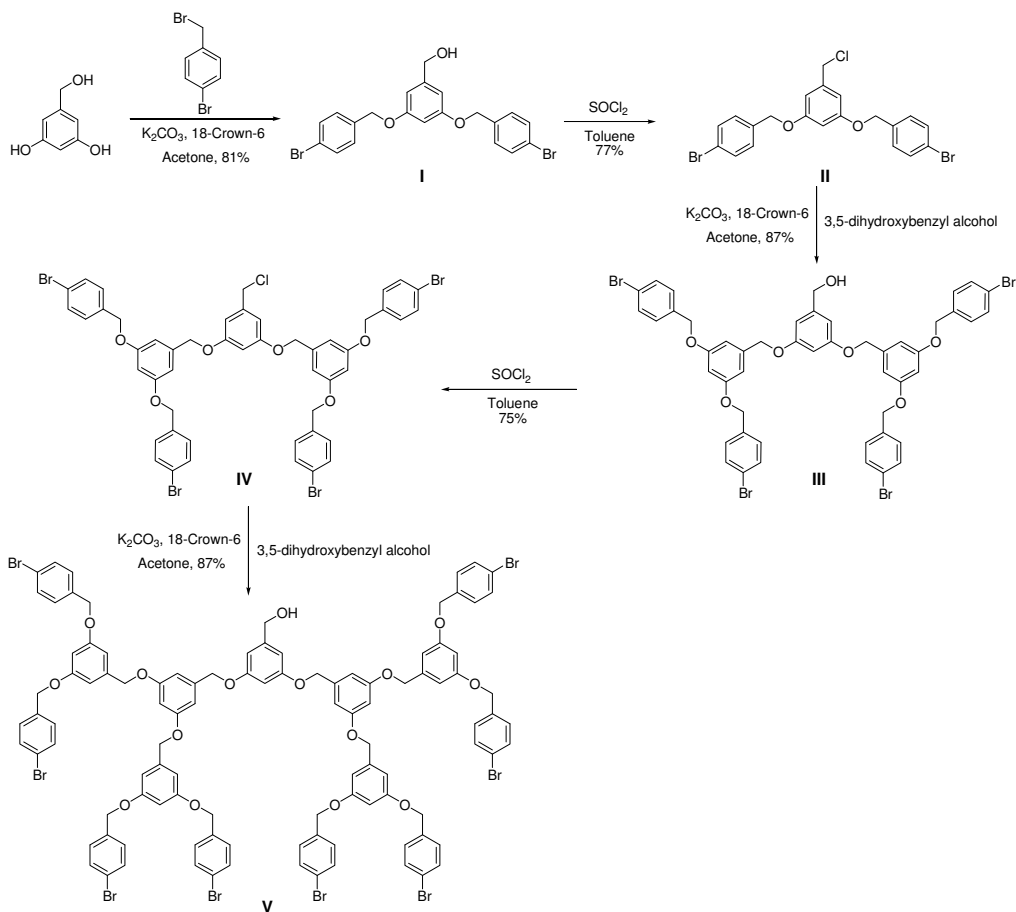
Table of Contents

Materials	S2
Synthesis of the monomers	S2
Formulations	S8
Sample preparation	S8
Hologram recording	S8
M/# and Angular selectivity curves (polyurethane matrix)	S10
M/# and Angular selectivity curves (polycarbonate matrix)	S10
Holographic properties	S11
Shrinkage calculations	S11
Refractive index calculation	S16
Exposure time for recording each hologram	S16
Monomer conversion in thick film	S18
References	S19

General Methods and Materials

Materials. 2,4,6-trimethylbenzoyldiphenylphosphine oxide (Lucirine TPO) was purchased from BASF. Hexamethylenediisocyanate was purchased from Wako. Dioctyltin dilaurate (U810) was purchased from Nitto Kasei. Tribromophenyl acrylate (BR-30) was purchased from Dai-Ichi Kogyo Seiyaku. Polypropylene-triol (GP1000) (average molecular weight is 1000) was purchased from Sanyo Chemical Industries. All these chemicals were used as received. Analytical TLC was performed on commercial Merck plates coated with silica gel GF254 (0.24 mm thick). Column chromatography was performed on a Biotage SP1 Flash Purification System using FLASH 40+M and FLASH 25+M cartridges. Infrared spectra were recorded on a Perkin Elmer Spectrum 100 with a Universal ATR sampling accessory. ^1H NMR (400 MHz and 200 MHz) and ^{13}C NMR (100 MHz) measurements were performed on a Bruker AC 400 and 200 spectrometers at 23 ± 2 °C using residual protonated solvent signal as internal standard (^1H : $\delta(\text{CHCl}_3) = 7.26$ ppm and ^{13}C : $\delta(\text{CHCl}_3) = 77.0$ ppm. Differential Scanning Calorimetry (DSC) measurements were performed with a TA Instruments DCS 2920 with temp rate of 5 degrees per minute. Data was collected during third cycle in the selected temperature ranges. Calibrations were made using indium as a standard for both temperature transitions and the heats of fusion. Melting transition temperatures (T_m) were determined by peak maxima of the transition.

Synthesis of the dendritic monomers:¹



Scheme 1

Typical procedure for the synthesis of bromo substituted dendritic alcohols;

Br₂-G1-OH (I): A mixture of 4-bromobenzyl bromide (28.90 g, 116 mmol), 18-crown-6-ether (3.06 g, 12 mmol) and 3,5-dihydroxybenzyl alcohol (6.48 g, 46 mmol) in dry acetone (90 mL) was refluxed under nitrogen for 12 h. The mixture was cooled and the solvent was removed *in vacuo*. The resulting solid was dissolved in CH_2Cl_2/H_2O and extracted with CH_2Cl_2 (x3). The combined organic layers were dried with $MgSO_4$, filtered, and concentrated *in vacuo*. The crude product was purified by column chromatography using CH_2Cl_2 as eluent to afford benzyl alcohol **I** as a white solid (18.00 g, 81%). 1H -NMR (500 MHz) $CDCl_3$, δ_H (ppm): 1.95 (t, 1 H, $-CH_2OH$, $^3J = 6.0$ Hz), 4.61 (d, 2 H, $-CH_2OH$, $^3J = 6.0$ Hz), 4.98 (s, 4 H, (Br)Ar- CH_2 -OAr), 6.48 (t, 1 H,

ArH, $^4J = 2.1$ Hz), 6.60 (d, 2 H, ArH, $^4J = 2.1$ Hz), 7.27 and 7.50 (ABq, 8 H, (Br)ArH, $^3J = 8.3$ Hz); ^{13}C -NMR (125 MHz) CDCl_3 , δ_{C} (ppm): 65.2 (1 C, Ar- CH_2OH), 69.4 (2 C, (Br)Ar- CH_2O -Ar), 101.5 (1 C, arom. CH), 106.0 (2 C, arom. CH), 122.0 (2 C, arom. CBr), 129.2 (4 C, (Br)arom. CH), 131.8 (4 C, (Br)arom. CH), 135.9 (2 C, (Br)arom. C- CH_2O), 143.7 (1 C, arom. C- CH_2OH), 160.0 (2 C, arom. C-O-); IR (cm^{-1}): 3290 (OH), 2920, 2875 (C-H), 1610, 1595 (C=C), 1160, 1010 (C-O); 825, 800 (1,4-Ar), 690 (1,3,5-Ar); MS (m/z, EI): 476, 478, 480 (1:2:1, M^+); $T_{\text{m}} = 98\text{-}99^\circ\text{C}$.

Typical procedure for the synthesis of bromo substituted dendritic chlorides;

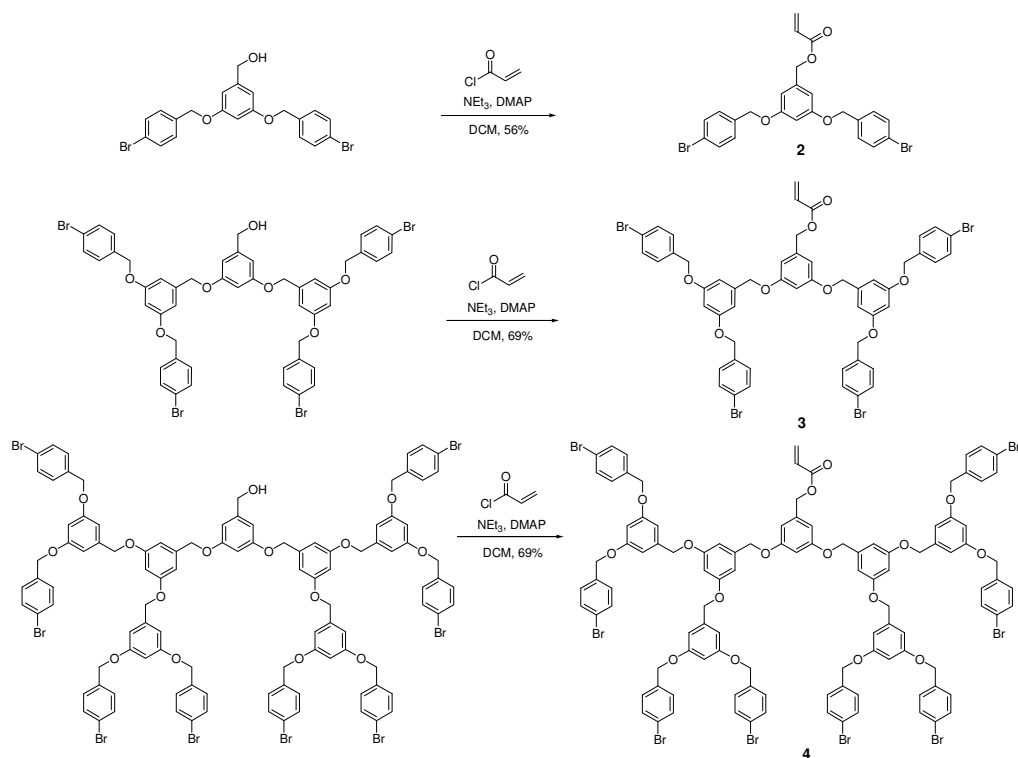
Br₂-G1-Cl (II): A solution of **I** (0.50 g, 1.0 mmol) in dry toluene (6.5 mL) was cooled to 0°C and pyridine (0.09 g, 1.1 mmol) was added. To the stirred mixture a solution of SOCl_2 (0.14 g, 1.1 mmol) in toluene (0.2 mL) was added dropwise. After addition the mixture was heated to reflux for 30 min. The reaction mixture was concentrated *in vacuo* and the residue was dissolved in CH_2Cl_2 and filtered through a silica gel plug. The obtained solid was recrystallized from hexane and the product was isolated as a white solid (0.40 g, 77%). ^1H -NMR (500 MHz) CDCl_3 , δ_{H} (ppm): 4.51 (s, 2 H, $-\text{CH}_2\text{Cl}$), 4.99 (s, 4 H, (Br)Ar- CH_2O Ar), 6.51 (t, 1 H, ArH, $^4J = 2.1$ Hz), 6.63 (d, 2 H, ArH, $^4J = 2.1$ Hz), 7.29 and 7.52 (ABq, 8 H, (Br)ArH, $^3J = 8.3$ Hz); ^{13}C -NMR (125 MHz) CDCl_3 , δ_{C} (ppm): 46.3 (1 C, Ar- CH_2Cl), 69.5 (2 C, (Br)Ar- CH_2O -Ar), 102.2 (1 C, arom. CH), 107.9 (2 C, arom. CH), 122.1 (1 C, arom. CBr), 129.2 (4 C, (Br)arom. CH), 131.9 (4 C, (Br)arom. CH), 135.8 (2 C, (Br)arom. C- CH_2O), 139.9 (1 C, arom. C- CH_2Cl), 160.0 (2 C, arom. C-O-); IR (cm^{-1}): 2920, 2875 (C-H); 1595 (C=C), 1170, 1060, 1010 (C-O), 835, 800 (1,4-Ar), 705 (C-Cl); MS (m/z, EI): 494, 496, 498, 500 (1:2:1.5:0.5, M^+); $T_{\text{m}} = 83\text{-}84^\circ\text{C}$.

Br₄-G2-OH (III): Compound **III** was prepared from **II** by the method reported for synthesis of molecule **I** and purified by column chromatography furnishing a white solid (12.80 g, 87%). ^1H -NMR (500 MHz) CDCl_3 , δ_{H} (ppm): 1.75 (t, 1 H, $-\text{CH}_2\text{OH}$, $^3J = 6.0$ Hz), 4.62 (d, 2 H, $-\text{CH}_2\text{OH}$, $^3J = 6.0$ Hz), 4.96, 4.97 (2 x s, 12 H, Ar- CH_2O Ar), 6.51 (2 x t, 3H, ArH, $^4J = 2.0$ Hz, $^4J = 2.0$ Hz), 6.59 (d, 2 H, ArH, $^4J = 2.0$ Hz), 6.65 (d, 4H, ArH, $^4J = 2.0$ Hz), 7.27 and 7.50 (ABq, 16H, (Br)ArH, $^3J = 8.3$ Hz); ^{13}C -NMR (125 MHz) CDCl_3 , δ_{C} (ppm): 65.3 (1 C, Ar- CH_2OH), 69.5 (4 C, (Br)Ar- CH_2O -Ar), 69.9 (2 C, Ar- CH_2O -Ar), 101.5 (1 C, arom. CH), 101.7 (2 C, arom. CH), 105.9 (2 C, arom. CH), 106.5 (4 C, arom. CH), 122.0 (4 C, arom. CBr), 129.2 (8 C, (Br)arom. CH), 131.8 (8 C, (Br)arom. CH), 135.9 (4 C, (Br)arom. C- CH_2O), 139.6 (2 C, arom. C- CH_2O),

143.6 (1 C, arom. C-CH₂OH), 160.0 (4 C, arom. C-O-), 160.1 (2 C, arom. C-O-); IR (cm⁻¹): 3325 (OH), 2920, 2880 (C-H), 1590 (C=C), 1150, 1070, 1010 (C-O), 825, 795 (1,4-Ar), 675 (1,3,5-Ar); MS (m/z, ESI/TOF): 1083 {M+Na}⁺, 1099 {M+K}⁺; T_m = 103-104°C.

Br₄-G2-Cl (IV): Compound **IV** was prepared from **III** by the general method described above for molecule **II** and purified by precipitation into hexanes from CH₂Cl₂, giving a white solid (7.69 g, 75%). ¹H-NMR (500 MHz) CDCl₃, δ_H (ppm): 4.50 (s, 2 H, -CH₂Cl), 4.96, 4.98 (2 x s, 12 H, Ar-CH₂-OAr), 6.51 (2 x t, 3H, ArH, ⁴J = 2.2 Hz, ⁴J = 2.2 Hz), 6.61 (d, 2 H, ArH, ⁴J = 2.2 Hz), 6.64 (d, 4H, ArH, ⁴J = 2.2 Hz), 7.27 and 7.49 (ABq, 16H, (Br)ArH, ³J = 8.4 Hz); ¹³C-NMR (125 MHz) CDCl₃, δ_C (ppm): 46.4 (1 C, Ar-CH₂Cl), 69.5 (4 C, (Br)Ar-CH₂O-Ar), 70.1 (2 C, Ar-CH₂O-Ar), 101.9 (2 C, arom. CH); 102.3 (1 C, arom. CH), 106.6 (4 C, arom. CH), 107.9 (2 C, arom. CH), 122.1 (4 C, arom. CBr), 129.2 (8 C, (Br)arom. CH), 131.9 (8 C, (Br)arom. CH), 135.9 (4 C, (Br)arom. C-CH₂O), 139.4 (2 C, arom. C-CH₂O), 139.8 (1 C, arom. C-CH₂Cl), 160.0 (6 C, arom. C-O-); IR (cm⁻¹): 3060, 2870 (C-H), 1590 (C=C), 1150, 1045, 1010 (C-O), 830, 800 (1,4-Ar), 710 (C-Cl), 680 (1,3,5-Ar); MS (m/z, ESI/TOF): 1079{M+H}⁺, 1101 {M+Na}⁺, 1117 {M+K}⁺; T_m = 104-105°C.

Br₈-G3-OH (V): Molecule **V** was synthesized from compound **IV** as described for compound **I** and purified by column chromatography (Solvent) furnishing an off-white glassy solid (0.51 g, 87%). ¹H-NMR (500 MHz) CDCl₃, δ_H (ppm): 1.68 (br-t, 1 H, -CH₂OH, ³J = 6.0 Hz), 4.61 (d, 2 H, -CH₂OH, ³J = 5.8 Hz), 4.97 (s, 28 H, Ar-CH₂-OAr), 6.51 (m, 7 H, ArH), 6.61 (d, 2 H, ArH, ⁴J = 1.9 Hz), 6.65 (m, 12 H, ArH), 7.28 and 7.50 (ABq, 32 H, (Br)ArH, ³J = 8.3 Hz); ¹³C-NMR (125 MHz) CDCl₃, δ_C (ppm): 65.3 (1 C, Ar-CH₂OH), 69.5 (8 C, (Br)Ar-CH₂O-Ar), 70.0 (6 C, Ar-CH₂O-Ar), 101.5 (1 C, arom. CH), 101.7 (2 C, arom. CH), 101.8 (4 C, arom. CH), 105.9 (2 C, arom. CH), 106.5 (4 C, arom. CH), 106.6 (8 C, arom. CH), 122.1 (8 C, arom. CBr), 129.2 (16 C, (Br)arom. CH), 131.8 (16 C, (Br)arom. CH), 135.9 (8 C, (Br)arom. C-CH₂O), 139.50 (2 C, arom. C-CH₂O), 139.53 (4 C, arom. C-CH₂O), 143.7 (1 C, arom. C-CH₂OH), 160.0 (8 C, arom. C-O-), 160.10 (4 C, arom. C-O-), 160.14 (2 C, arom. C-O-); IR (cm⁻¹): 3325 (OH), 3060, 2870 (C-H), 1590 (C=C), 1150, 1040, 1010 (C-O), 830, 800 (1,4-Ar), 680 (1,3,5-Ar); T_g = 51.4°C.



Scheme 2

Br₂-G1-Acrylate (2): Compound **I** (0.150 g, 0.3 mmol) was dissolved in CH₂Cl₂ (2 mL) after which DMAP (0.016 g, 0.1 mmol) and Et₃N (0.5 g, 0.7 mL, 5 mmol) were added. To this stirring mixture acryloyl chloride (0.114 g, 0.1 mL, 1.2 mmol) was added dropwise, and the resulting slurry was stirred for 16 h at room temperature under nitrogen atmosphere. The reaction mixture was filtered and the organic layer was extracted with NaHSO₄ (1 M, x3), NaHCO₃ (x3) and brine (x1). The organic layer was dried with MgSO₄, filtered and concentrated *in vacuo*. The product was obtained as an oil (0.093 g, 56%). ¹H-NMR (500 MHz) CDCl₃, δ_H (ppm): 4.98 (s, 4 H, (Br)Ar-CH₂-OAr), 5.12 (s, 2 H, -CH₂OCO-), 5.87 (dd, 1 H, CH₂=C, ²J=1.3 Hz, ³J=10.4 Hz), 6.16 (dd, 1 H, CH₂=CH-, ³J=10.4 Hz, ³J=17.3 Hz), 6.44 (dd, 1 H, CH₂=CH-, ²J=1.3 Hz, ³J=17.3 Hz), 6.51 (t, 1 H, ArH, ⁴J = 2.2 Hz), 6.59 (d, 2 H, ArH, ⁴J = 2.2 Hz), 7.28 and 7.50 (ABq, 8H, (Br)ArH, ³J = 8.4 Hz); ¹³C-NMR (125 MHz) CDCl₃, δ_C (ppm): 66.1 (1 C, Ar-CH₂OH), 69.5 (2 C, (Br)Ar-CH₂O-Ar), 102.0 (1 C, arom. CH), 107.3 (2 C, arom. CH), 122.1 (1 C, arom. C-Br), 128.3 (1 C, -CH=CH₂), 129.2 (4 C, (Br)arom. CH), 131.4 (1C, CH₂=CH), 131.9 (4 C, (Br)arom.

CH), 135.8 (2 C, (Br)arom. C-CH₂O), 138.5 (1 C, arom. C-CH₂OCO), 159.9 (2 C, arom. C-O-), 166.0 (1 C, C-COO-); IR (cm⁻¹): 3056, 2926, 2875 (C-H), 1722 (C=O), 1610, 1595 (C=C), 1152, 1011 (C-O), 832, 800 (1,4-Ar), 727 (1,3,5-Ar); MS (m/z, ESI/TOF): 552 {M+Na}⁺.

Br₄-G2-Acrylate (3): The product was obtained from compound **III** by the general procedure reported for compound **2** and the product was obtained as a solid (0.109 g, 69%). ¹H-NMR (500 MHz) CDCl₃, δ_H (ppm): 4.96, 4.98 (2 x s, 12 H, Ar-CH₂-OAr), 5.13 (s, 2 H, -CH₂OCO-), 5.84 (dd, 1 H, CH₂=C, ²J=1.3 Hz, ³J=10.4 Hz), 6.16 (dd, 1 H, CH₂=CH-, ³J=10.4 Hz, ³J=17.3 Hz), 6.44 (dd, 1 H, CH₂=CH-, ²J=1.3 Hz, ³J=17.3 Hz), 6.50 (m, 3H, ArH), 6.59 (d, 2 H, ArH, ⁴J = 2.1 Hz), 6.64 (d, 4H, ArH, ⁴J = 2.1 Hz), 7.27 and 7.49 (ABq, 16H, (Br)ArH, ³J = 8.3 Hz); ¹³C-NMR (125 Mhz) CDCl₃, δ_C (ppm): 66.2 (1 C, Ar-CH₂OH), 69.5 (4 C, (Br)Ar-CH₂O-Ar), 70.0 (2 C, Ar-CH₂O-Ar), 101.8 (1 C, arom. CH), 101.9 (2 C, arom. CH), 106.6 (4 C, arom. CH), 107.2 (2 C, arom. CH), 122.1 (4 C, arom. C-Br), 128.3 (1 C, OOC-CH=CH₂), 129.2 (8 C, (Br)arom. CH), 131.4 (1 C, -CH=CH₂), 131.9 (8 C, (Br)arom. CH), 135.9 (4 C, (Br)arom. C-CH₂O), 138.4 (1 C, arom. C-CH₂OCO), 139.5 (2 C, arom. C-CH₂O), 160.0 (6 C, arom. C-O-), 166.0 (1 C, COO-); IR (cm⁻¹): 3063, 2920, 2880 (C-H); 1724 (C=O); 1592 (C=C), 1150, 1050, 1010 (C-O); 827, 800 (1,4-Ar); 680 (1,3,5-Ar).MS (m/z, ESI/TOF): 1132 {M+Na}⁺; T_m = 101°C.

Br₈-G3-Acrylate (4): Compound **4** was prepared from **V** by the general procedure reported for compound **2** and the product was obtained as a solid (0.105 g, 69%). ¹H-NMR (500 MHz) CDCl₃, δ_H (ppm): 4.95 (s, 28 H, Ar-CH₂-OAr), 5.11 (s, 2 H, -CH₂OCO-), 5.82 (dd, 1 H, CH₂=C, ²J=1.3 Hz, ³J=10.4 Hz), 6.15 (dd, 1 H, CH₂=CH-, ³J=10.4 Hz, ³J=17.3 Hz), 6.42 (dd, 1 H, CH₂=CH-, ²J=1.3 Hz, ³J=17.3 Hz), 6.51 (m, 6 H, ArH), 6.54 (t, 1 H, ArH, ⁴J=2.1 Hz), 6.59 (d, 2 H, ArH, ⁴J = 2.1 Hz), 6.63 (m, 12 H, ArH), 7.24 and 7.47 (ABq, 32H, (Br)ArH, ³J = 8.3 Hz); ¹³C-NMR (125 MHz) CDCl₃, δ_C (ppm): 66.2 (1 C, Ar-CH₂OCO), 69.4 (8 C, (Br)Ar-CH₂O-Ar), 70.0 (4 C, Ar-CH₂O-Ar), 70.1 (2 C, Ar-CH₂O-Ar), 101.8 (6 C, arom. CH), 101.9 (1 C, arom. CH), 106.6 (12 C, arom. CH), 107.2 (2 C, arom. CH), 122.0 (8 C, arom. C-Br), 128.3 (1 C, OOC-CH=CH₂), 129.2 (16 C, (Br)arom. CH), 131.4 (1 C, -CH=CH₂), 131.8 (16 C, (Br)arom. CH), 135.9 (8 C, (Br)arom. C-CH₂O), 138.4 (1 C, arom. C-CH₂OCO), 139.3 (2 C, arom. C-CH₂O), 139.5 (4 C, arom. C-CH₂O), 160.0 (10 C, arom. C-O-), 160.1 (4 C, arom. C-O-), 166.0 (1 C, COO-); MS (m/z, ESI/TOF): 2294 {M+Na}⁺; IR (cm⁻¹): 3060, 2870 (C-H), 1723 (C=O), 1590 (C=C), 1155, 1040, 1010 (C-O), 825, 800 (1,4-Ar), 680 (1,3,5-Ar); T_m = 86°C.

Formulations.

	Polyols (wt%)			Isocyanate (wt%)	Monomer (wt%)	Initiator (wt%)	Catalyst (wt%)
	polycarbonate- diol	polypropylene- triol	trimethyl- olpropane	HMDI	1, 2, 3, or 4	TPO	dioctyltin- dilaurate
Polyurethane matrix formulation	0.0	77.2	0.0	19.48	3	0.3	0.02
polycarbonate matrix formulation	63.0	0.0	7.0	26.68	3	0.3	0.02

Sample Preparation. To fabricate optical films, several drops of the mixture of solutions A and B were placed between two 3 x 1 inch glass plates separated by Teflon spacers of 0.5mm thicknesses. Clips were placed on both ends of the glass slides to hold them in proper position. The whole assembly was then placed in a heating oven set at 60 °C for 15 hrs. After curing the films, the sample sandwiched between two glass slides was mounted on the holographic setup and exposed.

Hologram Recording and Evaluation. Experimental setup for recording of holograms was assembled on an optical table suspended on vibration damping supports. The output of a blue diode laser (SONY SBL-N001A, 407 nm, 45 mW, single longitudinal mode) was split into two beams with equal power using a continuously adjustable beam splitter consisting of two half-wavelength plates and a polarizer cube.² The resulting beams passed through spatial filters and collimating lenses, which produced beams with diameter of ~ 5 mm. The angle between the recording beams was 37.4°. Optical power density in a single recording beam was ~6 mW/cm². A sample was placed at the intersection point of the recording beams on a computer-controlled rotation stage (Sigma Koki SGSP-120YAW, 0.025° positioning accuracy). Intensities of the diffracted and transmitted beams were measured by Si photodiodes protected from ambient light by interference filters. Exposure of a sample to the recording beams was controlled by a computer-operated shutter (Suruga Seiki F77-4). Overall controls over the experiment and data acquisition were carried out by a home-brew program running on a PC. The experimental setup allowed us to control the amount of optical energy used for recording of a hologram, record multiple diffraction gratings, determine their diffraction efficiency (M# measurements), and

measure angular selectivity of diffraction gratings to evaluate the amount of volume shrinkage due to the recording.

Diffraction efficiency was determined using the following formula:

$$\eta = \frac{I_D}{I_D + I_T}$$

here I_D and I_T are intensities of diffracted and transmitted beams, respectively. Holograms recorded in our experiments are transmission volume holograms (transmission Bragg holograms).²

Sensitivity of the material was estimated using the following equation:

$$S = \frac{\sqrt{\eta}}{dtI}$$

where t is the recording time, d is the thickness of a hologram and I is the combined intensity of recording beams.

Multiplexing capabilities of the recording material were evaluated using M# parameter:

$$M\# = \sum_{i=1}^N \sqrt{\eta_i}$$

In these experiments, we recorded consecutively N holographic gratings on the same spot on the sample. The sample was rotated by a certain angle between the recordings. For each hologram, we measured diffraction efficiency η_i .

M/# and Angular selectivity curves of data storage systems in polyurethane matrix.

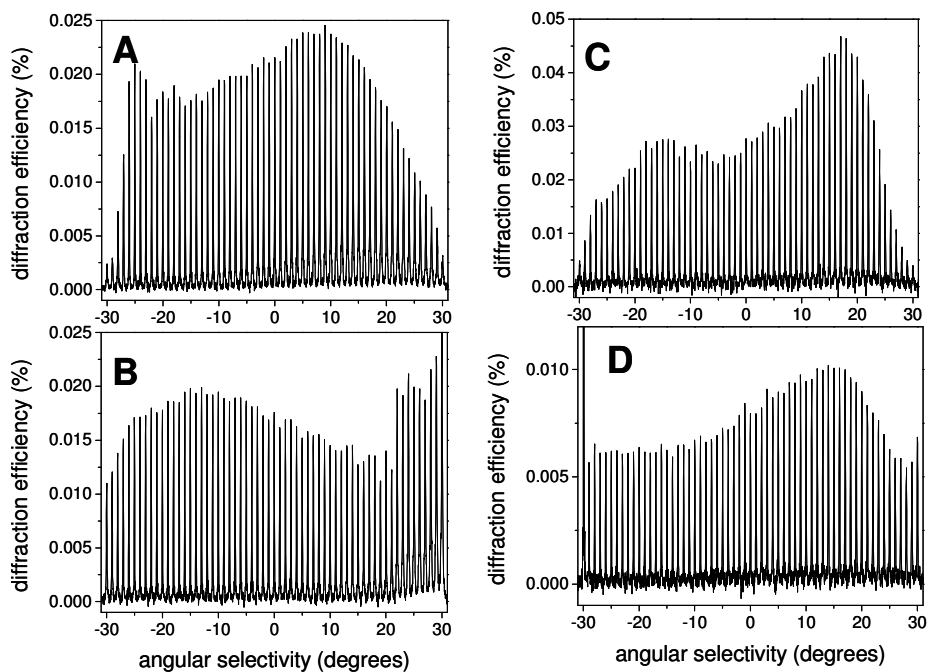


Figure 1. Angular selectivity curves of the holograms recorded in 0.5 mm thick films containing; a) monomer **1**, b) monomer **2**, c) monomer **3**, and d) monomer **4**.

M/# and Angular selectivity curves of data storage systems in polycarbonate matrix.

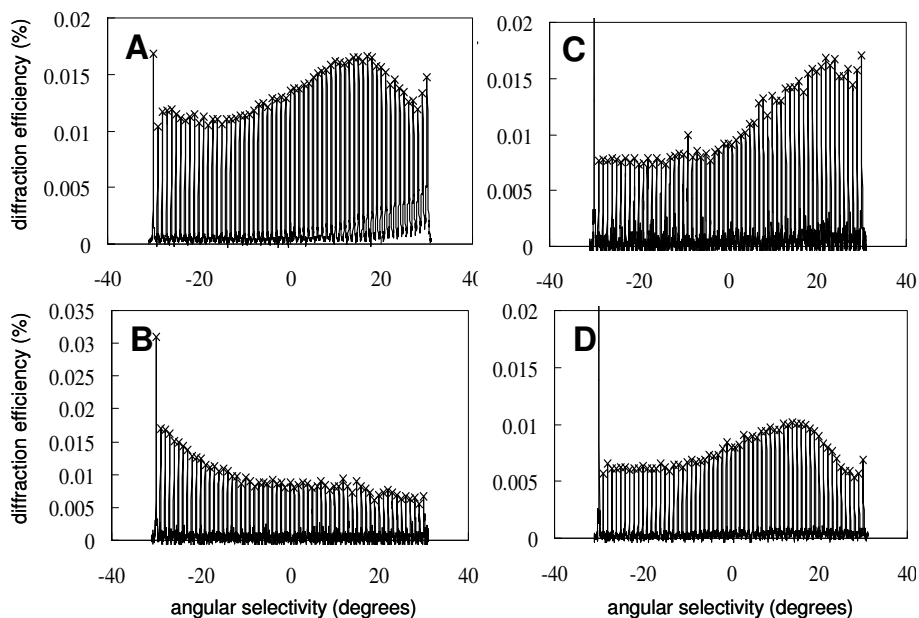


Figure 2. Angular selectivity curves of the holograms recorded in 0.5 mm thick films containing; a) monomer **1**, b) monomer **2**, c) monomer **3**, and d) monomer **4**.

Table 1. Holographic properties of the different data storage systems in the polycarbonate matrix.

Monomer	Storage Capacity (M/#)	Sensitivity (cm/mJ)	Volume Shrinkage (%)
1	7	0.14	0.23
2	6	0.06	0.1
3	6.5	0.04	0.04
4	6	0.05	0.03

Shrinkage Calculation. Shrinkage due to the recording was evaluated in accordance with Dhar's report.³ A set of fifteen holograms was angle multiplexed from -28° to $+28^\circ$ by 4° step. After recording of the holograms, the material was post-cured for 5 minutes with LEDs (Bivar Inc., 400 nm, 10 mW/cm^2). In order to evaluate the volume shrinkage taken place in the out-of-plane direction, σ , the shift in the Bragg angle, $\Delta\theta_{\text{Bragg}}$, experimentally obtained was fitted to the following equation:

$$\Delta\theta_{Bragg} = \arcsin \left[n_1 \sin \left\{ \phi_1 - \frac{\pi}{2} + \arcsin \left(\frac{\lambda}{2\Lambda_1 n_1} \right) \right\} \right] - \arcsin \left[n_0 \sin \left\{ \phi_0 - \frac{\pi}{2} + \arcsin \left(\frac{\lambda}{2\Lambda_0 n_0} \right) \right\} \right],$$

where λ , ϕ , Λ and n are the recording laser wavelength, the grating tilt angle, the grating fringe spacing and the refractive index, respectively. The subscripts 1 and 0 represent the states with and without the volume shrinkage. ϕ_1 and Λ_1 are the functions of σ and described, respectively, as $\phi_1 = \pi/2 - \arctan\{\tan(\pi/2 - \phi_0)/(1 + \sigma)\}$ and $\Lambda_1 = \Lambda_0 \sin \phi_1 / \sin \phi_0$. In this study, $n_0 = n_1 = 1.510$ was used for the shrinkage evaluation.

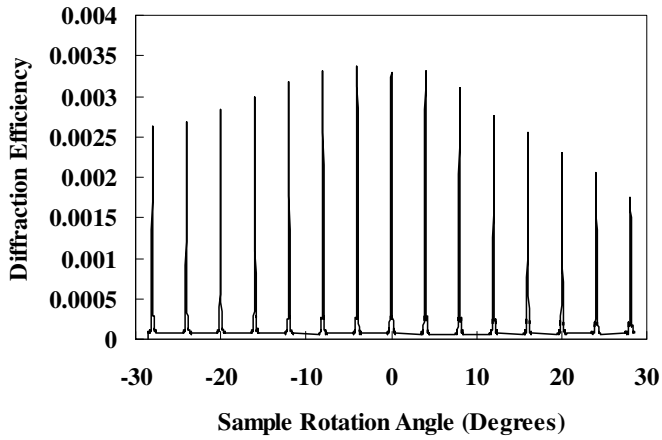


Figure 3. Diffraction efficiency of the fifteen recorded holograms as a function of sample rotation angle for holographic system containing monomer **1**. The angle of the maximum diffraction efficiency for each hologram was found by fitting each peak to a Gaussian line shape.

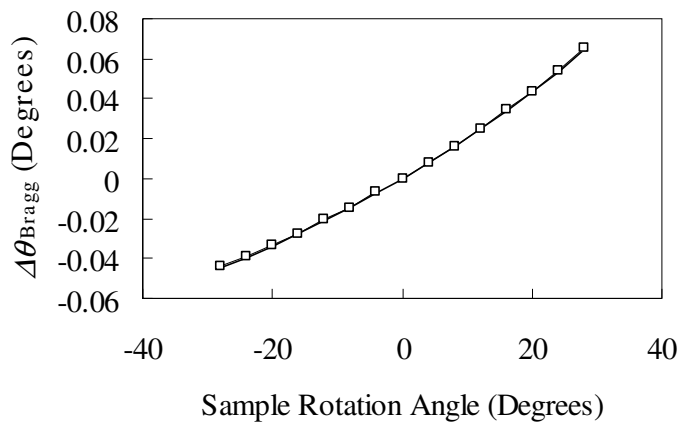


Figure 4. Shift in the Bragg angle as a function of sample rotation angle for **1**.

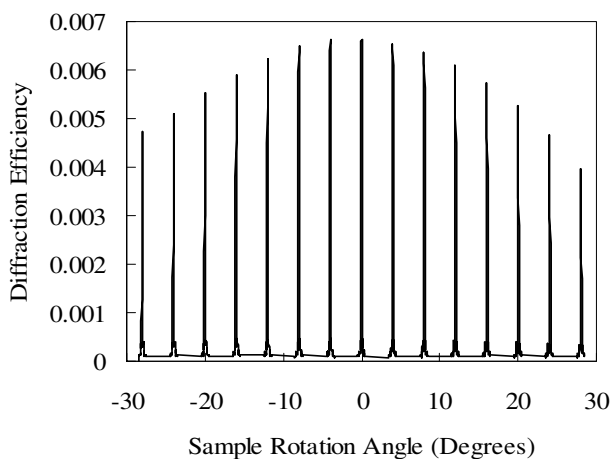


Figure 5. Diffraction efficiency of the fifteen recorded holograms as a function of sample rotation angle for holographic system containing Monomer **2**. The angle of the maximum diffraction efficiency for each hologram was found by fitting each peak to a Gaussian line shape.

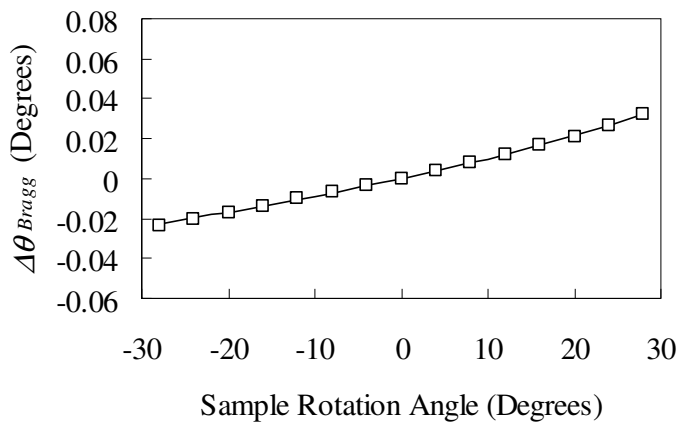


Figure 6. Shift in the Bragg angle as a function of sample rotation angle for Monomer 2 system. The solid line represents the fit to the Bragg shift using the theoretical equation.

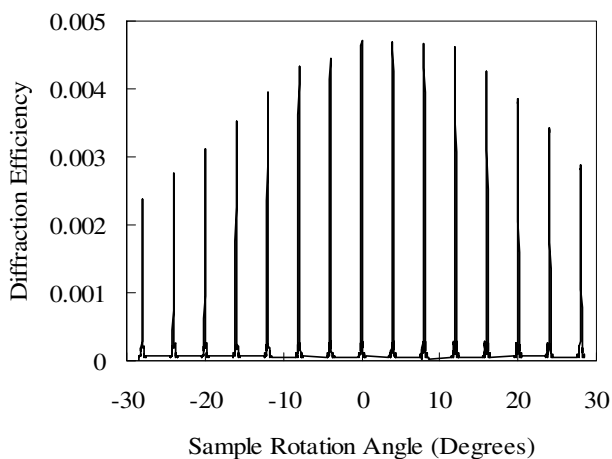


Figure 7. Diffraction efficiency of the fifteen recorded holograms as a function of sample rotation angle for holographic system containing Monomer 3. The angle of the maximum diffraction efficiency for each hologram was found by fitting each peak to a Gaussian line shape.

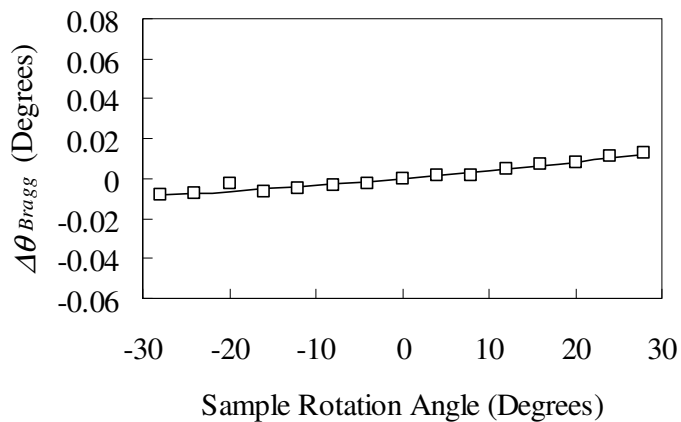


Figure 8. Shift in the Bragg angle as a function of sample rotation angle for Monomer **3** system. The solid line represents the fit to the Bragg shift using the theoretical equation.

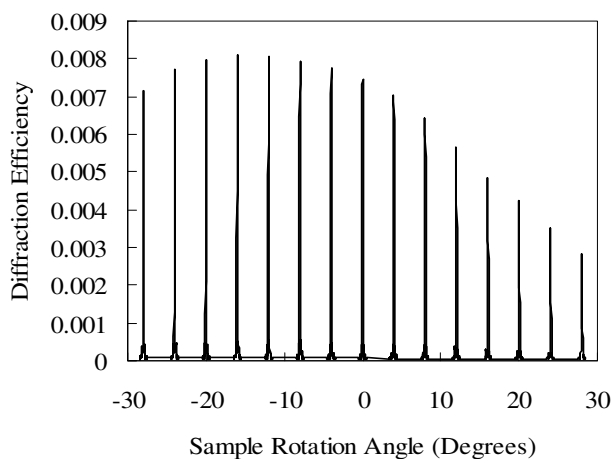


Figure 9. Diffraction efficiency of the fifteen recorded holograms as a function of sample rotation angle for holographic system of Monomer **4**. The angle of the maximum diffraction efficiency for each hologram was found by fitting each peak to a Gaussian line shape.

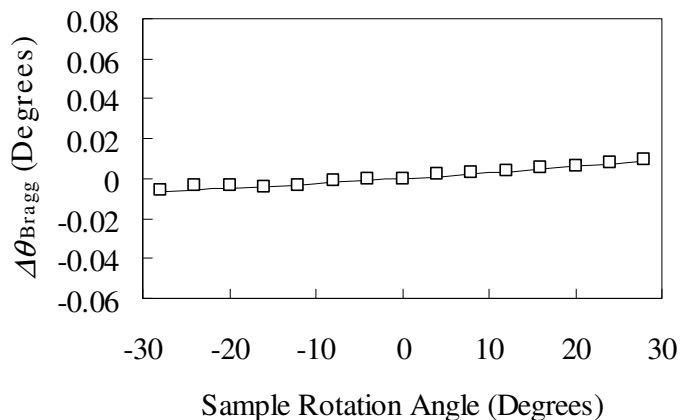


Figure 10. Shift in the Bragg angle as a function of sample rotation angle for Monomer 4.

Refractive index calculation;

Theoretical refractive indices of the acrylate monomers **1**, **2**, **3**, and **4** were calculated using software by Polymer-Design Tools™ (<http://www.hallogram.com/polymerdesign/index.html>).

Exposure time for each hologram;

	Monomer 1	Monomer 2	Monomer 3	Monomer 4
Recording Angle	Exposure time (msec)	Exposure time (msec)	Exposure time (msec)	Exposure time (msec)
-30	4000	8000	10000	15000
-29	720	2120	2180	2500
-28	720	2080	2180	2500
-27	720	2040	2180	2520
-26	720	2020	2180	2520
-25	720	2020	2200	2520
-24	720	2000	2200	2540
-23	720	2020	2220	2560
-22	740	2020	2240	2580
-21	740	2020	2260	2620
-20	740	2020	2280	2640
-19	760	2040	2320	2680

-18	760	2060	2340	2720
-17	780	2080	2380	2760
-16	800	2100	2420	2820
-15	800	2120	2460	2880
-14	820	2140	2520	2940
-13	840	2180	2580	3000
-12	860	2200	2620	3080
-11	880	2240	2700	3160
-10	900	2280	2760	3240
-9	920	2340	2840	3340
-8	960	2380	2920	3440
-7	980	2440	3000	3540
-6	1020	2500	3100	3660
-5	1040	2560	3200	3800
-4	1080	2640	3300	3940
-3	1120	2720	3420	4100
-2	1160	2800	3540	4260
-1	1200	2880	3680	4440
0	1260	2980	3840	4620
1	1300	3080	4000	4840
2	1360	3200	4160	5060
3	1420	3320	4340	5300
4	1480	3440	4560	5560
5	1560	3580	4760	5840
6	1640	3740	5000	6160
7	1720	3900	5260	6500
8	1800	4080	5520	6860
9	1900	4260	5820	7260
10	2020	4480	6140	7680
11	2120	4700	6500	8160
12	2260	4940	6880	8680
13	2380	5200	7300	9240
14	2540	5480	7740	9860

15	2700	5800	8240	10520
16	2860	6140	8780	11260
17	3060	6500	9360	12060
18	3280	6900	10000	12960
19	3500	7340	10700	13940
20	3760	7800	11460	15000
21	4020	8320	12300	16200
22	4320	8900	13240	17500
23	4660	9520	14260	18960
24	5020	10200	15380	20560
25	5440	10940	16600	22340
26	5880	11760	17980	24320
27	6580	12680	20120	27460
28	7400	14080	22600	31100
29	8620	15680	26340	36700
30	10100	18100	30840	43520

Monomer Conversion in the holographic disc;

A holographic disk containing the photoactive monomer was exposed to blue light for 5 minutes at each side (note that this is a blanket exposure and not a holographic exposure). The optical power of the light source was 10 mW/cm^2 . After the exposure, the sample was immersed in THF to extract the unreacted monomer, and then the concentration of the monomer in the THF solution was measured by using liquid chromatography. The conversion was calculated from the concentration change before and after the light exposure. The concentration of the monomer in the holographic disk before the light exposure was also measured as a reference.

Monomer	Monomer conversion (%)
1	99
2	68
3	46
4	45

References.

- (1) K. L. Wooley, C. J. Hawker, J. M. J. Fréchet, *J. Chem. Soc. Perkin Trans. 1*, 1991, 1059
- (2) P. Hariharan, "Optical holography Principles, techniques, and applications", Cambridge University Press, 2nd ed., 1996.
- (3) Dhar et al. *Appl. Phys. Lett.* 73, 1337 (1998).

Appendix E

A.E. Dugaard, S. Hvilsted, T.S. Hansen and N.B. Larsen. “Conductive Polymer Functionalization by Click Chemistry”. *Macromolecules* **2008**, *41*, 4321–4327.

Conductive Polymer Functionalization by Click Chemistry

Anders Egede Daugaard and Søren Hvilsted*

Danish Polymer Centre, Department of Chemical and Biochemical Engineering, Technical University of Denmark, Building 423 Produktionstorvet, DK-2800 Kgs. Lyngby, Denmark

Thomas Steen Hansen and Niels B. Larsen

Polymer Department, POL-313, P.O. Box 49, Frederiksborgvej 399, DK-4000 Roskilde, Denmark

Received December 7, 2007; Revised Manuscript Received April 21, 2008

ABSTRACT: Click chemistry is used to obtain new conductive polymer films based on poly(3,4-ethylenedioxythiophene) (PEDOT) from a new azide functional monomer. Postpolymerization, 1,3-dipolar cycloadditions in DMF, using a catalyst system of CuSO_4 and sodium ascorbate, and different alkynes are performed to functionalize films of PEDOT- N_3 and copolymers prepared from EDOT- N_3 and 3,4-ethylenedioxythiophene (EDOT). This approach enables new functionalities on PEDOT that could otherwise not withstand the polymerization conditions. Reactions on the thin polymer films have been optimized using an alkynated fluorophore, with reaction times of ~ 20 h. The applicability of the method is illustrated by coupling of two other alkynes: a short chain fluorocarbon and a MPEG 5000 to the conductive polymer; this alters the advancing water contact angle of the surface by $+20^\circ$ and $-20^\circ/-25^\circ$, respectively. The targeted chemical surface modifications have been verified by X-ray photoelectron spectroscopy analysis.

Introduction

Conductive polymers have been extensively studied during the past few decades for applications such as biosensors,¹ strain gauges,² organic solar cells,³ or organic light-emitting diodes.⁴ Many challenges have to be met in the development of new functional conducting polymers, including synthesis of monomers with the required functionality and establishment of polymerization conditions compatible with the targeted function. Specific problems may be instability of large biological molecules for biosensors under the typically harsh polymerization conditions or inhibition of the polymerization process by a side reaction with a functional group in the monomer. Functionalization of the conductive polymer may result either from incorporation of the functional entity into the monomer during monomer synthesis or by postpolymerization coupling of the targeted functionality to built-in generic coupling sites in the monomer unit. Recently, the term “click chemistry” was defined by Sharpless et al.⁵ as selection criteria for highly efficient coupling reactions. Ideally, the click reaction can be performed in water or organic solvents at room temperature, making the method suitable for most applications. Click chemistry has mainly been based on the use of 1,3-dipolar cycloadditions of azides and alkynes under copper catalysis^{6,7} and Diels–Alder reactions. In polymer chemistry it has been used in numerous ways e.g. for end-group functionalization,⁸ polymer to polymer couplings,⁹ functionalization of linear polymers with selected groups,¹⁰ dendrons,¹¹ and poly(ethylene glycol) (PEG).¹² Also, in reactions on surfaces the cycloaddition has been used with good results e.g. to bond metal surfaces together.¹³ It has been used with carbon nanotubes¹⁴ and for functionalization of self-assembled monolayers on gold.^{15,16} Recently click chemistry has also been used for surface reactions on cotton¹⁷ and glass.^{18,19} A bioactive surface has been prepared by introduction of biotin by click chemistry on a polymer substrate.²⁰ For sensor applications especially biological systems are of great interest, and these often require mild reaction conditions, which can be obtained using click chemistry.²¹ A comprehensive review on

macromolecular click chemistry has recently been published by Binder et al.²²

The new developed conducting polymer is based on PEDOT, used in numerous applications due to its high electrical conductivity and high stability in ambient and aqueous environments.²³ During polymerization the polymer becomes insoluble, and further functionalization becomes difficult. Combination of the conductive properties of PEDOT and the advantages of modularity, high selectivity, and high yields of click chemistry permits preparation of new PEDOTs for many different applications, e.g., surfaces with conductive properties or sensors. Both pre- and postfunctionalization have been studied by others. With regards to biological active molecules the most successful methods so far is physical adsorption after polymerization or entrapment during polymerization.²⁴ Covalent postfunctionalization has been achieved through peptide bonding.^{25,26} The click approach is a good alternative that gives a controlled functionalization without protective groups through high selectivity. In our group we have focused on the use of PEDOT for different applications^{27–30} and the use of click chemistry for polymer functionalization.³¹ Here we present a standardized method for postpolymerization functionalization of PEDOT to obtain conductive polymer surfaces with various functionalities.

Experimental Section

General Methods. Thin layer chromatography (TLC) was performed on Merck plates coated with silica gel F254. Kieselgel for column chromatography was Merck Kieselgel 60 (230–400 mesh). ^1H NMR was run on a 250 MHz cryomagnet from Spectrospin and Bruker at room temperature. Infrared spectroscopy (IR) was performed on a Perkin-Elmer Spectrum One model 2000 Fourier transform infrared system with a universal attenuated total reflection sampling accessory on a ZnSe/diamond composite. Differential scanning calorimetry (DSC) was performed on a DSCQ1000 from TA Instruments. The thermal analyses were performed at a heating and cooling rate of $10^\circ\text{C}/\text{min}$. The melting temperatures (T_m) are reported as the peak temperatures of the endothermic melting peaks. The conductivity was measured with a four-point probe (Jandel Engineering Ltd., Linslade, UK) connected to a four-point source meter (Keithley 2400, Cleveland, OH). Film thicknesses were measured with an Ambios XP-2 (Ambios

* Corresponding author. E-mail: sh@kt.dtu.dk.

Technology, Inc., Santa Cruz, CA) profilometer using a stylus force of 0.5 mg. Optical microscopy images was recorded with a AxioCam MRc 5 camera mounted on a Zeiss Axioskop 40 microscope (Oberkochen, Germany). Fluorescence analysis was conducted with a Zeiss Filter Set 09 (excitation 450–490 nm, emission >515 nm). XPS analysis was performed on a Thermo Fisher Scientific K Alpha (East Grinstead, UK) using monochromatized aluminum K α radiation in a 400 μ m spot on the sample. Survey and high-resolution spectra were acquired and analyzed using the manufacturer's Advantage software package. Spectra were generally acquired with electron charge compensation in operation to avoid sample charging, except for a series of measurements to determine the detrimental effects of electron flooding on azide functional groups. Atomic force microscopy analysis proceeded on a PSIA XE-150 instrument operating in intermittent contact mode with BudgetSensor Tap-300 cantilevers.

Chemicals. Chemicals except for Baytron C were acquired from Aldrich and were used as received unless otherwise specified. Baytron C was purchased from H.C. Starck. Fluorescein methyl ester was prepared in accordance with Moore et al.³²

3,4-(1-Bromomethylethylene)dioxythiophene, 1 (EDOT-Br). 3,4-Dimethoxythiophene (0.41 g, 2.8 mmol), 3-bromo-1,2-propanediol (1.11 g, 7.2 mmol), and *p*-toluenesulfonic acid (0.08 g, 0.4 mmol) were dissolved in toluene (30 mL) and stirred at 100 °C for 48 h. Toluene was removed in vacuo, and the residue was dissolved in CH₂Cl₂ and extracted with Na₂CO₃ and H₂O. The organic phase was dried with MgSO₄, filtered, and concentrated in vacuo, and the crude product was purified by column chromatography with a gradient eluent of heptane/ethyl acetate (EtOAc). The product was isolated as a colorless oil (0.24 g, 37%). IR (cm⁻¹): 3112 (C–H stretch). ¹H NMR (CDCl₃, 250 MHz, δ_{H} , ppm): 3.4–3.6 (m, 2H, CH₂–Br); 4–4.44 (m, 3H, O–CH₂–CH–O); 6.36/6.37 (2 \times d, ⁴*J* = 3.7 Hz, 2H, S–CH).

3,4-(1-Azidomethylethylene)dioxythiophene, 2 (EDOT-N₃). 1 (0.22 g, 0.9 mmol) and NaN₃ (0.08 g, 1.2 mmol) were dissolved in DMF (10 mL) and stirred at room temperature (RT) for 17 h. The reaction mixture was diluted with H₂O (15 mL), and the aqueous DMF was extracted with EtOAc (5 \times 15 mL). The organics were combined and extracted with H₂O (3 \times 15 mL) and brine (1 \times 15 mL), dried with MgSO₄, filtered, and concentrated in vacuo to give the product as a colorless oil (0.18 g, 97%). IR (cm⁻¹): 3114 (C–H stretch); 2097 (–N₃ stretch). ¹H NMR (CDCl₃, 250 MHz, δ_{H} , ppm): 3.4–3.6 (m, 2H, CH₂–N₃); 4–4.44 (m, 3H, O–CH₂–CH–O); 6.36/6.39 (2 \times d, ⁴*J* = 3.7 Hz, 2H, S–CH).

General Polymerization Method for 2, to PEDOT-N₃. 3. The polymerization method was based on an earlier published method for the polymerization of EDOT.³³ A number of microscope slides were thoroughly cleaned using acetone, isopropanol, ethanol, and water. The glass slides were surface modified by vapor phase hexamethyldisilazane (HMDS) in a dedicated oven (Yield Engineering Systems 6112). 2 (20 mg, 0.15 mmol), Baytron C (0.48 mL, ~40 wt % Fe(III)Tos in butanol), and butanol (0.48 mL) were mixed and spin-coated on the glass-slides (10 s at 1000 rpm). The samples were placed on a hot plate at 65 °C for 5 min and subsequently washed with water and blown dry in a nitrogen flow, yielding films with a thickness of 200–250 nm.

General Copolymerization Method for Poly(3,4-ethylenedioxythiophene-co-3,4-(1-azidomethylethylene)dioxythiophene). The copolymerization method was based on an earlier published method for the polymerization of EDOT.³³ A solution of 3,4-ethylenedioxythiophene (EDOT, 0.22 mL), Baytron C (6.5 mL), butanol (6.5 mL), and pyridine (0.15 mL) was mixed with the EDOT-N₃ solution mentioned above to yield solutions containing 5 (4), 10 (5), 20 (6), 40 (7), 60 (8), and 80 mol % (9) EDOT-N₃ of the total monomer content. The polymerization mixtures were then spin-coated onto the HDMS treated glass slides (10 s at 1000 rpm). The samples were placed on a hot plate at 65 °C for 5 min and subsequently washed with water and blown dry in a nitrogen flow.

General Ester Synthesis, 2,2,3,3,3-Pentafluoropropyl Pent-4-ynoate, 10. A solution of 4-pentynoic acid (0.60 g, 6.1 mmol), dimethylaminopyridine (DMAP, 0.12 g, 0.9 mmol), and 2,2,3,3,3-

pentafluoropropanol (0.97 g, 6.5 mmol) in CH₂Cl₂ (15 mL) was stirred at RT, and a solution of *N,N'*-dicyclohexylcarbodiimide (DCC, 1.58 g, 7.6 mmol) in CH₂Cl₂ was added dropwise. The reaction mixture was stirred overnight at RT, filtered, and concentrated in vacuo. The crude product was purified by column chromatography using a gradient eluent of pentane/ether and gave a colorless oil (1.24 g, 88%). IR (cm⁻¹): 3314 (C≡C–H stretch); 2119 (C≡C stretch); 1761 (O–C=O stretch); 1197, 1143, 1107 (C–F stretch). ¹H NMR (CDCl₃, 250 MHz, δ_{H} , ppm): 1.99 (t, ⁴*J* = 2.6 Hz, 1H, H–C≡); 2.54 (m, 2H, ≡C–CH₂–); 2.67 (m, 2H, –CH₂–COO–); 4.57 (tq, ⁴*J* = 1 Hz, ³*J* = 12.9 Hz, 2H, O–CH₂–CF₃).

Methyl 2-(3-Oxo-6-(prop-2-ynoxy)xanthen-9-yl)benzoate, 11. Fluorescein methyl ester (2.00 g, 5.8 mmol), triphenylphosphine (TPP, 4.55 g, 17.3 mmol), and propargyl alcohol (0.98 g, 17.5 mmol) were stirred in acetonitrile/THF (50/50) at 0 °C. Diethylazodicarboxylate (DEAD, 3 mL, 17.3 mmol) was added slowly, and the mixture was stirred overnight at RT. The crude mixture was poured onto a Kieselgel column and chromatographed using an eluent of 80/20 CH₂Cl₂/ether, followed by a gradient of CH₂Cl₂/EtOAc. The product was collected from the top of the column with EtOAc as a yellow crystalline compound (1.08 g, 49%, *T*_m = 206 °C). IR (cm⁻¹): 3193 (–C≡C–H stretch); 2123 (C≡C stretch); 1729 (O–C=O stretch). ¹H NMR (CDCl₃, 250 MHz, δ_{H} , ppm): 3.59 (s, 3H, O–CH₃); 5.00 (s, 2H, ≡C–CH₂–O); 6.26 (s, 1H, Ar–H); 6.40 (m, 1H, Ar–H); 6.7–7.0 (m, 3H, Ar–H); 7.28 (s, 1H, Ar–H); 7.50 (m, 1H, Ar–H); 7.7–8.0 (m, 2H, Ar–H); 8.21 (s, 1H, Ar–H).

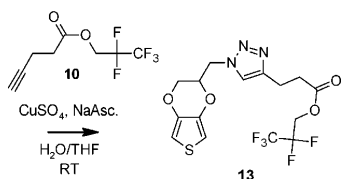
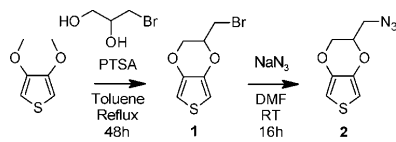
α -Methoxypoly(ethylene glycol)- ω -pent-4-ynoate, 12. The product was prepared according to the general procedure for ester synthesis by DCC coupling, using a commercially available methoxypoly(ethylene glycol) (*M*_n = 5010, PDI = 1.1), 1.2 equiv of 4-pentynoic acid, DCC and 1 equiv of DMAP relative to the end group. The crude product was purified by precipitation in cold dry diethyl ether and dried in vacuo to give 12 as a solid polymer (3.54 g, 87%, *T*_m = 56 °C, *M*_n = 5290, PDI = 1.1). IR (cm⁻¹): 1738 (O–C=O stretch); 1099 (C–O stretch). ¹H NMR (CDCl₃, 250 MHz, δ_{H} , ppm): 1.96 (t, 2.5 Hz, 1H, H–C≡); 2.4–2.6 (m, 4H, –OC–CH₂–CH₂–C≡); 3.35 (s, 3H, –OCH₃); 3.4–3.8 (m, O–CH₂–CH₂–O); 4.23 (t, 4.8 Hz, 2H, –COO–CH₂–).

Click Reaction of 2 with 10 and 13. 2 (49.8 mg, 0.25 mmol) and 10 (62.8 mg, 0.27 mmol) were dissolved in H₂O/THF (50/50, 25 mL), aqueous CuSO₄ (0.21 mL, 1 M, 0.21 mmol) and sodium ascorbate (0.43 mL, 1 M, 0.43 mmol) were added, and the reaction mixture was stirred at RT overnight. THF was removed in vacuo, and the residue was dissolved in CH₂Cl₂, extracted with brine, H₂O, dried with MgSO₄, filtered, and concentrated in vacuo. The crude product contained a minor residue of starting material that could be removed by column chromatography (EtOAc/heptane); the product was a colorless oil (77.7 mg, 72%). IR (cm⁻¹): 3112 (C–H stretch); 1756 (O–C=O stretch); 1190, 1140, 1106 (C–F stretch). ¹H NMR (CDCl₃, 250 MHz, δ_{H} , ppm): 2.87 (m, 2H, ≡C–CH₂–); 3.08 (m, 2H, –CH₂–COO–); 3.84 (dd, 12 Hz, 6.2 Hz, 1H, –CH₂–N); 4.26 (dd, 12 Hz, 1.9 Hz, 1H, –CH₂–N); 4.4–4.7 (m, 5H, –CH₂–O, –CH–O, CH₂–CF₃); 6.37/6.39 (2 \times d, ⁴*J* = 3.7 Hz, 2H, S–CH); 7.47 (s, 1H, N–CH=C).

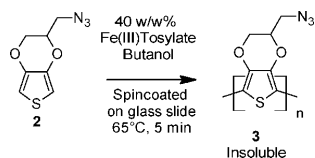
General Procedure for Click Reaction of Polymers 3, 4, 5, 6, 7, 8, and 9 to Give Respectively 14, 15, 16, 17, 18, 19, and 20. 11 (2.2 mg, 5.7 μ mol) was dissolved in DMF (0.2 mL) and mixed with a solution of CuSO₄ (10 μ L, 0.1 M, 1 μ mol) and sodium ascorbate (20 μ L, 0.1 M, 2 μ mol) in DMF (0.1 mL). The reaction mixture was placed on the surface of 3 and left there for 20 h. The surface was rinsed with H₂O and DMF and finally dried with pressurized air. The films were reoxidized by immersion in 10 mL of 10% Baytron C in water (~4 wt % Fe(III)Tos) in 5 min, followed by rinsing with H₂O and drying with pressurized air.

Click Reaction of 3 and 10, 21. The product was prepared according to the general click procedure on 3 using 10 (4.0 mg, 17.4 μ mol), CuSO₄ (10 μ L, 0.1 M, 1 μ mol), and sodium ascorbate (20 μ L, 0.1 M, 2 μ mol) in DMF for 20 h.

Scheme 1. Monomer Synthesis



Scheme 2. Polymerization of the Azide Functional Monomer 2



Click Reaction of 3 and 12, 22. The product was prepared according to the general click procedure on 3, using **12** (12.3 mg, 2.4 μmol), CuSO_4 (10 μL , 0.1 M, 1 μmol), and sodium ascorbate (20 μL , 0.1 M, 2 μmol) in DMF or H_2O for 20 h.

Results and Discussion

In order to prepare a PEDOT for use in the click approach, it was necessary to synthesize either an alkyne or an azide functional monomer based on 3,4-ethylenedioxythiophene (EDOT). It was decided to prepare the azide monomer, since that was expected to be able to withstand the polymerization conditions. The new monomer was synthesized as shown in Scheme 1. A transesterification using 3-bromo-1,2-propanediol gives the bromine functional monomer, **1**, and this is subsequently substituted using NaN_3 to give the product monomer EDOT- N_3 , **2**. The reactivity of the monomer was checked in a model reaction using standard click conditions and gave the expected product, **13**.

The polymerization method published earlier³³ was not efficient with this new monomer that appears to have a lower reactivity compared to ordinary EDOT. The polymerization rate under standard conditions is limited by pyridine. However, by omitting pyridine from the mixture, the polymerization of EDOT- N_3 occurred under otherwise similar conditions as shown in Scheme 2.

The prepared polymer is insoluble and thus cannot be characterized using NMR or SEC. However, surface characterization using XPS gives a good correlation between the expected composition and the formed substrate.

To monitor the reaction on the surface, it was decided to produce a fluorescent alkyne and detect this by fluorescence microscopy/spectroscopy. Fluorescein was chosen as precursor since it is an inexpensive fluorophore and has a high quantum yield, even after modification of the phenol and the acid group. It was expected that only a surface layer would be functionalized, and this would be difficult to detect with other techniques. In addition to this, the UV/vis spectrum of fluorescein could also be used to estimate the degree of reaction at higher concentrations.

The alkyne functional fluorophore was synthesized as shown in Scheme 3. First the methyl ester of fluorescein was prepared

through an ester synthesis in accordance with the method by Moore et al.³² In the second step the alkyne was introduced using a Mitsunobu ether synthesis in moderate yields, 48%.

At first the approach was to perform the click reactions on the polymer in H_2O with a catalyst system of CuSO_4 and sodium ascorbate. To make the fluorophore water-soluble, it was attempted to deprotect **11** by the method of Balakirev et al.³⁴ in order to perform the click reactions in water. This approach was ineffective and was abandoned. The solvent was replaced by DMF, and the catalyst system of CuSO_4 /sodium ascorbate was applied together with **11**, which was much more efficient as shown in Scheme 4.

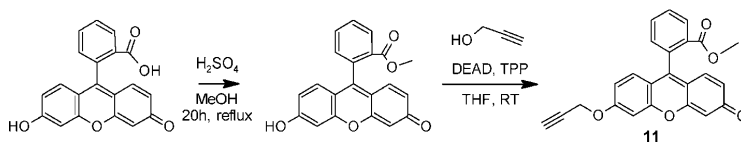
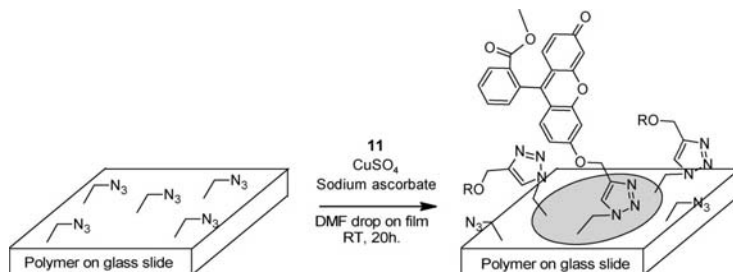
A reference reaction was performed without the CuSO_4 catalyst but with otherwise equivalent conditions. Fluorescent microscopy images of the clicked surface and the reference surface are presented in Figure 1. The distinct fluorescence of the clicked surface clearly shows that the reaction has proceeded, while the low fluorescence level of the nonclicked reference surface suggests that physical adsorption of the fluorescent reactant can be disregarded.

Fluorescent microscopy was performed on a pristine film of **11** spin-coated on a glass slide (not shown) and compared to the clicked sample. The detected fluorescence from **11** was significantly stronger than the clicked sample. This can be attributed to a combination of incomplete surface coupling and fluorescence quenching by the conducting polymer backbone. Ramanaviciene et al.³⁵ report that the conducting polymer polypyrrole significantly quenches fluorescein and rhodamine B fluorescence. A similar behavior was observed when a thin layer of **11** was deposited on a PEDOT- N_3 film.

The thickness of the clicked film and a reference film exposed to the same conditions except CuSO_4 was measured with a mechanical profilometer before and several days after the reaction. The thickness of the clicked film increased from 240 to 420 nm (± 10 nm), corresponding to an increase of 75%. The thickness of the reference film was approximately unchanged by the exposure to the reaction mixture without CuSO_4 , and a thickness of 235 nm before and 220 nm after the exposure was found. The significant volume expansion of the clicked film shows that the reaction not only is limited to the surface layer but also is occurring in the bulk phase. In addition to this the unchanged thickness of the reference film shows that the increase in thickness cannot be due to swelling or adhered reagents. The topography of the clicked sample (**14**) was investigated by atomic force microscopy (AFM) as shown in Figure 2. The surface is relatively uniform even after the large increase in thickness, and the roughness is only a few nanometers. This clearly shows that the reaction has been conducted evenly across the polymer film surface and that reactions in the bulk did not give rise to topographic differences on the surface.

X-ray photoelectron spectroscopy (XPS) was additionally used to investigate the clicked surfaces. The high-resolution peak of nitrogen shown in Figure 3 can be used to check for remaining azides on the surface due to the difference in binding energies of nitrogen in the triazole and the azide. The azide nitrogens exist in two different oxidation states resulting in two XPS peaks, one at 405 eV and one at 400 eV in a ratio of 1:2, whereas the triazole should give only one peak at 400 eV. The ratio of the two peaks in PEDOT- N_3 shown in Figure 3 is between 1:3 and 1:4. This deviation is a result of degradation of the azides during the XPS analysis. The analyses were generally undertaken with electron charge compensation to avoid charging of the less conductive film samples. XPS analysis without electron charge compensation on the highly conductive pure PEDOT- N_3 showed a constant peak ratio of exactly 1:2 for extensive analysis times, followed by an immediate decrease

Scheme 3. Fluorophore Synthesis

Scheme 4. Schematic of the Film Reaction of 3 with 11, Where R Substitutes 11^a

^a The gray area indicates where the film has been exposed to the reaction mixture and thus also that there are unreacted azides around this area.

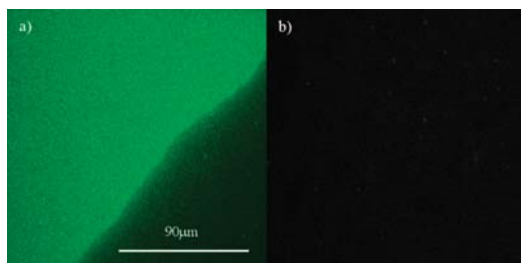


Figure 1. Fluorescence microscopy of the (a) clicked surface (14) and (b) the reference prepared without CuSO_4 under otherwise equivalent conditions. The drop of the reaction mixture did not cover the lower right corner in (a), and thus this part of the film has not been functionalized. The images are recorded using equal lighting and camera settings.

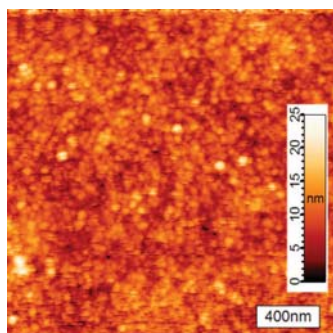


Figure 2. AFM topography image of the clicked surface of 14.

in ratio to below 1:3 after switching on charge compensation. The relative nitrogen content also decreases with analysis time (see Table 1, second column), where especially the intensity of the peak at 405 eV is weakened. This deviation from the 1:2 ratio is in agreement with the results obtained by Shannon et al.¹⁹ The XPS results clearly show the difference in binding energies from PEDOT- N_3 to the product triazole, where no

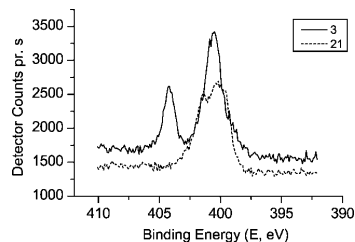


Figure 3. N (1s) high-resolution peak for PEDOT- N_3 (3) and the product triazole (21).

Table 1. XPS Results of PEDOT- N_3 (3) and the Triazoles 21 and 22 (All Numbers in atom %)

	theoretical 3 ^a	3 ^b	3 ^c	21	22, DMF	22, H ₂ O
C	56	61.5 (58.7)	62.0	59.5	64.4	63.2
O	18	19.5 (18.4)	20.9	17.5	26.6	21.1
N	18	9.3 (13.6)	8.6	6.7	4.6	8.4
S	8	9.6 (9.1)	8.5	5.7	4.5	7.3
F				10.6		

^a Inclusive 33% tosylate from reoxidation based on XPS analysis of pure PEDOT films showing tosylate to EDOT ratios of approximately 1:3 in oxidized conductive films. ^b Reference sample, PEDOT- N_3 without any further treatment. Quantification in parentheses refer to analysis without electron charge compensation. ^c Reference sample, PEDOT- N_3 exposed to equivalent reaction conditions except that CuSO_4 was omitted.

residual azide was detected. The absence of azide nitrogens thus shows that the reaction has proceeded, though it cannot be concluded that all azides have reacted, since nonreacted azides could be degraded during the analysis. In combination with the data from the model reaction, fluorescence spectroscopy, thickness measurements, and UV/vis data (examples given in Figures 4, 5, and 8), this clearly shows that the click reaction has been performed on the polymer substrate.

The conductivity of the films is not surprisingly affected by the treatment. Before reaction the conductivity of the films is around 60 S/cm. During the reaction the films are reduced with sodium ascorbate, causing a dramatic reduction in conductivity to around 0.2–0.3 S/cm. Some of the conductivity is however regained by reoxidation in an aqueous solution of Fe(III) tosylate ending at ~ 15 S/cm. The actual loss in film conductance is

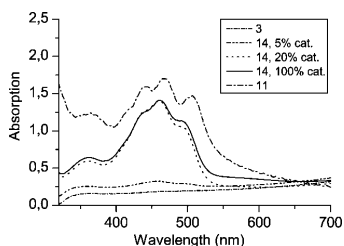


Figure 4. UV/vis spectroscopy of the fluorophore (**11**) loading on PEDOT-N₃ (**3**) as effect of catalyst concentration using a constant reaction time of 20 h.

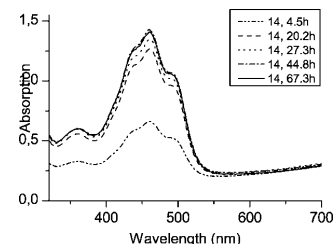


Figure 5. UV/vis spectroscopy of the fluorophore (**11**) loading on PEDOT-N₃ (**3**) as a function of reaction time using a constant catalyst loading of 20%.

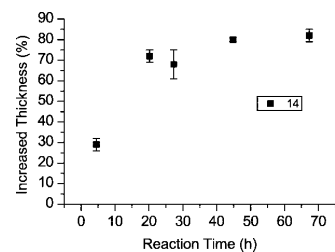


Figure 6. Increased thickness of the triazole functional polymer (**14**) as a function of reaction time using a constant catalyst loading of 20%.

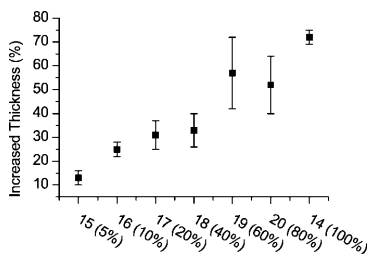


Figure 7. Increase in thickness by the click reaction as a function of EDOT-N₃ content in the copolymer.

considerably smaller than the reduction in conductivity, since the film thickness is increased by 75% after the click reaction, which in its own effect gives a reduction in conductivity.

Mechanical stirring is not possible with the polymer film, and all mixing of reagents is thus dependent on diffusion. Therefore, the necessary catalyst concentration within reasonable time frames was investigated. UV/vis spectroscopy of the films produced with a catalyst amount of 5, 20, and 100% catalyst

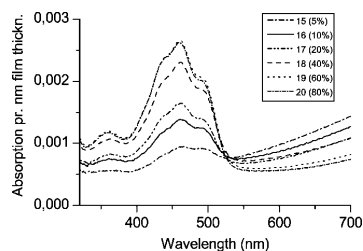


Figure 8. UV/vis absorptions per nm film thickness of the clicked copolymers, **15–20**.

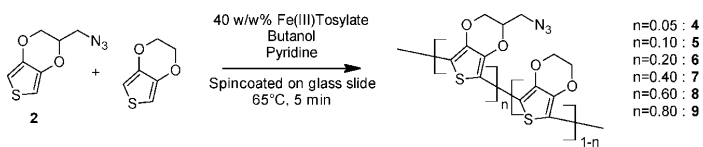
relative to the alkyne (**11**) is presented in Figure 4 and compared to a thin layer of **11** spin-coated on a glass slide. The UV/vis spectrum shows that the 20% and 100% samples have the same three characteristic peaks as **11**, although they are blue-shifted by 5–10 nm. The strong absorption peaks supports the assumption that more than a surface layer of fluorescein is present after the reaction.

The UV/vis absorption of the three fluorescein peaks reaches a maximum already at 20% catalyst, and conducting the reaction with 100% catalyst made no significant difference. Two explanations for this result seem feasible. Either 20% is sufficient, given the diffusion, to make the reaction proceed to completion within reasonable time or the concentration of azides is lower than assumed and all reactive sites can be initialized with 20% of the alkynes. The concentration of azides on the surface estimated based on the film thickness, film size, and the density of PEDOT that gives approximately 0.1–0.2 mg/cm² of azide polymer. In addition to this, access to all the azides in the film must be limited by sterical hindrance and diffusion into the polymer film, and it is expected that some of the sites may be inaccessible.

Using 20% catalyst loading the reaction time was monitored using UV/vis as shown in Figure 5. The reaction proceeds mainly within the first 20 h, and then the increase in intensity gradually decreases over time. This rate decrease is believed to be due to steric hindrance in the bulk of the polymer film as the loading increases and less free sites are available for reaction. It would demand unreasonable long reaction times to obtain complete reaction of all azides, and thus the loading obtained after 20 h has been found sufficiently high.

Film thickness measurements by profilometry corroborate these results (see Figure 6) by showing a slow progression toward larger film thickness for reactions occurring over several days.

The results from polymer films of pure EDOT-N₃ show a very high density of accessible reactive sites. Many applications may benefit from a lower density of sites with controllable average spacing, e.g., uses targeting the immobilization of large biomolecules as sensors or cellular stimulants. In order to be able to load the surface with a lower amount of azides, the copolymerization of EDOT and EDOT-N₃ was investigated. As mentioned earlier, EDOT-N₃ was less reactive than EDOT and thus polymerized without pyridine. In the copolymer formulation mixture it was necessary to include some pyridine in order to limit the EDOT polymerization since that would otherwise be too fast. It was decided to simply mix the reaction mixtures for homopolymerization of the two monomers in the ratio desired of the copolymer. This is a tradeoff as polymerization has to be slowed down sufficiently to control the EDOT reactivity without inhibiting the polymerization of EDOT-N₃ completely. The reaction was performed as shown in Scheme 5, and as with the homopolymer the product is insoluble and cannot be characterized using NMR or SEC.

Scheme 5. Copolymerization of EDOT-N₃ (**2**) and EDOT^a

^a Pyridine was added with EDOT to inhibit the polymerization.

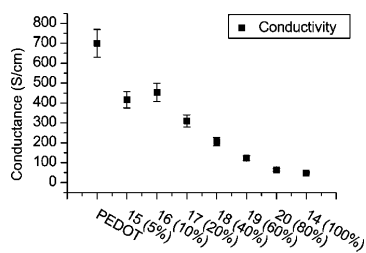


Figure 9. Conductivity of the clicked copolymers, **15–20**, compared to PEDOT.

Film thickness analysis of the copolymer films by profilometry revealed that increasing EDOT-N₃ content and decreasing pyridine content led to thicker polymer films. An explanation could be that more EDOT-N₃ remains after spin-coating and subsequent heating of the monomers as EDOT-N₃ is less volatile or simply that lower pyridine concentration gives less inhibition. If a specific film thickness was desired, it would have to be optimized for every ratio of the monomers in the copolymer. Since our interest in the copolymers are merely in creating a controllable density of reactive groups in the polymer, this has not been investigated further. Functionalization of the copolymers with **11** using equivalent reaction conditions was performed. As mentioned, the copolymer films are of different thickness, and thus the increased thickness by the click reaction was investigated as shown in Figure 7.

The increase in thickness was found to be dependent on the EDOT-N₃ content, which indicates that the reaction is conducted on the bulk film. This has been corroborated with fluorescence spectroscopy performed on the backside of the films which shows fluorescence. The degree of loading was also investigated using UV/vis spectroscopy as shown in Figure 8. To eliminate the effects of different film thicknesses, the results were recalculated and the relative absorbance per nm was plotted.

The corrected data clearly show that an increasing amount of reactive groups can be obtained using the copolymer approach. Interestingly, an upper degree of loading seems to be reached with 60% EDOT-N₃.

The effect on conductivity with the varied loading of the copolymer was simultaneously investigated, as shown in Figure 9. As mentioned above the functional polymers have a lower conductivity than pure PEDOT, and it is clear that the conductivity decreases with decreasing contents of EDOT. Consequently, the gain in functionality is balanced by a loss in conductivity.

To show that the method can be used as a general method for PEDOT functionalization, 2,2,3,3,3-pentafluoropropyl pent-4-ynoate, **10**, and an alkyne-functionalized MPEG 5000, **12**, were prepared. Both alkynes were produced through an ester synthesis using DCC in 88% and 87% yield, respectively. The fluorous and MPEG-functionalized polymers, **21** and **22**, have no special UV/vis absorptions that could be used to confirm the reaction. However, the changes in the surface energy

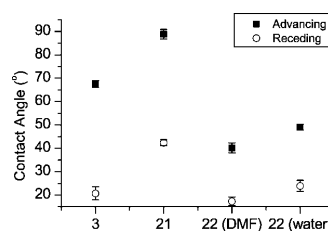


Figure 10. Contact angles of H₂O with the fluorous (**21**) and MPEG-functionalized triazole (**22**, reaction in DMF or aqueous environment) compared to the starting material PEDOT-N₃ (**3**).

properties of the PEDOT-N₃ after reaction are substantial, as can be seen from the water contact angle measurements shown in Figure 10.

It is known that introduction of fluorous compounds on a surface will decrease the surface energy and make the surface more hydrophobic.³⁶ By attaching the fluorous **10** to the conductive polymer, there was a distinct increase in both the advancing and receding contact angle by ~20°, which clearly shows that the reaction has proceeded and a more hydrophobic surface has been formed. The contact angle hysteresis is ~50°, indicating substantial chemical heterogeneity at the surface. It would normally be expected to obtain a higher advancing contact angle on a fluorous surface like **21**, but the effects from the tosylate ions that were introduced into the polymer through the reoxidation are believed to affect the surface oppositely. Covalent attachment of poly(ethylene glycol) entities to PEDOT-N₃ is expected to increase its surface energy, resulting in lower water contact angles. Immobilization of MPEG 5000 on the surface in **22** yields the expected lowering of the advancing contact angle by 20°–25°, depending on using either H₂O or DMF as solvent. The receding contact angle shows no significant development in either solvent compared to the untreated PEDOT-N₃. This is again consistent with a chemically heterogeneous surface, where the PEDOT/tosylate base polymer presents more hydrophilic functionalities amidst the PEG chains.

Profilometry measurements on these samples showed that the reaction performed in DMF increased the thickness by ~130 nm, corresponding to 60% for the fluorous hydrocarbon, **21**, and 60 nm corresponding to 30% for the MPEG functionalized polymer prepared in DMF, **22**. **22** prepared in H₂O had approximately the same thickness in the product as in the starting material.

XPS analysis of the clicked surfaces corroborates the results found by contact angle and by thickness goniometry and profilometry, as shown in Table 1. As mentioned earlier, the quantifications are deviating due to degradation of the azides in the sample during the analysis. However, the relative differences between PEDOT-N₃ (**3**) and the respective products can still be used for qualitative assessments. Reaction of **3** with **10** to give **21** introduced 10.6% fluorine to the surface layer, and the high-resolution nitrogen peak shows no residual azide. Thereby the reaction is confirmed, though the extent of reaction cannot be conclusively determined. The results with MPEG

coupling to give **22** also correlate well with the contact angle measurements, where there is clearly a higher loading of MPEG with DMF as solvent compared to H₂O. The high-resolution peak of nitrogen shows in both cases residual azide nitrogen (not shown), which would be expected since diffusion of the long MPEG chains of **12** into the PEDOT-N₃ is much more difficult than with the smaller **10**. Regarding the MPEG experiments, the reaction is much more likely to occur only in the upper surface or perhaps only on the surface. However, there is an increased loading in the case of DMF compared to water. One may speculate that this is due to water being inefficient in swelling and wetting the PEDOT-N₃ surface. Access to reactive groups would be limited to the azides on the actual surface; thus, after reaction of about one layer of MPEG the reaction would stop. The higher loading observed with MPEG reactions in DMF could be an effect of better wetting and swelling of the surface, which would give access to an increased number of reactive sites.

Conclusion

We have developed the synthesis of a new azide monomer, EDOT-N₃, and demonstrated that it can be polymerized to PEDOT-N₃, which can be used as a precursor to obtain conductive polymers with different functionalities. A click reaction with a fluorescein derivative has been performed on the surface, and the reaction conditions have been optimized for other applications. It is possible to copolymerize EDOT-N₃ and EDOT in different ratios and to functionalize these after polymerization. Through the copolymer it is possible to control the number of reactive sites on the surface, in case a lower loading is desirable. The copolymers have also been shown to be a good way to obtain functional conductive polymers while minimizing the loss in conductivity.

By coupling the fluororous alkyne and the MPEG alkyne to the surface, we have shown the versatility of the method. We believe that this method can be applied for other alkynes with different functional groups. The approach is well suited for new sensor devices, and we are currently working on the development of different systems.

Acknowledgment. The Danish Research Council for Technology and Production Sciences (through the framework program "Design and Processing of Polymers for Microfluidic Applications", grant 26-04-0074) is thanked for financial support.

References and Notes

- Dai, L. M.; Soundarrajan, P.; Kim, T. *Pure Appl. Chem.* **2002**, *74*, 1753–1772.
- Mateiu, R.; Lillemose, M.; Hansen, T. S.; Boisen, A.; Geschke, O. *Microelectron. Eng.* **2007**, *84*, 1270–1273.
- Goetzberger, A.; Hebling, C.; Schock, H. W. *Mater. Sci. Eng., R* **2003**, *40*, 1–46.
- Hung, L. S.; Chen, C. H. *Mater. Sci. Eng., R* **2002**, *39*, 143–222.
- Kolb, H. C.; Finn, M. G.; Sharpless, K. B. *Angew. Chem., Int. Ed.* **2001**, *40*, 2004–2021.
- Rostovtsev, V. V.; Green, L. G.; Fokin, V. V.; Sharpless, K. B. *Angew. Chem., Int. Ed.* **2002**, *41*, 2596–2599.
- Tornøe, C. W.; Christensen, C.; Meldal, M. *J. Org. Chem.* **2002**, *67*, 3057–3064.
- Lutz, J. F.; Börner, H. G.; Weichenhan, K. *Macromol. Rapid Commun.* **2005**, *26*, 514–518.
- Opsteen, J. A.; van Hest, J. C. M. *Chem. Commun.* **2005**, 57–59.
- Sumerlin, B. S.; Tsarevsky, N. V.; Louche, G.; Lee, R. Y.; Matyjaszewski, K. *Macromolecules* **2005**, *38*, 7540–7545.
- Helms, B.; Mynar, J. L.; Hawker, C. J.; Frechet, J. M. J. *J. Am. Chem. Soc.* **2004**, *126*, 15020–15021.
- Parrish, B.; Breitenkamp, R. B.; Emrick, T. *J. Am. Chem. Soc.* **2005**, *127*, 7404–7410.
- Diaz, D. D.; Punna, S.; Holzer, P.; Mcpherson, A. K.; Sharpless, K. B.; Fokin, V. V.; Finn, M. G. *J. Polym. Sci., Part A: Polym. Chem.* **2004**, *42*, 4392–4403.
- Li, H. M.; Cheng, F. O.; Duft, A. M.; Adronov, A. *J. Am. Chem. Soc.* **2005**, *127*, 14518–14524.
- Collman, J. P.; Devaraj, N. K.; Chidsey, C. E. D. *Langmuir* **2004**, *20*, 1051–1053.
- Zirbs, R.; Kienberger, F.; Hinterdorfer, P.; Binder, W. H. *Langmuir* **2005**, *21*, 8414–8421.
- Chen, G. J.; Tao, L.; Mantovani, G.; Ladmiral, V.; Burt, D. P.; Macpherson, J. V.; Haddleton, D. M. *Soft Matter* **2007**, *3*, 732–739.
- Gallant, N. D.; Lavery, K. A.; Amis, E. J.; Becker, M. L. *Adv. Mater.* **2007**, *19*, 965–969.
- Prakash, S.; Long, T. M.; Selby, J. C.; Moore, J. S.; Shannon, M. A. *Anal. Chem.* **2007**, *79*, 1661–1667.
- Nandivada, H.; Chen, H. Y.; Bondarenko, L.; Lahann, J. *Angew. Chem., Int. Ed.* **2006**, *45*, 3360–3363.
- Brennan, J. L.; Hatzakis, N. S.; Tshikhudo, T. R.; Dirvianskyte, N.; Razumas, V.; Patkar, S.; Vind, J.; Svendsen, A.; Nolte, R. J. M.; Rowan, A. E.; Brust, M. *Bioconjugate Chem.* **2006**, *17*, 1373–1375.
- Binder, W. H.; Sachsenhofer, R. *Macromol. Rapid Commun.* **2007**, *28*, 15–54.
- Groenendaal, B. L.; Jonas, F.; Freitag, D.; Pielartzik, H.; Reynolds, J. R. *Adv. Mater.* **2000**, *12*, 481–494.
- Ahuja, T.; Mir, I. A.; Kumar, D.; Rajesh, *Biomaterials* **2007**, *28*, 791–805.
- Rahman, M. A.; Park, D. S.; Chang, S. C.; Mcneil, C. J.; Shim, Y. B. *Biosens. Bioelectron.* **2006**, *21*, 1116–1124.
- Higgins, S. J.; Mouffoukand, F. Patent WO2006018643-A2, **2006**.
- Hansen, T. S.; West, K.; Hassager, O.; Larsen, N. B. *Adv. Mater.* **2007**, *19*, 3261–3265.
- Hansen, T. S.; West, K.; Hassager, O.; Larsen, N. B. *J. Micromech. Microeng.* **2007**, *17*, 860–866.
- Hansen, T. S.; West, K.; Hassager, O.; Larsen, N. B. *Synth. Met.* **2006**, *156*, 1203–1207.
- Hansen, T. S.; West, K.; Hassager, O.; Larsen, N. B. *Adv. Funct. Mater.* **2007**, *17*, 3069–3074.
- Thomsen, A. D.; Malmstrom, E.; Hvilsted, S. *J. Polym. Sci., Part A: Polym. Chem.* **2006**, *44*, 6360–6377.
- Adamczyk, M.; Grote, J.; Moore, J. A. *Bioconjugate Chem.* **1999**, *10*, 544–547.
- Winther-Jensen, B.; Breiby, D. W.; West, K. *Synth. Met.* **2005**, *152*, 1–4.
- Mugherli, L.; Burchak, O. N.; Chatelain, F.; Balakirev, M. Y. *Bioorg. Med. Chem. Lett.* **2006**, *16*, 4488–4491.
- Ramanaviciene, A.; Kurilcik, N.; Jursenas, S.; Finkelsteinas, A.; Ramanaviciene, A. *Biosens. Bioelectron.* **2007**, *23*, 499–505.
- Borkar, S.; Jankova, K.; Siesler, H. W.; Hvilsted, S. *Macromolecules* **2004**, *37*, 788–794.

MA702731K

Department of Chemical
and Biochemical Engineering
DTU Building 229
Søltofts Plads
DK-2800 Kgs. Lyngby
www.kt.dtu.dk